International Telecommunication Union

ITU-R

Radiocommunication Sector of ITU

Report ITU-R S.2462-0
(07/2019)

Sharing between 50/40 GHz geostationary networks and non-geostationary systems

S Series
Fixed-satellite service

Foreword

The role of the Radiocommunication Sector is to ensure the rational, equitable, efficient and economical use of the radio-frequency spectrum by all radiocommunication services, including satellite services, and carry out studies without limit of frequency range on the basis of which Recommendations are adopted.

The regulatory and policy functions of the Radiocommunication Sector are performed by World and Regional Radiocommunication Conferences and Radiocommunication Assemblies supported by Study Groups.

Policy on Intellectual Property Right (IPR)

ITU-R policy on IPR is described in the Common Patent Policy for ITU-T/ITU-R/ISO/IEC referenced in Resolution ITU-R 1. Forms to be used for the submission of patent statements and licensing declarations by patent holders are available from http://www.itu.int/ITU-R/go/patents/en where the Guidelines for Implementation of the Common Patent Policy for ITU-T/ITU-R/ISO/IEC and the ITU-R patent information database can also be found.

Series of ITU-R Reports

(Also available online at http://www.itu.int/publ/R-REP/en)

Series	Title
BO	Satellite delivery
BR	Recording for production, archival and play-out; film for television
BS	Broadcasting service (sound)
BT	Broadcasting service (television)
F	Fixed service
M	Mobile, radiodetermination, amateur and related satellite services
P	Radiowave propagation
RA	Radio astronomy
RS	Remote sensing systems
S	**Fixed-satellite service**
SA	Space applications and meteorology
SF	Frequency sharing and coordination between fixed-satellite and fixed service systems
SM	Spectrum management

***Note**: This ITU-R Report was approved in English by the Study Group under the procedure detailed in Resolution ITU-R 1.*

Electronic Publication
Geneva, 2019

REPORT ITU-R S.2462-0

Sharing between 50/40 GHz geostationary networks and non-geostationary systems

(2019)

Annexes 1 through 12 in this Report contain the results of studies into technical issues relating to sharing between non-geostationary fixed-satellite service (non-GSO FSS) satellite systems using circular orbits and GSO networks in the 50/40 GHz frequency bands to provide that detail for World Radiocommunications Conference 2019 (WRC-19) agenda item 1.6.

TABLE OF CONTENTS

Page

Policy on Intellectual Property Right (IPR) ii
1 Background 5
2 Characteristics of non-GSO FSS systems 5
3 Technical characteristics of GSO FSS networks 6
4 GSO protection criteria 6
5 Sharing between non-GSO systems and GSO FSS networks 6
5.1 Application of non-GSO operational parameters in determining sharing considerations 6
5.2 Protection of GSO networks based on fading statistics only 7
5.3 Application of Methodology A' from Recommendation ITU-R S.1323 8
5.4 Protection of the Earth-to-space GSO links 8
6 Frequency sharing in the 50/40 GHz frequency bands 8
7 Summary of Studies 9
7.1 Summary of Study 1 9
7.2 Summary of Study 2 10
7.3 Summary of Study 3 10
7.4 Summary of Study 4 10
7.5 Summary of Study 5 11
7.6 Summary of Study 6 11
7.7 Summary of Study 7 12
7.8 Summary of Study 8 12
7.9 Summary of Study 9 13
7.10 Summary of Study 10 13
7.11 Summary of Study 11 14
7.12 Summary of Study 12 14
Annex 1 – Study #1 for the development for sharing between non-GSO and GSO in the 50/40 GHz frequency bands 14
1 Non-GSO system parameters 14
2 GSO system parameters 15
3 Background on methodology for deriving aggregate epfd limits using Recommendation ITU-R S.1323 15

Page

4 Description of sharing studies to develop a framework for sharing between non-GSO and GSO in the 50/40 GHz frequency bands 17
4.1 Derivation of aggregate epfd limits using an iterative approach and Recommendation ITU-R S.1323 17
4.1.1 Limitations of iterative derivation of epfd curves based on Recommendation ITU-R S.1323 18
4.1.2 epfd curves based on Recommendation ITU-R S.1323 taking into account propagation losses on the interfering signal path 21
4.2 Sharing between non-GSO and GSO FSS systems using Recommendation ITU-R S.1323 21
4.3 Sharing between non-GSO and GSO FSS systems by allowing single system GSO unavailability increase allowances 22
4.4 Sharing between non-GSO and GSO FSS systems by allowing single system GSO unavailability increase allowances 24
5 Summary 25
Annex 2 – Study #2 for the development for sharing between non-GSO FSS and GSO FSS in the 50/40 GHz frequency bands 26
1.1 Non-GSO FSS system 26
1.2 GSO system parameters 30
1.3 Propagation models 32
1.4 Time step calculation 33
1.5 Statistics gathered 34
1.6 Results 34
1.6.1 *I*/*N* and epfd cumulative distribution functions 34
1.6.2 Convolution of interference and wanted signals 35
1.7 Discussion 36
1.7.1 *I*/*N* vs. epfd 36
1.7.2 Propagation and correlation 37
2.1 Non-GSO system 39
2.2 GSO system parameters 40
2.3 Propagation models 41
2.4 Description of simulation 42
2.5 Results of Simulation 42
2.5.1 Calculations of the impact of the non-GSO system on the unavailability of the GSO link 42
2.6 Conclusion 45
Annex 3 – Study #3: Assessment of sharing of aggregate GSO interference allowance among non-GSO systems in the 50/40 GHz frequency band 46
1 Comparison of Study #1 and Study #2 46
1.1 Comparison of VLEO and VMEO analysis studies 46
2 VLEO and VMEO composite epfd profiles 47
3 Observations 48
Annex 4 – Study 4: Considerations on non-GSO/GSO FSS sharing in the 50/40 GHz band 49
1 Introduction 49
2 Methodology, parameters and assumptions 49

Page

3 Results 52
3.1 Interference from a LEO satellite system into receiving GSO earth stations 52
3.2 Interference from LEO earth stations into a GSO satellite 55
3.3 Interference from an equatorial MEO satellite system into receiving GSO earth stations 57
3.4 Interference from earth stations operating with an equatorial MEO satellite system into a GSO satellite 58
4 Conclusions 60
Annex 5 – Study 5: Research on epfd limits for a typical non-GSO system to GSO system in the 50/40 GHz band 61
1 Introduction 61
2 System parameters 61
2.1 Non-GSO system parameters 61
2.2 GSO system parameters 63
3 Parameters of interference simulation scenarios 65
3.1 Time step and simulation duration 65
3.2 Rain attenuation models 66
4 Results 66
4.1 GSO beam pointing low latitude area 66
4.1.1 Downlink 66
4.1.2 Uplink 67
4.2 GSO beam pointing medium latitude area 68
4.2.1 Downlink 68
4.2.2 Uplink 69
5 Conclusion 70
Annex 6 – Study 6: Interference by a non-GSO system to a GSO system in the 50/40 GHz frequency band 71
1 Non-GSO system 71
2 GSO system parameters 74
3 Propagation models 76
4 Simulation run time 76
5 Statistics collection 77
6 Results 77
6.1 Scenario 1 77
6.1.1 Downlink for Gateway 78
6.1.2 Uplink for Gateway 79
6.1.3 Downlink for user terminal 80
6.1.4 Uplink for User Terminal 81
6.2 Scenario 2 81
6.2.1 Downlink for gateway 82
6.2.2 Uplink for Gateway 83
6.2.3 Downlink for User Terminal 84
6.2.4 Uplink for User Terminal 85
7 Conclusion 85

Page

Annex 7 – Study 7: Sharing studies relevant to developing aggregate V-band epfd limits 86
1 Introduction 86
2 GSO network parameters 87
2.1 Impact of degradation on data rate 87
3 epfd↓ technical analysis 90
4 epfd↑ technical analysis 91
5 Calculation of average percent throughput degradation from degradation statistics 92
5.1 Model 1 92
5.2 Model 2 93
6 Application of the average percent throughput degradation calculation to propagation fades and interference from non-GSO systems 94
Annex 8 – Study 8: Protection of GSO links from aggregate interference from non-GSO networks based on fading statistics only 96
Annex 9 – Study 9: Study of sharing between GSO and non-GSO FSS systems in the 50/40 GHz frequency bands 100
1 Introduction 100
2 Current approaches 101
3 Study details and characteristics 101
Attachment 1 to Annex 9 – Analysis of interference into systems using transparent transponders: joint effects of uplink and downlink fading and interference 108
A.1 Technical Analysis 108
A.1.1 Uplink Analysis 108
A.1.2 Downlink Analysis with Transparent Transponder 109
A.1.3 Combined Uplink/Downlink Analysis with Transparent Transponder 111
Attachment 2 to Annex 9 – Derivation of overall uplink and downlink degradation in carrier-to-noise ratio 114
Annex 10 – Study 10: Sharing study relating (*I*/*N*) to spectral efficiency of satellite networks using ACM 115
1 Introduction 116
2 GSO Network Parameters 116
2.1 Earth Station Parameters 116
2.2 Satellite Parameters 116
3 Impact of degradation in (*C*/*N*) on spectral efficiency 117
4 Definitions and assumptions 121
4.1 Basic definitions 121
4.2 Basic Assumptions 121
5 Uplink considerations 122
5.1 Clear-sky conditions 122
6 Downlink considerations 124
6.1 Clear-Sky conditions 124
6.2 Rain faded conditions 125
6.2.1 Degradation in downlink carrier-to-noise ratio 125
6.2.2 Effect of rain fade and interference on percent degraded throughput 129
6.2.3 Case study of percent degraded throughput on downlink 132

Page

7 Long-Term considerations on sensitivity of percent degraded throughput (%DTp) to *I*/*N* level in clear-sky 147
8 Conclusions 154
Annex 11 – Sharing studies relating to protection of GSO FSS networks using adaptive coding and modulation from the operation of non-GSO FSS systems 154
1 Introduction 154
2 Overview of percent degraded throughput concept 155
3 Overview of percent degraded throughput on sharing studies using time average approach 155
4 Percent degraded throughput as applied for non-GSO sharing computations 156
5 Overview of reserve capacity approach 158
6 Alternative reserve capacity approach 159
7 Conclusion 161
Annex 12 – Study #12 for the development for sharing between non-GSO and GSO in the 50/40 GHz frequency bands 161
Attachment 1 to Annex 12 166
Attachment 2 to Annex 12 166
Annex 13 – GSO/FSS system parameters used in studies 167

1 Background

World Radiocommunications Conference 2015 (WRC-15) established agenda item 1.6 for WRC-19: "to consider the development of a regulatory framework for non-GSO FSS satellite systems that may operate in the frequency bands 37.5-39.5 GHz (space-to-Earth), 39.5-42.5 GHz (space-to-Earth), 47.2-50.2 GHz (Earth-to-space) and 50.4-51.4 GHz (Earth-to-space), in accordance with Resolution **159 (WRC-15)**." It also developed the associated Resolution **159 (WRC-15)** entitled: "Studies of technical, operational issues and regulatory provisions for non-geostationary fixed-satellite services satellite systems in the frequency bands 37.5-39.5 GHz (space-to-Earth), 39.5-42.5 GHz (space-to-Earth), 47.2-50.2 GHz (Earth-to-space) and 50.4-51.4 GHz (Earth-to-space)."

Article **22** of the Radio Regulations (RR) contains provisions to ensure compatibility of non-GSO FSS operations with GSO networks for the 14/11 GHz and 30/20 GHz frequency bands. Among these provisions are uplink and downlink equivalent power flux-density (epfd↑ and epfd↓) limits to protect GSO networks from unacceptable interference pursuant to RR No. **22.2**. There are currently no regulatory provisions for sharing between non-GSO systems and GSO networks in the 50/40 GHz frequency bands. In response to WRC-19 agenda item 1.6, the work represented in this document seeks to develop a regulatory framework to facilitate co-frequency operation of GSO networks and non-GSO FSS systems in the 50/40 GHz frequency bands.

2 Characteristics of non-GSO FSS systems

The type of non-GSO FSS systems considered for this study will utilize circular-orbit non-GSO satellites to provide global broadband communications. These systems are designed with a view to facilitate effective FSS intra-service spectrum sharing by utilizing interference mitigation techniques, including GSO arc avoidance. While the technical details, such as the specific GSO arc avoidance angles employed, vary between non-GSO systems, this mitigation technique can be an effective means of co-frequency sharing between non-GSO systems and GSO networks. These systems can

greatly enhance spectrum efficiency by using next-generation satellite and earth station technology and efficiently use existing FSS satellite spectrum, while providing worldwide connectivity.

3 Technical characteristics of GSO FSS networks

The characteristics of GSO FSS, MSS, and BSS systems for studies under WRC-19 agenda item 1.6 have been consolidated into Annex 6.

4 GSO protection criteria

Protection of FSS networks operating in the 50/40 GHz frequency bands is being developed by the ITU-R.

5 Sharing between non-GSO systems and GSO FSS networks

This section presents considerations of different methodologies for performing sharing calculations between non-GSO and GSO FSS systems. Any methodology to assess the sharing conditions between GSO networks and non-GSO systems requires establishing a representative set of GSO networks. The studies presented in Annexes 1 through 9 provide examples of the procedures described in this section protect GSO networks.

5.1 Application of non-GSO operational parameters in determining sharing considerations

In their operation, non-GSO systems may implement mitigation strategies involving a variety of techniques in various combinations in order to avoid harmful interference into GSO networks. Possible mitigation strategies include: GSO-arc avoidance to prevent harmful interference when a non-GSO satellite passes near the main beam of a GSO link, satellite diversity, satellite selection strategies, frequency channelization, spread spectrum coding techniques, alternate polarization, and advanced antenna characteristics.

While the technical details of such mitigation techniques vary between non-GSO systems, they can be used as an effective means of co-frequency sharing between non-GSO systems and GSO networks. Furthermore, these mitigation techniques could be useful to limit the probability of degradation to GSO links in the 50/40 GHz frequency bands.In the 50/40 GHz frequency bands, propagation impairments such as rain, cloud and gaseous absorption can substantially affect FSS satellite links. Not only are rain fade and gaseous absorption propagation effects more severe than in lower frequency bands but effects such as cloud attenuation can also impact the FSS intra-service sharing environment in the 50/40 GHz frequency bands. The following steps can be taken in performing an assessment of non-GSO sharing with GSO in the 50/40 GHz frequency band. This methodology is based on protection criteria being developed by the ITU-R, which is derived from Methodology A from Recommendation ITU-R S.1323 and is illustrated by the studies contained in Annexes 1 through 3. This methodology aims to increase the spectrum efficiencies of FSS systems in the 50/40 GHz by accounting for the operational parameters of all types of non-GSO systems, while protecting GSO systems in these bands.

Step 1: Determine the mitigation strategies (e.g., GSO-arc avoidance angle values) to be used to protect all relevant scenarios of interference to GSO networks from the non-GSO system.

Step 2: Calculate relevant interference statistics (e.g., visibility, satellite hand-offs, satellite track time, link availability, etc.) throughout the service area of the non-GSO system, employing the mitigation strategies determined in Step 1.

Step 3: Characterization of degradation due to fading and other short-term variations in link characteristics. Even though Recommendation ITU-R S.1323 considers only degradations due to rain fading; additional degradations that become significant at the 50/40 GHz frequency bands can be taken into account such as cloud attenuation, scintillation and atmospheric gas attenuation.

Step 4: The total degradation can be calculated as a convolution of the pdf GSO link fading and the pdf of the degradation due to interference statistics from step 2.

Step 5: The resulting total degradation model is used to compute the permitted levels of interference. In order to take into account the propagation impairments affecting the interfering signals from non-GSO systems, compare the interference statistics of the non-GSO system to verify the GSO protection requirements specified in section 45 above.

Step 6: The results of steps 1 to 3 will define the requirements of the non-GSO system analyzed to ensure the protection of compatibility between GSO networks and non-GSO systems.

The studies presented in Annexes 1 through 3 provide examples of the procedures discussed above.

5.2 Protection of GSO networks based on fading statistics only

This methodology aims to establish the interference mask for non-GSO systems in order to protect the GSO links in the space-to-Earth direction, which is the protection of the receiving GSO earth stations.

Based on a representative set of GSO networks for which detailed link budget information is necessary, it is possible to perform *C/N+I* analyses. Those analyses include clear sky conditions and also fading conditions when the earth stations locations (Gateway and user) are known. All this information is only inherent to the GSO network and to the 'long-term interference' [1] considerations, which are well assessed by the GSO operators and do not include the operation of non-GSO systems.

For every *C/N+I* value of the GSO link, it is possible to determine the corresponding unavailability purely due to propagation effects using Recommendation ITU-R P.618. Limiting the increase of such unavailability (or decrease in capacity for networks using adaptive coding) is the basis to establish the constraints to be imposed to non-GSO systems. Indeed, the non-GSO interference on the GSO links should be limited in a way that the unavailability of the GSO systems is not increased above a defined level that is often expressed in percentage of the unavailability due to propagation effects. For GSO networks using adaptive coding and modulation, this approach considered that the non-GSO interference may be limited in a way that it is at the origin of a specific maximum percentage of decrease the throughput of the GSO network.

It is clear that different GSO links may lead to different non-GSO interference limits, depending on the GSO link characteristics and performance objectives; that is the reason why a representative set of GSO links should be duly established. It is also clear that different non-GSO systems (i.e. low-Earth orbit (LEO) orbit versus medium-Earth orbit (MEO) orbit) will lead to different interference profiles into the GSO reference links. However, this approach assumes that the permissible interference levels induced by non-GSO systems on a GSO link are completely independent of the

[1] Long-term interference is written here in the same sense as used in the Recommendation ITU-R S.1323 and refers to the interference component that is permanently experienced by the GSO link. It includes intra-system interference, interference from other GSO networks and also to sharing with terrestrial services. Intra-system interference is due to different factors such as limitations in the isolation frequency reuse, of intermodulation and polarization. Interference from other GSO networks and terrestrial services is typically assessed in terms of uplink and downlink *C/I* as detailed in Annex 7 to this Report for each GSO link.

characteristics or number of non-GSO system(s) and are only dependent on the GSO link to be protected.

In order to verify whether the GSO protection criterion is satisfied by a particular non-GSO system, the procedure described in § 5.1 can be used. Annex 8 provides an example illustrating this approach.

NOTE – There was no agreement with the validity of this methodology on the process of the generation of epfd values to protect GSO networks. Questions were raised about whether it was appropriate to apply the same probability used in the Recommendation ITU-R P.618 (ITU-R P.618) rain fade calculation to the derived epfd threshold as this is an assumption of full correlation between the two. In particular, during the full convolution process in Recommendation ITU-R S.1323 Method A, the probability used in the ITU-R P.618 rain fade calculation and the probability used to select an epfd level are selected fully independent of each other. For example, during a deep (low probability, short term) rain fade, it is most likely that the epfd level is close to average values (medium probability, long term), and it is very unlikely that there be simultaneously high interference and high fading.

5.3 Application of Methodology A' from Recommendation ITU-R S.1323

This approach allows for the definition of epfd masks independently of a particular non-GSO system. It is based on the Methodology A' from Recommendation ITU-R S.1323. Under this methodology, specific parametric representations are chosen for the pdfs of rain fading and interference, in order to establish the joint probability of fading and interference and to ensure that the joint cumulative probability meets the specified link performance criteria, which is characterized by a set of degradations in $(C/N+I)_i$ and the corresponding fractions of time p_i for which the degradations may be exceeded.

It should be noted that this approach is a simplification of the approach of Methodology A as this approach does not take into account the actual interference profiles of non-GSO operations but base the interference statistics on predetermined pdfs of rain fading and interference. This predetermination of pdfs may inherently result in epfd limits that favor some non-GSO systems and disadvantage other non-GSO systems.

5.4 Protection of the Earth-to-space GSO links

The protection of GSO satellite stations from the non-GSO systems is in practice less complex to address than that of the GSO earth stations protection. The reason is that the lower altitude of the non-GSO satellites with respect to the GSO space stations makes it easier to comply with epfd limitations at the GSO arc than for the case of the epfd limits on Earth's surface to protect earth stations.

By using the GSO link budgets contained in Annex 7 of this Report, it is possible to deduce the maximum permissible interference at the GSO satellite receiver by using, for instance, the protection criteria $\Delta T/T=6\%$ (with T as the total system noise) commonly applied to other GSO networks.

6 Frequency sharing in the 50/40 GHz frequency bands

It is important to develop regulations that facilitate maximizing the spectral efficiency of satellite use of the 50/40 GHz frequency bands. Optimal use of the orbit and spectrum resources at 50/40 GHz requires a more equitable regulatory environment between GSO and non-GSO systems than has been established in bands below 30 GHz. GSO networks and non-GSO FSS systems should have equitable access to enable the most efficient use of the spectrum and realize the full benefits of both types of orbits.

A key aspect of such an approach is to find a mechanism that is truly equitable amongst all co-frequency non-GSO systems, and maximizes the available spectrum and orbit resources.

In order to achieve a high-quality candidate mechanism to guide frequency sharing, a good initial step is to identify the requirements that should be addressed by such a sharing mechanism. The following is a list of key considerations that an effective frequency sharing approach should address:

– Maximize the opportunity for equitable co-frequency operation of non-GSO systems while observing aggregate GSO protection criteria.

– Establish an agreed set of GSO reference links that will enable both non-GSO systems and GSO networks to compatibly provide high-quality, co-frequency fixed-satellite services based on allowable aggregate interference levels from non-GSO systems into GSO networks.

– Apportion the maximum allowable aggregate non-GSO interference commensurate with the services provided by each non-GSO system.

One possible solution that has been presented to facilitate multiple non-GSO systems in the 50/40 GHz FSS bands would be to allow the first system deployed in these frequency bands access to the full FSS intra-service aggregate interference allowance required to protect co-frequency GSO networks until another co-frequency non-GSO system gets deployed. If and when subsequent non-GSO systems are deployed in the same band, each system would need to reduce their epfd contribution in an equitable manner so that the aggregate interference from all active constellations still meets the GSO protection criteria. This approach will ensure protection of GSO networks while maximizing the use of orbit and spectrum resources.

Technical studies have shown that sharing of aggregate epfd is possible while meeting the GSO protection criteria. However, regulatory difficulties have been identified. If a suitable process to share epfd were to be identified, this approach would ensure protection of GSO networks while maximizing the use of orbit and spectrum resources.

Another approach that has been considered to facilitate multiple non-GSO systems in the 50/40 GHz band is to apportion the unavailability limit of non-GSO systems to GSO networks. This type of approach allows for a single system limit for each non-GSO system to enable fixed and measurable protection of GSO systems as determined by GSO reference links and GSO protection requirements. This approach also allows for the measurement of the aggregate impact of multiple non-GSO systems by the linear addition of epfd impacts from non-GSO systems. Further details and studies of this approach is presented in study #1 under Annex 1.

7 Summary of Studies

7.1 Summary of Study 1

The study in Annex 1 points to the need to develop regulations that facilitate maximizing the spectral efficiency of use of the 50/40 GHz frequency bands and presents sharing considerations that should be taken into account, including technology and natural considerations such as propagation losses in such sharing considerations. The study presents an analysis of the generation of an epfd profile masks based on generic low-Earth orbit (LEO) constellations of 2 000 and 4 000 service vehicles. The LEO constellations are at an altitude of 1 200 km and a minimum service elevation angle of 45 degrees.

The analysis presents a background on the methodology for deriving aggregate epfd limits based on procedures carried out in lower frequency using Recommendations ITU-R S.1503, ITU-R P.618 and the sharing considerations given in Recommendation ITU-R S.1323. Given that this analysis deduced epfd↓ masks based on a particular representative LEO constellation, the epfd↓ masks are system specific and they are variable, depending on the particular operations of the non-GSO constellation chosen for defining a particular mask. The analysis shows that situations can arise where a particular system cannot meet a specific limit mask (deduced from a different system) but meets the GSO protection criteria given in Recommendation ITU-R S.1323. An analysis is also presented that shows

the effect of accounting for propagation losses on the interfering path. The result of this study shows that there can be significant operational margin available to the GSO networks when propagation impairments are taken into account.

7.2 Summary of Study 2

Study 2 shown in Annex 2 provides a simulation and results of a study of the sharing between a non-GSO FSS satellite system in a circular equatorial orbit and a GSO system in the 48/38 GHz frequency bands. It includes descriptions of the non-GSO and GSO systems along with the assumptions for the propagation model used. The results are shown in both epfd and *I*/*N* statistics. The *C*/*N* and *C*/*(N+I)* curves of the GSO system and the effect on availability due to interference from the non-GSO system are also provided.

Based on the input assumptions, the results show that the unavailability targets in Recommendation ITU-R S.1323 of 10% increase are met. This suggests that these could be acceptable epfd levels for the GSO network and non-GSO system assumed. It is noted that these levels are the results from a single non-GSO FSS network. This study acknowledges that it is necessary to consider aggregation affects taking into account different constellation types rather than a single equatorial circular orbit non-GSO system.

7.3 Summary of Study 3

The study in Annex 3 presents a comparison of the LEO system presented in Annex 1 and the MEO system presented in Annex 2. The purpose of the comparison in this study is to present an assessment of potential sharing between these two systems, with a view to maximize spectral efficiency in the 50/40 GHz band.

The analysis provides a comparison of the representative interference profiles derived in the studies from Annexes 1 and 2 relating to non-GSO constellations in LEO and MEO orbits. The analysis shows that the methodology used in both studies derive a potential epfd mask on the basis of the relevant non-GSO system considered, therefore, they are completely dependent on the characteristics of the systems being evaluated. While using this methodology, potential epfd masks can be developed for a particular system, it is difficult to define epfd masks that would allow all non-GSO systems to operate and provide for maximum spectrum efficiency, while still assuring that GSO protection criteria will always be observed.

The analysis also shows that if masks are developed for the operation of one particular non-GSO system, a separate non-GSO system may not be able to meet the requirements from that mask. However, each system independently, and even in composite form, are able to meet the protection criteria given in Recommendation ITU-R S.1323 with excess margin available.

7.4 Summary of Study 4

The study in Annex 4 considers both the uplink and downlink interference from two different non-GSO systems into a GSO network at varying elevation angles. The two non-GSO systems modelled were a LEO system at 1 200 km and a MEO system at 8 062 km. Two sets of five earth stations with five different elevation angles to the GSO were simulated, with the victim and interfering earth stations always being co-located. It is noted that in future versions of this study, an increased number of earth stations could be considered to reflect more realistic deployment scenarios. It is also noted that this study did not include any propagation impairments other than free space path loss, although it is recognized that at these frequencies, rain and cloud attenuation have significant impacts on both the wanted and interfering signal. If other attenuation losses are taken into account, it is expected that the resulting *I*/*N* would be lower.

The results of the study provide levels of interference into a GSO system from two different non-GSO systems, and should be considered when examining the co-existence between these two types of implementations of the FSS:

– For the first interference scenario (LEO and GSO), in the downlink, the study shows that the receiving GSO earth stations at lower elevation angles to the GSO satellite were more susceptible to interference from non-GSO systems. In the uplink, the interference into a GSO satellite from LEO earth stations was studied showing low levels of interference at the GSO satellite from earth stations located at most elevation angles to the GSO. When the elevation angles of the earth stations to the GSO were increased, the results showed higher levels of interference, but for small percentages of time.

– For the second interference scenario (MEO and GSO), the study shows that receiving GSO earth stations at lower elevation angles to the satellite receive lower *I*/*N* from the equatorial MEO system. When earth stations with higher elevation angles to the GSO were studied, higher levels of interference were received, with the greatest impact to earth stations with elevation angles of 10° and 0° to the GSO. It is important to note that no geostationary arc avoidance was used in the MEO study. In terms of the uplink interference to the GSO satellite the *I*/*N* levels were found to be relatively low (under the conditions assumed), except for when the interfering earth stations were located at high elevation angles to the GSO.

7.5 Summary of Study 5

Study 5 in Annex 5 is an analysis with a circular orbit LEO non-GSO FSS system using parameters similar to the 3ECOM-2 satellite network (IFIC2788), as an example of a typical non-GSO constellation deployment. The system consists of 12 orbits with 28 satellites in each orbit, which provides a total of 336 satellites in the system.

Assuming that the protection criterion for GSO FSS networks is a 10% increase to unavailability caused by the interference, the criterion was not exceeded for GSO beams from both low latitude and medium latitude scenarios in this study. The level of emissions from the non-GSO system depicted in this Study were acceptable based on the assumptions in this study. Although the downlink pfd values of non-GSO system exceeded the pfd requirement in RR Table **21-4**, the compatibility between these two FSS systems depicted in this Study was achieved. Given that the non-GSO FSS system downlink transmitting power would need to be decreased to meet the RR Table **21-4** pfd limits, this lower power would further aid the sharing of non-GSO and GSO systems.

With the parameters of non-GSO and GSO systems depicted in Study 5, the calculated epfd limits were −152 dBW/m^2/MHz for uplink and −148 dBW/m^2/MHz for downlink. These calculated results are for this specific case of frequency sharing between non-GSO and GSO systems. Additional analysis and calculation for different cases may be conducted in the future research.

7.6 Summary of Study 6

Study 6 in Annex 6 is an analysis regarding interference by a non-GSO system to a GSO system in the 50/40 GHz band under different conditions in two scenarios.

The configuration and orbital parameters of the simulated non-GSO system is extracted from 3ECOM-3 filing with some characteristics modification to scale it in the 50/40 GHz band. The Worst-Case Geometry location for non-GSO system is calculated based on Recommendation ITU-R S.1503 and standard propagation models are used for simulations as referenced in Recommendation ITU-R P.525 and Recommendation ITU-R P.618 to model free space loss and rain attenuation.

The operational scenarios for tracking the non-GSO satellites are as follows:

Scenario 1:

– Minimum elevation angle: 20°

– GSO avoidance angle: 2°

– The related satellite is chosen based on the highest elevation angle.

Scenario 2:

– Minimum elevation angle: 40°

– GSO avoidance angle: 10°

– The related satellite is chosen based on the highest elevation angle.

Based on Recommendation ITU-R S.1323, if criterion is 10% increase in the unavailability caused by interference, the increase in unavailability from non-GSO system for scenario 1 has not been met but for scenario 2 it has been met. Then the interference from non-GSO system with scenario 2 tracking strategy depicted in this Study is acceptable.

The effects of interference on User Terminal antenna are more than Gateway antenna.

By the change in some of the parameters in tracking strategy, it is possible to decrease interference from a non-GSO system. Therefore, it could be concluded that frequency sharing between GSO and non-GSO satellite networks is possible provided that appropriate changes would be made on some of the parameters in tracking strategy.

7.7 Summary of Study 7

Study 7 in Annex 7 is an analysis of the operation of non-GSO systems into GSO networks that use Adaptive Coding and Modulation (ACM). This analysis discuss the operation of ACM in next generation GSO systems and potential procedures in terms of impact on data rate that can be taken into account for protection of these types of ACM operations. The analysis produces several results regarding the impact of non-GSO systems on GSO operations using ACM. The analysis concludes that further work is required to address how to account for the operations of non-GSO systems and the protection of GSO operations employing ACM.

7.8 Summary of Study 8

An example of Methodology 5.2 described above is contained in Annex 8. In this study, for every $C/N+I$ value of the GSO link, it is possible to determine the corresponding unavailability purely due to propagation effects using Recommendation ITU-R P.618. Limiting the increase of such unavailability (or decrease in capacity for networks using adaptive coding) is the basis to establish the constraints to be imposed to non-GSO systems. Indeed, the non-GSO interference on the GSO links should be limited in a way that the unavailability of the GSO systems is not increased above a defined level that is often expressed in percentage of the unavailability due to propagation effects. For GSO networks using adaptive coding and modulation, the non-GSO interference should be limited in a way that it is at the origin of a specific maximum percentage of decrease in the amount of throughput of the GSO network. Using this approach, the permissible interference levels induced by non-GSO systems on a GSO link are completely independent of the characteristics or number of non-GSO system(s) and are only dependent on the GSO link to be protected. Based on this approach, maximum interference levels based on the; then, the interference levels can be transformed into aggregate epfd limits.

NOTE – There was no agreement with the validity of this methodology on the process of the generation of epfd values to protect GSO networks. Questions were raised about whether it was appropriate to apply the same probability used in the ITU-R P.618 rain fade calculation to the derived epfd threshold as this is an assumption of full correlation between the two. In particular, during the

full convolution process in rn Recommendation ITU-R S.1323 Method A, the probability used in the ITU-R P.618 rain fade calculation and the probability used to select an epfd level are selected fully independent of each other. For example, during a deep (low probability, short term) rain fade, it is most likely that the epfd level is close to average values (medium probability, long term), and it is very unlikely that there be simultaneously high interference and high fading.

7.9 Summary of Study 9

Study 9 in Annex 9 provides simulations and results to verify the applicability of the methodology to calculate the increase in unavailability to GSO reference links from interference of non-GSO systems. For the simulations, a COTS software (Visualyse) is used to simulate the interference from a non-GSO system into the reference GSO links. The technical characteristics of the GSO reference links used were from links provided by SES and Telesat. The non-GSO systems modelled had altitudes of 1200 km and 1400 km, both with circular orbits.

For each link assessed in this study, rain fading was modelled using Recommendation ITU-R P.618, with the local rain rates provided by Recommendation ITU-R P.837. The fading noise temperature was calculated in accordance with rain characteristics. It was assumed that the rain fade of the wanted links and the interference links were 100% correlated (as the software was limited to 0% or 100%). The percentage of unavailability due to rain was determined for each segment of the forward and return links. For the purpose of these simulations, it was assumed that the GSO links were unavailable if the C/N was below the specified thresholds. The percentage of unavailability due to the combined impact of the rain and the non-GSO interference was then determined, using a $C/(N+I)$ objective of 12 dB. In order to avoid main-beam interference, GSO arc avoidance of 3º and 6º was applied in the uplink.

Results demonstrate that the highest increase in unavailability created by one non-GSO system is 2.7%. It is also shown that when a larger GSO arc avoidance angle is applied, the increase in unavailability of the GSO link is reduced. The absence of GSO arc avoidance leads to high increases in unavailability. Finally, it is noted that most of the increase in unavailability is caused by interference into the downlink segments of the GSO links, while the impact on the uplink is almost negligible.

NOTE - The methodology used to obtain the total unavailability of the system and the corresponding results in the table below need to be assessed further, taking into account the overall (uplink and downlink) $C/N+I$ obtained for each link.

7.10 Summary of Study 10

Study 10 in Annex 10 investigates the impact on the spectral efficiency of a GSO network employing Adaptive Coding and Modulation (ACM) that is subjected to interference from a non-GSO network. The study considers the sensitivity of ACM systems to variations in I/N rather than epfd.

Operation of V-Band non-GSO systems has the potential to cause interference to GSO networks operating in this band – downlinks in 37.5-42.5 GHz (space-to-Earth), and uplinks in 47.2-50.2 GHz (earth-to-space) and 50.4-51.4 GHz (Earth-to-space). The ITU has addressed similar concerns in FSS bands below 30 GHz by imposing epfd limits on non-GSO systems. In this study, we demonstrate that imposing fixed limits on epfd or I/N are not necessarily good protection measures considering the characteristics of the interference generated by non-GSO systems and the capabilities of satellite networks employing ACM; the spectral efficiency of an ACM system subject to interference is a better indicator. Two scenarios of interference from a non-GSO system into the downlink of a GSO network were considered. In the first case, the GSO earth station was assumed to be at a higher lattitude (Saskatoon, Canada). In this case the interference had minimal impact on the spectral efficiency of a link employing ACM. In the second case, the GSO earth station was assumed to be at a lower lattitude

(Peru). We have provided the time function of the interference for the second case, which had short duration *I*/*N* peaks at around 33 dB. The analysis and calculations show that even with such high peaks in *I*/*N*, the long-term spectral reduction in efficiency for the second case was about 2%.

These results demonstrate that imposing a constraint on epfd, which is equivalent to imposing a constraint on *I*/*N* is not an equitable sharing criteria. The results further support the concept of a criterion that limits the reduction in spectral efficiency for systems employing ACM.

7.11 Summary of Study 11

Study 11 considers concepts for the protection of FSS systems utilizing adaptive coding and modulation in the 50/40 GHz frequency bands. The use of adaptive coding and modulation allows a satellite to maintain a connection in spite of degraded conditions but at lower throughput data rates. To consider the impact to satellite systems using ACM, and to allow those systems to adjust to degraded link conditions, it is necessary to account for all foreseeable fade effects, such as time-varying propagation conditions and interference. As presented in this study, the concept of percent degraded throughput may represent a methodology to assess interference into GSO FSS links as applied on a long-term average basis and presents a methodology that can provide a metric to protect the operations of satellite systems employing ACM.

7.12 Summary of Study 12

This study shows that the impact of interference caused by non-GSO systems to a victim GSO FSS link cannot be assessed exclusively by considering the time allowance for degradation exceeding the minimum short-term performance objectives (Recommendation ITU-R S.1323 *recommends* 3.1) and, in the case of GSO networks using ACM, the reduction of the time-averaged spectral efficiency of the victim link (Recommendation ITU-R S.1323 *recommends* 3.2). Therefore, this study may represent a methodology to assess the interference into FSS links using Adaptive Code and Modulation (ACM) techniques. In particular, this study considers assessing the impact that the interference from a non-GSO system operating co-frequency has on a victim GSO FSS link by evaluating the degradation of spectral efficiency (SE) that is exceeded for various percentages (95, 99, 99.5 and 99.9%) of an average year.

Annex 1

Study #1 for the development for sharing between non-GSO and GSO in the 50/40 GHz frequency bands

1 Non-GSO system parameters

The design space of possible non-GSO systems that can utilize circular-orbit non-GSO satellites is extremely varied due to system goals and design targets. For the purposes of this analysis, a set of parameters were chosen for each simulation run for two generic low-Earth orbit (LEO) constellations comprising 2 000 and 4 000 representative non-GSO co-frequency satellites. These are referred to below as the “2000-SV Constellation” and the “4000-SV Constellation”, respectively, where “SV” stands for space vehicle. Table A1-1 presents the LEO constellation parameters used in the analysis and Table A1-2 presents the simulated representative non-GSO satellite transmit parameters. These parameters may not be fully representative of all proposed systems that are planning to operate in the 50/40 GHz band and further studies may be needed for other non-GSO constellations.

All constellations are assumed circular, with a typical LEO altitude of 1200-km and 45° inclination. The satellite coverage area is defined by a minimum service elevation angle of 45°.

TABLE A1-1

Non-GSO constellation parameters

LEO altitude	1 200-km	
LEO inclination angle	45°	
ES minimum operational elevation angle	45°	
Total number of LEO satellites	**LEO planes**	**SVs per plane**
2 000	20	100
4 000	40	100

TABLE A1-2

Non-GSO Tx link parameters

Frequency	40 GHz
Maximum pfd	−129 dB(W/(m^{2}*4 kHz))
Peak gain	57 dBi
Beam pattern	S.672, L_N = −25
Number of beams	200 per polarization
Maximum covering beams (N_{co})	unlimited

2 GSO system parameters

For the purposes of this analysis, a set of representative GSO parameters were chosen for the simulations. Table A1-3 presents the simulated GSO earth station receiver parameters.

TABLE A1-3

GSO link parameters

Antenna diameters	0.3, 0.5, 1.0, 2.5-m
Reference pattern	Recommendation ITU-R S.1428
Earth station latitudes	1°N, 15°N, 30°N, 45°, 60°N
System temperature	350 K

3 Background on methodology for deriving aggregate epfd limits using Recommendation ITU-R S.1323

Part 1, § 6 of Annex 1 to Recommendation ITU-R S.1323-2 currently provides an example analysis of the application of Methodology A using a 19-GHz GSO downlink earth station located in New York City and assuming a link availability objective of 99.9% of the time. That analysis calculates a design degradation margin (X_{max}) of 7.923 dB as shown in Table A1-4.

TABLE A1-4

Methodology A example parameters

Parameter	Value
Location	New York City (41°N 074°W)
Elevation to GSO at 74W	42.43°
I_{self} fraction, α	20%
Frequency	19 GHz
Atmospheric loss	0.3 dB
System temperature, T_{sys}	323.6 K
Design margin, X_{max}	7.923 dB

The same 19-GHz GSO downlink example was analysed again using the Recommendation ITU-R S.1323 Methodology A, but using the updated propagation models provided in Recommendation ITU-R P.618-12 resulting in an 8.260 dB design degradation margin as shown in Table A1-5.

The same analysis was then used to calculate the comparable threshold design degradation margin to use for a downlink at 40 GHz using the same GSO link geometry and availability objective. The comparable 40 GHz atmospheric loss and GSO ES receiver system noise temperature were calculated based on the frequency difference and these link parameters are shown in the third column of Table A1-5. The conclusion is that for the 40 GHz GSO downlink, a threshold design degradation margin (X_{max}) of 25.62 dB would be comparable to the 8.26 dB for the example 19 GHz downlink.

TABLE A1-5

Methodology A example parameters using Recommendation ITU-R P.618-12 for an example GSO downlink operating in NYC with 99.9% availability at 19 GHz and 40 GHz

Parameter	Value	
Location	New York (41°N 074°W)	
Elevation	42.43°	
I_{self} fraction, α	20%	
Frequency	19 GHz	40 GHz
Atmospheric loss	0.286 dB	0.680 dB
System temperature, T_{sys}	323.6 K	356.5 K
Design margin, X_{max}	8.260 dB	25.620 dB

For this study, a number of candidate epfd limit masks were studied as a basis for frequency sharing between non-GSO and GSO systems during previous study cycles. Figure A1-1 presents an illustrated overview of the analysis flow and associated ITU-R Recommendations that were used as a basis for the generation and verification of the aggregate epfd limits.

FIGURE A1-1

Analysis flow of the derivation and verification of aggregate epfd limits

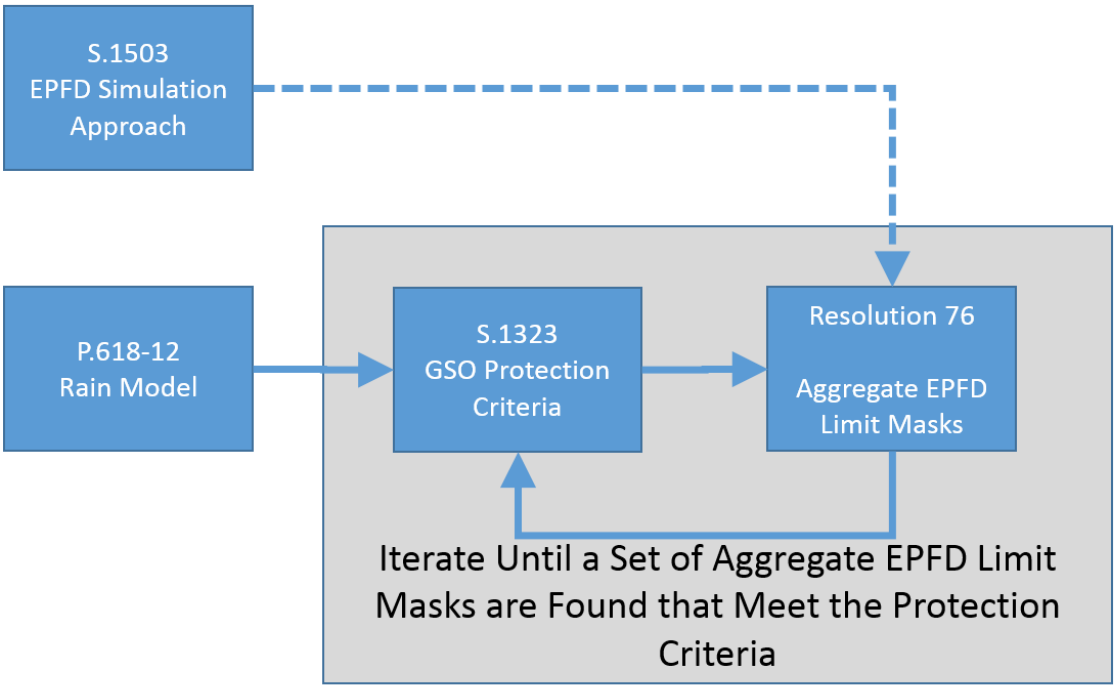

Methodology A of Recommendation ITU-R S.1323 is based upon convolving the probability distribution function (pdf) of degradation due to propagation loss (based on a fading model that includes the effects of rain), with the pdf of degradation due to interference and verifying that the resultant link degradation is less than 1/0.9 of the degradation due to propagation losses alone. Recommendation ITU-R S.1323 Methodology A does not provide a means to derive aggregate epfd limit masks, but rather provides a method to evaluate if a calculated aggregate non-GSO interference epfd curve meets the GSO protection criteria.

Recommendation ITU-R P.618 provides guidance on how to compute the pdf of rain loss as a function of frequency, earth station (ES) location and elevation angle. This propagation pdf is a key input to the Recommendation ITU-R S.1323 Methodology A analysis.

Recommendation ITU-R S.1503 provides recommendations on how to compute the epfd from a non-GSO system into victim GSO earth stations and satellites. The computed epfd can be provided as input into a Recommendation ITU-R S.1323 Methodology A analysis.

4 Description of sharing studies to develop a framework for sharing between non-GSO and GSO in the 50/40 GHz frequency bands

The sections below indicate potential solutions to deriving a sharing framework between non-GSO and GSO FSS systems in the 50/40 GHz frequency bands. For each potential sharing solution, a description of the approach is indicated.

4.1 Derivation of aggregate epfd limits using an iterative approach and Recommendation ITU-R S.1323

In developing sharing considerations between non-GSO FSS systems and GSO FSS networks in the 50/40 GHz frequency band, Recommendation ITU-R S.1323 Methodology A can be used to evaluate a set of potential candidate aggregate epfd curves. Parameters used in the sharing studies include

non-GSO operational parameters as described in § 2, minimum propagation margin assumptions based on 50/40 GHz propagation characteristics, and minimum GSO link availability assumptions based on the minimum operational elevation angle as a function of propagation margin. GSO minimum link availability assumptions are made to determine the minimum performance criteria needed to achieve protection as outlined in Recommendation ITU-R S.1323 for bands below 30 GHz.

The sharing approach given in Methodology A of Recommendation ITU-R S.1323 for GSO/non-GSO frequency sharing is then applied by convolving the probability distribution function (pdf) of degradation due to propagation loss with the pdf of degradation due to aggregate interference from the operation of the non-GSO satellites. The resultant combined link degradation is then compared to the maximum allowable degradation due to propagation losses plus interference per the GSO performance criteria, which is currently under development for the 50/40 GHz frequency bands. For bands below 30 GHz, Recommendation ITU-R S.1323 recommends that the degradation due to interference can be responsible for no more than 10% of the degradation due to propagation losses. That protection criterion is provisionally used for this study with the recognition that new GSO/non-GSO sharing criteria for the 50/40 GHz frequency bands may result from the studies under Resolution **159 (WRC-15)**.

This approach can be used to study aggregate non-GSO interference into representative reference GSO satellite links based on link performance characteristics. Reference GSO links for the 50/40 GHz frequency bands are included in Annex 7 of this Report. This approach can then be used on an iterative basis to generate aggregate epfd limits from non-GSO systems that will appropriately protect the reference GSO links.

4.1.1 Limitations of iterative derivation of epfd curves based on Recommendation ITU-R S.1323

As noted above, a series of candidate aggregate epfd curves can be created based on the simulated aggregate interference due to all non-GSO satellites in view to a reference GSO earth station. Then an analysis method, such as Methodology A in Recommendation ITU-R S.1323, can be used to evaluate if the resultant aggregate non-GSO interference into reference GSO links meets the GSO protection criteria. Note that there exists an infinite number of potential epfd limit masks that can meet the GSO protection criterion. A single 'representative' set of aggregate epfd limit masks corresponding to an agreed set of reference GSO links could then be selected. These reference GSO links will include not just earth station diameter (as in the existing Resolution **76 (WRC-15)** aggregate epfd limit tables), but also some additional parameters to be agreed that can be used as a basis for sharing between GSO networks and non-GSO FSS systems

Currently, for the frequency bands under 30 GHz with single-system epfd limit masks covered under RR Article **22**, in order to receive a favourable finding, all non-GSO epfd interference simulation results (from the ITU's epfd Validation Tool) would need to be completely under the limit masks. Using the various latitude and link elevation simulation results associated with a particular reference GSO antenna diameter, a composite mask (corresponding to different GSO satellite longitudes) can be created to satisfy all links. For illustrative purposes only, Fig. A1-2 presents the results of an example composite mask for the epfd↓ results from the 2000-SV representative constellation into 2.5-m diameter reference GSO earth station located at 30°N.

Simulated epfd↓ results for these two independent GSO links are highlighted (dashed blue representing a profile with a maximum short-term level and dashed orange highlighting a link with high long-term levels). The light grey curves represent the simulated epfd↓ results for GSO satellites located at different longitudes, but serving the same reference GSO ES. The solid red curve represents a potential epfd↓ limit mask that the composite of all the simulated epfd↓ curves would just meet.

FIGURE A1-2

Simulated aggregate epfd↓ curves and example composite mask for 2.5 m GSO ES antenna – 2000-SV Constellation

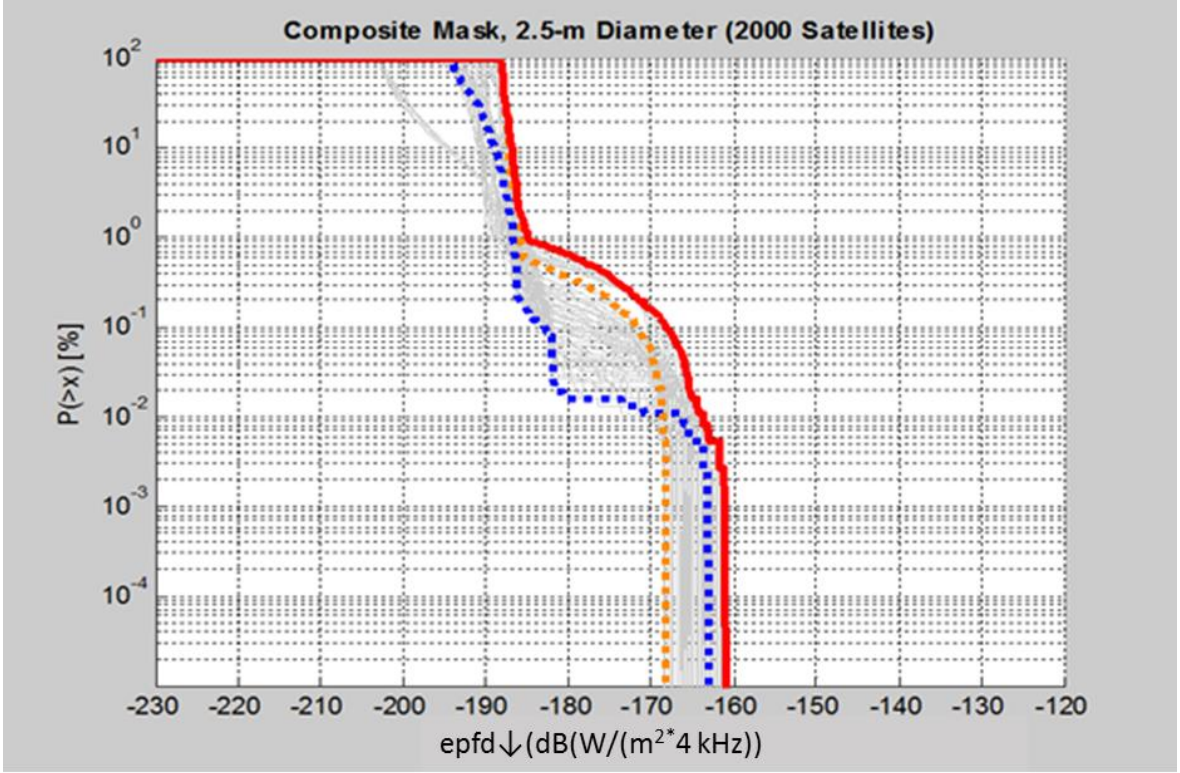

Note however, that using this approach to establish a reference aggregate epfd limit mask (such as the red mask of Fig. A1-2), scenarios can arise in which a particular aggregate set of non-GSO satellites may not meet this limit mask even though it passes the GSO protection criteria outlined in Recommendation ITU-R S.1323 when applied against each reference GSO link. Correspondingly, scenarios can also arise in which a particular non-GSO constellation will meet a particular epfd limit mask but will not pass the sharing criteria outlined in Recommendation ITU-R S.1323. These results are the direct cause of non-GSO systems in higher frequency bands being able to limit the probability of interference into GSO networks. These potential issues are important to address to establish appropriate regulations for GSO/non-GSO sharing in the 50/40 GHz frequency bands due to the heightened variability in propagation losses.

To determine if a candidate composite epfd limit mask is valid, Methodology A in Recommendation ITU-R S.1323 can be used to test a variety of GSO link elevations (corresponding to a variety of GSO satellite longitudes) to each reference GSO ES location. The results can be analysed to obtain for each reference GSO ES location, a family of curves as shown in Fig. A1-3. Each different coloured curve corresponds to a different GSO link elevation angle.

The vertical axis is the relative interference margin which is calculated as 1-X/Z. The GSO protection criteria require the values of 1-X/Z to be 10% or less. This protection criterion is considered satisfied once the relative interference margin calculated for all of the links to the reference GSO ES (colored curves in Fig. A1-3) drop and stay below a value of 10%. The horizontal axis is the calculated degradation to the GSO reference link. For the example in Fig. A1-3, it can be seen that the simulated 2000-SV Constellation would just satisfy a GSO link design margin, X_{max}, of 8.16 dB, which provides 99.7542% availability at the simulated location. If a higher GSO link design margin (e.g., X_{max} of 25.62 dB as calculated in Table A1-6 for NYC) were used, then higher levels of epfd could be tolerated without violating GSO protection criteria.

As an illustration of testing the validity of a candidate epfd limit mask using the Methodology A approach, the example composite mask of Fig. A1-2 was applied to reflect the aggregate external interference from the 2000-SV Constellation to determine the required GSO link margin for a site at 30°N, 042°E. Based on this simulation, it was found that the current Recommendation ITU-R S.1323 10% time allowance is achieved if a minimum margin of 8.16 dB is provided as shown in Fig. A1-3.

FIGURE A1-3

Methodology A convolution 30N042E – 2000-SV Constellation

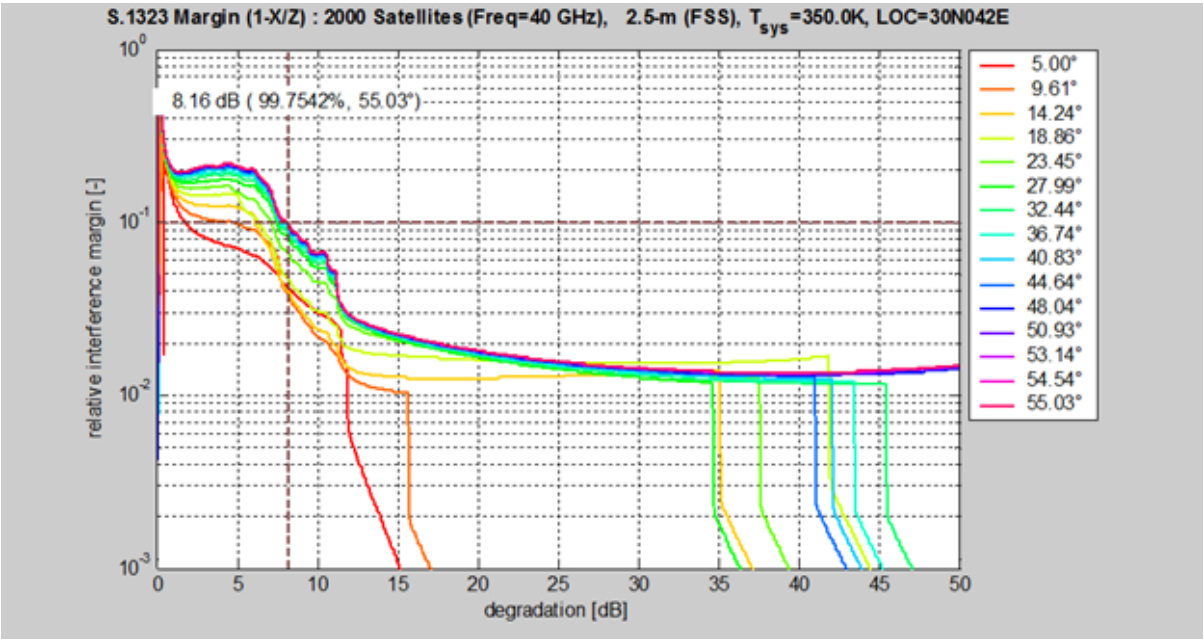

However, if the Recommendation ITU-R S.1323 Methodology A convolution is performed using the aggregate epfd curves calculated for each reference GSO earth station location and elevation angle, the required degradation drops to only 2.45 dB. This is illustrated in Fig. A1-4.

FIGURE A1-4

Per link convolution 30N042E – 2000-SV Constellation

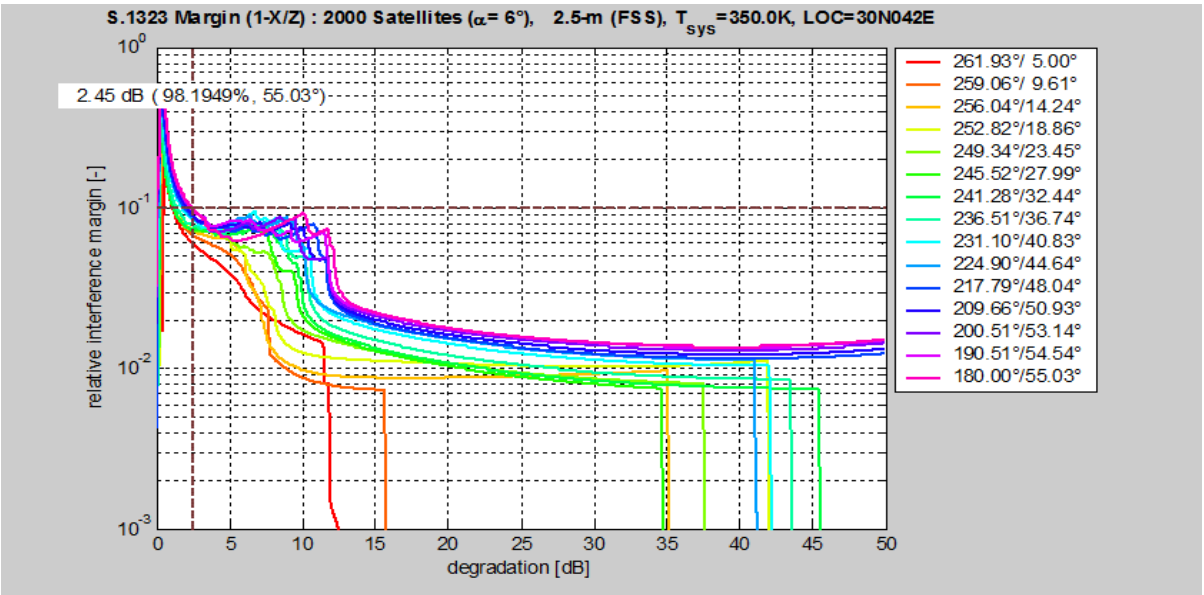

As illustrated in the examples above, using this approach to define an epfd mask results in significantly variable profiles dependent on each particular non-GSO constellation and reference GSO link location and elevation angle. This situation can result in spectrum inefficiencies. In the example scenario presented above, the sharing analysis represented by Recommendation ITU-R S.1323 demonstrates that for both systems, there is margin available to allow for more efficient sharing of the 50/40 GHz spectrum bands.

4.1.2 epfd curves based on Recommendation ITU-R S.1323 taking into account propagation losses on the interfering signal path

As previously described, atmospheric propagation losses can be significant in the 50/40 GHz band. The current Methodology A approach assumes that only the desired GSO link is attenuated by atmospheric propagation losses, but not the interfering signals. The analysis conducted in § 4.1.1 can be repeated using an approach where atmospheric propagation effects are also accounted for on the interfering path, as well as the wanted path. Figure A1-5 presents the results of such an analysis.

FIGURE A1-5

Per link convolution with interferer propagation losses 30N095W – 2000-SV Constellation

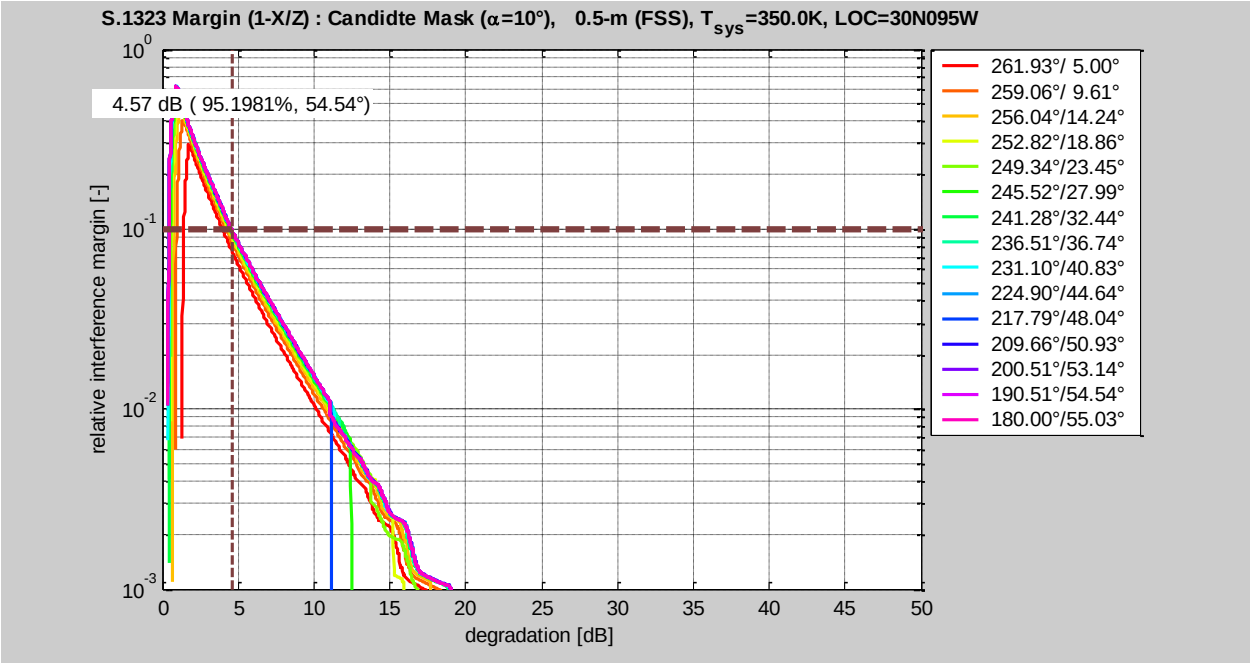

As can be seen from the analysis that includes propagation losses, when atmospheric propagation affects are accounted for on the interfering path, there is significant interference degradation margin available for the operation of both the non-GSO system and GSO network. In both cases assessed in §§ 4.1.1 and 4.1.2, the non-GSO system meets protection requirements being developed by the ITU-R. However, in the case of accounting for the additional atmospheric losses in the 50/40 GHz band, significant additional operating margin is available to the GSO links.

4.2 Sharing between non-GSO and GSO FSS systems using Recommendation ITU-R S.1323

Given the magnitude and wide variability of propagation losses in the 50/40 GHz frequency bands, a possible approach to sharing, given the limitations of the iterative approach described above, is to evaluate non-GSO to GSO FSS sharing based on calculations of aggregate epfd from proposed non-GSO constellations to reference GSO links. This approach would avoid the problems illustrated above of having epfd curves that fail the sharing criteria under Recommendation ITU-R S.1323 while

not exceeding the limit masks, or viceversa. This would allow for the most efficient use of FSS spectrum in the 50/40 GHz band that will enable both non-GSO systems and GSO networks to provide high-quality broadband satellite services. Under this sharing approach, the operation of non-GSO would be used to determine if a particular non-GSO constellation meets the GSO FSS protection criteria as described by Recommendation ITU-R S.1323, Methodology A.

4.3 Sharing between non-GSO and GSO FSS systems by allowing single system GSO unavailability increase allowances

As discussed above, the methodology to determine the epfd limits based on interference profiles is extremely dependent on the characteristics of the systems being evaluated. While epfd masks can be developed for individual systems, it is not spectrally efficient to define a single epfd mask that would allow all non-GSO system design types (LEO, HEO, MEO) to operate while assuring GSO protection. The study presented in this section discusses a possible regulatory mechanism for an alternative approach for non-GSO/GSO sharing that aims to maximize the spectral efficiency of use of the 50/40 GHz frequency bands. The objective of this study is to identify means to enable use of these bands by non-GSO systems for use of the orbit and spectrum resources in the 50/40 GHz frequency bands while ensuring GSO protection.

To facilitate sharing between non-GSO FSS systems in the 50/40 GHz frequency bands, the criteria for sharing should be defined by the maximum permissible level of interference into a wanted GSO FSS system. This permissible level is defined by ITU-R Recommendations and defines the aggregate interference caused by all non-GSO FSS systems into a GSO system. The study presented in this section apportions the aggregate interference into single entry permissible levels to be met by individual non-GSO FSS systems, taking into account the mechanisms by which all the interference sources cumulate.

In this methodology, each non-GSO system would be allocated a specific permissible level of interference, which is a portion of the overall aggregate allowable interference to each defined GSO reference link based on the time allowance for degradation based on *C*/*N* of the desired system. Figures A1-6 and A1-7 below show examples of unavailability increase that a single non-GSO system in the 50/40 GHz band can operate based on a specific single-system allowance. This analysis was conducted using worldwide GSO reference links. This analysis shows that while specifying a specific portion of the aggregate interference allowance to individual non-GSO systems, multiple other non-GSO can operate co-frequency in the bands identified under WRC-19 agenda item 1.6 while meeting similar or lower single entry unavailability allowances.

FIGURE A1-6

Unavailability increase from ITU-R defined reference links

47S063W ES 220 cm antenna
1.30% unavailability increase

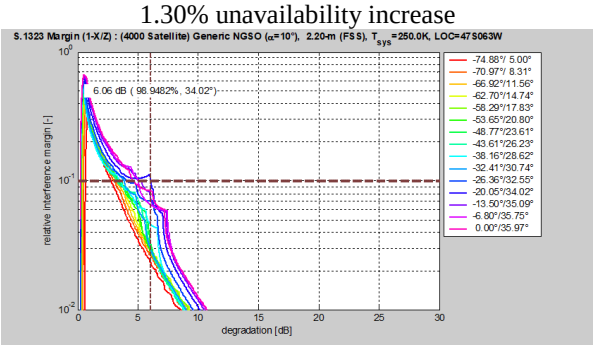

47S063W ES 45 cm antenna
1.98% unavailability increase

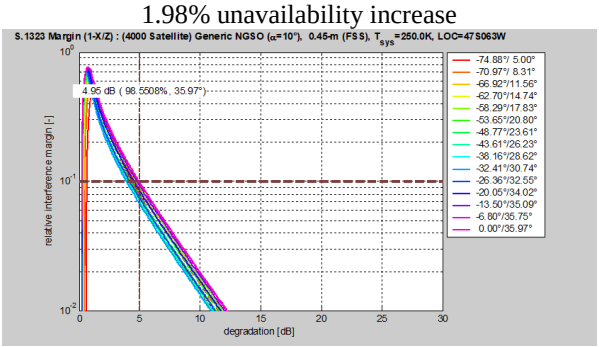

FIGURE A1-7

Unavailability increase from worldwide GSO reference links

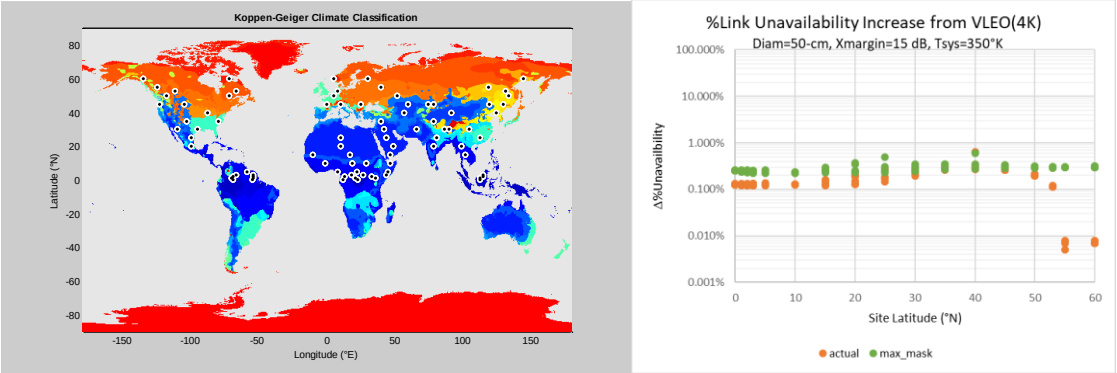

In addition to the single entry non-GSO system allowance, there is a need to provide a regulatory mechanism that would ensure protection of GSO FSS networks from the maximum aggregate interference levels produced by multiple non-GSO FSS systems in the frequency bands identified under WRC-19 agenda item 1.6. As described above, a single entry allowance for each individual non-GSO single-system contribution would be known based upon a requirement to provide a showing at the time of a bringing into use of the non-GSO system.

A key assumption in ITU-R Recommendations on allowable aggregate interference between non-GSO and GSO systems is that the time allowance for each interference entry are subdivided by the number of total systems. ITU-R studies have also confirmed that this worst-case bound on aggregate interference can be found by linear addition of the single-system contributions from each co-frequency non-GSO system. The ability to track the amount of single entry interference levels produced by any individual non-GSO system provides a method for evaluating that the aggregate limits are never exceeded.

A sample flow of the technical requirements to assure protections to GSO is presented in Fig. A1-8. Based on the analysis conducted in this study, this technical and regulatory process can be used as a basis for provided additional spectrum efficiency for FSS systems in frequency bands above 30 GHz. It may be useful to reflect this procedure in an ITU-R Recommendation with sample calculations.

FIGURE A1-8

Example flow of technical implementation of sharing implementation

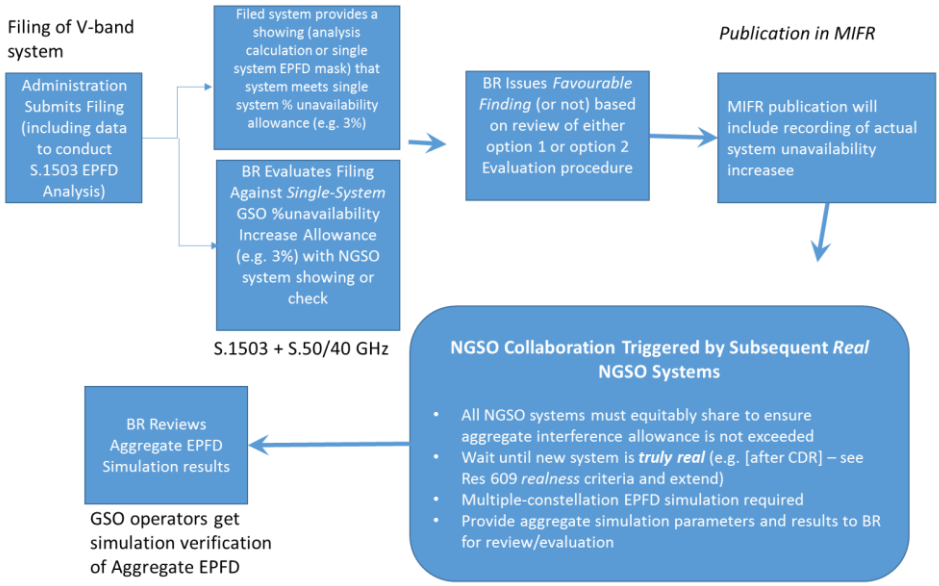

4.4 Sharing between non-GSO and GSO FSS systems by allowing single system GSO unavailability increase allowances

This section presents an example implementation of the procedures discussed in § 4.3 and shown graphically in Fig. A1-8. In this example implementation, it is assumed that a non-GSO network is operating based on the parameters presented in the section above and a second non-GSO system is planned to be operated. This section will present a comparison of the methodology as shown in Fig. A1-8 and compared to a similar methodology used in frequency bands below 30 GHz. For illustrative purposes, the first operational non-GSO system will be assumed to be based on a system similar to the one analysed in this study and will be referred to as "VLEO". The second representative non-GSO system will be based on the system studied in Study #2 and will be referred to as "VMEO".

The VLEO system, as shown in § 4.3 above, increases the link unavailability based on worldwide reference links by approximately ~1%. This value is safely below the proposed 3% allocation of a single-entry limit. The VLEO system would file their system and the provision of 0.98% unavailability use would be recorded.

A similar single-entry percent unavailability analysis was conducted for the VMEO system described in Study #2 below. The maximum unavailability increase from the VMEO system is approximately ~0.8%.

FIGURE A1-9

Unavailability increase from VMEO based on worldwide GSO reference links

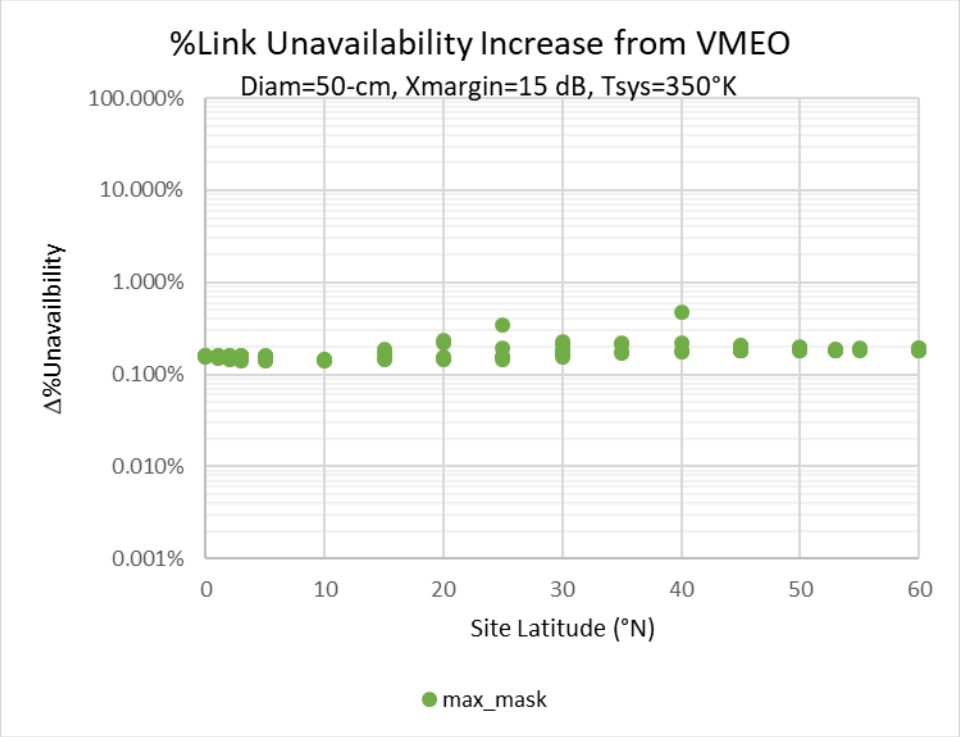

Once the VMEO system is of sufficient maturity as discussed in the process flow diagram in Fig. A1-8, the VLEO and VMEO systems would engage in coordination discussions. In this example, the single-entry contribution from VLEO was found to be ~1% unavailability increase and the contribution from VMEO was found to be ~0.8% unavailability increase. As previously described, the measurement of the aggregate impact of multiple non-GSO systems can be accounted for by the linear addition of total single entry epfd impacts from non-GSO systems. In this case, the addition of the two single-entry impacts would be ~1.8%, which is significantly less than the 10% aggregate

limit. The VLEO and VMEO systems would not need to directly engage in direct coordination and the total aggregate use of non-GSO systems would be notified to the BR as ~1.8%.

To illustrate this process, an analysis of the combined degradation effects from the VMEO and VLEO systems was conducted and the results are illustrated in Fig. A1-10. As can be seen, the combined results from these two systems results in an aggregate percent unavailability increase that is less than the sum of the percent unavailability increases from the individual systems. This is in large part due the differences in the non-GSO system geometries and the fact that the maximum degradation from each system does not occur in the same geographic region.

FIGURE A1-10

Unavailability increase from VLEO+VMEO based on worldwide GSO reference links

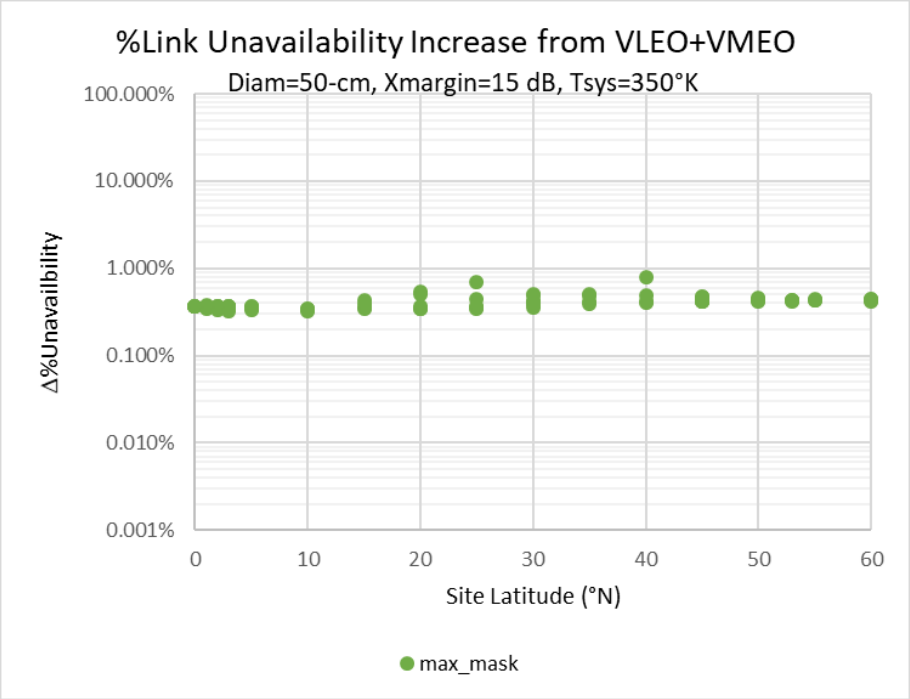

It is interesting to compare the results presented above to those found in Study #3, which compares the generation of epfd limit masks for VLEO and VMEO. In that study, it was found that the development of epfd masks for either VLEO or VMEO, results in inefficiencies for the other system. Further, it is found that if a mask was developed for one system, the other system would not meet the criteria of the other systems. However, when these results are plotted against the protection criteria as shown in Fig. A1-10, it is found that the two systems operating together use less than 1/10 of the interference budget allocated to non-GSO FSS systems.

5 Summary

The studies presented above show that sharing methodologies between non-GSO and GSO FSS systems based on defining epfd limit masks as was done in frequency bands below 30 GHz are extremely system dependent. It is important to develop regulations that facilitate maximizing the spectral efficiency of use of the 50/40 GHz FSS bands for all FSS systems. The analysis above presents sharing considerations that may be taken into account in these higher frequency bands, including technology considerations and propagation losses. Optimal use of the orbit and spectrum resources in the 50/40 GHz FSS bands requires a more equitable regulatory environment between GSO networks and non-GSO FSS systems than has been established in bands below 30 GHz in order

to take advantage of next generation satellite technology to provide high capacity broadband services, while utilizing benefits of both non-GSO and GSO satellite orbits.

As presented in the studies of this Annex, one sharing consideration that could be taken into account to allow a more flexible regulatory environment for non-GSO systems, while protecting GSO networks, is to apportion the allowable aggregate allowance for GSO systems to individual non-GSO systems. This regulatory methodology would allow for spectrally efficient operation of non-GSO systems by allowing each individual non-GSO system to define operations based on a single system unavailability allowance. This methodology would also allow for the tracking of aggregate interference as to ensure that GSO FSS systems are fully protected based on ITU-R defined protection levels.

Annex 2

Study #2 for the development for sharing between non-GSO FSS and GSO FSS in the 50/40 GHz frequency bands

1.1 Non-GSO FSS system

The non-GSO system was an equatorial circular orbit system with parameters similar to the O3B-B satellite system but scaled to the 50/40 GHz band. The reference for this configuration was taken from IFIC 2713 for O3B-B with orbit parameters as in Table A2-1.

TABLE A2-1

Non-GSO system orbit parameters

Height (km)	8062
Number of satellites	24
Inclination angle (degree)	0
Eccentricity	0

The non-GSO satellite antenna characteristics were as in Table A2-2.

TABLE A2-2

Non-GSO system satellite antenna properties

Number of beams per satellite	10
Dish size (m)	0.3 (1)
Efficiency	0.65
Gain pattern	Rec. ITU-R S.1528 Ls = –25
Noise temperature (K)	600

(1) Note that the filing parameters equated to a dish size of 0.4 m.

For the non-GSO Earth station (ES), a number of antenna sizes could be conceived and the filing contains a range of typical ES. For the purposes of this study, a single antenna size was to be considered. A number of factors can be considered when selecting the appropriate size: while the trend is for smaller antennas, there is likely to be significant rain fade at these higher frequencies and so it might be beneficial to avoid the very smallest size. Hence, it was decided to baseline on a 1.8 m dish, similar to this one: http://www.o3bnetworks.com/wp-content/uploads/2015/02/O3b_General-Dynamics_1.8m-Dual-Tracking-Antenna.pdf.

The parameters selected are shown in Table A2-3:

TABLE A2-3

Non-GSO system ES antenna properties

Dish size (m)	1.8
Efficiency	0.65
Gain pattern	Rec. ITU-R S.580-6 APL [1]
Noise temperature (K)	300

[1] APL stands for Antenna Pattern Library and is the ITU-R's implementation of this Recommendation.

The following frequencies were used for the non-GSO and GSO systems:

TABLE A2-4

50/40 GHz band frequencies

Uplink frequency (GHz)	48
Downlink frequency (GHz)	38

As noted in the section below, these frequency bands will involve significant rain fades and it is likely that automatic transmit power control (ATPC) will be one of the techniques used to compensate for deep fades. This means that rather than a single transmit power figure, three values must be provided:

1 Minimum transmit power

2 ATPC range

3 Target receive signal level.

The following approach was used for the transmit power:

– The ATPC range was taken to be 10 dBW to be consistent with the non-GSO system (as described below).

– The maximum ES transmit power was taken to be 17 dBW, taken from the highest power from the GD reference sheet plus 1 dBW.

– Hence the minimum transmit power was 7 dBW.

The power densities and e.i.r.p. are shown in Table A2-5, assuming a carrier bandwidth of 115 MHz.

TABLE A2-5

Non-GSO system powers and e.i.r.p.

Power, peak gain and e.i.r.p.	UL	DL
Minimum TX power (dBW)	7	7
Maximum TX power (dBW)	17	17
Maximum TX power density (dBW/Hz)	–63.6	–63.6
Peak gain (dBi)	56.9	39.7
Minimum e.i.r.p. (dBW)	63.9	46.7
Maximum e.i.r.p. (dBW)	73.9	56.7

For the target receive level a number of techniques could be used. If a single modulation were used then the *C/(N+I)* required to achieve a certain BER could be used together with the noise and margin for interference. But it is likely that the 50/40 GHz band systems will use adaptive modulation whereby if the wanted signal is reduced then the modulation would be adjusted accordingly.

However as the ATPC requires a target, it is suggested that a baseline modulation could be used to derive the receive signal threshold, accepting that the system could go below this point and still provide a service if faded. The following methodology was therefore used:

$$C_{Target} = T\left(\frac{C}{N+I}\right) + M_i + 10log_{10}(kTB) \quad (1)$$

where:

$$T\left(\frac{C}{N+I}\right) = 10.5\ dB$$

$$M_i = 1\ dB$$

TABLE A2-6

ATPC target signal levels

Uplink target C (dBW)	–108.7
Downlink target C (dBW)	–111.7

The ES were deployed across major landmasses: while some traffic is expected at sea or in the air, it is considered these will be secondary markets. In total 100 non-GSO ES were deployed with a bias towards the equator as that was considered to have more critical geometry with respect to the GSO arc. However, in order to protect the GSO arc it was necessary to avoid locating ES directly to the equator. It was noted that many of the locations considered would have high rainfalls and hence be susceptible to fading.

At the 50/40 GHz band the ES antenna beamwidths are significantly narrower than at Ku or Ka band. Hence, it is possible to operate non-GSO very close to the equator and with a tracking strategy that points very close to the GSO arc.

The following tracking strategy was used:

– Minimum elevation of $\varepsilon_0 = 20°$
– GSO avoidance angle $\alpha_0 = 1°$
– The highest available elevation satellite was selected
– The satellite was assumed to point a beam directly at the ES.

This permitted operation on non-GSO ES within about 1.7° of the equator, with resulting deployment is as in Fig. A2-1.

FIGURE A2-1

Deployment of non-GSO ES

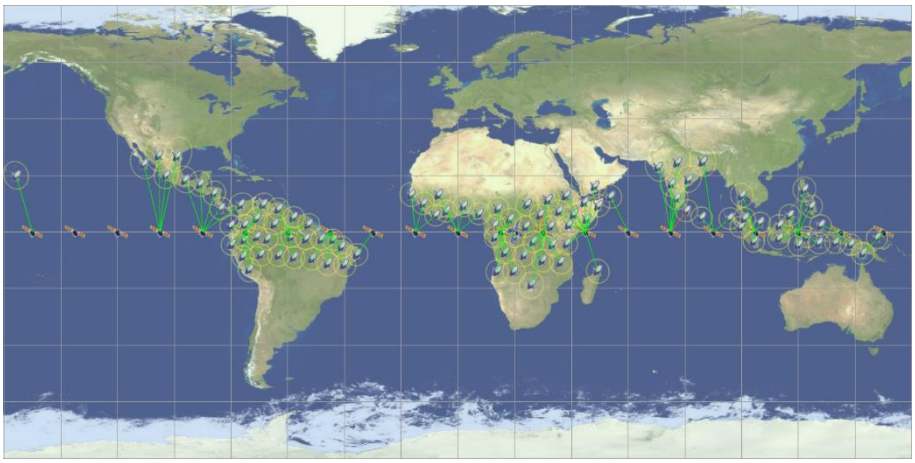

Example link budgets (UL and DL) for one ES are shown in Table A2-7.

TABLE A2-7

Example link budgets at 0 dB gain contour

Example link budget	UL	DL	Units
Frequency	48	38	GHz
Bandwidth	115	115	MHz
Transmit power	7	7	dBW
Transmit peak gain	56.9	39.7	dBi
Transmit relative gain contour	0.0	0.0	dB
Path loss	207.5	210.7	dB
Freespace	204.7	202.7	dB
676 dry	0.9	0.2	dB
676 water	0.7	0.5	dB
618 rain	1.1	7.3	dB
Receive peak gain	41.7	54.9	dBi
Receive relative gain contour	0.0	0.0	dB
Receive feeder loss	0.0	0.0	dB
C (signal strength)	−101.9	−109.1	dBW
N	−120.2	−123.2	dBW
C/*N*	18.3	14.1	dB

These link budgets are an example for one of the links from the non-GSO satellite to non-GSO ES for one time step in the simulation. The rain rate and percentage of time is likely to vary between non-GSO ES and time step respectively and be different from those used in the GSO link budget in Table A2-11.

When the simulation was run for 24 hours, this gave average availability over all time steps and all non-GSO ES of 99.2% for the UL (with range from 98.6% to 99.9%) and 99.5% for the DL (with range from 99.2% to 99.9%). Actual service availability would be higher due to adaptive modulation.

1.2 GSO system parameters

A similar approach was used for the GSO system parameters as for the non-GSO above.

The ES parameters are given in Table A2-8.

TABLE A2-8

GSO ES parameters

Dish size (m)	2.4
Efficiency	0.65
Gain pattern	Rec. ITU-R S.1428-1
Noise temperature (K)	300

The dish size was selected as it was one of the GSO ES antenna diameters that was identified in other documents and was shown to produce link budgets that could provide a service with a reasonable availability. Other dish sizes should also be considered.

The satellite antenna parameters are given in Table A2-9.

TABLE A2-9

GSO satellite spot beam parameters

Direction	**RX = UL**	**TX = DL**
Peak gain (dB)	52	50
Beamwidth (degrees)	0.445	0.561
Gain pattern	Rec. ITU-R S.672-4 Ls = −25	Rec. ITU-R S.672-4 Ls = −25
Noise temperature (K)	600	n/a

The GSO ES was assumed to be located at the edge of the GSO RX beam's −3 dB footprint. The transmit and powers were as given in Table A2-10 assuming a 100 MHz carrier.

TABLE A2-10

GSO satellite spot beam parameters

Direction	**UL**	**DL**
Minimum TX power (dBW)	10.0	10.0
Maximum TX power (dBW)	20.0	20.0
Maximum TX power density (dBW/Hz)	−60.0	−60.0
Peak gain (dBi)	59.8	52.0
Minimum e.i.r.p. (dBW)	69.8	62
Maximum e.i.r.p. (dBW)	79.8	72.0
ATPC target (dBW)	−109.3	−112.3

The GSO systems were located at low latitudes as it was considered that this would be near the worst case geometry (WCG) with the GSO ES co-located with the non-GSO ES. The locations are shown in Fig. A2-2.

FIGURE A2-2

Location of GSO systems

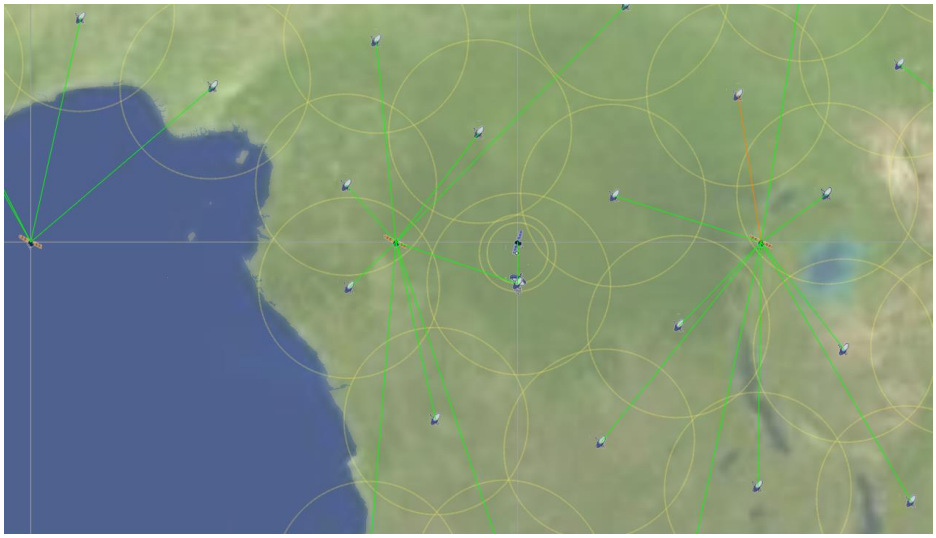

Note that this would also be where there could be significant rain fades.

The resulting link budgets are shown in Table A2-11.

TABLE A2-11

GSO link budgets

Direction	UL	DL
Frequency (GHz)	48.0	38.0
Receive temperature (K)	600.0	300.0
Bandwidth (MHz)	100.0	100.0
TX power (dBW)	20.0	20.0
TX peak gain (dBi)	59.8	50.0
TX relative gain contour (dB)	0.0	−1.9
Total path loss (dB)	238.1	238.2
RX peak gain (dBi)	52.0	57.7
RX relative gain contour (dB)	−3.0	0.0
RX feed loss (dB)	0.0	0.0
RX wanted signal (dBW)	−109.3	−112.3
Rec. ITU-R P.676 dry air loss (dB)	0.8	0.2
Rec. ITU-R P.676 water vapour loss (dB)	0.6	0.4
Rec. ITU-R P.618 rain loss (dB)	19.5	22.4
Rec. ITU-R P.618 percentage (%)	0.9	0.6
Rec. ITU-R P.618 rain rate (mm/h)	76.8	76.8
Wanted signal *C*/*N* (dB)	11.5	11.5

The resulting availabilities were 99.1% for the UL and 99.4% for the DL with 1 dB of margin for interference. Actual service availability would be higher due to adaptive modulation.

1.3 Propagation models

The following propagation models were used for the baseline analysis.

TABLE A2-12

Propagation models

Radio path	Propagation models
Wanted	Rec. ITU-R P.525 (free space) Rec. ITU-R P.676-10 (gaseous attenuation) Rec. ITU-R P.618-12 (rain fade)
Interfering	Rec. ITU-R P.525 (free space)

This is consistent with the definition of epfd which is effectively clear air, i.e.:

$$epfd = e.i.r.p. - L_s + G_{rel} \quad (2)$$

Where L_s is the spreading loss and G_{rel} the receive relative gain. Further runs considered the impact of alternative propagation models for the interfering signal.

It was noted that availability for both the GSO and non-GSO systems were less than 99.9% and the key factor involved was the increased rain fade for the frequencies involved. For the example consider the following parameters for a high-rain area near the equator:

Rain rate: 47 mm/hour for 0.01% of an average year

Elevation angle: 76°

For these parameters the rain fade predicted by Recommendation ITU-R P.618-12 is as shown in Fig. A2-3.

FIGURE A2-3

Rec. ITU-R P.618-12 rain fade at the 50/40 GHz band

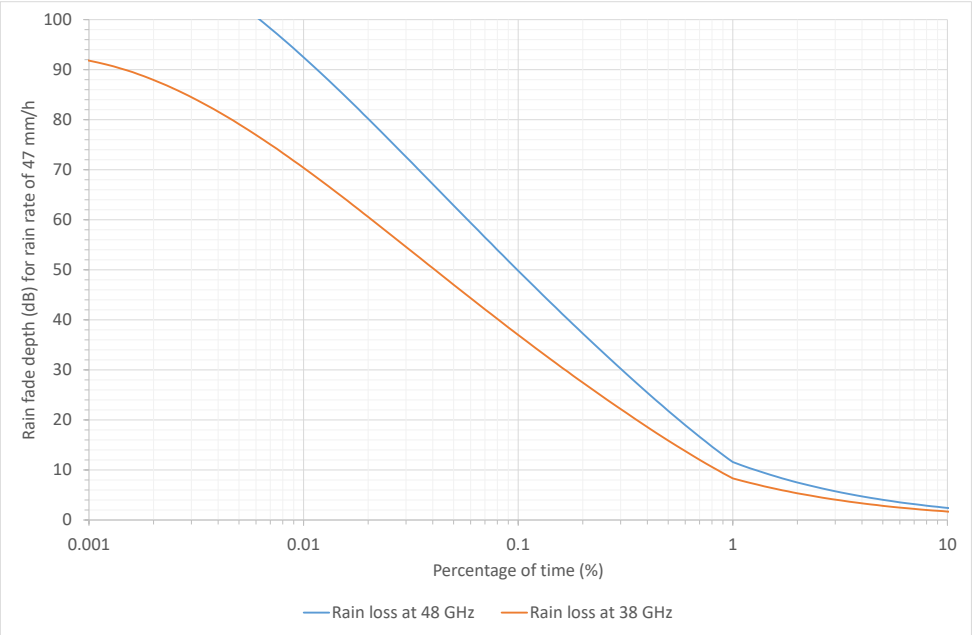

It can be seen that there can be extremely large rain fades which would make closing the link infeasible for 100% of the time. Note that Recommendation ITU-R P.618-12 is valid for "frequencies up to 55 GHz".

The Recommendation also describes a method to calculate the noise rise due to re-radiated energy during rain, but this has not been modelled in these simulations.

During the analysis, rain rates were taken from Recommendation ITU-R P.837-6.

1.4 Time step calculation

It is necessary to ensure that the time step is sufficiently fine that there are enough samples within the main beam for the statistics to be stable. This can be calculated using the parameter N_{hit} which identifies how many samples are required. In Recommendation ITU-R S.1503-2 this is set as:

$$N_{hit} = 16$$

From this and the geometry involved it is feasible to calculate the time step required for the uplink (UL) and downlink (DL) directions, as in Table A2-13.

TABLE A2-13

Time step calculation

Case	epfd(down)	epfd(up)
Frequency (GHz)	38	48
ES type	GSO	non-GSO
Dish size (m)	2.4	1.8
Beamwidth (degree)	0.2303	0.2431
Height (km)	8 062	8 062
N_{hit}	16	16
Time step (s)	0.4	0.4

When undertaking an assessment against the thresholds in RR Article **22** it is also necessary to have sufficient samples to give statistics at the lowest percentage of time specified in the tables. However, as there are no thresholds for the 50/40 GHz band currently in the Radio Regulations the run duration was taken from the repeat period of the constellation. For a satellite system at a height of 8 062 km the time for a satellite to return to the same position with respect to the Earth can be calculated as in Table A2-14.

TABLE A2-14

Run length calculation

Orbit repeat period (s)	1.73E+04
Earth sidereal period (s)	86164.09
Satellite mean motion (rad/s)	3.64E-04
Earth mean motion (rad/s)	7.29212E-05
Repeat time (s)	21 597.5

Therefore, the run number and time step size were as in Table A2-15.

TABLE A2-15

Run time step and number of time steps

Time step (s)	0.4
Number of time steps	53 994

1.5 Statistics gathered

The following statistics were gathered for the GSO systems uplink and downlink.

TABLE A2-16

Run statistics gathered

Interference metric (*X*)	**epfd**	***C*/(*N*+*I*)**	***C*/*N***	***I*/*N***
Reference bandwidth	1 MHz	n/a	n/a	n/a
CDF resolution	0.1 dB	0.1 dB	0.1 dB	0.1 dB
Threshold *T*(*X*)	n/a	10.5 dB	10.5 dB	–10 dB

1.6 Results

1.6.1 *I*/*N* and epfd cumulative distribution functions

The plots below show the CDFs of *I*/*N* and epfd into the GSO UL and DL. These CDFs use the worst-case geometry for the GSO system.

FIGURE A2-4

CDF of *I*/*N* into the GSO UL and DL

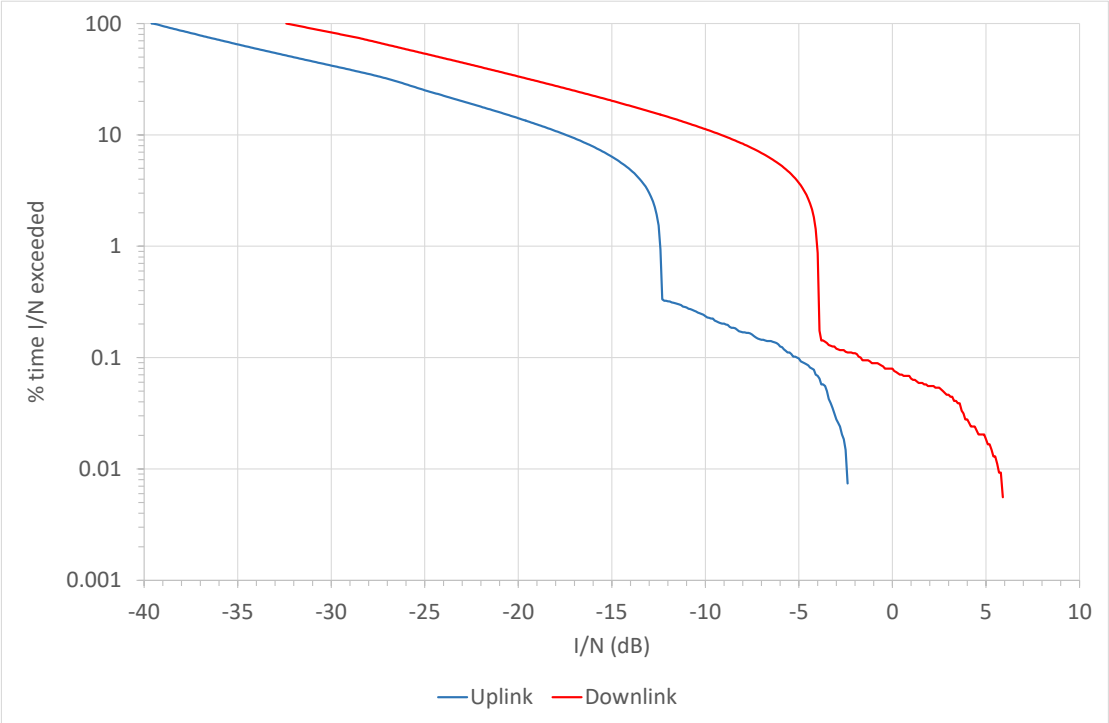

The $T(I/N)$ was exceeded for 0.2% of time for the UL and 11.3% of time for the DL.

FIGURE A2-5

CDF of epfd into the GSO UL and DL

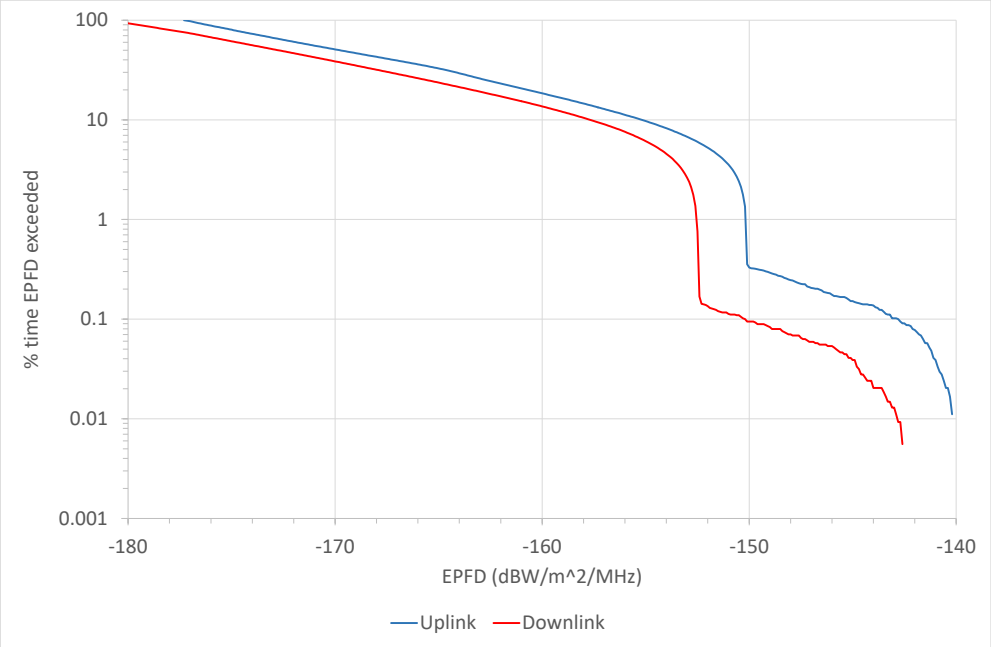

It is noted that the maximum epfd values of around −140 dBW/m^2/MHz would be similar to thresholds in RR Article **22** for Ka band.

1.6.2 Convolution of interference and wanted signals

The degradation of the *C*/*N* curve due to interference to *C*/(*N*+*I*) was also generated for the GSO UL and DL directions by calculating the wanted and interfering signals for each sample (which had the effect of convolving the two distributions), as shown in Figs A2-6 and A2-7.

FIGURE A2-6

CDF of *C*/*N* and *C*/(*N*+*I*) for the GSO UL

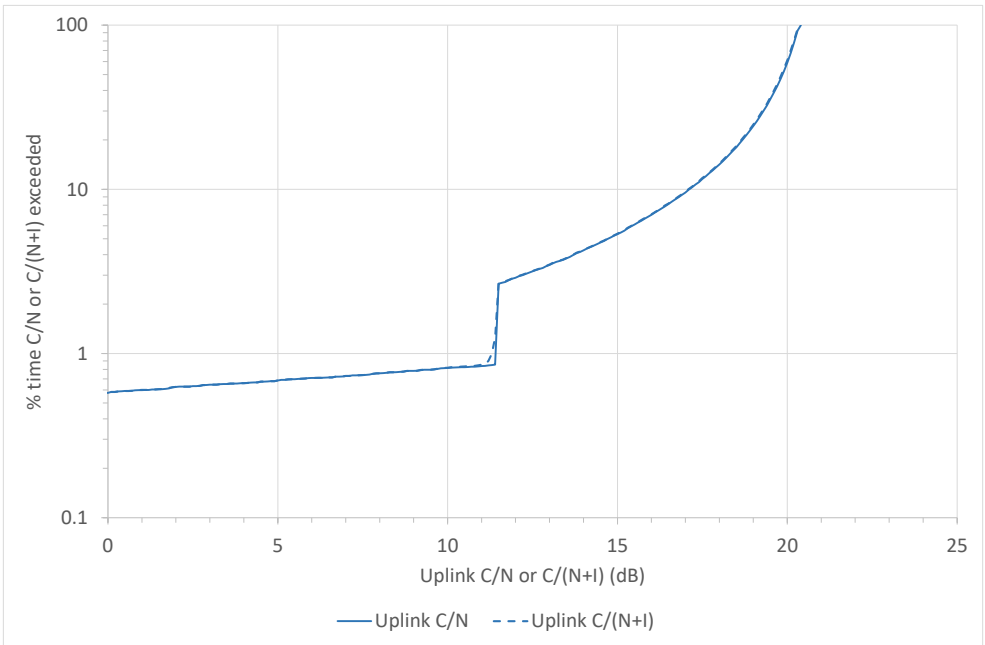

FIGURE A2-7

CDF of *C*/*N* and *C*/(*N*+*I*) for the GSO DL

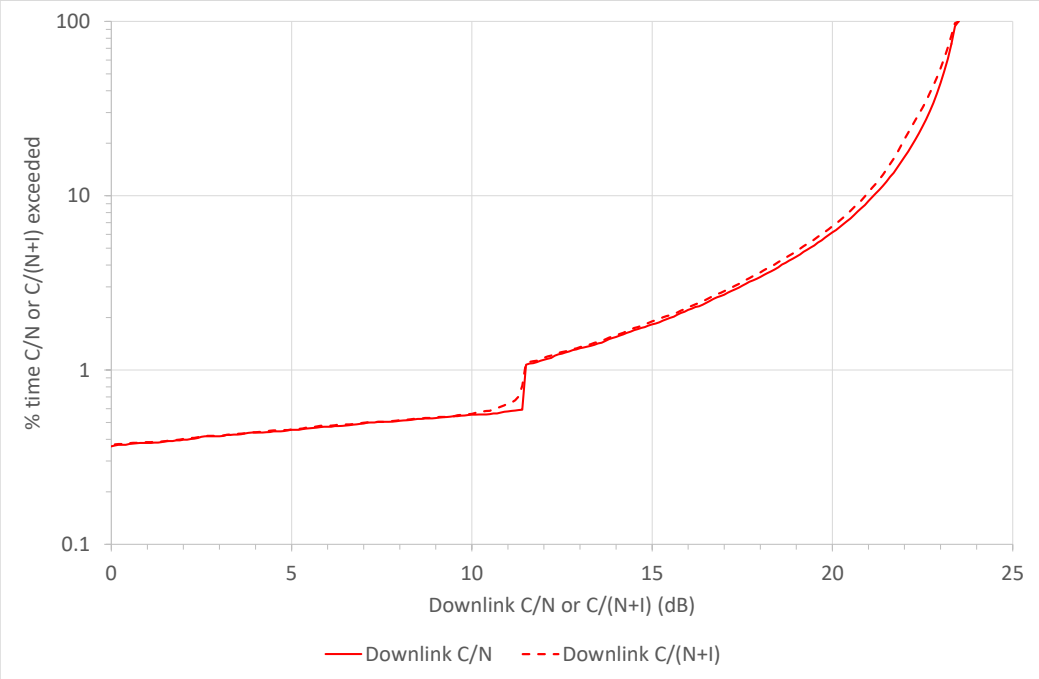

The addition of interference into the GSO system resulted in a decrease in availability i.e. an increase in unavailability as in Table A2-17.

TABLE A2-17

Increase in unavailability

Direction	*UL*	*DL*
Unavailability with no interference (%)	0.826	0.556
Unavailability with interference (%)	0.832	0.582
Increase in unavailability (%)	0.006	0.026
Percentage increase unavailability (%)	0.673	4.667

It can be seen that the unavailability targets in Recommendation ITU-R S.1323 of 10% increase are met, suggesting that these could be acceptable epfd levels. However, it is noted that these levels are the results from a single non-GSO FSS network and it would also be necessary to consider aggregation affects. This could take into account different constellation types rather than solely equatorial circular orbit.

1.7 Discussion

1.7.1 *I*/*N* vs. epfd

It was noted that the highest *I*/*N* was highest for the DL while the epfd was highest for the UL and the reasons for this was investigated further.

The epfd equation can be written as:

$$EPFD = e.i.r.p. - L_s + G_{rel} \quad (3)$$

where L_s is the spreading loss and G_{rel} the receive relative gain (relative to peak gain), and it is noted that the spreading loss is dependent upon distance, *d*, but not frequency, *f*.

Therefore the difference between the *UL* and *DL* epfd is therefore:

$$\Delta\text{epfd} = (e.i.r.p._{UL} - e.i.r.p._{DL}) - 20log_{10}\left(\frac{d_{UL}}{d_{DL}}\right) + \left(G_{rel,UL} - G_{rel,DL}\right) \quad (4)$$

The *I*/*N* equation can be written as:

$$\frac{I}{N} = e.i.r.p. - L_{fs} + G_{max} + G_{rel} - 10log_{10}(kTB) \quad (5)$$

Here L_{fs} is the free space path loss which depends upon both distance and frequency, *T* is the receive temperature in Kelvin, *B* the bandwidth and *k* Boltzmann's constant.

Then the difference between *UL* and *DL I/N* is:

$$\frac{\Delta I}{N} = (EIRP_{UL} - EIRP_{DL}) - 20log_{10}\left(\frac{d_{UL}}{d_{DL}}\right) - 20log_{10}\left(\frac{f_{UL}}{f_{DL}}\right) + \left(G_{max,UL} - G_{max,DL}\right) + \left(G_{rel,UL} - G_{rel,DL}\right) - 10log_{10}\left(\frac{T_{UL}}{T_{DL}}\right) \quad (6)$$

Then the delta between the epfd and *I/N* differences is:

$$\Delta\text{epfd} - \frac{\Delta I}{N} = 20log_{10}\left(\frac{f_{UL}}{f_{DL}}\right) - \left(G_{max,UL} - G_{max,DL}\right) + 10log_{10}\left(\frac{T_{UL}}{T_{DL}}\right) \quad (7)$$

This is consistent with the results as in Table A2-18.

TABLE A2-18

Differences *UL*/*DL* between *epfd* and *I*/*N*

Highest	***UL***	***DL***
Frequency (GHz)	48	38
GSO G_{max} (dBi)	52.0	57.7
GSO RX temperature (K)	600	300
Maximum *epfd* (dBW/m^2/MHz)	–140.1	–142.6
Maximum *I*/*N* (dB)	–2.4	6.0

This shows that the delta between the *epfd* and *I*/*N* differences should be around 10.8 dB.

This is a useful sanity check and also identifies the key differences between the *epfd* and *I*/*N* results, namely the {frequency, peak gain, noise temperature} parameters. In this case the most significant factor was the higher peak gain on the GSO ES antenna compared to the GSO satellite antenna.

1.7.2 Propagation and correlation

It is noted that at the 50/40 GHz band there can be extremely high rain fades and hence modelling propagation loss accurately is important. A number of factors have to be included, in particular:

1 Fading of the wanted and interfering signals due to rain loss;

2 Variation in transmit power of wanted and interfering signals due to power control adjusting to rain loss;

3 Correlation between propagation loss between wanted and interfering paths.

The last of these is shown in Fig. A2-8, considering interference from a non-GSO FSS systems into a GSO downlink:

FIGURE A2-8

Rain loss on wanted and interfering paths

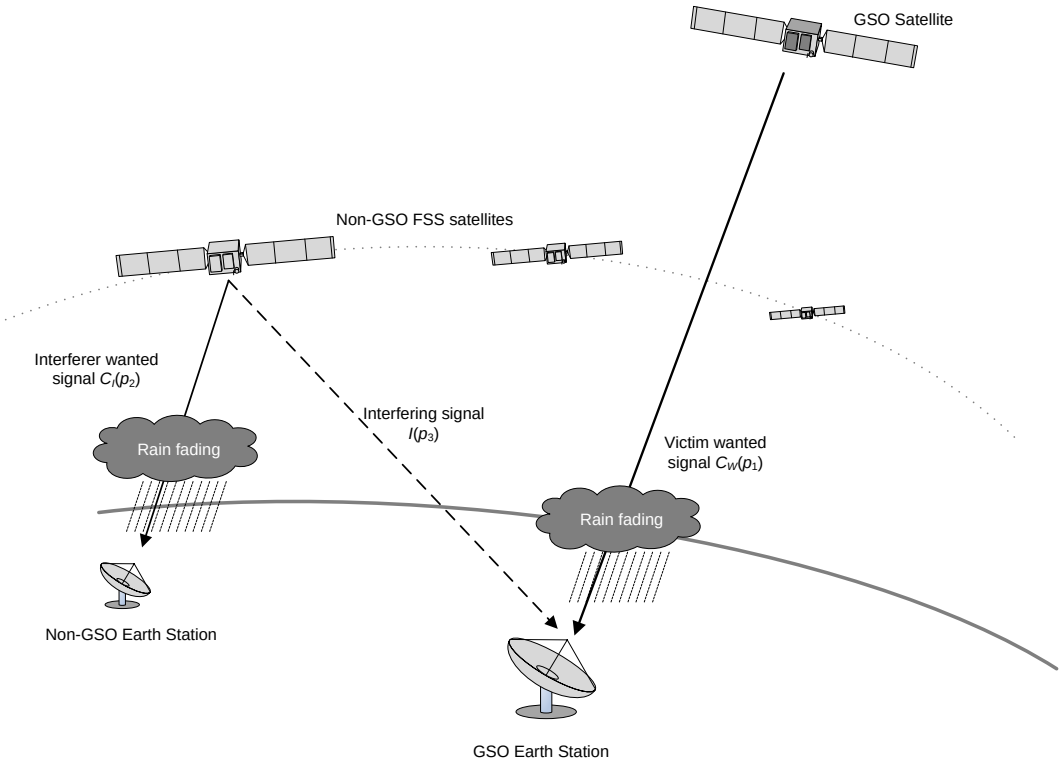

Factors to consider in modelling include:

1 Fading of GSO DL wanted signal due to rain fade.

2 Increase in interfering satellite's transmit power for the non-GSO DL.

3 Decrease in interfering signal due to rain fade around the GSO ES.

When using the rain fade model in Recommendation ITU-R P.618 it is necessary to select a percentage of time to use for each path, namely $\{p_1, p_2, p_3\}$. A number of options could be considered:

– Do not include rain fade on the interfering link: this could be considered a worst case.

– Assume rain fade on the wanted and interfering links are not correlated, so that $\{p_1, p_2, p_3\}$ are selected independently.

– Assume rain fade on the wanted and interfering links are correlated, so that $p_1 = p_3$ but that p_2 is selected independently.

These assumptions can have significant impact on the results, as shown in Table A2-19.

TABLE A2-19

Impact on interfering propagation model on the increase in unavailability

Propagation models used for interfering path	P.525	P.525 + P.676	P.525 + P.676 + P.618 uncorrelated	P.525 + P.676 + P.618 correlated
Unavailability with no interference (%)	0.556	0.556	0.593(1)	0.605(1)
Unavailability with interference (%)	0.582	0.578	0.606	0.605
Increase in unavailability (%)	0.026	0.022	0.013	0.000
Percentage increase unavailability (%)	4.667	4.000	2.156	0.000

(1) There was some variation in this figure between runs due to the sequence of random numbers being used differently. Longer runs showed a convergence towards an unavailability of around 0.59%.

This is a topic that could benefit from further consideration and analysis. Two approaches could be considered:

a) assume maximum e.i.r.p. for the non-GSO system PFD and e.i.r.p. masks: this will result in higher levels of epfd in RR Article **22**;

b) allow the e.i.r.p. and pfd masks in RR Appendix **4** to be exceeded as part of a power control mechanism as for Recommendation ITU-R S.524: this would result in lower levels of epfd in RR Article **22**.

2.1 Non-GSO system

The non-GSO system parameters considered were derived from Study #2; it is an equatorial circular orbit system with parameters similar to the O3B-B satellite system but scaled to the 50/40 GHz bands.

The automatic transmit power control (ATPC) was not considered in the simulation and as a consequence, the transmit power of the non-GSO system was adjusted. Other than the change in the transmit power, the other parameters remain the same as Study #2. The revised power and e.i.r.p. levels are shown below.

TABLE A2-20

Non-GSO system power and e.i.r.p. levels

Maximum transmit power (dBW)	21
Maximum transmit power density (dBW/Hz)	−59.6
Satellite transmit peak gain (dBi)	39.7
Maximum downlink e.i.r.p. (dBW)	60.7

Example link budget for the downlink of one non-GSO earth station is shown in Table A2-21.

TABLE A2-21

Example link budget at 0 dB gain contour for a non-GSO earth station

Example link budget	DL
Frequency (GHz)	38
Bandwidth (MHz)	115
Transmit power (dBW)	21
Transmit peak gain (dBi)	39.7
Transmit relative gain contour (dB)	0.0
Path loss (dB)	225.8
Receive peak gain (dBi)	55.2
Receive relative gain contour (dB)	0.0
Receive feeder loss (dB)	0.0
C (signal strength) (dBW)	–109.9
N (dBW)	–123.2
C/*N* (dB)	13.3

2.2 GSO system parameters

The GSO parameters were derived from ITU documentation (Annex 13). The links were considered in this study and the parameters are summarized in the Tables below.

For the forward link, the total link performance was dominated by the downlink. Therefore the simulation was run only in the downlink direction.

TABLE A2-22

Forward link (Gateway to user) parameters

GSO Parameters	Values
Frequency (GHz)	38
Carrier size (MHz)	500
Satellite transmit gain(dBi)	49.8
Spot beamwidth (degrees)	0.5737
Satellite roll-off pattern	ITU-R S.672-4 Annex 1 $L_S = -25$
Satellite transmit power (dBW)	29.7
Receive wanted signal (dBW)	−109.3
Earth station Longitude, Latitude (North, East)	(3.13, 101.6)
Satellite longitude (East)	100.3
e.i.r.p. (dBW)	79.5
Frequency (GHz)	38
Path loss (dB)	233.2
Earth station antenna size (m)	0.75
Earth station antenna gain(dBi)	47.6
Relative contour from beam peak (dB)	−3
Wanted signal *C*/*N* (dB)	5.6

The resulting availability for the above Table A2-22 is approximately 98.6%. If adaptive modulation is used, the actual service availability would be higher.

The receiving earth station is co-located with the non-GSO earth station at the centre of the non-GSO satellite spot beam. The GSO earth station location has significant rain fades but is slightly outside of the worst-case geometry (WCG) as the minimum alpha at this location is around 1.9° which is in the side lobe of the GSO earth station antenna.

This study does not utilise automatic transmit power control (ATPC) for the simulation since the GSO links had not considered ATPC

FIGURE A2-9

Location of GSO earth station

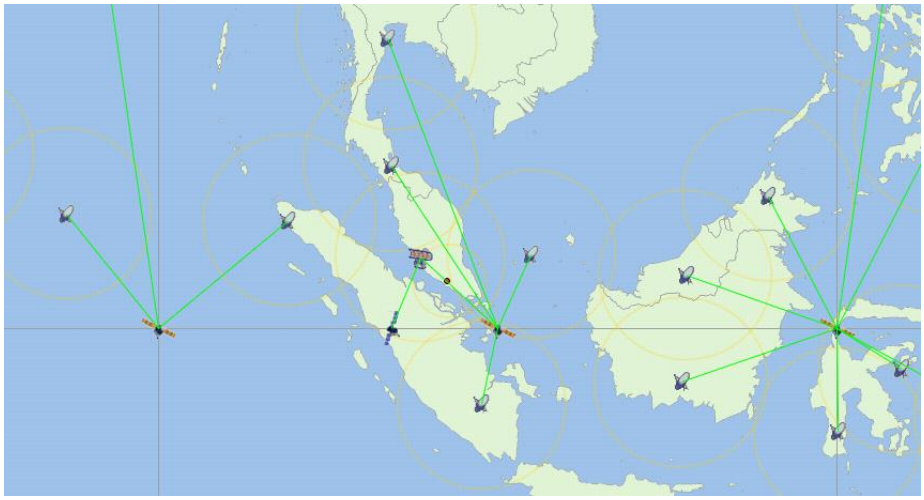

2.3 Propagation models

The following propagation models were used for the baseline analysis. Compared to the original Study 2, Recommendation ITU-R P.840 was included in the simulation since attenuation due to clouds and fog is significant in the 50/40 GHz bands.

Recommendation ITU-R P.525 (free space)

Recommendation ITU-R P.676-10 (gaseous attenuation)

Recommendation ITU-R P.618-12 (rain fade)

Recommendation ITU-R P.840-7 (cloud and fog)

The rain rates for the simulation were taken from Recommendation ITU-R P.837-6. Table A2-23 depicts the different types of path losses experienced by the GSO link.

TABLE A2-23

Example of path losses for the GSO link in the downlink

Path loss (dB)	232.6
Free space (dB)	215.1
676 dry (dB)	12.3
676 water (dB)	0.2
618 rain (dB)	12.3
840 cloud and fog (dB)	4.5

2.4 Description of simulation

The study aims to assess the amount of allowable interference from a single non-GSO system into a GSO network by assessing the impact of the non-GSO interference on the unavailability of the GSO link. The Visualyse software was used to perform these simulations.

The short-term interference allowance from non-GSO systems to GSO networks is assumed to be at most 10% of the time allowance for degradation exceeding the minimum short-term performance objectives, in terms of *C*/*N* value. The 10% increase in unavailability of the GSO link is an aggregate interference from all non-GSO systems and the simulation looks at the suitable percentage of unavailability to be apportioned to a single non-GSO system.

To assess the impact on unavailability, Visualyse was used to calculate the *C*/*N* and *C*/(*N*+*I*) percentage of bad steps which were then used to derive these values:

– The percentage of unavailability without interference = $\left(\frac{p2-p1}{p1}\right) * 100$

– The percentage of unavailability due to interference = $\left(\frac{p2-p1}{p2}\right) * 100$

where:

$p1$: unavailability of link due to rain fading alone:

$$p1 = p[C/N < T(C/N)]$$

$p2$: unavailability of link due to rain fading and interference:

$$p2 = p[\ C/(N+I) < T(C/N)]$$

The threshold used for the short-term interference is $T(C/N)$ = 4.7 dB.

For the sake of comparison, the simulations are done for three scenarios:

– Scenario 1: No rain fade is experienced by the interfering path

– Scenario 2: Wanted and interfering propagation paths are not correlated

– Scenario 3: Wanted and interfering propagation paths are correlated

In addition, the following statistics were gathered for the GSO system downlink:

TABLE A2-24

Run statistics gathered

Interference metric (X)	*C*/(*N*+*I*)	*C*/*N*
Reference bandwidth	n/a	n/a
CDF resolution	0.1 dB	0.1 dB
Threshold T(X)	4.7 dB	4.7 dB

2.5 Results of Simulation

2.5.1 Calculations of the impact of the non-GSO system on the unavailability of the GSO link

Scenario 1: No rain fade is experienced by the interfering path

The key outputs of the simulation are shown in the watch window below:

FIGURE A2-10

Percentage of bad steps of *C*/*N* and *C*/(*N*+*I*) for scenario 1

Variable	Value
GSO links.GSO DL.Statistics.C/(N+I) statistics.Percentage bad steps	1.316789
GSO links.GSO DL.Statistics.C/N statistics.Percentage bad steps	1.303824

Scenario 2: Wanted and interfering propagation paths are not correlated

The key outputs of the simulation are shown in the watch window below:

FIGURE A2-11

Percentage of bad steps of *C*/*N* and *C*/(*N*+*I*) for scenario 2

Variable	Value
GSO links.GSO DL.Statistics.C/(N+I) statistics.Percentage bad steps	1.313085
GSO links.GSO DL.Statistics.C/N statistics.Percentage bad steps	1.303824

Figure A2-12 shows the plots of the ITU-R P.618 rain fade for the wanted GSO link and worst interferer against time.

FIGURE A2-12

Rain fades of the wanted and worst interferer are not correlated

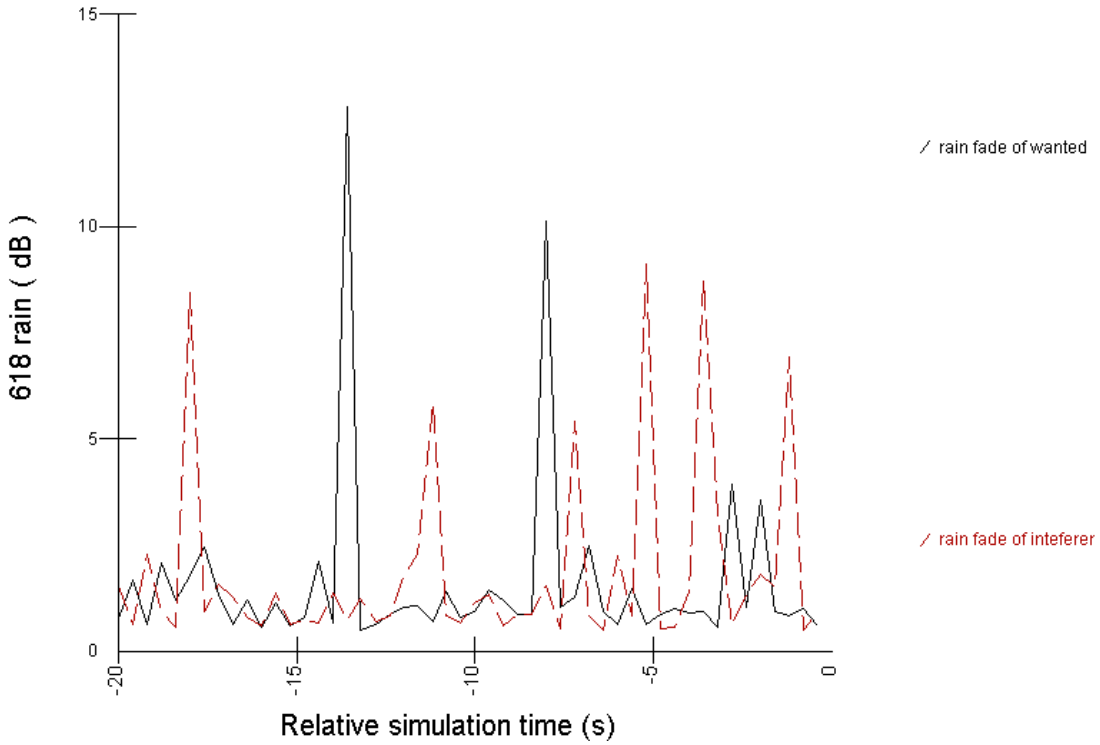

Scenario 3: Wanted and interfering propagation paths are correlated

The key outputs of the simulation are shown in the watch window below.

FIGURE A2-13

Percentage of bad steps of *C*/*N* and *C*/(*N*+*I*) for scenario 3

Variable	Value
GSO links.GSO DL.Statistics.C/(N+I) statistics.Percentage bad steps	1.277896
GSO links.GSO DL.Statistics.C/N statistics.Percentage bad steps	1.277896

Figure A2-14 shows the plots of the ITU-R P.618 rain fade for the wanted GSO link and worst interferer against time. The Visualyse software was used to correlate the wanted and interfering paths so that there is a high degree of correlation between the two rain fades.

FIGURE A2-14

Rain fades of the wanted and worst interferer are correlated

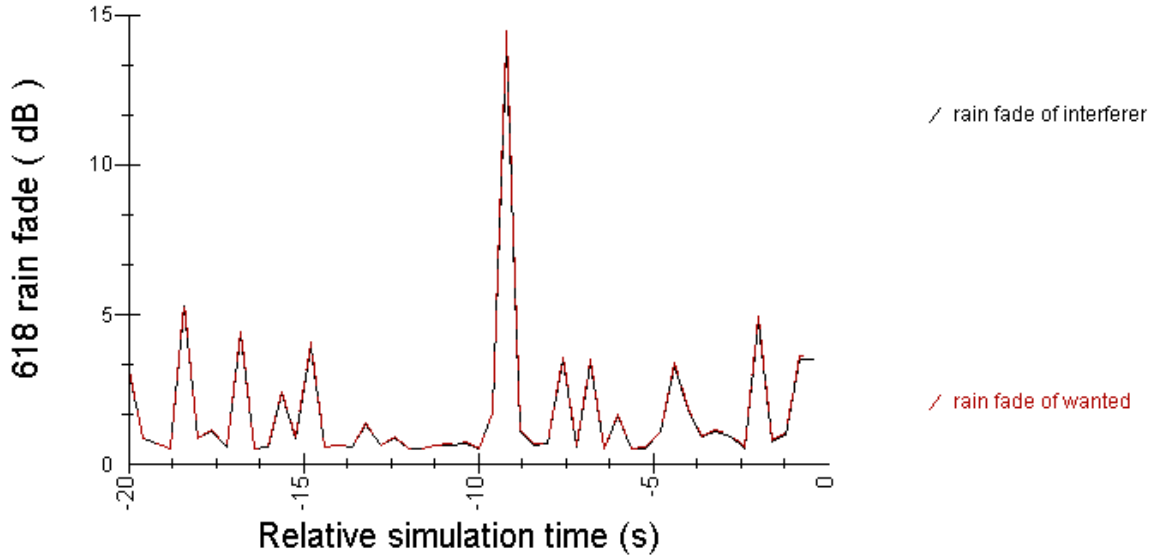

Based on the above results, the percentages of unavailability were calculated for the three scenarios, using the formulas described in § 2.5. A comparison of the unavailability results obtained is made in Table A2-25.

TABLE A2-25

Increase in unavailability for threshold of 4.7 dB

Propagation models used	**Scenario 1 P.525 + P.676 + P.840**	**Scenario 2 P.525 + P.676 + P.840 + P.618 uncorrelated**	**Scenario 3 P.525 + P.676 + P.840 + P.618 correlated**
Unavailability with no interference (%)	1.303824	1.303824	1.277896
Unavailability with interference (%)	1.316789	1.313085	1.277896
Increase in unavailability (%)	0.012965	0.009261	0
Percentage increase unavailability (%)	0.994383	0.710295	0
Percentage increase unavailability due to interference (%)	0.984592	0.705286	0

The simulation was repeated for higher thresholds of 6.8 dB and 16.6 dB. Tables A2-26 and A2-27 show the increase in unavailability for these thresholds with lower GSO link availability.

TABLE A2-26

Increase in unavailability for threshold of 6.8 dB

Propagation models used	**Scenario 1 P.525 + P.676 + P.840**	**Scenario 2 P.525 + P.676 + P.840 + P.618 uncorrelated**	**Scenario 3 P.525 + P.676 + P.840 + P.618 correlated**
Unavailability with no interference (%)	1.666821	1.666821	1.646449
Unavailability with interference (%)	1.687193	1.687193	1.646449
Increase in unavailability (%)	0.020372	0.020372	0
Percentage increase unavailability (%)	1.222207	1.222207	0
Percentage increase unavailability due to interference (%)	1.207449	1.207449	0

TABLE A2-27

Increase in unavailability for threshold of 16.6 dB

Propagation models used	**Scenario 1 P.525 + P.676 + P.840**	**Scenario 2 P.525 + P.676 + P.840 + P.618 uncorrelated**	**Scenario 3 P.525 + P.676 + P.840 + P.618 correlated**
Unavailability with no interference (%)	10.49356	10.49356	10.66765
Unavailability with interference (%)	10.83989	10.74174	10.83619
Increase in unavailability (%)	0.346329	0.248171	0.168535
Percentage increase unavailability (%)	3.300394	2.364983	1.579869
Percentage increase unavailability due to interference (%)	3.194949	2.310344	1.555298

2.6 Conclusion

The results show that at a lower threshold value which is associated with higher GSO link availability and rain fade, the impact of interference on the increase in GSO unavailability is less pronounced. For GSO links with higher threshold values which experienced lesser rain fade, the increase in its unavailability due to non-GSO interference becomes evident.

All results show that after considering the correlation of wanted and interfering propagation paths, the increase in unavailability for the GSO links due to interference from the non-GSO system is less than 3%.

Annex 3

Study #3: Assessment of sharing of aggregate GSO interference allowance among non-GSO systems in the 50/40 GHz frequency band

1 Comparison of Study #1 and Study #2

The analysis presented in Annex 1 was performed using Recommendation ITU-R S.1323 to derive epfd masks corresponding to a representative non-GSO LEO system ("VLEO"). The analysis presented in Annex 2 was performed using Recommendation ITU-R S.1323 to derive epfd masks corresponding to a representative non-GSO MEO system ("VMEO"). These two studies represent instances of proposed non-GSO systems that may operate in the 50/40 GHz frequency bands. This annex presents an assessment of potential sharing of aggregate GSO interference allowance among non-GSO systems presented in Annex 1 and Annex 2 based on principles outlined in section 6.

1.1 Comparison of VLEO and VMEO analysis studies

To perform a comparison of the results of the studies of VLEO and VMEO in Annex 1 and Annex 2, respectively, the interference profiles derived for each of the constellations can be compared with the protection criteria given in Recommendation ITU-R S.1323. The resultant interference profiles can be convolved with rain degradation statistics for a variety of globally distributed reference GSO earth station locations (with corresponding rain fade statistics) to determine the minimum GSO link margin required for the interference profile to meet the 10% of time allowance in *recommends* 3.1 of Recommendation ITU-R S.1323.

This analysis is presented in Fig. A3-1 for VLEO and Fig. A3-2 for VMEO.

FIGURE A3-1

VLEO epfd↓ profile and Recommendation ITU-R S.1323 analysis

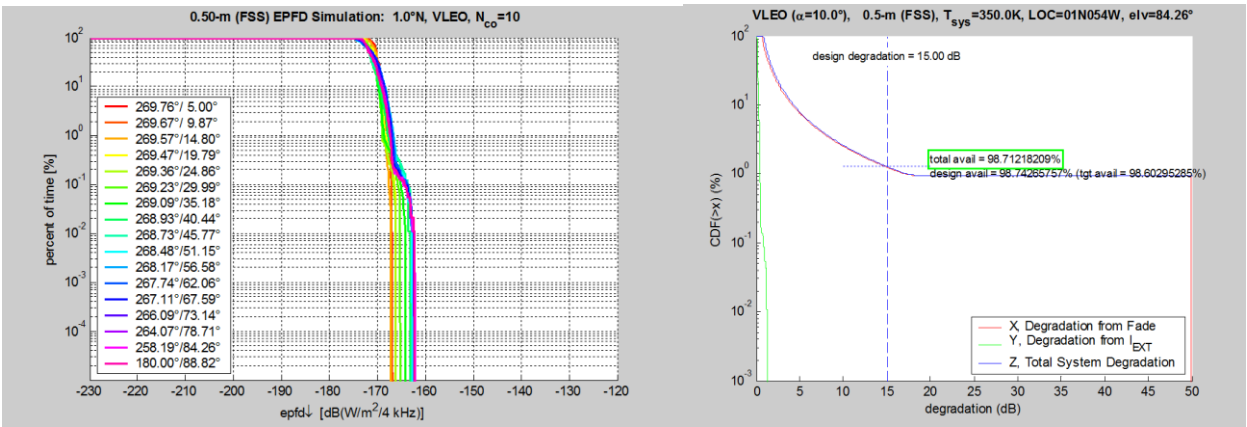

FIGURE A3-2

VMEO epfd↓ profile and Recommendation ITU-R S.1323 analysis

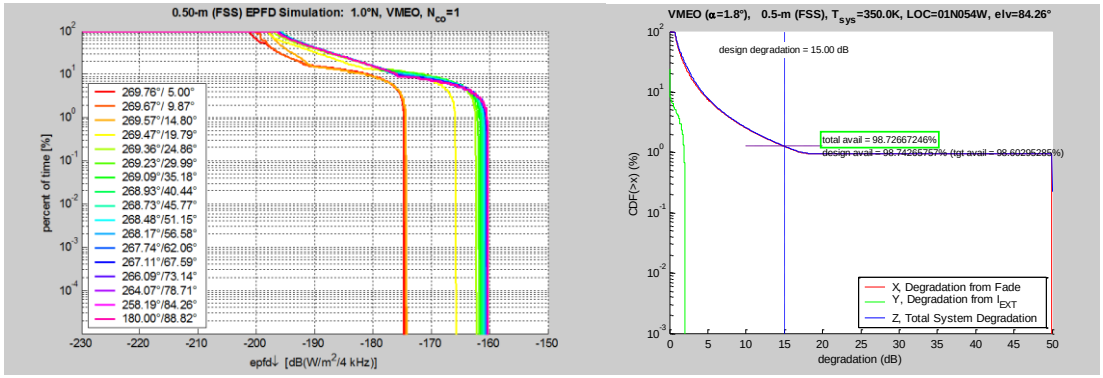

As can be seen by Figs A3-1 and A3-2, as expected, the representative masks of both VLEO and VMEO allow for sufficient GSO link margin when compared to the protection criteria given in Recommendation ITU-R S.1323.

Next, an analysis was performed to evaluate how each system performs using the derived representative interference profile of the other system. Figure A3-3 shows the performance of the VLEO system as applied to the representative interference profile developed by the VMEO system.

FIGURE A3-3

VMEO system performance based on vLeo interference profile

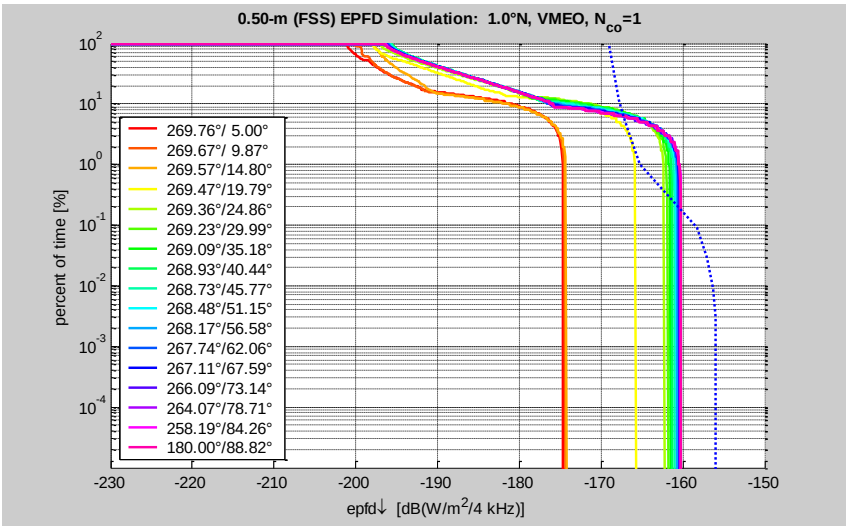

2 VLEO and VMEO composite epfd profiles

A composite interference profile was generated based on the system performance of both VLEO and VMEO and compared with the protection criteria given in Recommendation ITU-R S.1323. This composite profile is presented in Fig. A3-4 and the comparison to the protection criteria given in Recommendation ITU-R S.1323 is presented in Fig. A3-5.

FIGURE A3-4

VLEO + VMEO composite epfd↓ profile

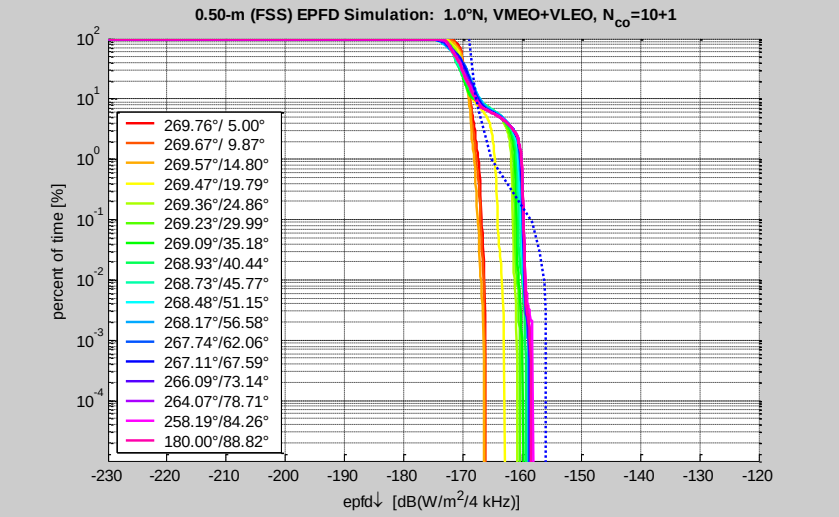

FIGURE A3-5

VLEO + VMEO Recommendation ITU-R S.1323 analysis

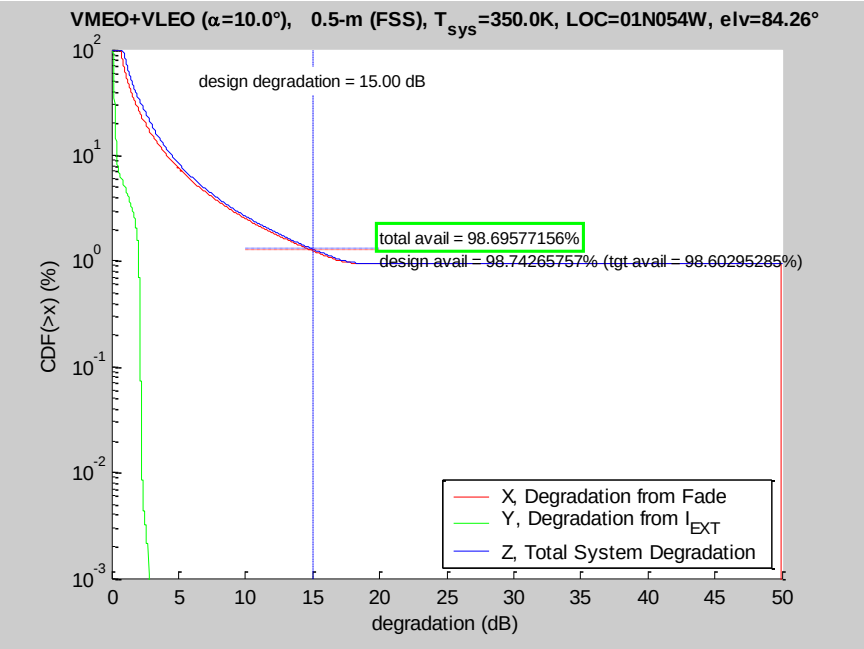

3 Observations

The analysis presented above provides a comparison of the representative interference profiles derived in the studies from Annex 1 and Annex 2 relating to non-GSO constellations in LEO and MEO orbits. The analysis shows that the methodology to determine the epfd interference profiles is extremely dependent on the characteristics of the systems being evaluated. While epfd masks can be developed for a particular system, it is very difficult, if not impossible, to define epfd masks that might not allow all non-GSO systems to operate and provide for maximum spectrum efficiency, while still assuring that GSO protection criteria will always be observed.

The analysis also shows that if masks are developed for the operation of one particular non-GSO system, a separate non-GSO system may not be able to meet the requirements from that mask. However, each system independently, and even in composite form, are able to meet the protection

criteria given in Recommendation ITU-R S.1323 with excess margin available. Given the additional propagation margins that should be taken into account on the interference path, the operating margins for GSO operations might be greater. Given these observations, a more equitable sharing procedure could be established such as one highlighted in § 7 of this Report.

Annex 4

Study 4: Considerations on non-GSO/GSO FSS sharing in the 50/40 GHz band

1 Introduction

This study looks at the interference statistics (*I*/*N*) from two non-GSO systems (LEO type and MEO type)[2] into a GSO satellite network. This contribution presents the interference statistics from the non-GSO FSS systems into a GSO FSS satellite network. An *I*/*N* approach was used as it provides a preliminary, worse case assessment of the potential for interference. The study includes descriptions of the following:

– non-GSO and GSO FSS system parameters;

– the simulation configuration; and

– the *I*/*N* statistics generated.

The following scenarios were analyzed:

– Interference from a LEO satellite system into receiving GSO earth stations (§ 3.1).

– Interference from LEO earth stations into a GSO satellite (§ 3.2).

– Interference from an equatorial MEO satellite system into receiving GSO earth stations (§ 3.3).

– Interference from earth stations operating with an equatorial MEO satellite system into a GSO satellite (§ 3.4).

The study finishes with a discussion on the results and identifies potential areas for further study.

2 Methodology, parameters and assumptions

This study investigated the resulting *I*/*N* from two types of non-GSO FSS satellite networks: a low-earth orbit constellation and an equatorial medium earth orbit constellation into a GSO system. Two deployment scenarios were modelled: 1) the GSO earth stations are located with varying elevation angles with respect to a GSO satellite and 2) the GSO earth stations are located at the equator but retain the same elevation angle to the GSO.

---

[2] A LEO satellite system is a Low Earth Orbit satellite system and is generally accepted to have an orbit below 1 500 km in altitude above the Earth's surface. A MEO satellite system is a Medium Earth Orbit satellite system and is generally accepted to have an orbit above 8 000 km and below 18 000 km in altitude above the Earth's surface. These definitions are taken from the ITU's Handbook on Satellite Communications, third edition.

The earth stations of the non-GSO and GSO systems were assumed to be co-located. The earth station locations were varied based on different elevation angles to the GSO satellite and with the location of the earth stations separated in longitude by a specified amount from the GSO satellite.

The studies did not include any propagation impairments other than free space loss, although it is recognized that at these frequencies, rain and cloud attenuation have significant impacts on both the wanted and interfering signal. As the studies assumed no additional propagation impairments, the *I*/*N* results will be worst-case and actual values under normal operating conditions would be lower. The studies were modelled using a commercial off-the-shelf (COTS) satellite simulation program.

The majority of the FSS system parameters (shown in Tables A4-1, A4-2 and A4-3) used in the studies were chosen from the lists of space system parameters that were contributed to the ITU; other assumed parameters are indicated. The constellations are representative of satellite filings that have been submitted to the ITU. The studies were done on a co-frequency basis assuming full bandwidth overlap in all the studies. The uplink and downlink frequencies used in the simulations were 51 GHz and 41 GHz, respectively.

As stated, the five sets of co-located earth stations were modelled and co-frequency operation was assumed. It is recognized that this is a worst-case analysis, because in reality, all would not operate on the same frequency. The total interference was calculated from all the co-located non-GSO earth stations in the uplink and from all the non-GSO satellites communicating with the non-GSO earth stations in the downlink. It should be noted that the interference into the GSO network came from the five non-GSO links (user terminals) that were established between the five non-GSO earth stations (co-located with the GSO earth stations) and the non-GSO satellites.

TABLE A4-1

GSO parameters

Uplink	
Carrier	#01
Peak receiving satellite antenna gain	51.8 dBi
Receiving satellite antenna pattern	S.672-4, $L_s = -20$
Receiving satellite temperature	1000 K
Downlink	
Carrier	#23
Receiving antenna diameter	0.6 metres
Peak receiving gain	46 dBi
Receiving antenna pattern	S.465-6
Receive system noise temperature	400 Kelvin
Satellite PFD	Art. **21-4** limits

TABLE 4-2

LEO parameters

Satellite system	
Number of satellites	774
Coverage	Global
Altitude	1 200 km
Inclination	89.7°
Number of planes	18
Number of satellite per plane	43 evenly spaced
Type of orbit	Circular polar
Phasing between planes	180°
Uplink	
Carrier	#27
Transmitting Peak power density	−78.7 dBW/Hz
Transmitting Antenna diameter	0.2 metres
Peak Transmitting Gain	36.9 dBi
Transmitting Antenna Pattern	S.465-6
Tracking Strategy	Highest elevation angle of at least 25°
Time step	0.25 seconds
Elapsed time	24 hours
Downlink	
Satellite PFD	Article **21-4** limits
Assumed tracking strategy	Have at least an angle of 6° away from the GSO; minimum elevation angle of 30°
Time step	0.25 seconds
Elapsed time	24 hours

TABLE A4-3

Equatorial MEO parameters

Satellite system	
Number of satellites	12
Coverage	Standard service < 45° latitude
Altitude	8 062 km
Inclination	0
Number of planes	1
Number of satellite per plane	12 evenly spaced
Type of orbit	Circular equatorial

TABLE A4-3 *(end)*

Uplink	
Carrier	#34
Transmitting Peak power density	−73.7 dBW/Hz
Transmitting Antenna diameter	1.8 metres
Peak Transmitting Gain	56.9 dBi
Transmitting Antenna Pattern	S.465-6
Tracking Strategy	Highest elevation angle
Time step	0.25 seconds
Elapsed time	24 hours
Downlink	
Carrier	#20
Peak satellite e.i.r.p. spectral density	−34.6 dBW/Hz
Satellite peak transmitting gain	39 dBi
Transmitting Antenna Pattern	S.1528, L_s = 25
Tracking strategy	Highest elevation angle
Time step	0.25 seconds
Elapsed time	24 hours

3 Results

3.1 Interference from a LEO satellite system into receiving GSO earth stations

In terms of communication of the downlink from the satellite to earth stations, earth stations with low elevation angles to the GSO look through a greater area of the orbital shell and therefore 'see' more satellites and higher levels of interference. In addition, there are more satellites in the polar region of the LEO constellation modelled, and thus the satellites will be physically closer. Earth station antenna side lobes and back lobes are independent of the antenna diameter and thus there is no impact on the levels of the interference received from directions well off the antenna main beam. However, the physical diameter of the receiving antenna has the largest impact in terms of the maximum value of interference that is received.

Scenario 1: The receiving GSO earth stations are located north of the equator and at the same longitude of the GSO satellite. The earth stations are situated such that the elevation angles to the GSO satellite are 10°, 15°, 20°, 25°, and 30°. The range of elevation angles was chosen to illustrate the impact of lower GSO earth station elevation angles even though it is not expected that earth stations at these frequency bands would operate at the lower end of this range due to operational constraints. Additional measures such as larger earth stations and use of Adaptive Coding and Modulation (ACM) would be needed if GSO links were to be viable even in drier climates at some of the lower elevation angles.

Figure A4-1 is a snap shot of the simulation modelled, showing the LEO satellites, two sets of co-located GSO and non-GSO earth stations at varying elevation angles and the GSO satellite.

FIGURE A4-1

Graphical representation of Scenario 1

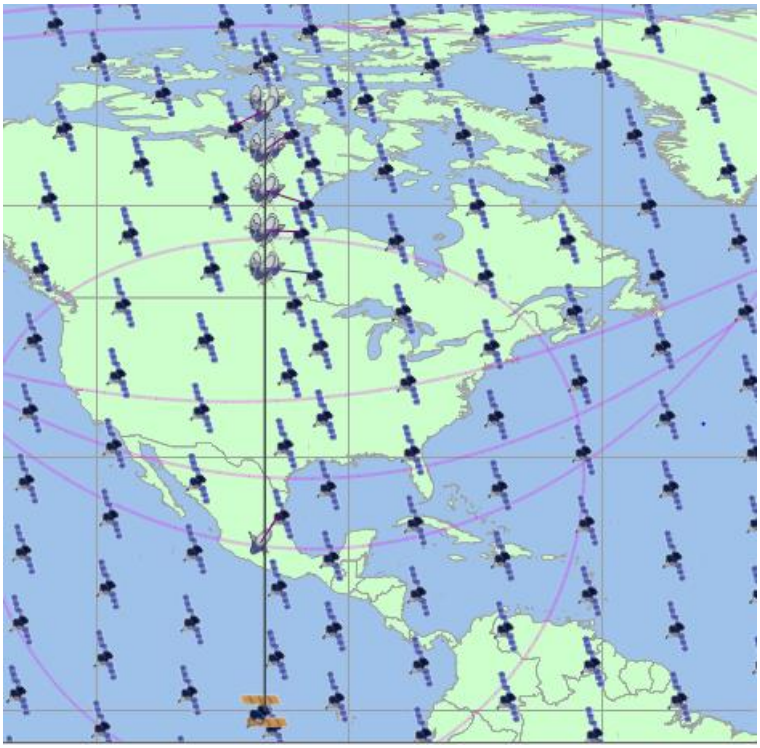

FIGURE A4-2

LEO interference into receiving earth stations (same longitude as GSO satellite)

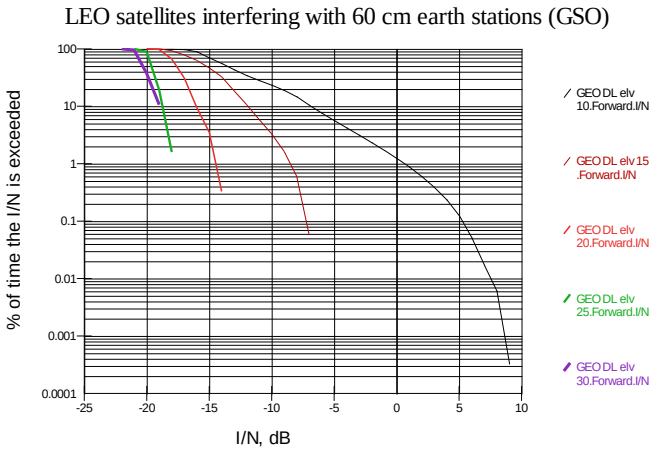

From Fig. A4-2, it is shown that there is an increase in interference as the elevation angle of the receiving GSO earth station decreases. A simulation was also carried out for a receiving antenna diameter of 3.5 metres, and there was no significant difference aside from the minor difference for very small percentage of time, which is probably a result of the simulation time and start times used. The main beam does not figure into the interference statistics given the orbital avoidance strategy practised by the non-GSO system.

The shape of the *I*/*N* CDFs for both the 0.6 m and the 3.5 m GSO earth station antenna were the same, though the 60 cm GSO receiving earth station had a higher aggregate *I*/*N* compared to the larger antennas for a smaller percent of the time; however, the *I*/*N* of 9 dB exceeded for 0.0003% of the time represented only one time step in the simulation. For this reason, the curves for a 3.5 m antenna are

not reproduced here. A longer simulation time or even a different start time may have yielded the same result for the 3.5 m antenna.

Scenario 2: The receiving non-GSO and GSO earth stations are located at the equator. The earth stations are situated at longitudes west of the satellite such that elevation angles to the GSO satellite remain identical to those in scenario 1: 10°, 15°, 20°, 25°, and 30°. This scenario was carried out to see the effects of the evenly spaced non-GSO satellites on the GSO link when they cross the equator – at higher latitudes the non-GSO satellites are closer together.

FIGURE A4-3

LEO interference into 60 cm receiving earth stations at the equator

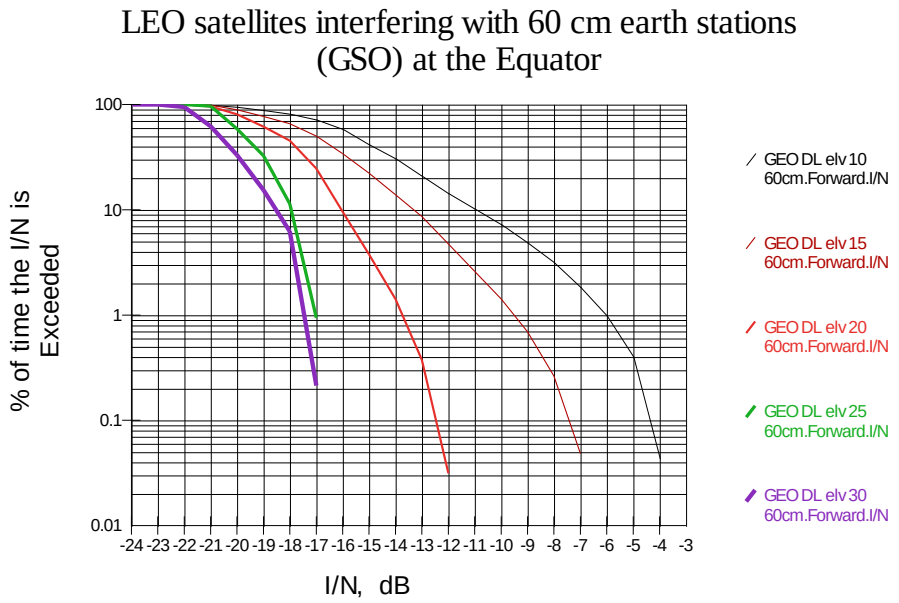

Figure A4-3 shows that GSO receiving earth stations at the lowest elevation angles are impacted by higher *I*/*N* as compared to GSO receiving earth stations at higher elevation angles.

Discussion

Figure A4-1 shows the aggregate interference coming into the GSO receiving earth stations, from the LEO satellites as they transmit to the LEO earth stations. Both sets of receiving earth stations (GSO and LEO) have the same orbital longitude as the GSO satellite but with varying elevation angles to the satellite. The figure shows that there is an increase in *I*/*N* with a decrease in the earth station angles to the GSO satellite. This decrease is caused by the discrimination in the receiving antenna gain and when the LEO satellites are close to the receiving earth stations. The simulations showed that the receiving earth stations received more interference in the back and side lobes of the antenna.

The variation of the *I*/*N* in different scenarios is predominantly influenced by the elevation angle of the earth station to the GSO and number of satellites coming adjacent to the main beam of elevation angle to the GSO.

Some variation will also occur from the change in distance of the interfering LEO satellites to the GSO earth station as the satellite moves closer to or further away from the earth station, which affects the free space loss.

Figure A4-2 shows the aggregate interference into the GSO receiving earth stations from the LEO satellites as they transmit to the co-located LEO earth stations. Both sets of receiving earth stations

are located at the equator and have varying elevation angles to the GSO due to their different longitudinal positions. The GSO receiving earth stations with lower elevation angles to the GSO are impacted more by interference than earth stations with a higher elevation angle to the GSO.

Comparing the levels of *I*/*N* produced in Scenarios 1 and 2, the levels of *I*/*N* are lower in the second scenario, when the earth stations are located at the equator. In this scenario, the tracking strategy of avoiding the GSO arc by 6° impacts the levels of interference received. In all cases, the long-term *I*/*N* (20% of the time) is well under −16 dB for elevation angles greater than 20° or greater.

3.2 Interference from LEO earth stations into a GSO satellite

In terms of communication on the uplink to the GSO satellite from transmitting earth stations, the analysis is not dependent on the size of the transmitting GSO earth station antenna diameter since this value will not affect the *I*/*N*. The main factor affecting the *I*/*N* will be the off-axis transmitting gain of the interfering LEO earth stations, since GSO arc avoidance was modelled. The receiving GSO satellite gain is assumed to be at a maximum towards each of the co-located transmitting earth stations. This analysis investigates the *I*/*N* of co-located stations north of the equator and the effect of the longitudinal separation of the earth stations at the equator on the interference received by the GSO satellite.

Scenario 3: The transmitting earth stations are located north of the equator, at the same longitude as the GSO satellite, and at latitudes such that elevation angles to the GSO satellite are 10°, 15°, 20°, 25° and 30°.

FIGURE A4-4

LEO earth stations (same longitude as GSO) interfering into a GSO satellite

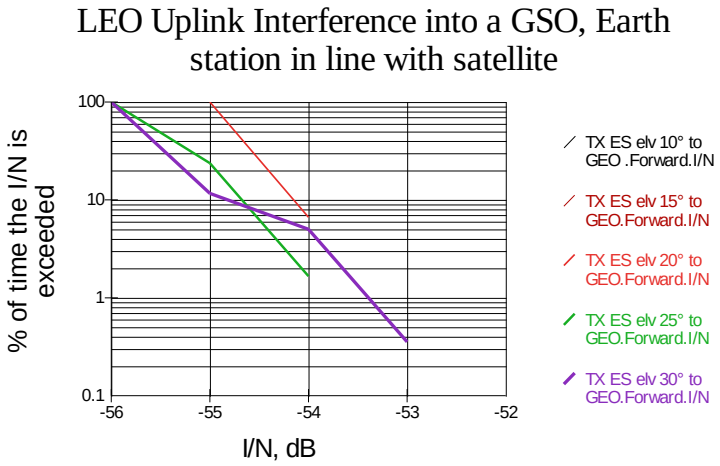

The *I*/*N* into the satellite from the transmitting LEO earth stations are static for earth stations at 10° and 15° elevation angles to the GSO and thus do not appear in Fig. A4-4. The *I*/*N* into the satellite from the transmitting LEO earth stations at higher elevation angles to the GSO are less than −53 dB and have little variance.

Scenario 4: The transmitting earth stations are situated at the equator and at longitudes west of the satellite such that elevation angles to the GSO satellite are 10°, 15°, 20°, 25°, and 30°.

FIGURE A4-5

LEO earth stations (at the equator) interfering into a GSO satellite

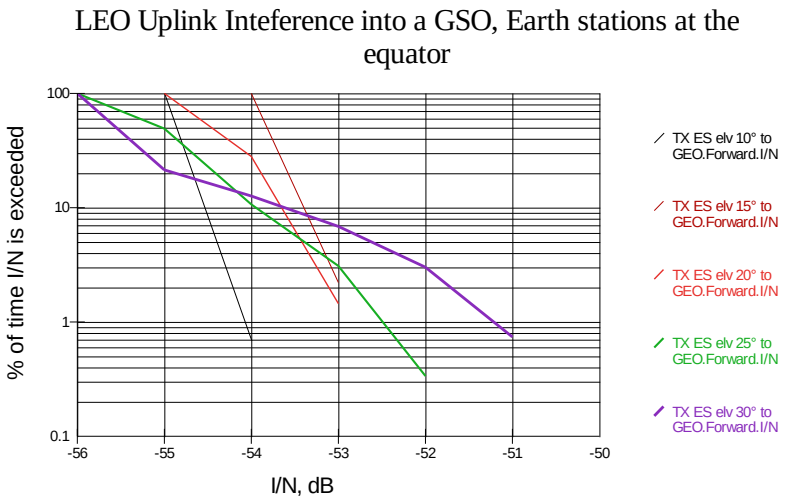

In Fig. A4-5, the *I*/*N* into the satellite from the transmitting LEO earth stations are less than −51 dB for the interference from all the earth stations (elevation angles to GSO of 10°, 15°, 20°, 25°, and 30°).

Scenario 5: The transmitting earth stations are located north of the equator and at the same orbital longitude as the GSO satellite, and are at latitudes such that the elevation angles to the GSO satellite are 40°, 50°, 60°, 70°, and 80°.

FIGURE A4-6

LEO earth stations (same longitude as GSO satellite) interfering into a GSO satellite

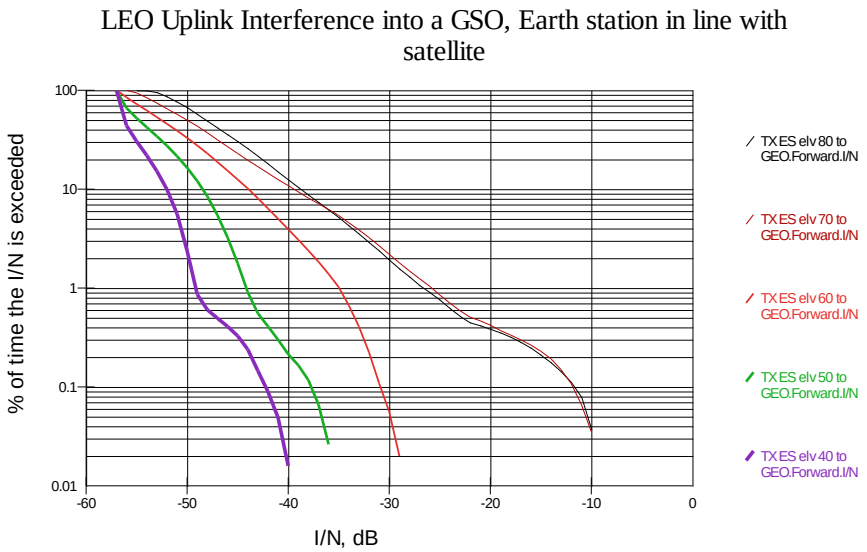

Figure A4-6 shows that the receiving GSO satellite receives less interference, as expected, from the earth stations that are further away from the satellite.

Discussion

In these uplink scenarios, the dominating varying factor in the *I*/*N* is the off-axis transmitting gain coming from the LEO earth stations, which is about 40 to 50 dB down from the main lobe. The resulting *I*/*N* are quite low for earth stations with elevations angles to the GSO satellite that are less than 30°, as seen in Figs A4-4 and A4-5. Another factor to consider is that the power from the LEO earth stations are at levels significantly lower than what would be expected to communicate with a GSO satellite. When the co-located transmitting LEO earth stations were situated at higher elevation angles to the GSO satellite, more interference was received into the GSO satellite, with an *I*/*N* of −10 dB for no more than 0.03% of the time.

3.3 Interference from an equatorial MEO satellite system into receiving GSO earth stations

This following section studies the interference levels from the equatorial MEO satellites into a set of receiving GSO earth stations. Since the MEO satellite system studied has an equatorial orbital and is not designed to serve earth stations at high latitudes, but typically <45°, the earth stations are situated at the equator. Further analysis is carried out with earth stations situated at the equator, but with larger elevation angles to the GSO satellite.

Scenario 6: The receiving earth stations are located at the equator, west of the satellite such that the elevation angles to the GSO satellite are 10°, 15°, 20°, 25°, and 30°.

FIGURE A4-7

Interference into 60 cm receiving earth stations located at the equator

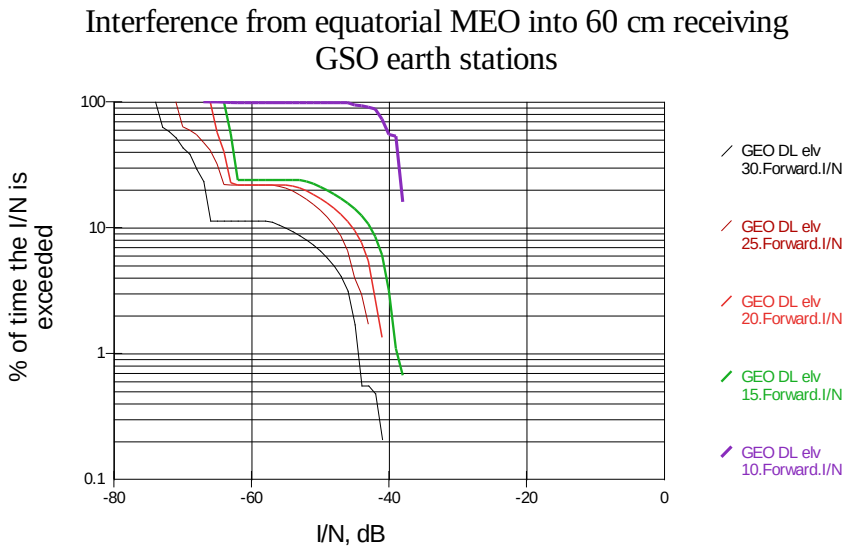

Figure A4-7 shows that very low *I*/*N* are seen at the receiving GSO earth stations, indicating that all the interfering power is well off the main beam of the receiving antenna.

Scenario 7: The receiving earth stations are located at the equator, west of the GSO by 0°, 10°, 20°, 30°, and 40°, resulting in elevation angles to the GSO of 90°, 78.2°, 66.6°, 55°, and 43.7°, respectively.

FIGURE A4-8

Interference into earth stations located at the equator

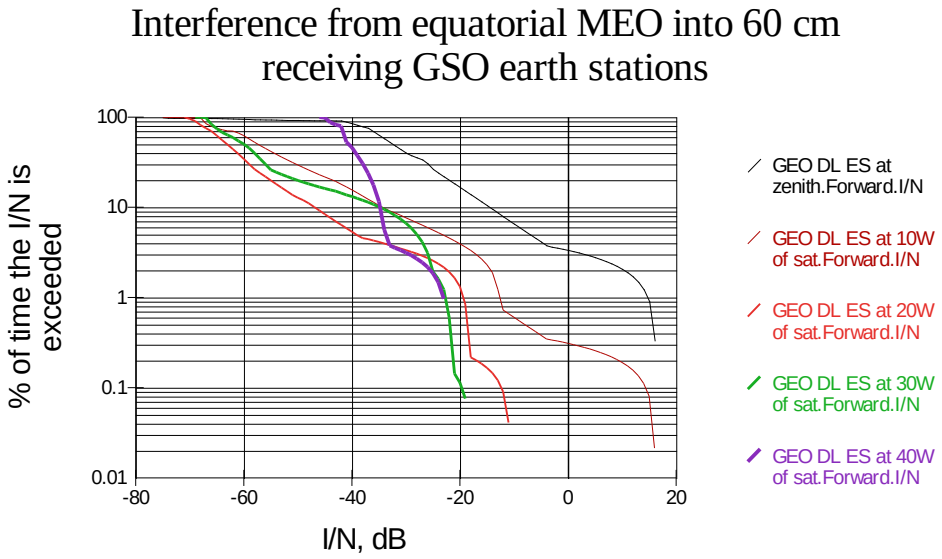

Figure A4-8 shows that the receiving GSO earth stations, with higher elevation angles to the GSO than in Fig. A4-7, have higher levels of *I*/*N* than was seen in Fig. A4-7.

Discussion

Overall, the receiving GSO earth stations that have a low elevation angle to the GSO satellite, have lower *I*/*N*. Generally, as the stations come closer to the GSO, the discrimination is reduced between the look angles between equatorial MEO satellites and the GSO satellite, and thus the receiving GSO earth station has a higher gain towards the interfering satellites. The exception to this is between the two receiving GSO earth stations, one at zenith, and the other 10° west of the GSO satellite. These two receiving GSO earth stations receive similar amounts of interference, as seen in Fig. A4-8; however, the receiving GSO earth station at 10° west of the GSO receives more incidences of the interference events. This is explained by the fact that the *I*/*N* at the receiving GSO earth station's main beam located at 0°N and having the same longitude of the GSO satellite, intersects the MEO's orbital shell with a minimum area when pointed straight up. The receiving earth station further west, and at a lower elevation angle, has its antenna's main beam intersecting a larger volume, possibly seeing more than one satellite at a time.

Finally, as in the LEO scenario, a larger receiving antenna diameter was modelled, but the results are not included. The size of the receiving GSO earth stations has an impact as the receiving GSO earth stations are located closer to the GSO satellite. Interference is seen closer to the main beam and there were incidences of in-line events, which can be seen as the difference in the maximum *I*/*N* ratios received by the GSO earth station antenna diameters at zenith and 10° of the satellite (shown in Fig. A4-8).

3.4 Interference from earth stations operating with an equatorial MEO satellite system into a GSO satellite

Since the equatorial MEO constellation modelled has an equatorial orbit and does not aim to serve absolute altitudes much greater than 45°, this study investigate the impact of these systems at low elevation angles to the GSO, but the earth stations were situated at the equator.

Scenario 8: The transmitting MEO earth stations are located at the equator and situated such that the elevation angles to the GSO satellite are: 10°, 15°, 20°, 25°, and 30°.

FIGURE A4-9

Equatorial MEO earth stations at the equator interfering into a GSO satellite

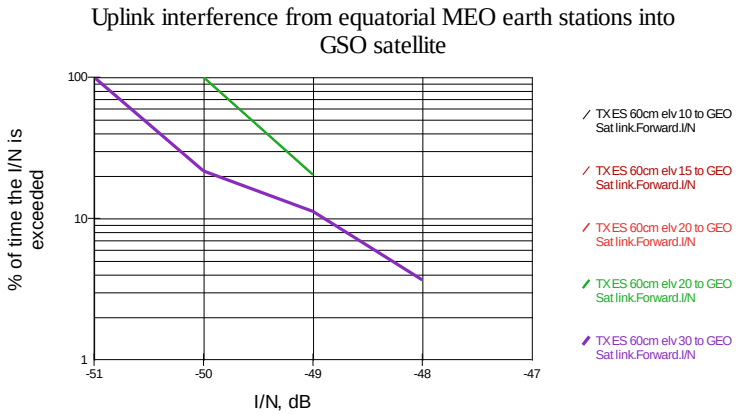

The *I*/*N* into the satellite from the transmitting MEO earth stations are static for earth stations at 10°, 15° and 20° elevation angles to the GSO and thus do not appear in Fig. A4-9. The *I*/*N* into the satellite from the transmitting equatorial MEO earth stations at higher elevation angles to the GSO are less than -48 dB and have little variance between minimum and maximum levels.

Scenario 9: The transmitting earth stations are located at the equator, west of the GSO by 0°, 10°, 20°, 30°, and 40°, resulting in elevation angles to the GSO of 90°, 78.2°, 66.6°, 55°, and 43.7°, respectively.

FIGURE A4-10

Interference from earth stations located at the equator into a GSO satellite

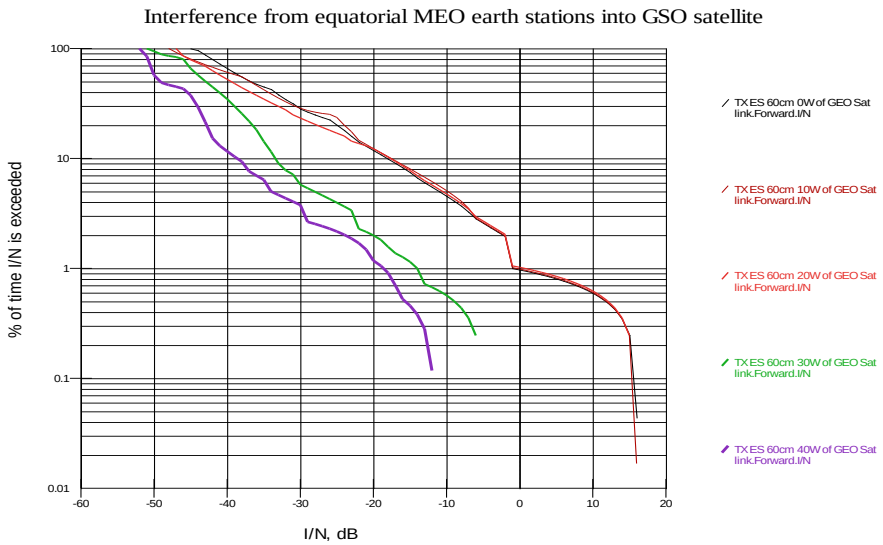

Figure A4-10 shows that the receiving GSO satellite receives less interference from the earth stations that are further away from the satellite.

Discussion

The dominating varying factor in the *I*/*N* is the off axis transmitting gain coming from the MEO earth stations. The resulting *I*/*N* are quite low for earth stations with elevations angles to the GSO satellite that are less than 30°, as seen in Fig. A4-9. In addition, the transmitting power from the MEO earth stations are at levels lower than what would be expected to communicate with a GSO satellite. The levels of *I*/*N* are quite high (~17 dB) from the interference received from the earth stations located 0°, 10°, and 20° west of the satellite, indicating in-line events for about 0.02% of the time.

4 Conclusions

The contribution studied the effect of varying the location of earth stations on the interference received into a GSO network from two different non-GSO satellite systems (a circular-orbit LEO and an equatorial MEO).

For the first interference study (LEO vs GSO), in the downlink, it is shown that the receiving GSO earth stations at lower elevation angles to the GSO satellite were more susceptible to interference from non-GSO systems.

These studies only examined attenuation due to free space losses. However, if other attenuation losses were taken into account, the *I*/*N* would be lower. In the uplink scenarios, the interference into a GSO satellite from LEO earth stations was studied showing low levels of interference at the GSO satellite from earth stations located at most elevation angles to the GSO. When the elevation angle of the earth stations to the GSO was increased, the results showed higher levels of interference, but for small percentages of time, taking into account 5 terminals.

For the second interference study (MEO vs GSO), it is shown that receiving GSO earth stations at lower elevation angles to the satellite receive lower *I*/*N* from the equatorial MEO system. When earth stations with higher elevation angles to the GSO were studied, higher levels of interference were received, with the greatest impact to earth stations with elevation angles of 10° and 0° to the GSO. It is important to note that no geostationary arc avoidance was used in the MEO study. In terms of the uplink interference to the GSO satellite, the *I*/*N* levels were not significant, except for when the interfering earth stations were located with high elevation angles to the GSO.

Previous ITU studies have demonstrated that providing service to elevation angles below 20° to the GSO could require undue complexity and cost due to higher propagation impairments, e.g., gaseous absorption, cloud and rain. To serve lower elevation angles, GSO satellite operators will need to take additional measures in their system design, such as implementing larger antenna diameters and heavy coding. These conclusions may be taken into account when considering the use of these bands for GSO and non-GSO systems and when examining co-existence between these two types of implementations of the FSS.

Further areas of study could include different types of non-GSO systems and studying the impact of *C*/*(N+I)*, based on a range of carrier powers for GSO systems, into the victim networks to study the effect of correlated fading on interference into the two types (GSO versus non-GSO) of FSS systems. In addition, it would be interesting to see the effect of GSO interference into the non-GSO systems.

Annex 5

Study 5: Research on epfd limits for a typical non-GSO system to GSO system in the 50/40 GHz band

1 Introduction

Based on Resolution **159 (WRC-15)**, ITU-R is invited to complete the research for the WRC-19 agenda 1.6 that includes the following item:

> to consider the development of a regulatory framework for non-GSO FSS satellite systems that may operate in the frequency bands 37.5-39.5 GHz (space-to-Earth), 39.5-42.5 GHz (space-to-Earth), 47.2-50.2 GHz (Earth-to-space) and 50.4-51.4 GHz (Earth-to-space), in accordance with Resolution **159 (WRC-15)**.

And some studies shall be conducted, such as:

> studies carried out under resolves to invite ITU-R shall focus exclusively on the development of equivalent power flux-density limits (epfd)produced at any point in the GSO by emissions from all the earth stations of a non-GSO system in the fixed-satellite service or into any geostationary FSS earth station, as appropriate.

During the study period of ITU-R in 2016, study on interference by non-GSO to GSO system, in which the parameters of non-GSO system were similar to a typical MEO satellite system.

Apparently, LEO orbit could also be a good option for the future non-GSO system with a deployment of global coverage. This paper conducted a study on epfd limits of a typical non-GSO system with LEO orbit.

2 System parameters

2.1 Non-GSO system parameters

The non-GSO system is an LEO circular orbit system with parameters similar to the 3ECOM-2 satellite network (IFIC2788) which was chosen just as an example based on the typical deployment of non-GSO constellation. It is with 12 orbits and 28 satellites in each, so the system has 336 satellites totally. The key parameters were shown in the Tables below.

TABLE A5-1

Non-GSO parameters for satellites

Carrier frequency (GHz)	48/38
Orbit height (km)	1425
Orbit period (hour/minute)	1 hour 45 minutes
Inclination angle (°)	89
Carrier bandwidth (MHz)	81
Peak transmit power (dBW)	24.8
Max receive Gain (dBi)	34.1
Max transmit Gain (dBi)	34.1
Beam steerable or not	Yes
Gain pattern	Rec. ITU-R S.1528 Ls = −25
Receive noise temperature (K)	564
C/N requirement (dBc)	10

NOTE – The calculated space-to-Earth pfd value of this non-GSO system was not in accordance with the related limits in RR Table **21-4**.

TABLE A5-2

Non-GSO parameters for earth stations

Carrier frequency (GHz)	48/38
Dish size (m)	1.8
Carrier bandwidth (MHz)	81
Peak power (dBW)	24.8
Max receive Gain (dBi)	56.1
Max transmit Gain (dBi)	58.2
Steerable or not	Yes
Transmit Gain pattern	Rec. ITU-R S.580
Receive Gain pattern	Rec. ITU-R S.580
Receive noise temperature (K)	444
C/N requirement (dBc)	10
Total number of earth station	336 (global distributing)

Typically, under the condition that there is certain avoidance angle between the non-GSO and GSO communication links, the tracking strategy could be summarized as below:

(1) All the earth stations are with uniform orientation direction, the related satellite is chosen based on the maximum antenna Gain identification.

(2) Every earth station is with an unfixed orientation direction, the related satellite is chosen based on the best elevation angle.

According to the first strategy, the epfd into GSO system could be effectively controlled by setting of suitable space orientation. It's simple but with a drawback that the space-to-earth or earth-to-space communication link is always not optimal, which may affects the system capacity.

According to the second strategy, if the smallest avoidance angle is met, an optimal communication link is always available. It is with a drawback that the beam shifting strategy is complicated.

Until now, it is preferred by more engineers that the second tracking strategy could satisfy the best communication capacity. Based on this analysis, an assumption for the simulation was made:

The tracking strategy with unfixed orientation is adopted by non-GSO system, with a minimal avoidance angle of 10 degrees and a minimal elevation angle of 45 degrees. The satellite could use steerable beam that the beam centre aims at the related earth station.

C/*N* should be deduced by the equation below and the calculated results are shown in Table A5-3.

$$\frac{C}{N} = P_t + G_t + G_r - G_{relative} - \text{FSL} - 10\log_{10}(\text{kTB}) \quad (8)$$

where:

P_t : transmit power (dBW)

G_t : transmit peak gain (dBi)

G_r : receive peak gain (dBi)

$G_{relative}$: receive relative gain to the peak (dBi)

FSL : free space loss (dB)

k : Boltzmann's constant (J/K)

T : noise temperature in receive end (K)

B : bandwidth of carrier/noise (Hz).

TABLE A5-3

Link budgets for non-GSO

Direction	**Uplink**	**Downlink**
Frequency (GHz)	48	38
Bandwidth (MHz)	81	81
Transmit power (dBW)	24.8	24.8
Transmit peak gain (dBi)	58.2	34.1
Free space loss at elevation angler of 45°(dB)	192.15	190.12
Receive peak gain (dBi)	34.1	56.1
Receive relative gain (dBi)	0.0	0.0
Calculated *C*/*N* (dBc) (in case of clear sky)	55.14	47.92

It was shown that the *C*/*N* requirements were met for both uplink and downlink in the case of clear sky.

2.2 GSO system parameters

The parameters used in GSO system come from contribtuions to the ITU, collected in Annex 13 and are in the Tables that follow. According to Article **22** of the Radio Regulations, the epfd limits are focused on the equivalent interference effect at any point on GSO orbit or any location within the service area on earth, which are related to specific reference points. On the hand of the interfered, only some typical points should be involved in the interference calculation. It was assumed that the named GSO system adopted multi-beams as the deployment for the 50/40 GHz band telecommunications service. Considering the global coverage by 3ECOM-2, two pairs of typical beams (transmit and receive) of GSO system were chosen as the references in low latitude and medium latitude area respectively.

FIGURE A5-1

Interfering scenario

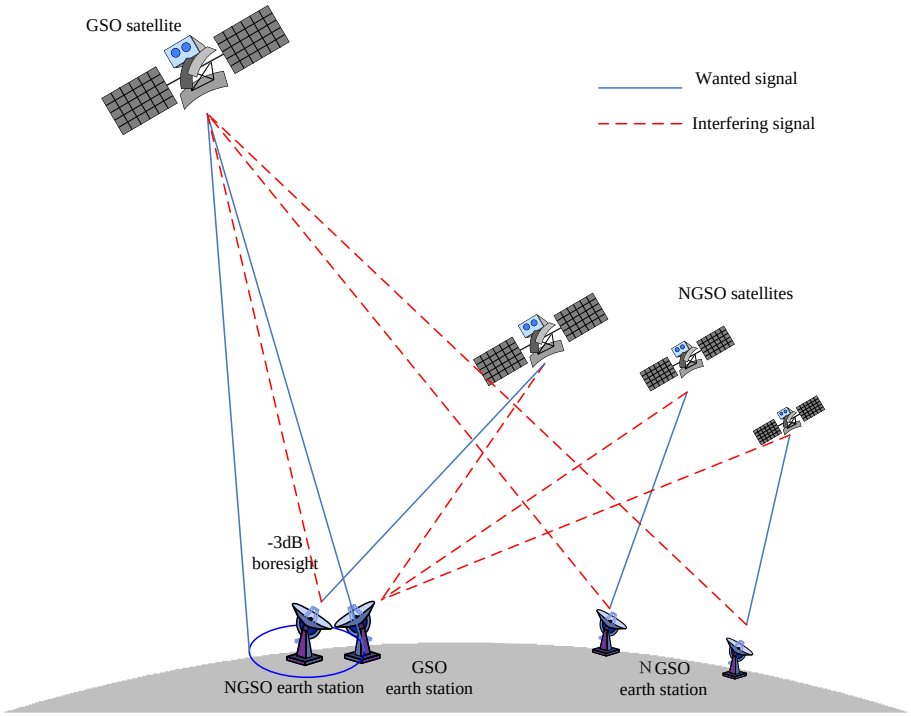

At the same time, GSO earth stations in this paper were assumed on GSO transmit/receive beam's negative 3 dB footprints and non-GSO earth stations were in their related non-GSO satellite beam centres, as the relatively worst cases, which were depicted in Fig. A5-1. The locations of GSO earth stations are "North 5 degrees, East 120 degrees" and "North 40 degrees, East 120 degrees", as the reference points in downlink case, and the GSO satellite was located at East 120 degrees, as the reference points in uplink case for epfd study.

TABLE A5-4

GSO parameters for satellites

Carrier frequency (GHz)	48/38
Carrier bandwidth (MHz)	110
Peak e.i.r.p. power (dBW)	61.8
Max receive Gain (dBi)	51.8
Transmit Gain pattern	Rec. ITU-R S.672-4 Ls = −25
Receive Gain pattern	Rec. ITU-R S.672-4 Ls = −25
Receive noise temperature (K)	700

TABLE A5-5

GSO parameters for earth station

Carrier frequency (GHz)	48/38
Dish size (m)	2.2
Carrier bandwidth (MHz)	110
Peak e.i.r.p. power (dBW)	83.5
Max receive Gain (dBi)	56.6
Transmit Gain pattern	Rec. ITU-R S.580
Receive Gain pattern	Rec. ITU-R S.580
Receive noise temperature (K)	250

TABLE A5-6

Link budgets for GSO

Location of earth station	**Low (N 5°, E 120°)**		**Medium (N 40°, E 120°)**	
Direction	**Uplink**	**Downlink**	**Uplink**	**Downlink**
Earth station size (m)	2.2	2.2	2.2	2.2
Frequency (GHz)	48.0	38.0	48.0	38.0
Receive temperature (K)	700	250	700	250
Bandwidth (MHz)	110.0	110.0	110.0	110.0
Transmit e.i.r.p. power (dBW)	83.5	61.8	83.5	61.8
Free space loss (dB)	217.15	215.12	217.55	215.52
Receive peak gain (dBi)	51.8	56.6	51.8	56.6
Receive relative gain (dB)	–3.0	-3.0	–3.0	-3.0
Rec. ITU-R P.618 rain loss (dB)	19.59	9.19	19.19	8.79
Rec. ITU-R P.618 percentage (%)	99.006	98.039	98.976	97.898
Unavailability (%)	0.994	1.961	1.024	2.102
Rec. ITU-R P.618 rain rate (mm/h)	85	85	85	85
Wanted *C*/*N* (dBc)	15.3	15.3	15.3	15.3
Calculated *C*/*N* (dBc)	15.3	15.3	15.3	15.3

3 Parameters of interference simulation scenarios

3.1 Time step and simulation duration

According to the ITU recommended documents (Recommendations ITU-R S.1503 and ITU-R S.1325), the calculation result of time step in the simulation was calculated to be 0.16s. Considering the repeat period of the named non-GSO satellites is 12 5612 days, approximately $12\frac{1}{2}$ days, and that means in every two days the satellites return to the locations which is very close to the original ones, so the simulation duration was set to be 1080000 steps (two days).

TABLE A5-7

Time step

Direction	Uplink	Downlink
Frequency (GHz)	48	38
Earth station type	Non-GSO	GSO
Dish size (m)	1.8	2.2
Beamwidth (degree)	0.243	0.230
Non-GSO height (km)	1425	1425
Non-GSO inclination (degree)	89	89
N_{hit}	5	5
Time step (s)	0.16	0.16

3.2 Rain attenuation models

The rain attenuation coincides with rain probability, carrier frequency, and other factors. In this paper, the 50/40 GHz band communication links are more sensitive to the rain attenuation. The propagation models in Recommendation ITU-R P.618 were used for the analysis.

4 Results

4.1 GSO beam pointing low latitude area

4.1.1 Downlink

(1) epfd

FIGURE A5-2

Downlink epfd

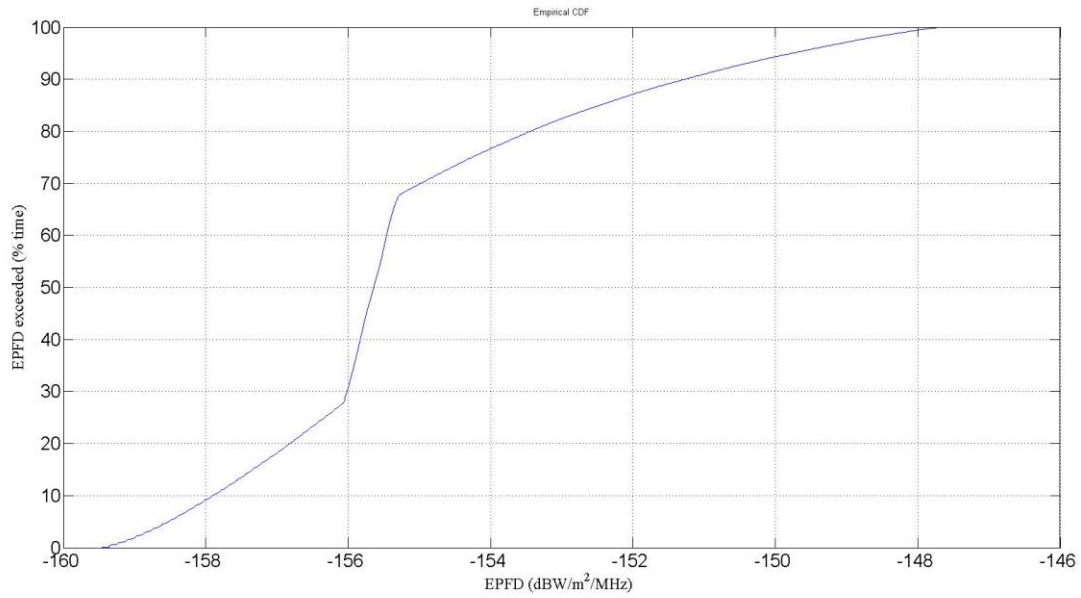

It was shown that the maximum epfd value was approximately −148 dB(W/m^2/MHz).

(2) *C/(N+I)*

FIGURE A5-3

Downlink *C/(N+I)*

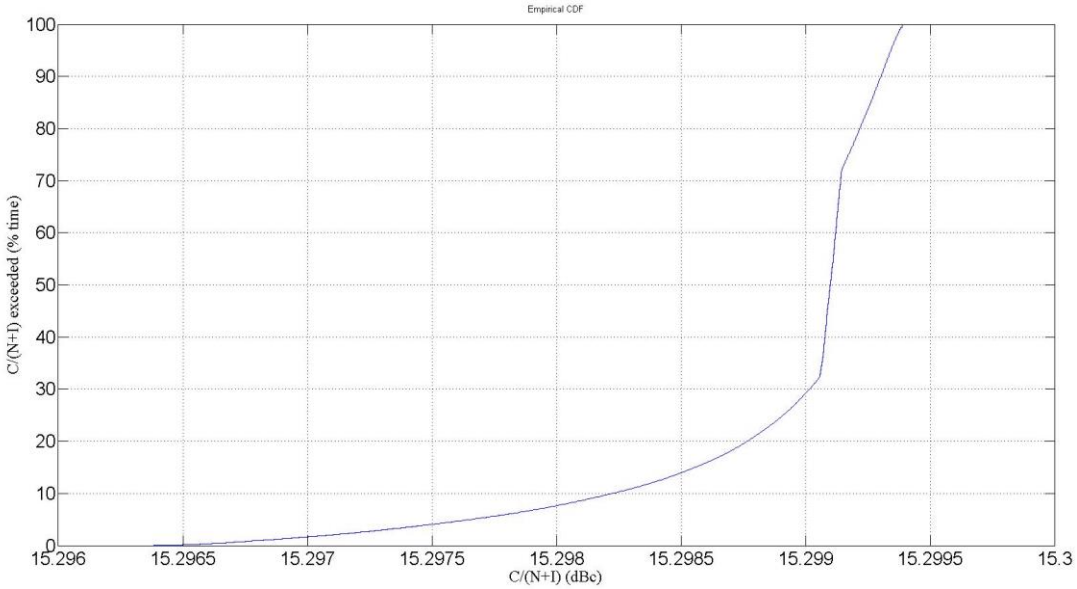

4.1.2 Uplink

(1) epfd

FIGURE A5-4

Uplink epfd

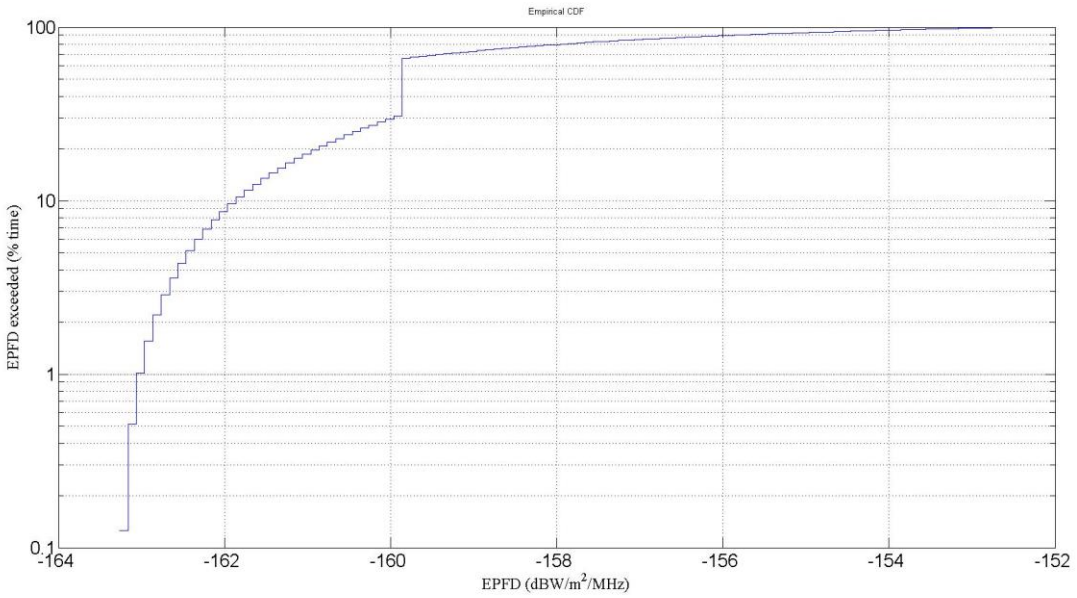

It was shown that the maximum epfd value was approximately −152 dB(W/m^2/MHz).

(2) *C/(N+I)*

FIGURE A5-5

Uplink *C/(N+I)*

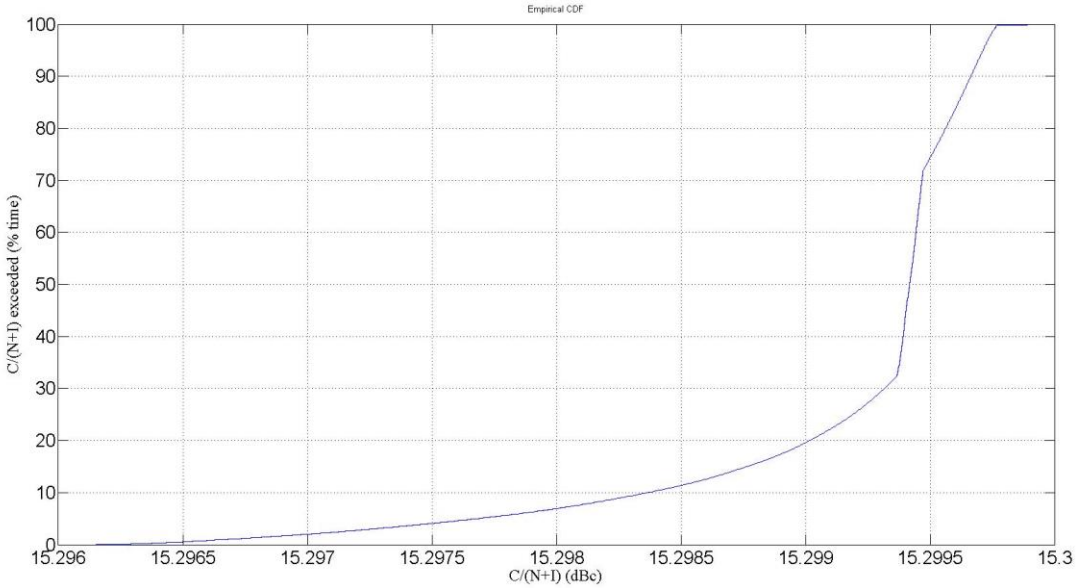

4.2 GSO beam pointing medium latitude area

4.2.1 Downlink

(1) epfd

FIGURE A5-6

Downlink epfd

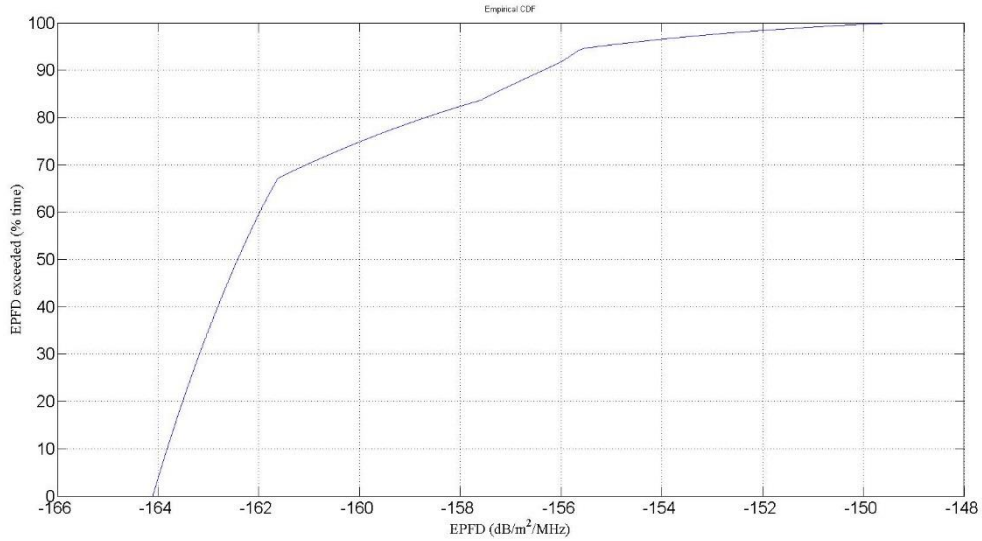

It was shown that the maximum epfd value was approximately −148 dB(W/m^2/MHz).

(2) *C/(N+I)*

FIGURE A5-7

Downlink *C/(N+I)*

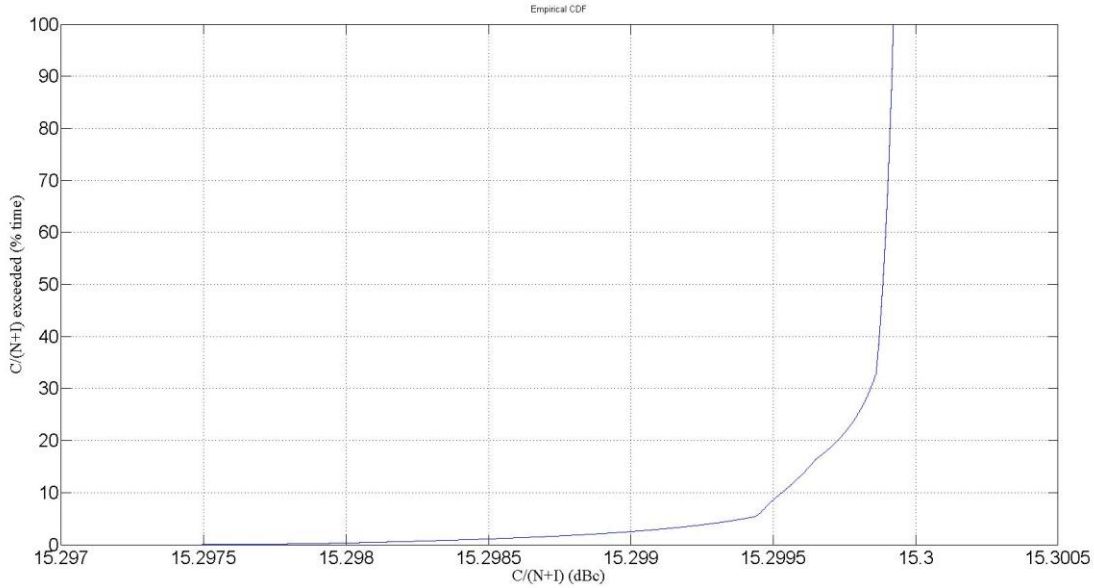

4.2.2 Uplink

(1) epfd

FIGURE A5-8

Uplink epfd

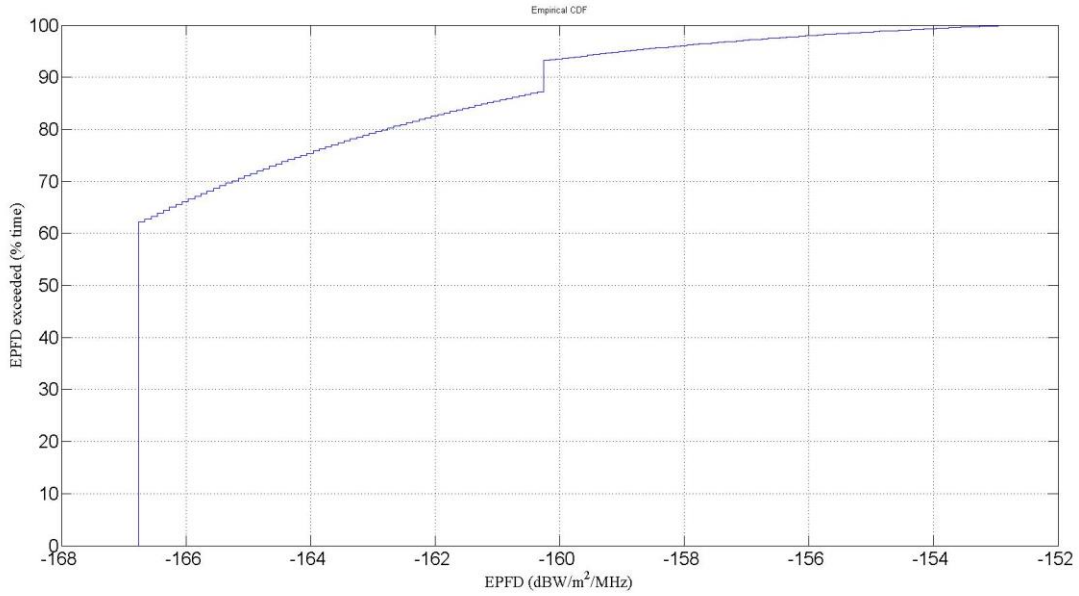

It was shown that the maximum epfd value was approximately −152 dB(W/m^2/MHz).

(2) *C/(N+I)*

FIGURE A5-9

Uplink *C/(N+I)*

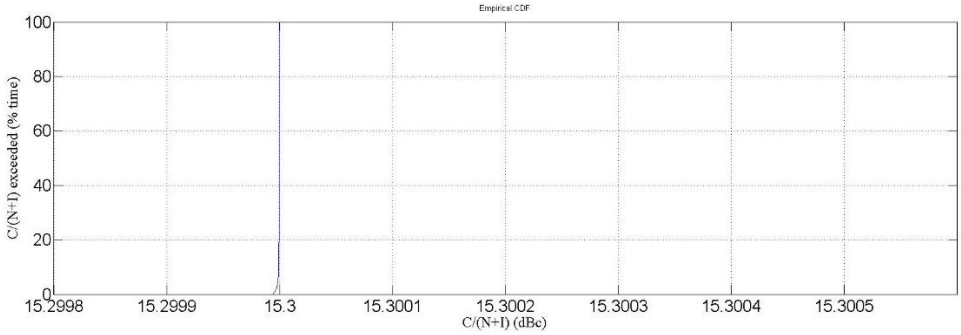

5 Conclusion

It could be deduced that, the interference from low latitude area of global covering non-GSO system is more to GSO system, especially in uplink, and that could be explained by the following equation:

$$\frac{I}{N} = (EIRP + G_r - FSL)/N \quad (9)$$

where:

G_r : relative Gain in receiving end of GSO beam of uplink

FSL : free space loss, which is affected by wave length and propagation distance.

Under the same bandwidth and noise temperature, the uplink noise powers in low latitude GSO beam and medium latitude GSO beam are same. But the free space loss of interference of both beams are different, that is because the key sources of interference to low latitude GSO beam are mainly from the uplink earth stations of non-GSO system in low latitude area, whose signals propagate shorter distance to reach the GSO. There is similar situation on the parameter G_r, which means interference signals into low latitude GSO beam have smaller avoidance angle and bigger G_r at most times. The comparing of CDF of *I*/*N* in uplink from different GSO beams was completed in Fig. A5-10.

FIGURE A5-10

Contrast of CDF of *I*/*N* from different GSO beams

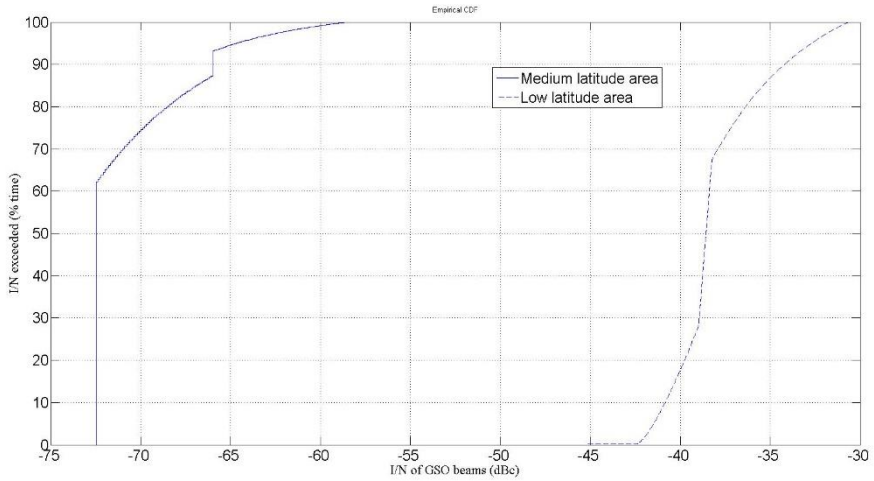

Table A5-8 showed the unavailability contrast between GSO beams pointing low latitude area and medium latitude area. From Table A5-8, the percentage of increase in unavailability at low latitude area GSO beam was higher than that of medium latitude area in uplink.

TABLE A5-8

Contrast in unavailability

GSO beam pointing	**Low latitude area**		**Medium latitude area**	
Direction	**Uplink**	**Downlink**	**Uplink**	**Downlink**
Unavailability with no interference (%)	0.994	1.961	1.024	2.102
Unavailability with interference (%)	1.042	1.967	1.025	2.114
Increase in unavailability (%)	0.048	0.006	0.001	0.012
Percentage increase unavailability (%)	4.6	0.31	0.1	0.57

On the assumption that the criterion is 10% increase of the unavailability caused by the interference, the unavailability from both low latitude GSO beam and medium latitude GSO beam apparently met that standard. Based on the above assumption, the interference from the non-GSO system depicted in this document was acceptable. Although the downlink pfd values of non-GSO system did not meet the pfd requirement in RR Table **21-4**, the compatibility between these two system depicted in this document was achieved. Given that the downlink transmitting power of non-GSO system is decreased to guarantee the pfd limits in RR Table **21-4** and the other parameters without any modifications, the sharing of non-GSO and GSO systems could definitely be realized.

With the precondition of the parameters of non-GSO and GSO systems depicted in this paper, the calculated values of epfd limits were −152 dB(W/m^2/MHz) for uplink and −148 dB(W/m^2/MHz) for downlink. The calculation results is just for one specific case of frequency sharing between non-GSO and GSO systems, it is necessary for consequent analysis and calculation for different cases to be conducted in the future research.

Annex 6

Study 6: Interference by a non-GSO system to a GSO system in the 50/40 GHz frequency band

1 Non-GSO system

The non-GSO system is a circular orbit system with parameters similar to the **3ecom-3** satellite system but scaled to the 50/40 GHz band. The reference for this configuration was taken from IFIC 2809 for **3ecom-3** satellite network. In this simulation, orbit parameters have been extracted from the related filing. Moreover, parameters for earth station and satellite have been extracted with a few modifications. This satellite system is a constellation of 288 satellites with orbit parameters in Table A6-1:

TABLE A6-1

Non-GSO system orbit parameters

Height (km)	1050
Number of satellites	288
Number of plane	12
Number of satellite per plane	24
Inclination angle (degree)	89
Eccentricity	0

Also, non-GSO parameters for earth stations and satellites have been shown in the Tables A6-2 and A6-3:

TABLE A6-2

Non-GSO parameters for satellites

Frequency (GHz)		48/38
Bandwidth (MHz)		125
Transmit peak gain (dBi)		39.7
Receive peak gain (dBi)		41.7
ATPC (dBW)	Min power	6
	Max power	16
	Receive level	−90
Number of beams per satellite		8
Dish size (m)		0.3
Efficiency		0.65
Gain pattern		Rec. ITU-R S.1528 Ls = −25
Noise temperature (K)		600

TABLE A6-3

Non-GSO parameters for earth stations

Frequency (GHz)		48/38
Bandwidth (MHz)		125
Transmit peak gain (dBi)		53.7
Receive peak gain (dBi)		51.7
ATPC (dBW)	Min power	10
	Max power	20
	Receive level	−84
Number of beams per satellite		8
Dish size (m)		1.2
Efficiency		0.65
Gain pattern		ITU-R S.580
Noise temperature (K)		300

Furthermore, two scenarios have been considered for tracking strategy of the above-mentioned non-GSO system:

Scenario 1:

– Minimum elevation angle: 20°

– GSO avoidance angle: 2°

– The related satellite is chosen based on the highest elevation angle.

Scenario 2:

– Minimum elevation angle: 40°

– GSO avoidance angle: 10°

– The related satellite is chosen based on the highest elevation angle.

Worst case geometry

Based on Recommendation ITU-R S.1503 WCG locations for this non-GSO satellite system have been determined. WCG locations are calculated as following:

TABLE A6-4

WCG of non-GSO system

WCG	Latitude	Longitude
Worst earth station	10	20
Worst GSO	–	30

In the proposed scenario, GSO earth station has been considered at WCG near the −3dB GSO Beam footprint It is assumed that 64 non-GSO earth stations are located in Region of (lat: −10, long: 0) to (lat: 30, long: 40) around the WCG, with the one co-located with GSO earth station.

Deployment of GSO and non-GSO earth stations has been shown in Fig. A6-1.

FIGURE A6-1

Deployment of non-GSO and GSO ES

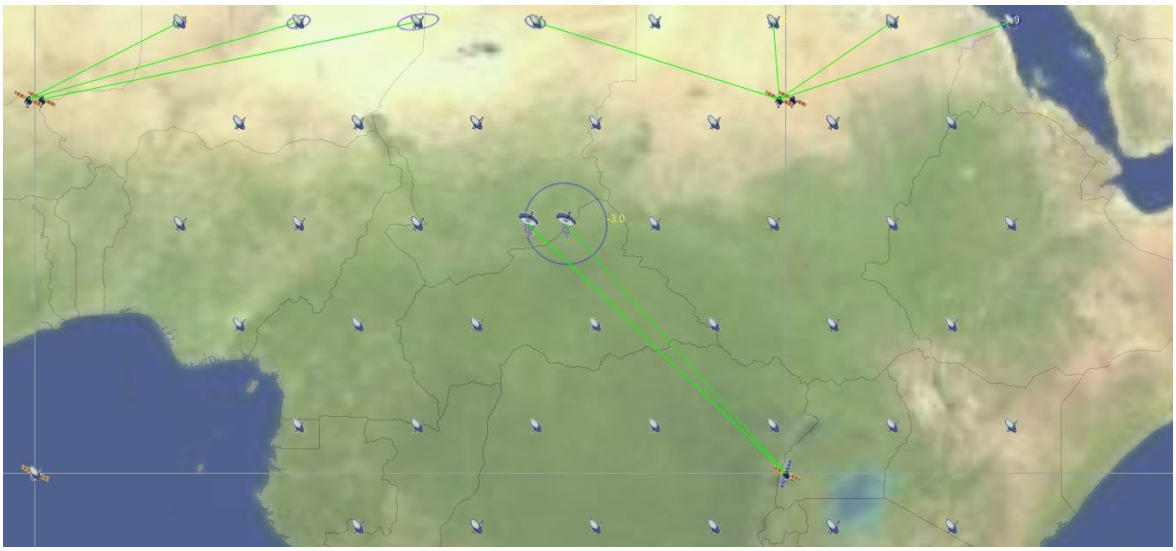

Based on the characteristics of non-GSO system discussed in above-mentioned Tables and deployment of non-GSO ES's at WCG, a snapshot of resulting link budget for one ES has been shown in Table A6-5.

TABLE A6-5

Link budgets for non-GSO

Example link budget	UL	DL	Units
Frequency	48	38	GHz
Bandwidth	125	125	MHz
Transmit power	10	6	dBW
Transmit peak gain	53.7	39.6	dBi
Transmit relative gain contour	0.0	0.0	dB
Path loss	187.8	184.57	dB
Rec. ITU-R P.525	186.1	184	dB
Rec. ITU-R P.618	1.75	0.57	dB
Receive peak gain	41.7	51.7	dBi
Receive relative gain contour	0.0	0.0	dB
C (signal strength)	−82.4	–87.2	dBW
N	−119.8	–122.8	dBW
C/*N*	37.4	35.6	dB

2 GSO system parameters

Having considered WCG for non-GSO system, GSO system was assumed to be in an orbital position that concludes the worst result; orbital position of 30° E in this case.

GSO parameters for satellite have been shown in Table A6-6.

TABLE A6-6

GSO parameters for satellites

Frequency (GHz)		48/38	
Bandwidth (MHz)		110	
Transmit peak gain (dBi)		49.7	
Receive peak gain (dBi)		51.8	
ATPC (dBW)	Direction	GatewayToUser	UserToGateway
	Min power	18	4
	Max power	28	14
	Receive level	−110	−107.5
Number of beams per satellite		8	
Efficiency		0.65	
Gain pattern		Rec. ITU-R S.672-4 Ls = −25	
Noise temperature (K)		523	

Moreover, two types of earth stations were considered: User Terminal and Gateway. GSO parameters for User Terminal and Gateway have been shown in Tables A6-7 and A6-8.

TABLE A6-7

GSO parameters for User Terminal

Frequency (GHz)		48/38
Bandwidth (MHz)		110
Transmit peak gain (dBi)		45.2
Receive peak gain (dBi)		43
ATPC (dBW)	Min power	28
	Max power	38
	Receive level	−107
Efficiency		0.65
Gain pattern		Rec. ITU-R S.580
Noise temperature (K)		350

TABLE A6-8

GSO parameters for Gateway

Frequency (GHz)		48/38
Bandwidth (MHz)		110
Transmit peak gain (dBi)		59
Receive peak gain (dBi)		57
ATPC (dBW)	Min power	17.7
	Max power	27.7
	Receive level	−87.4
Efficiency		0.65
Gain pattern		Rec. ITU-R S.580
Noise temperature (K)		350

With regard to the fact that GSO Station are located at WCG according to Fig. A6-1 the resulting link budgets for User Terminal and Gateway GSO Links have been shown in Table A6-9.

TABLE A6-9

GSO link budgets

Earth Station Type	User Terminal		Gate Way	
Direction	**UL**	**DL**	**UL**	**DL**
Earth Station Size (m)	0.45	0.45	2.2	2.2
Frequency (GHz)	48	38	48	38
Bandwidth (MHz)	110	110	110	110
Transmit power (dB)	38	28	27.7	14
Transmit peak gain (dBi)	45.2	50	59	50
Transmit relative gain (dBi)	0	0	0	0
Path loss (dB)	242	233	238.4	230.4
Rec. ITU-R P.525 (dB)	217.2	215	217.2	215
Rec. ITU-R P.618 (dB)	24.8	18	21.2	15.3
Rec. ITU-R P.618 Percentage (%)	0.4	0.4	0.4	0.4
Get Rain Rate from ITU-R P.837-6 (mm/h)	43.8	43.8	43.8	43.8
Receive peak gain	52	43	52	57
Receive relative gain	−3	−3	−3	−3
C (signal strength)	−110.8	−114.4	−103.7	−112
N	−121	−122.7	−120.6	−122.7
C/*N*	10.2	8.29	16.8	10.7

3 Propagation models

Apart from free space loss, the impact of rain attenuation in the 50/40 GHz frequency bands is also noticeable compared to other propagation models.

Therefore, in our simulation we have considered free space loss based on Recommendation ITU-R P.525 and rain attenuation model based on Recommendation ITU-R P.618 for wanted and interferer signals.

It should be mentioned that rain rate come from Recommendation ITU-R P.837 and associated percentage of time have been generated by random Monte Carlo analysis.

The 50/40 GHz band frequencies will involve significant rain fades and automatic transmit power control (ATPC) will be one of the techniques used to compensate deep fades.

4 Simulation run time

According to Recommendation ITU-R S.1503, WCG (downlink) and time step have been calculated by orbit parameters. It is considered that constellation would be repeatable and return to its original configuration.

The run duration was taken from the repeat period of non-GSO system. For a satellite to return to the same position approximately, the run time duration is about two days. Thus, the time step and the number of time step for uplink and downlink directions have been calculated as shown in Table A6-10:

TABLE A6-10

Time step

Direction	Uplink	Downlink	
Frequency (GHz)	48	38	
Earth station type	Non-GSO	GSO	
Dish size (m)	1.2	2.2	0.45
Beamwidth (degree)	0.46	0.251	1.22
Non-GSO height (km)	1050	1050	1050
Non-GSO inclination (degree)	89	89	89
Nhit	16	16	16
Time step (s)	0.05	0.05	0.22
Number of time steps	3456000	3456000	785454

5 Statistics collection

The link statistics of GSO system uplink and downlink were considered as Table A6-11:

TABLE A6-11

Run statistics collection

Direction	Uplink			Downlink		
Link Statistics	**epfd**	***C/(N+I)***	***C/N***	***epfd***	***C/(N+I)***	***C/N***
Reference bandwidth	1 MHz	n/a	n/a	1 MHz	n/a	n/a
CDF resolution	0.1 dB	0.1 dB	0.1 dB	0.1 dB	0.1 dB	0.1 dB
Thresholds	n/a	15 dB	15 dB	n/a	7.5 dB	7.5 dB

6 Results

Simulations have been run for two scenarios of tracking strategy. In addition, two types of earth stations have been considered in simulations: User Terminal and Gateway.

The results of simulation for two scenarios of tracking strategy for User Terminal and Gateway earth stations were shown as follows.

6.1 Scenario 1

Tracking strategy has been developed based on scenario 1. Results of epfd, *C*/*N* and *C*/*(N+I)* for Gateway and User Terminal have been shown as following.

6.1.1 Downlink for Gateway

6.1.1.1 CDF of epfd

FIGURE A6-2

CDF of downlink epfd for Gateway

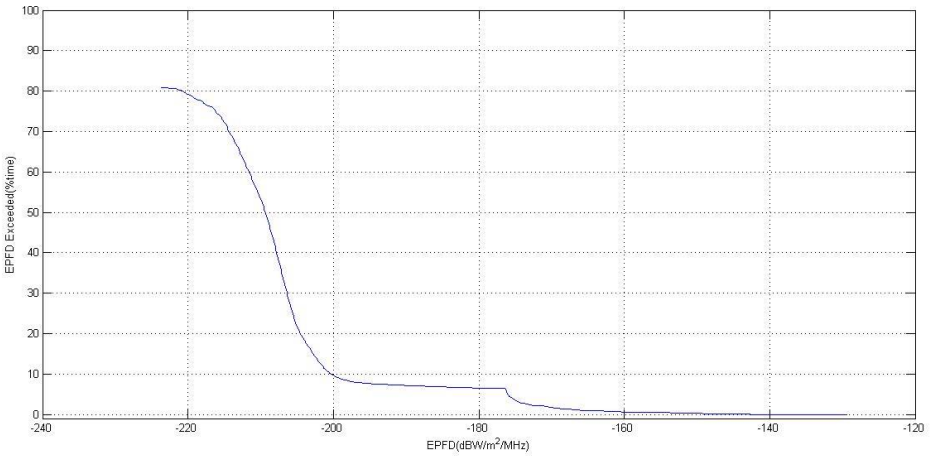

It has been shown (see Fig. A6-2) that the maximum epfd value is approximately −130 dB(W/m^2/MHz) which is more than thresholds in RR Article **22** for Ka band.

6.1.1.2 CDF of *C*/*N* and *C*/(*N*+*I*)

FIGURE A6-3

CDF of *C*/*N* and *C*/(*N*+*I*) for the Gateway GSO DL

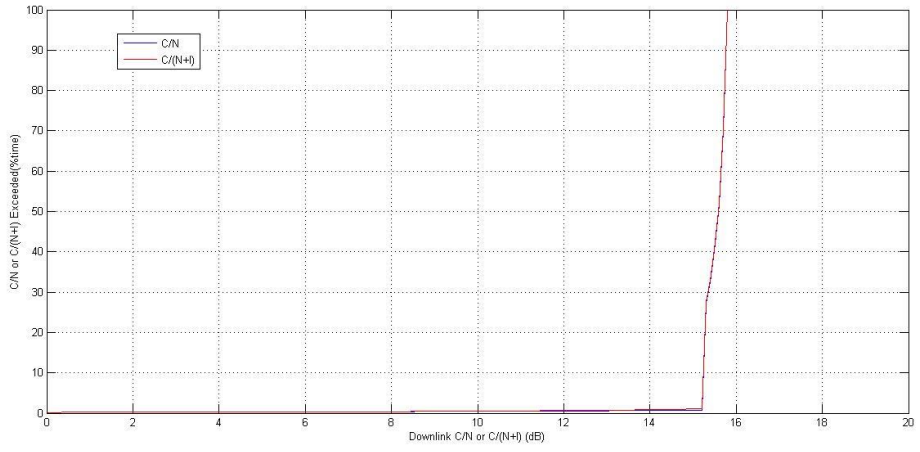

6.1.2 Uplink for Gateway

6.1.2.1 CDF of epfd

FIGURE A6-4

CDF of uplink epfd for Gateway

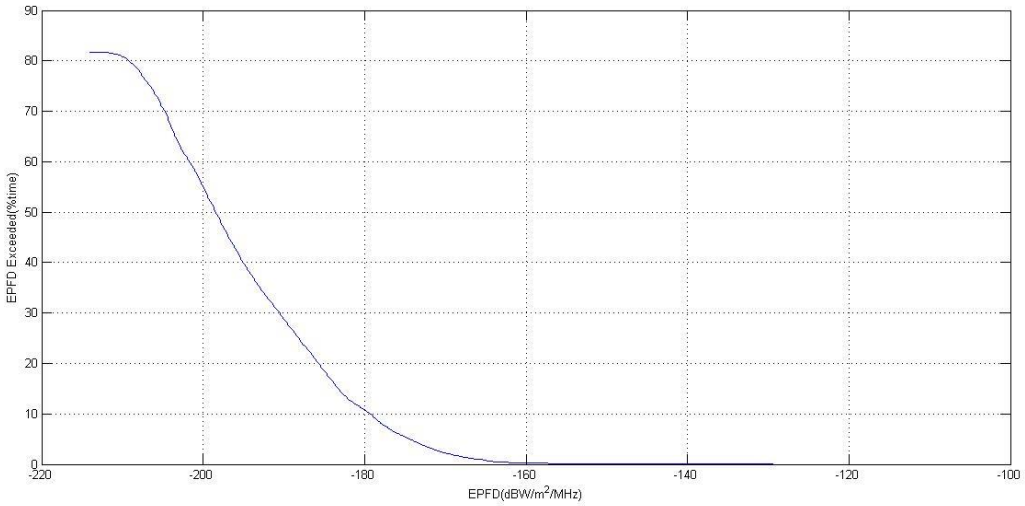

It has been shown in Fig. A6-4 that the maximum epfd value is approximately −130 dB(W/m^2/MHz) which is more than thresholds in RR Article **22** for Ka band.

6.1.2.2 CDF of *C*/*N* and *C*/*(N+I)*

FIGURE A6-5

CDF of *C*/*N* and *C*/*(N+I)* for the Gateway GSO UL

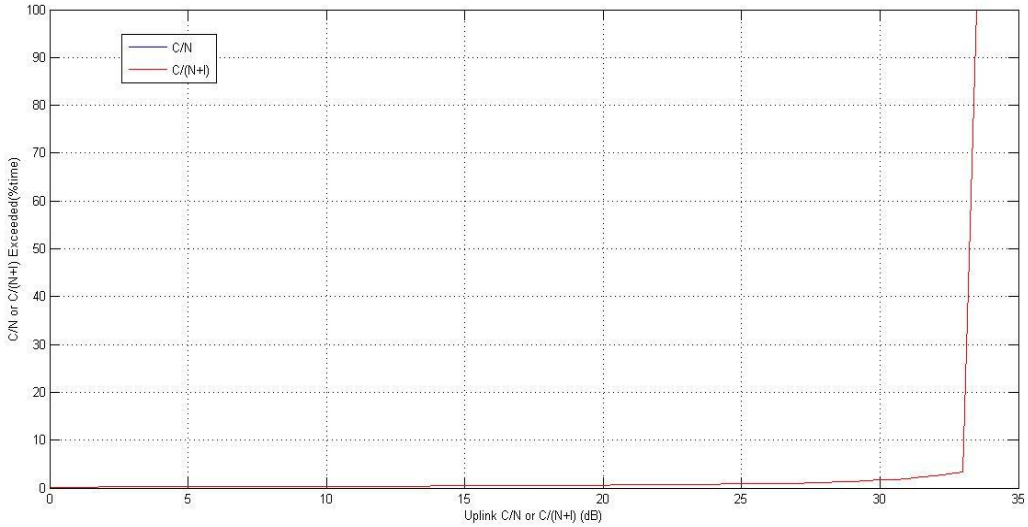

6.1.3 Downlink for user terminal

6.1.3.1 CDF of epfd

FIGURE A6-6

CDF of downlink epfd for user terminal

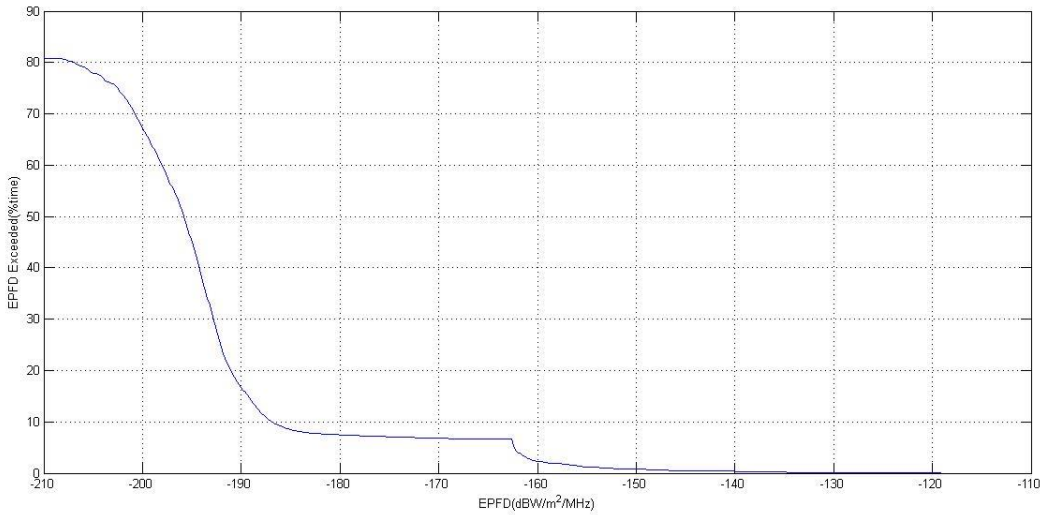

It has been shown (see Fig. A6-6) that the maximum epfd value is approximately −130 dB(W/m^2/MHz) which is more than thresholds in RR Article **22** for Ka band.

6.1.3.2 CDF of *C*/*N* and *C*/(*N*+*I*)

FIGURE A6-7

CDF of *C*/*N* and *C*/(*N*+*I*) for the User Terminal GSO DL

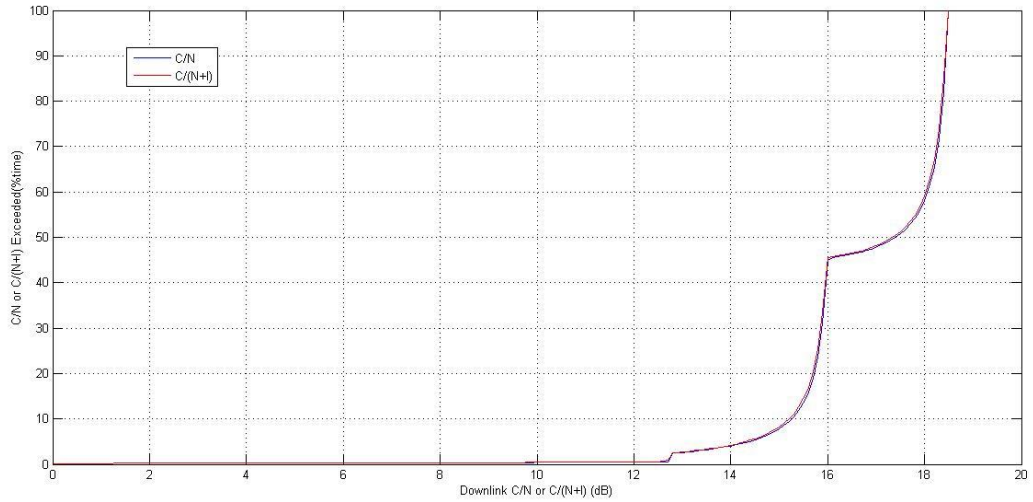

6.1.4 Uplink for User Terminal

6.1.4.1 CDF of epfd

FIGURE A6-8

CDF of uplink epfd for User Terminal

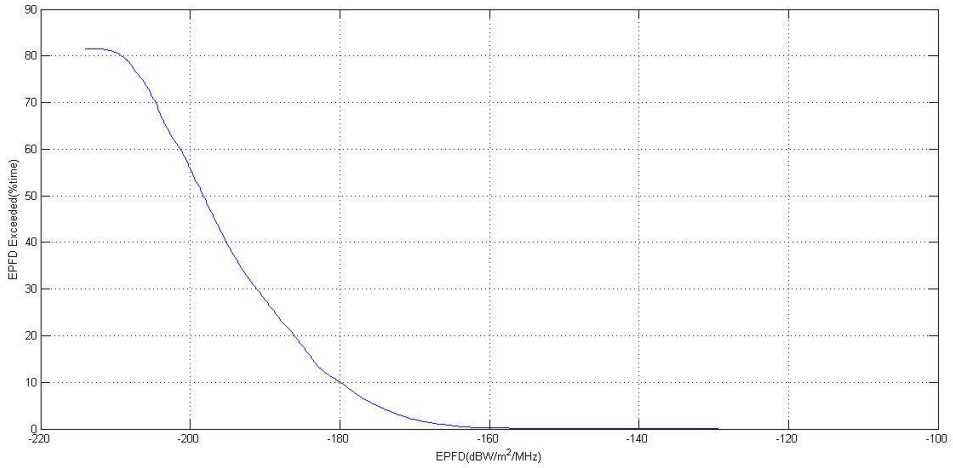

It has been shown (see Fig. A6-8) that the maximum epfd value is approximately −130 dB(W/m^2/MHz) which is more than thresholds in RR Article **22** for Ka band.

6.1.4.2 CDF of *C*/*N* and *C*/*(N+I)*

FIGURE A6-9

CDF of *C*/*N* and *C*/*(N+I)* for the User Terminal GSO UL

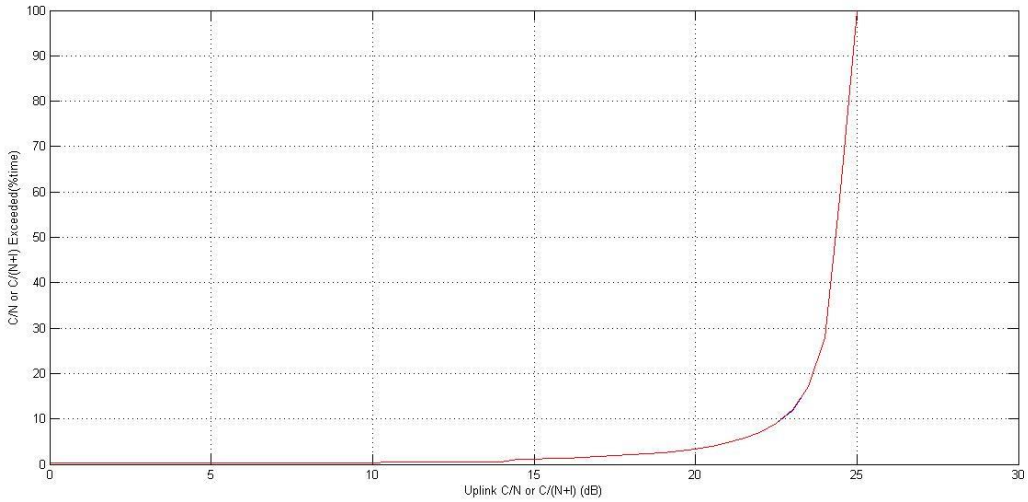

6.2 Scenario 2

Tracking strategy has been developed based on scenario 2. Results of epfd, *C*/*N* and *C*/*(N+I)* for gateway and User Terminal have been shown as following.

6.2.1 Downlink for gateway

6.2.1.1 CDF of epfd

FIGURE A6-10

CDF of downlink epfd for gateway

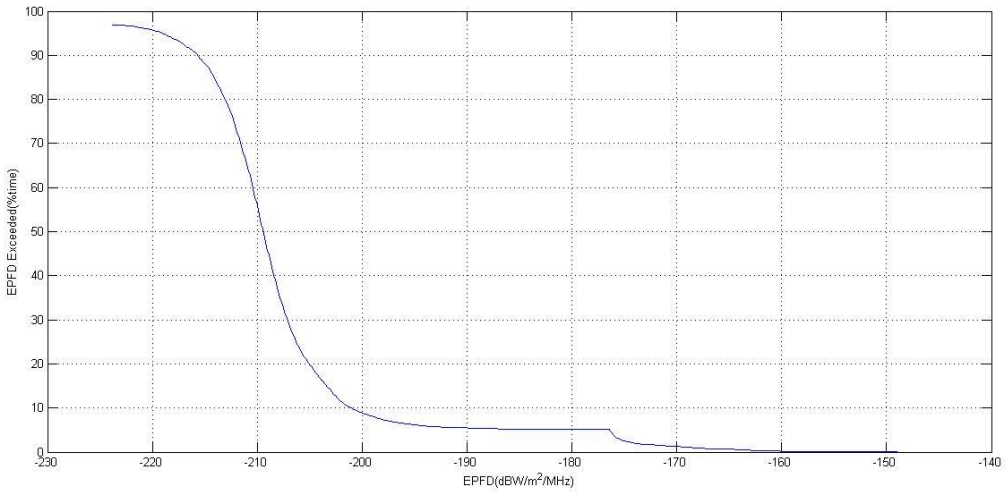

It has been shown (see Fig. A6-10) that the maximum epfd value is approximately −150 dB(W/m^2/MHz) which is lower than thresholds in RR Article **22** for Ka band.

6.2.1.2 CDF of *C*/*N* and *C*/(*N*+*I*)

FIGURE A6-11

CDF of *C*/*N* and *C*/(*N*+*I*) for the Gateway GSO DL

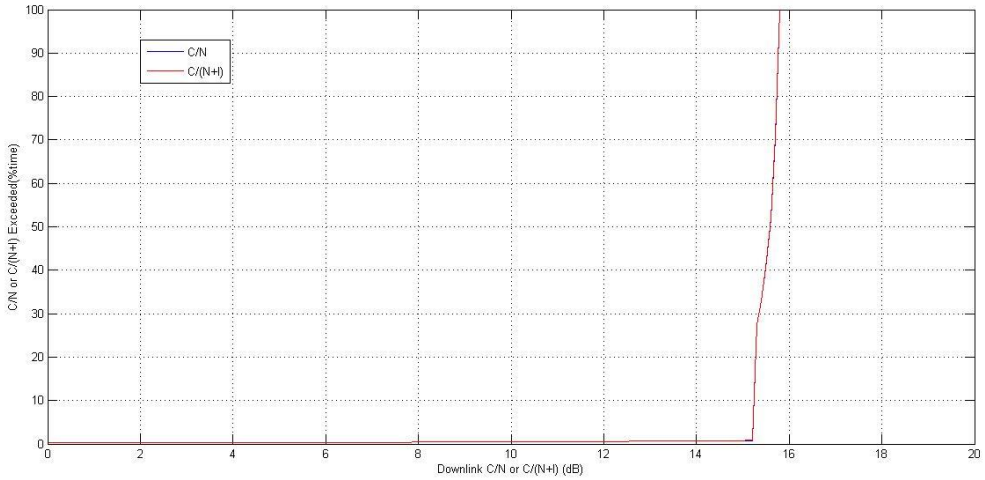

6.2.2 Uplink for Gateway

6.2.2.1 CDF of epfd

FIGURE A6-12

CDF of uplink epfd for Gateway

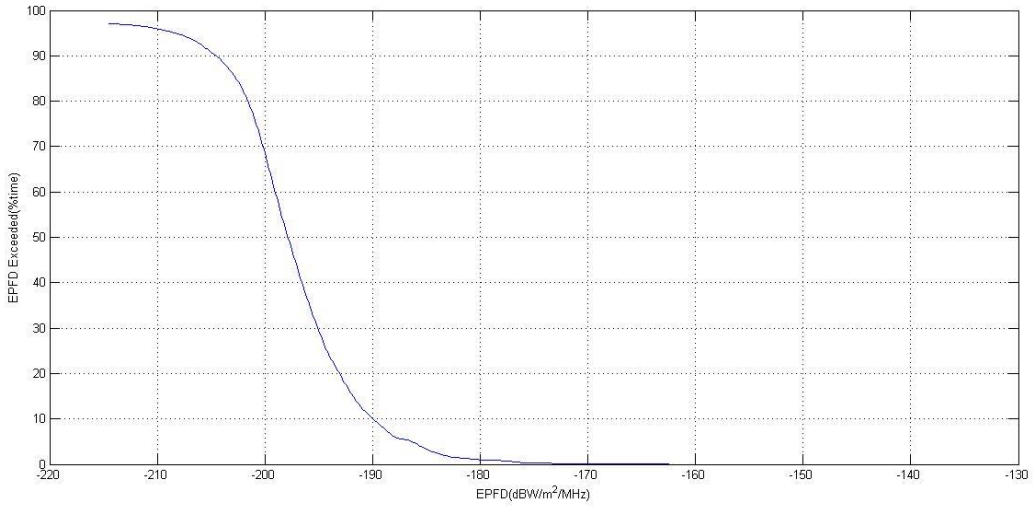

It has been shown (see Fig. A6-12) that the maximum epfd value is approximately −170 dB(W/m^2/MHz) which is lower than thresholds in RR Article **22** for Ka band.

6.2.2.2 CDF of *C*/*N* and *C*/*(N+I)*

FIGURE A6-13

CDF of *C*/*N* and *C*/*(N+I)* for the gateway GSO UL

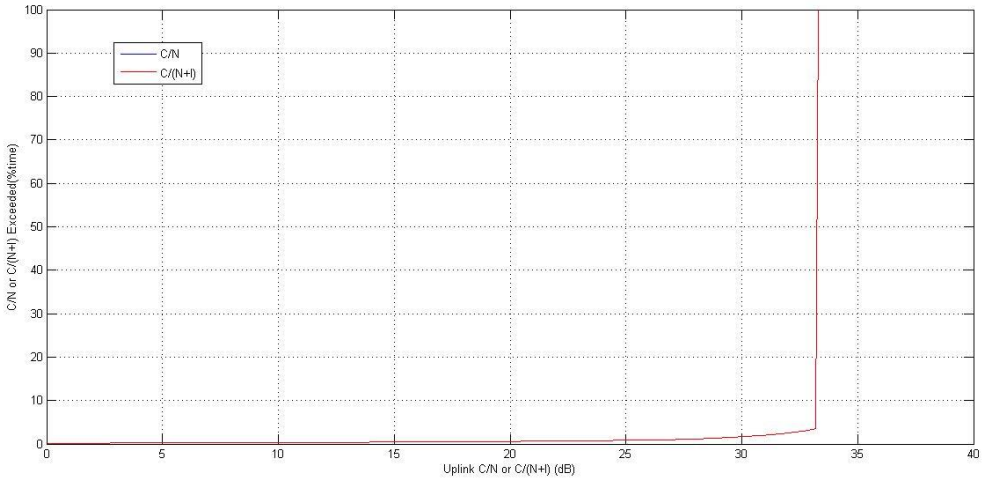

6.2.3 Downlink for User Terminal

6.2.3.1 CDF of epfd

FIGURE A6-14

CDF of downlink epfd for user terminal

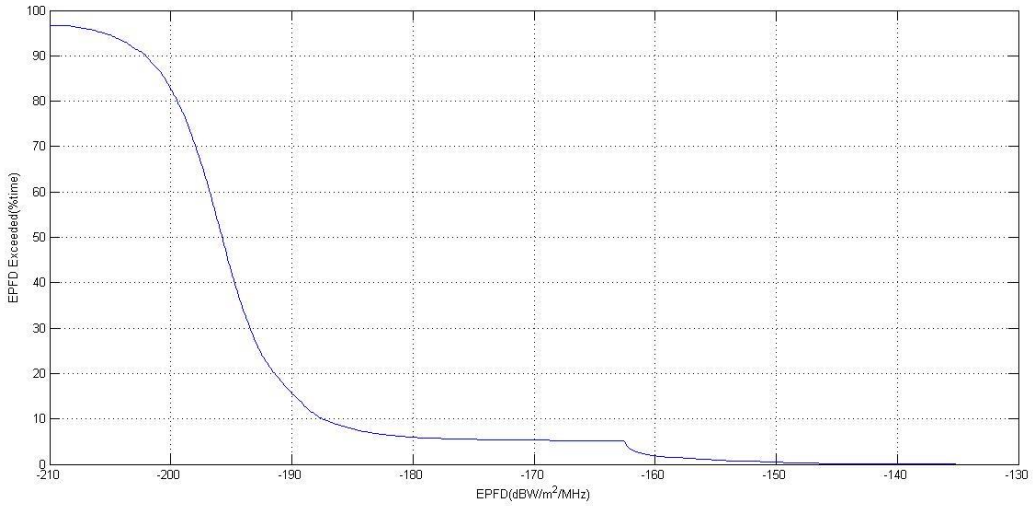

It has been shown (see Fig. A6-14) that the maximum epfd value is approximately −140 dB(W/m^2/MHz) which is similar to thresholds in RR Article **22** for Ka band.

6.2.3.2 CDF of *C*/*N* and *C*/(*N*+*I*)

FIGURE A6-15

CDF of *C*/*N* and *C*/(*N*+*I*) for the User Terminal GSO DL

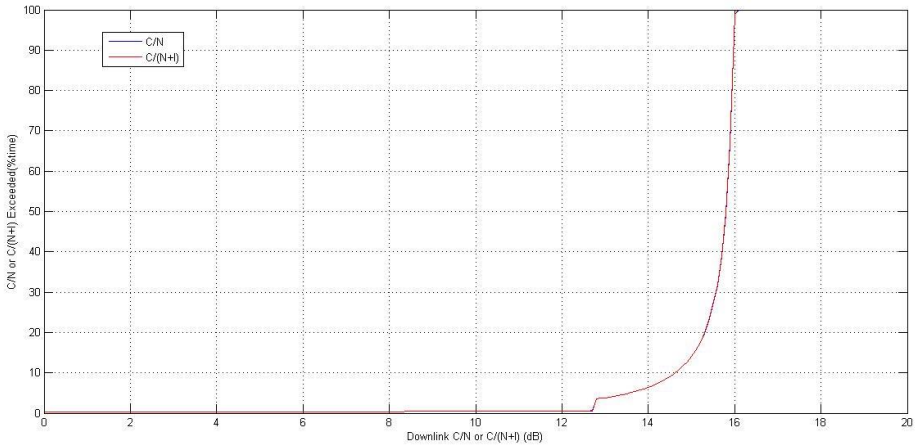

6.2.4 Uplink for User Terminal

6.2.4.1 CDF of epfd

FIGURE A6-16

CDF of uplink epfd for User Terminal

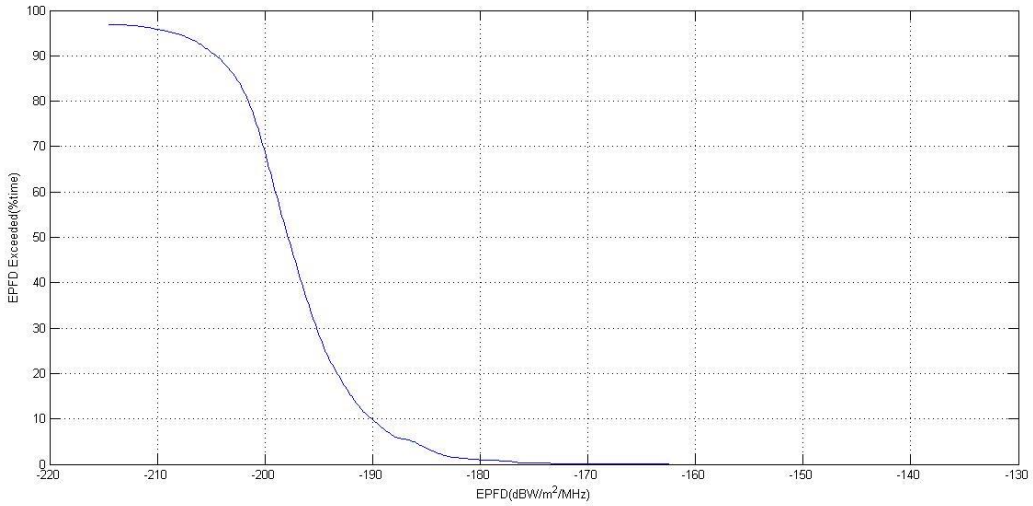

It has been shown (see Fig. A6-16) that the maximum epfd value is approximately −170 dB(W/m^2/MHz) which is lower than thresholds in RR Article **22** for Ka band.

6.2.4.2 CDF of *C*/*N* and *C*/(*N*+*I*)

FIGURE A6-17

CDF of *C*/*N* and *C*/(*N*+*I*) for the User Terminal GSO UL

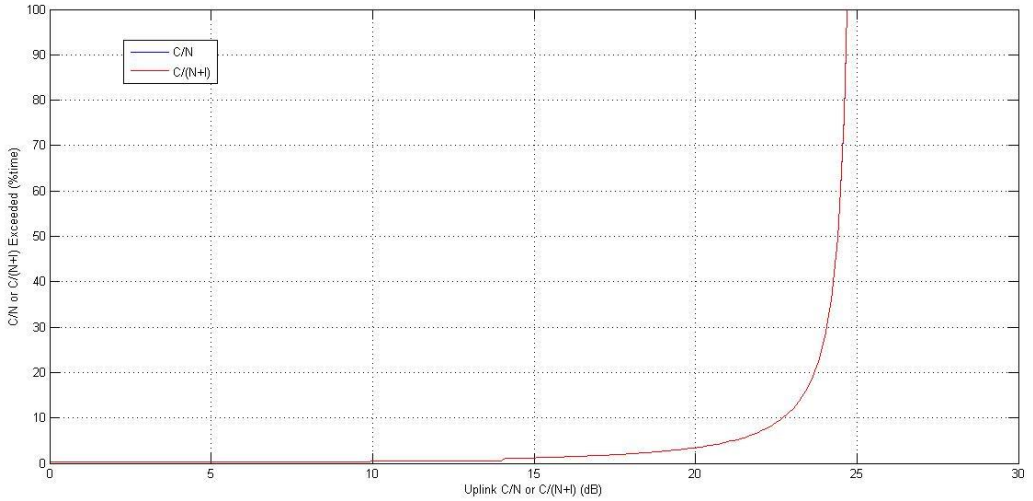

7 Conclusion

According to above-mentioned results, the increase in unavailability of GSO system for two scenarios could be shown in Table A6-12.

TABLE A6-12

Increase in unavailability

Scenario	**Scenario 1**				**Scenario 2**			
Earth Station Type	**GateWay**		**User Terminal**		**GateWay**		**User Terminal**	
Direction	Up	Dn	Up	Dn	Up	Dn	Up	Dn
Unavailability with no interference (%)	0.4774	0.372	0.51	0.375	0.43220	0.4710	0.4945	0.35150
Unavailability with interference (%)	0.4776	0.374	0.53	0.430	0.43225	0.4715	0.4960	0.35225
Increase in unavailability (%)	0.041	0.53	3.9	14.6	0.011	0.1	0.3	0.21

– Based on Recommendation ITU-R S.1323, if criterion is 10% increase in the unavailability caused by interference, the increase in unavailability from non-GSO system for scenario 1 has not been met but for scenario 2 it has been met. Then the interference from non-GSO system with scenario 2 tracking strategy depicted in this document is acceptable.

– The effects of interference on User Terminal antenna are more than Gateway antenna.

– By the change in some of the parameters in tracking strategy, it is possible to decrease interference from a non-GSO system. Therefore, it could be concluded that frequency sharing between GSO and non-GSO satellite networks is possible provided that appropriate changes would be made on some of the parameters in tracking strategy

Annex 7

Study 7: Sharing studies relevant to developing aggregate V-band epfd limits

1 Introduction

Operation of V-Band non-GSO systems has the potential to cause interference to GSO networks operating in this band – downlinks in 37.5-42.5 GHz (space-to-Earth), and uplinks in 47.2-50.2 GHz and 50.4-51.4 GHz (both Earth-to-space). The ITU has addressed similar concerns in FSS bands below 30 GHz by imposing epfd limits on non-GSO systems.

For frequency bands below 30 GHz, Radio Regulations Article **22** contains technical provisions for sharing between non-GSO systems and GSO networks. These technical provisions quantify RR No. **22.2**, and include single entry epfd limits that are derived from aggregate protection levels based on an assumed number of effective non-GSO systems of 3.5. RR No. **22.5C** specifies per system $epfd_{\downarrow}$ limits and

Resolution **76 (Rev.WRC-15)** specifies aggregate $epfd_{\downarrow}$ limits. RR No. **22.5D** specifies per system $epfd_{\uparrow}$ limits.

Radio Regulations No. **22.2** also applies in the V-band FSS frequencies above. Based on results from lower frequency bands, there are several options for defining technical provisions for sharing between non-GSO and GSO FSS networks in the 50/40 GHz frequency bands based on studies that have been carried out in ITU-R.

Recommendation ITU-R S.1323 Methodology A presents maximum permissible levels of interference between non-GSO and GSO FSS networks. This Recommendation was used as a basis for the development of epfd levels for frequency bands below 30 GHz. In this Recommendation, the protection criteria was based on a time allowance related to the BER (or *C*/*N*) performance of a satellite network. Using a single percentage time allowance based on a BER (or *C*/*N*) corresponding to unavailability as the metrics is designed to protect GSO networks providing constant bit rate services.

Modern GSO FSS networks tend to carry Internet traffic, so maintaining connections is more important than providing a constant bit rate. Given the large propagation losses experienced in V-band, these systems may utilize mitigation techniques such as adaptive coding and modulation (ACM) and power control to overcome the effects of propagation losses and interference.

This study investigates an alternative to the time allowance for degradation exceeding the minimum short-term performance objectives approach for establishing epfd limits. It considers an average decrease in the throughput approach that may be more applicable to networks implementing ACM.

2 GSO network parameters

2.1 Impact of degradation on data rate

Today's two-way satellite connections mainly carry Internet traffic, so maintaining connections is more important than providing a constant bit rate. Thus, even small amounts of link degradation, due to rain fades or interference, can have significant impact on GSO network performance. Modern GSO networks utilize adaptive coding and modulation (ACM), with power amplifier linearization techniques, to improve spectral efficiency and transmission performance. Linearization techniques allow the use of higher order, more spectrally efficient, modulations.

ACM combats the link degradation resulting from propagation fades and aggregate interference by maintaining the connection, but with reduced throughput. This decrease in throughput results in decreased satellite capacity. The impact of degradation is related to decrease in satellite link capacity by the slope of the ACM modem operating curve. Modem performance has improved significantly over the last two decades and is expected to continue improving in the future. Today's state-of-the-art modems provide DVB-S2X class performance.

Future modem performance is bounded by the Shannon limit, which relates the maximum achievable spectral efficiency to the available *C*/*N* (in this context, N is the total noise in the link, including thermal and interference). The Shannon limit is:

$$\varepsilon(bps/Hz) \;=\; \log_2\left(1 + 10^{C/N\,(dB)/10}\right) \tag{10}$$

The sensitivity of spectral efficiency to *C*/*N* of an ideal (Shannon limit) modem is given by

$$\dot{\varepsilon}\left(\frac{bps}{Hz}/dB\right) = \frac{d\varepsilon}{d(C/N)} = \frac{\ln(10)\times 10^{C/N\,(dB)/10-1}}{\ln(2)\times\left(1+10^{\,C/N(dB)/10}\right)} \tag{11}$$

And the relative sensitivity by

$$S\left(\frac{1}{dB}\right) = \frac{\ln(10)\times 10^{C/N\,(dB)/10-1}}{\ln(2)\times\left(1+10^{C/N\,(dB)/10}\right)\times\log_2\left(1+10^{C/N\,(dB)/10}\right)} \tag{12}$$

Figure A7-1 shows the Shannon limit curve, the DVB-S2X modem MODCOD's, and the least squares 2nd degree polynomial fit to the MODCOD's.

FIGURE A7-1

Modem operating curve

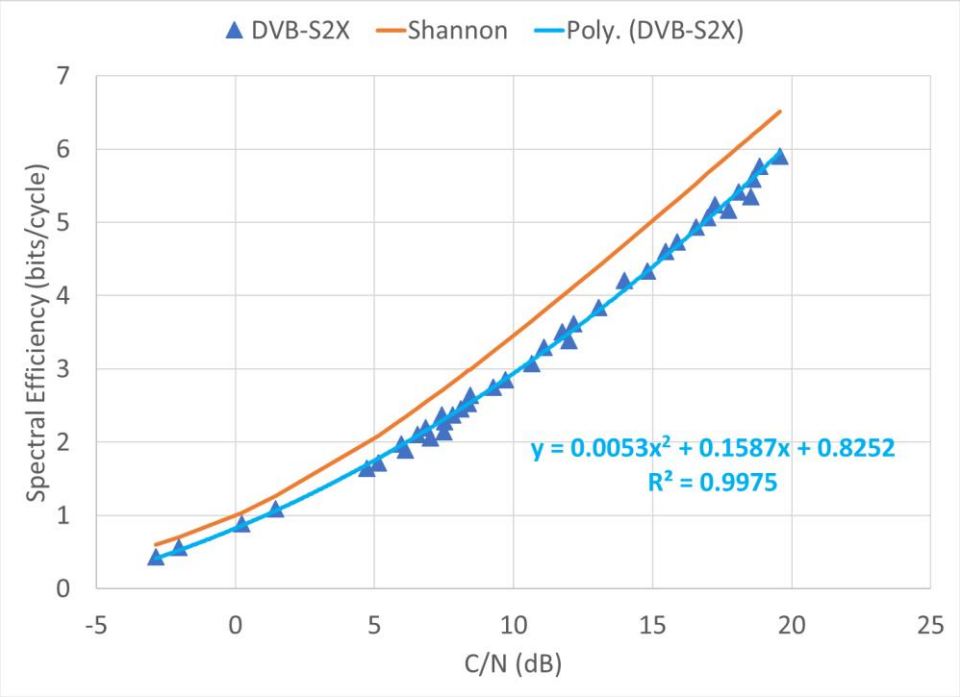

The fit equation,

$$\varepsilon\,(bps/Hz) = 0.0053 \times (C/N)^2 + 0.1587 \times (C/N) + 0.8252 \tag{13}$$

facilitates calculation of the sensitivity of spectral efficiency of the DVB-S2X modem to *C*/*N*:

$$\dot{\varepsilon}\,(\frac{bps}{Hz}/dB) = 0.0106 \times (C/N) + 0.1587 \tag{14}$$

The relative sensitivity of the DVB-S2X modem is given by

$$S\left(\frac{1}{dB}\right) = \frac{0.0106\times(C/N)+0.1587}{0.0053\times(C/N)^2+0.1587(C/N)+0.8252} \tag{15}$$

The DVB-S2X and Shannon relative sensitivities of spectral efficiency to changes in *C*/*N* are shown in Fig. A7-2. This Figure shows that the sensitivity is between 5% and 19% data rate reduction per dB for an ideal (Shannon limit) modem and between a 6% and 31% per dB for a DVB-S2X modem, depending on operating point. At a typical undegraded (clear-sky, no interference) GSO operating point of 12.3 dB, the sensitivity is 8% per dB for today's state-of-the-art DVB-SX2 modems, and slightly less for an ideal (Shannon limit) modem.

FIGURE A7-2

Data rate sensitivity to changes in *C/N*

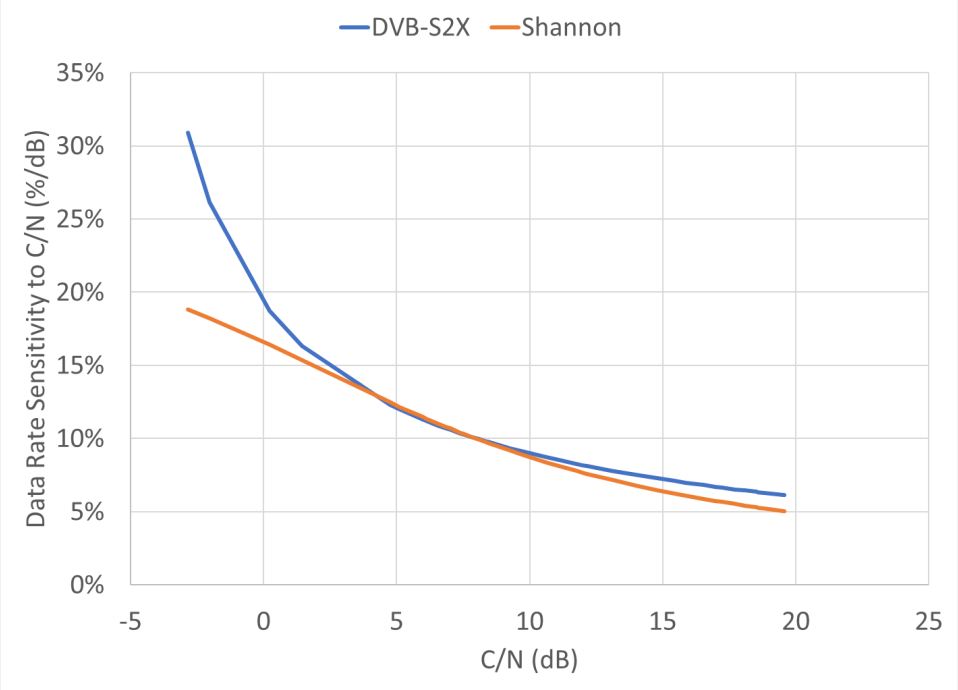

The percent degraded throughput, %DTp, is given by

$$\%DTp(\rho,\gamma) = 100\left[1 - \frac{\varepsilon(\rho-\gamma)}{\varepsilon(\rho)}\right] \quad (16)$$

where:

ρ : undegraded *C/N*

γ: degradation

ε(*x*) : spectral efficiency function.

The average percent degraded throughput ($\overline{\%DTp}$) is given by:

$$\overline{\%DTp}(\rho) = 100\left[1 - \int_0^\infty p(\gamma)\frac{\varepsilon(\rho-\gamma)}{\varepsilon(\rho)}d\gamma\right] \quad (17)$$

where:

ρ : undegraded *C/N*

p(γ) : probability density function (pdf) of degradation γ resulting from epfd, and is constrained by:

$$\int_0^\infty p(\gamma)\,d\gamma = 1 \quad (18)$$

ε(*x*) : spectral efficiency function.

The cumulative distribution function (cdf), the probability of degradation not exceeding γ, is given by:

$$cdf(\gamma) = \int_0^\gamma p(z)\,dz$$

3 epfd↓ technical analysis

The aggregate epfd↓ resulting from operation of co-frequency non-GSO FSS systems is potential interference into GSO FSS downlinks. The impact of this interference is characterized by the interference-spectral-density to thermal-noise-spectral-density ratio, I_0/N_0, which can be calculated as:

$$I_0/N_0(dB) = epfd_{\downarrow}\,(dBW/m^2) - 10\log_{10} B_R\,(Hz) + A_{eff}\,(dBm^2) - T\,(dBK) - k\,(dBW/(K{\times}Hz)) \quad (19)$$

where:

epfd↓ : aggregate effective PFD in the downlink direction (dBW/m^2)

B_R : reference bandwidth associated with the epfd↓ value (Hz)

A_{eff} : GSO satellite network ES antenna effective area (dBm^2).

$$A_{eff}(dBm^2) = 10\log_{10}\left[\frac{\pi{\times}D(m)^2{\times}\varepsilon}{4}\right] \quad (20)$$

where:

D : antenna diameter (m)

ε : antenna aperture efficiency

T : ES noise temperature (K)

K : Boltzmann's constant, −228.6 dBW/(K × Hz).

Assuming a 40-kHz reference bandwidth, 0.7 ES antenna aperture efficiency, and 250 K ES noise temperature, equation (19) reduces to:

$$I_0/N_0(dB) = epfd_{\downarrow}\,(dBW/m^2) + 20\log_{10}[D(m)] + 156\,dB \quad (21)$$

The degradation experienced by a GSO FSS downlink is a function of the I_0/N_0. It can be calculated as:

$$L(dB) = 10\log_{10}\left[1 + 10^{I_0/N_0(dB)/10}\right] \quad (22)$$

The relationship between aggregate epfd↓, ES antenna diameter, and downlink data rate reduction, assuming a typical undegraded (clear-sky, no interference) GSO modem operating point of 12.3 dB is shown in Table A7-1.

TABLE A7-1

Aggregate epfd↓ (dBW/(m^2 × 40-kHz)) that would result in indicated percentage throughput reduction (%DTp) for various ES antenna diameters (m)

Antenna diameter	Throughput reduction				
	1%	2%	3%	4%	5%
0.3 m	-161.1	-157.8	-156.1	-154.7	-153.6
0.45 m	-164.6	-161.3	-159.6	-158.2	-157.1
0.6 m	-167.1	-163.8	-162.1	-160.7	-159.6
1 m	-171.5	-168.3	-166.5	-165.1	-164.1
2 m	-177.5	-174.3	-172.5	-171.2	-170.1
5 m	-185.5	-182.3	-180.5	-179.1	-178.0

4 epfd↑ technical analysis

The aggregate epfd↑ resulting from operation of co-frequency non-GSO FSS systems is potential interference into a GSO FSS uplink. The impact of this interference is characterized by the interference-spectral-density to thermal-noise-spectral-density ratio, I_0/N_0, which can be calculated as:

$$I_0/N_0(dB) = epfd_{\uparrow}(dBW/m^2) - 10\log_{10} B_R(Hz) + G/T(dB/K) - G_1(dB/m^2) - k(dBW/(K \cdot Hz)) \quad (23)$$

where:

epfd↑ : aggregate effective PFD in the uplink direction (dBW/m^2)

B_R : reference bandwidth associated with the epfd↑ value (Hz)

G/T : GSO satellite receive beam G/T (dB/K)

G_1 : ideal gain of a 1-meter squared area at the uplink frequency (dB).

$$G_1(dB) = 10\log_{10}\left[\frac{4\pi \times F(Hz)^2}{c(m/s)^2}\right] \quad (24)$$

where:

F : uplink frequency (Hz)

C : speed of light, 299,792,458 m/s

k : is Boltzmann's constant, −228.6 dBW/(K×Hz).

Plugging in the 40-kHz reference bandwidth and using 49.26 GHz as the uplink frequency (< 0.2 dB error across the two bands), gives:

$$I_0/N_0(dB) = epfd_{\uparrow}\,(dBW/m^2) + G/T\,(dB/K) + 127.3\,dB \quad (25)$$

Alternatively, if the GSO satellite beam receive noise temperature, T (K), and effective antenna area are available, I_0/N_0, can calculated as

$$I_0/N_0(dB) = epfd_{\uparrow}(dBW/m^2) + A_{eff}(dBm^2) + 158.6\,dB \quad (26)$$

where A_{eff} is the GSO satellite receive beam antenna effective area (dBm^2) and a 250 K noise temperature has been assumed.

The degradation experienced by a GSO FSS uplink can be calculated as:

$$L(dB) = 10\log_{10}\left[1 + 10^{I_0/N_0(dB)/10}\right] \quad (27)$$

The relationship between aggregate epfd↑, satellite beam G/T, and uplink throughput reduction, assuming a typical undegraded (clear-sky, no interference) GSO modem operating point of 12.3 dB, is shown in Table A7-2.

TABLE A7-2

Aggregate epfd↑ (dBW/(m² × 40-kHz)) that would result in indicated percentage throughput reduction (%DTp) for various satellite beam G/Ts (dB/K)

G/T	Throughput Reduction				
	1%	2%	3%	4%	5%
33 dB/K	-175.8	-172.6	-170.8	-169.4	-168.4
33.5 dB/K	-176.3	-173.1	-171.3	-169.9	-168.9
34 dB/K	-176.8	-173.6	-171.8	-170.4	-169.4
34.5 dB/K	-177.3	-174.1	-172.3	-170.9	-169.9
35 dB/K	-177.8	-174.6	-172.8	-171.4	-170.4
35.5 dB/K	-178.3	-175.1	-173.3	-171.9	-170.9
36 dB/K	-178.8	-175.6	-173.8	-172.4	-171.4

5 Calculation of average percent throughput degradation from degradation statistics

The average percent throughput degradation ($\overline{\%DTp}$) is a function of the undegraded *C*/*N*, the degradation pdf, and the modem spectral efficiency function. It can be calculated using equation (8). Two models for the pdf are explored.

5.1 Model 1

Model 1 assumes that the pdf is a sum of delta functions

$$p(\gamma) = \sum_{k=1}^{N} p_k \delta(\gamma - \gamma_k) \tag{28}$$

where:

$\delta(x)$: Dirac delta function

$$\delta(x) = \begin{cases} 1 & x = 0 \\ 0 & x \neq 0 \end{cases} \tag{29}$$

γk : N degradations, constrained by: $\gamma 1 \geq 0$, $\gamma k+1 > \gamma k$, and $\gamma N \leq \infty$

pk : N probabilities constrained by:

$$\sum_{k=1}^{N} p_k = 1 \tag{30}$$

The Model 1 cdf is then an increasing staircase function, as shown in Fig. A7-3:

$$cdf(\gamma) = \sum_{k=1}^{N} p_k u(\gamma - \gamma_k) \tag{31}$$

where:

$u(x)$ is the unit step function

$$u(x) = \begin{cases} 0 & x < 0 \\ 1 & x \geq 0 \end{cases} \tag{32}$$

FIGURE A7-3

Model 1 CDF

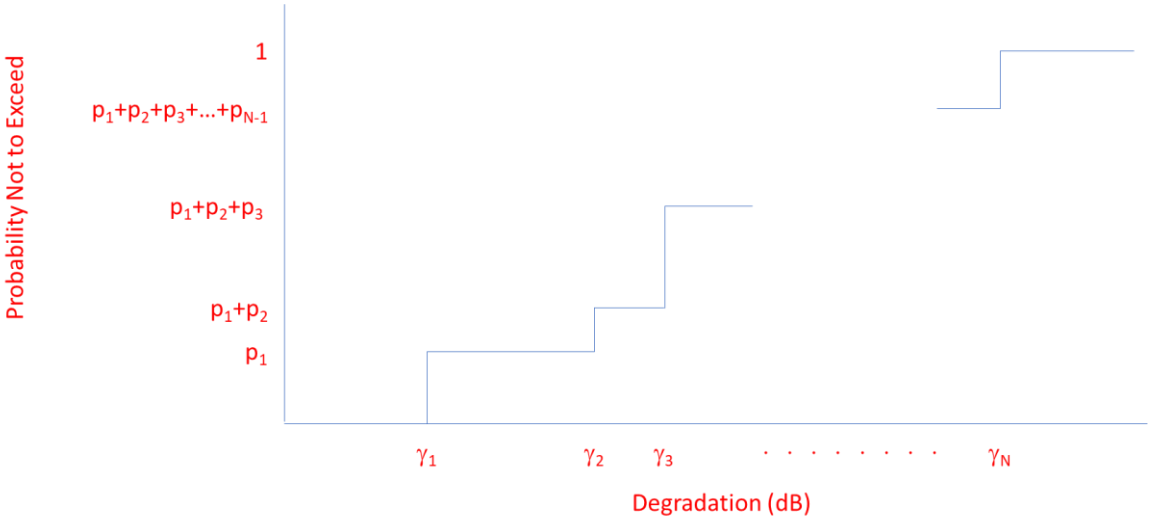

Substituting equation (28) into equation (17), gives:

$$\overline{\%DTp}(\rho) = 100\left[1 - \sum_{k=1}^{N} p_k \frac{\varepsilon(\rho - \gamma_k)}{\varepsilon(\rho)}\right] \tag{33}$$

5.2 Model 2

Model 2 assumes that the pdf is a staircase function:

$$p(\gamma) = \sum_{k=1}^{N-1} [u(\gamma - \gamma_{k+1}) - u(\gamma - \gamma_k)] \tag{34}$$

where:

γ_k : N degradations, constrained by $\gamma_1 \geq 0$, $\gamma_k > \gamma_{k-1}$, and $\gamma_N < \infty$

p_k : N-1 probabilities constrained by:

$$\sum_{k=1}^{N-1} p_k = 1 \tag{35}$$

The Model 2 cdf is then an increasing piecewise ramp function, as illustrated in Fig. A7-4:

$$cdf(\gamma) = \sum_{k=1}^{N-1} \frac{p_k}{\gamma_{k+1} - \gamma_k} [r(\gamma - \gamma_{k+1}) - r(\gamma - \gamma_k)] \tag{36}$$

Where *r(x)* is the ramp function

$$r(x) = \begin{cases} 0 & x < 0 \\ x & x \geq 0 \end{cases} \tag{37}$$

FIGURE A7-4

Model 2 CDF

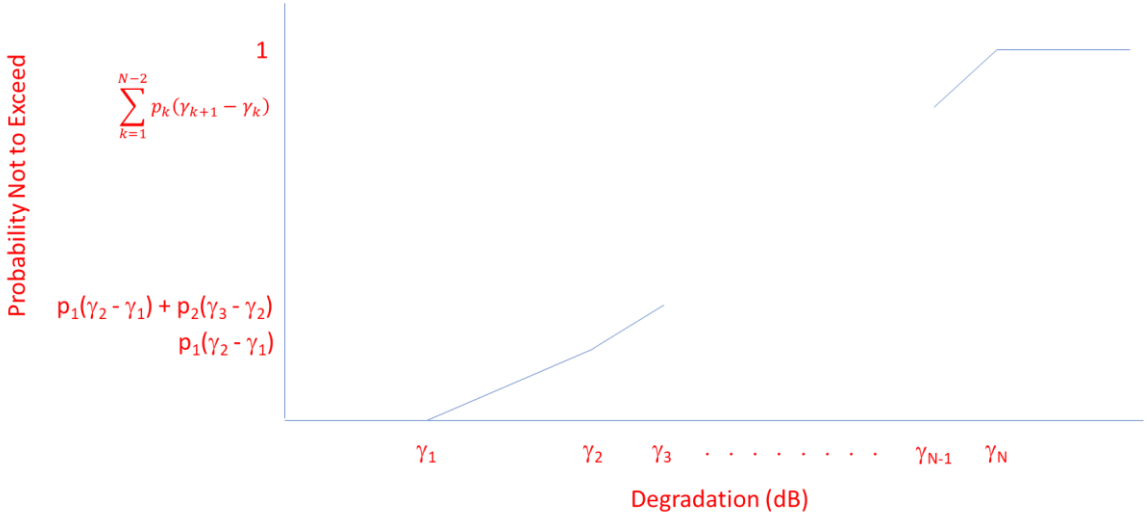

Substituting equation (10) into equation (17) gives:

$$\overline{\%DTp}(\rho) = 100\left[1 - \sum_{k=1}^{N-1} \frac{p_k}{\gamma_{k+1}-\gamma_k} \int_{\gamma_k}^{\gamma_{k+1}} \frac{\varepsilon(\rho-\gamma)}{\varepsilon(\rho)} d\gamma\right] \tag{38}$$

6 Application of the average percent throughput degradation calculation to propagation fades and interference from non-GSO systems

It should be noted that the Recommendation that governs the calculation of epfd statistics within the ITU, Recommendation ITU-R S.1503 assumes maximum power operation for non-GSO systems in all aspects of their operation. This assumption is reasonable when looking to find the worst-case, short-term, epfd generated by a non-GSO system. However, it can significantly over-estimate the long term interference introduced by non-GSO systems. The bandwidth efficiency of ACM systems is most sensitive to long-term interference. If ACM operations or mitigation of propagation impairments should be considered in the calculations of epfd statistics, the application of power control should similarly be applied to the calculation of interference statistics from non-GSO systems. This may result in a necessary revision to Recommendation ITU-R S.1503 for frequency bands above 30 GHz.

The analysis in this section looks at the impact of percent degraded throughput due to the epfd$_{\downarrow}$ from a non-GSO system utilizing power control to account for the same fade conditions that are being countered by the GSO system using ACM. For this analysis, a clear-sky pfd mask was used to generate a epfd$_{\downarrow}$ profile using the methodology of Recommendation ITU-R S.1503. This generated epfd$_{\downarrow}$ profile was then convolved with the non-GSO power control pfd profile which was assumed to be equal to the rain fade pdf at the GSO location Figure A7-5 presents the resulting epfd$_{\downarrow}$ profile from this analysis. Figure A7-6 presents the resulting convolution with the non-GSO power control profile with a 50 cm antenna and Fig. A7-7 presents the results with a 250 cm antenna. Table A7-3 and Table A7-4 present the resulting percent degradation of throughput based on rain fade on the GSO link versus rain fade plus interference.

FIGURE A7-5

epfd↓ profile from non-GSO operation into GSO link under Clear Sky Conditions

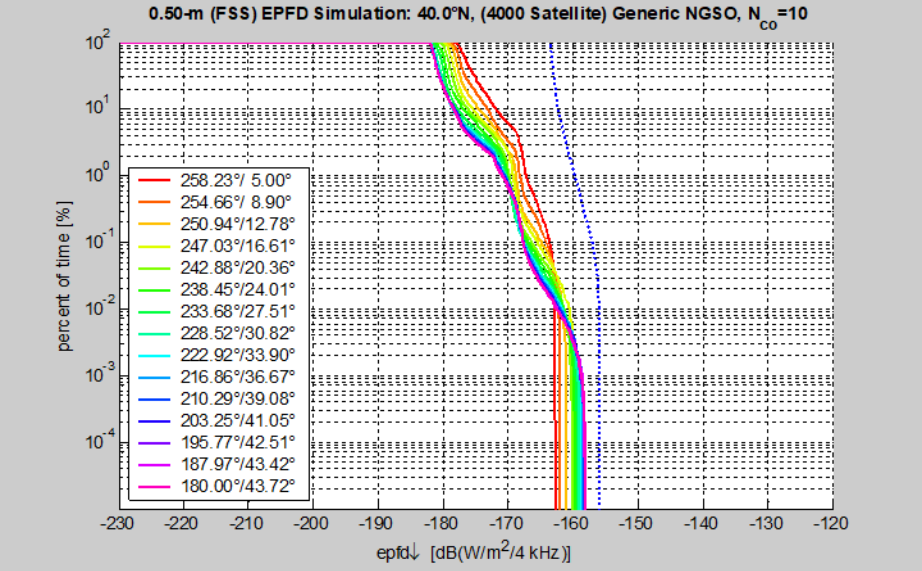

FIGURE A7-6

Bandwidth efficiency (bits/cycle) calculations from convolution results of epfd↓ with rain fade profile and 50 cm antenna

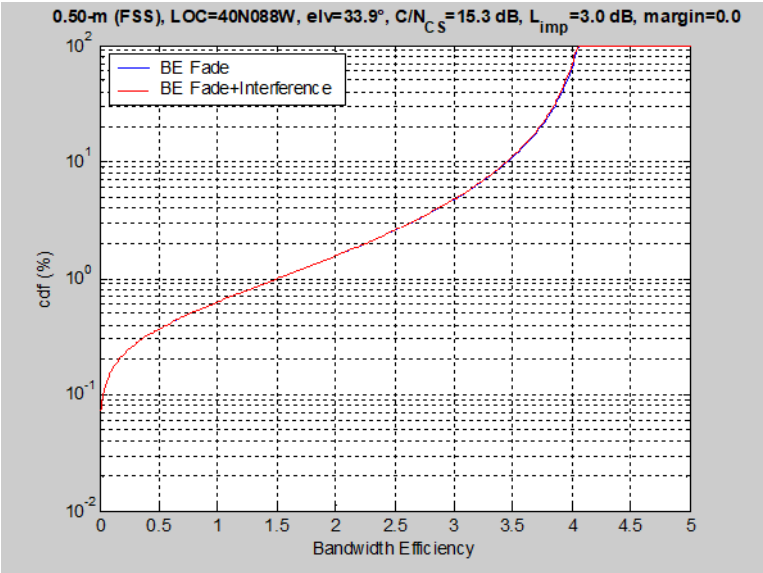

TABLE A7-3

Impact of fade and non-GSO epfd↓ on bandwidth efficiency (bits/cycle) for ACM with 50 cm antenna

MAX	AVG	MAX	AVG
Clear Sky	Fade	w/ Interference	Fade + Interference
4.06	3.81 (6.08%)	4.05 (0.25%)	3.80 (6.31%)

FIGURE A7-7

Bandwidth efficiency (bits/cycle) calculations from convolution results of epfd with rain fade profile and 250 cm antenna

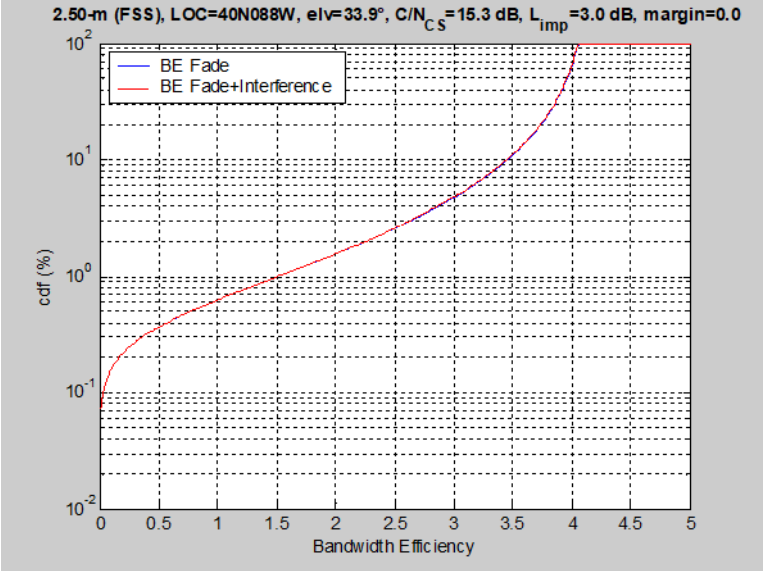

TABLE A7-4

Impact of fade and non-GSO epfd↓ on bandwidth efficiency (bits/cycle) for ACM with 250 cm antenna

MAX	AVG	MAX	AVG
Clear Sky	Fade	w/ Interference	Fade + Interference
4.06	3.81 (6.08%)	4.06 (0.00%)	3.81 (6.19%)

As can be seen from the results in Tables A7-3 and A7-4, the use of ACM to counter rain fade degradation will account for a 6.08% reduction in throughput based on only rain fade characteristics. The epfd↓ reduction in throughput, taking account similar rain fade performance for the non-GSO, will result in only 0.25%, for the 50 cm antenna, and close to 0%, for the 250 cm antenna. Thus, it can be seen that the impact of long-term throughput reduction based on ACM in the 50/40 GHz frequency bands will be dominated by propagation fades and additional epfd↓ from non-GSO operations are small. This reduction of 0.25% as seen from the example analysis above is much below the allowable 1% reduction as indicated by Recommendation ITU-R S.2131-0.

NOTE – Further work may be required to address the rate of change of degradation for ACM systems. While ACM modems can accommodate wide dynamic ranges, they are limited in the rate of change they can track. Further work may also be required to study potential use of Recommendation ITU-R S.2131-0.

Annex 8

Study 8: Protection of GSO links from aggregate interference from non-GSO networks based on fading statistics only

NOTE – There was no agreement with the validity of this methodology on the process of the generation of epfd values to protect GSO networks. Questions were raised about whether it was appropriate to apply the

same probability used in the Recommendation ITU-R P.618 rain fade calculation to the derived epfd threshold as this is an assumption of full correlation between the two. In particular, during the full convolution process in Recommendation ITU-R S.1323 Method A, the probability used in the Recommendation ITU-R P.618 rain fade calculation and the probability used to select an epfd level are selected fully independent of each other. For example, during a deep (low probability, short term) rain fade, it is most likely that the epfd level is close to average values (medium probability, long term), and it is very unlikely that there be simultaneously high interference and high fading.

The following Figures present the uplink, downlink and total system performance in clear sky and fading conditions in the absence of short-term interference (non-GSO systems). The propagation model considered for obtaining the fading of the carrier signals is Recommendation ITU-R P.618-12 associated with Recommendation ITU-R P.837-7. Additional attenuation accounting for atmospheric gas absorption was included by using Recommendation ITU-R P.676-11. The variation of the earth station receiver noise temperature as a function of the rain attenuation was also taken into account in the downlink calculations[3].

FIGURE A8-1

Uplink and downlink performance for reference link 4A/177 Forward (GW to User)

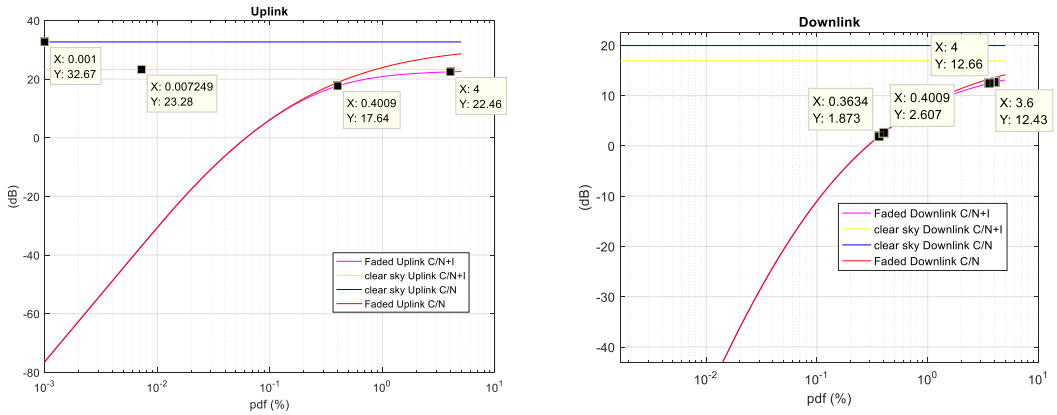

[3] In addition to the parameters provided in Annex 7, the following additional conditions are applied:

ES Gateway: To achieve a rain fall rate provided in Annex 7, with the specified latitude (41.98°), a longitude of 60°W.

GSO SS: To reach the elevation indicated in Annex 7, the GSO satellite longitude is around 49°W.

ES User terminal: To achieve the elevation angle from the latitude provided, a longitude of 38°W was used.

ES antenna noise temperature increase due to rain: In order to calculate the increase in the earth station receiver antenna noise depending on the rain loss, it is necessary to suppose the earth station feeder loss and the thermodynamic temperature of the feeder. To this effect the values of 0.5 dB and 290K were respectively used. In addition the sky temperature used for the downlink frequency at 40° elevation angle is 30K.

FIGURE A8-2

End to end link performance for reference link 4A/177 Forward (GW to User)

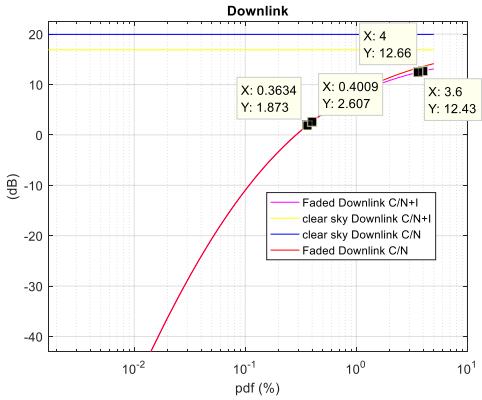

The performance objectives in Annex 11 are $C/(N+I)$ ratios associated to percentages of time for which those values should be exceeded. They are contained in the two left-hand columns of Table A8-1 below. The two right columns are the link performances achieved at the simulated locations.

TABLE A8-1

Objective $C/(N+I)$ (dB)	**Objective % of time**	**Calculated $C/(N+I)$ for % of time**	**% of time exceeding objective $C/(N+I)$**
−2.7	99.6	2.58	99.79
14	96	12.24	<95

The performance objectives are referred to link unavailability of 0.4% and 4% for $C/(N+I)$ of −2.7 dB and 14 dB respectively. From the simulations at the specified ES locations, it is observed that only the first objective is met. From Figs A8-1 and A8-2, it is observed that the dimensioning segment is the downlink.

The analysis here below to deduce the maximum interference permissible from non-GSO systems will be based on the downlink data in Fig. A8-1. This data contains only the long term interference (intra-system, other GSO networks interference and interference from FS).

Reference point 1: $C/(N+I)$ = 2.607 dB, p=0.4%

Decrease in GSO link availability:

The maximum decrease in the GSO link availability is the proposed approach to evaluate the performance objective associated with the lowest percentage of time.

For this point, C=−110.64 dBW, N=−113.3337 dBW

C/I_long_term = C-19.84 dB => I_long_term=−130.48 dBW

The non-GSO effect may degrade the GSO unavailability by at most 10% of the unavailability due to fading, that is, additional 0.04%. For such effect the propagation conditions leading to 0.4% of total unavailability should be those encountered for 0.36% of the time if we consider non-GSO effects.

For p = 0.36% of the time, only the target $C/N+I$ value that should be satisfied is considered. The carrier power, noise power and long term interference should be the same as for the reference point

(0.4%), only the new component of interference due to non-GSO systems changes from zero to a maximum value that is to be found to satisfy the increase in unavailability of 0.04%.

$C/(N+I)$ = 1.8 dB for p=0.36%, with I composed from long-term and short-term: $I=I_{lt}+I_{non\text{-}GSO}$

It is then used C=−110.64 dBW, N= −113.3337, $I= I_{lt}+I_{non\text{-}GSO}$ = −130.48 dBW+ $I_{non\text{-}GSO}$

The resulting $I_{non\text{-}GSO}$ is −120.15 dBW/600MHz = −147.93 dBW/MHz.

Therefore the resulting aggregate interference from non-GSO systems should satisfy the following:

$I_{non\text{-}GSO}$ < -147.93 dBW/MHz for 99.6% of time, which is equivalent to:

epfd = −147.93 dBW/MHz – G_{ES} – 10 log ($\lambda^2/4\pi$) = −137.73 dBW(m² MHz)

epfd<−137.73 dBW(m² MHz) for 99.6% of time

Reference point 2: $C/(N+I)$ = 12.66 dB, p=4%

For the performance objective associated to the highest percentage of time among the GSO link performance objectives, two approaches can be considered. On the one hand, the limitation of unavailability approach as for Reference point 1 or alternatively, an approach based on the maximum decrease of the GSO link capacity. The two approaches are developed here below:

Approach 1: Decrease in link availability: For this point, C=-100.579 dBW, N=−114.164 dBW,

C/I_long_term = C-19.84 dB => I_long_term=−120.42 dBW

The non-GSO effect may degrade the GSO unavailability by at most 10% of the unavailability due to fading, that is, additional 0.4%. For such effect the propagation conditions leading to 4% of total unavailability should be those encountered for 3.6% of the time if we consider non-GSO effects.

For p = 3.6% of the time, only the target $C/N+I$ value that should be satisfied is considered. The carrier power, noise power and long term interference should be the same as for the reference point (4%), only the new component of interference due to non-GSO systems changes from zero to a maximum value that is to be found to satisfy the increase in unavailability of 0.4%.

C/(N+I) = 12.43 dB for p=3.6%, with I composed from long-term and short-term: $I=I_{lt}+I_{non\text{-}GSO}$

It is then used C=-100.579 dBW, N=−114.164, $I=I_{lt}+I_{non\text{-}GSO}$ = −120.42 dBW+ $I_{non\text{-}GSO}$

The resulting $I_{non\text{-}GSO}$ is -125.649 dBW/600MHz = −153.43 dBW/MHz.

Therefore the resulting aggregate interference from non-GSO systems should satisfy the following:

$I_{non\text{-}GSO}$ < -153.43 dBW/MHz for 96% of time, or

epfd < -143.23 dBW/(m² MHz) for 96% of time

Approach 2: Decrease in GSO link capacity:

For this point, C=-100.579 dBW, N=-114.164 dBW,

C/I_long_term = C-19.84 dB => I_long_term=-120.42 dBW

According to the DVB-S2 standard, the corresponding MODCOD is 16 APSK with a FEC (forward error correction) code rate ρ = 7/9; which is coherent with the link information in Annex 7.

NOTE – The use of the Shannon curve should be used as the baseline rather then the DVB-S2 standard as the baseline standard for comparison.

$\Gamma = \log_2 M/(1+\alpha)$ where α is the roll-off factor and $m= \log_2 M$ is the number of bits per symbol

For 16 APSK and using a typical roll-off factor of 0.35, Γ = 2.963 (bit/s Hz^{-1})

Rc = Bcod • Γ = where Rc is the bit rate and Bcod is the bandwidth used

Rc = 600 (MHz) • 2.963 (bit/s Hz^{-1}) =1 777.8 Mbit/s

The information rate Rb is related to the coded bit rate Rc as follows: Rb=Rc • ρ

Rb = 1 382.7 Mbit/s

The decrease of 10% of the link capacity leads to an information rate Rb = 1 244.4 Mbit/s

The MODCOD just below the nominal performance is 16APSK 13/18, leading to Rb= 1 284 Mbit/s

The next MODCOD is 16APSK 25/36 and leads to Rb =1 234.6 Mbit/s, which is below the maximum decrease in capacity of 10%. Consequently, the degraded MODCOD to respect the 10% restriction is 16APSK 13/18.

The required $C/(N+I)$ for this MODCOD is 11.52 dB.

The carrier power, noise power and long term interference should be the same as for the reference point (4%), only the new component of interference due to non-GSO systems changes from zero to a maximum value that is to be found to satisfy the decrease in capacity of 10%.

$C/(N+I)$ = 11.52 dB with I composed from long-term and short-term: $I=I_{lt}+I_{non\text{-}GSO}$

It is then used C=-100.579 dBW, N=-114.164, $I= I_{lt}+I_{non\text{-}GSO}$ = -120.42 dBW+ $I_{non\text{-}GSO}$

The resulting $I_{non\text{-}GSO}$ is -118.46 dBW/600MHz = -146.24 dBW/MHz.

Therefore the resulting aggregate interference from non-GSO systems should satisfy the following:

$I_{non\text{-}GSO}$ < -146.24 dBW/MHz for 96% of time, or

epfd < -136.04 dBW/(m² MHz) for 96% of time

Following the same procedure, additional limitations for the interference from non-GSO systems can be calculated to obtain an epfd mask on the Earth surface to protect the GSO link under study.

The same analysis can be performed for all the GSO reference links so as to have a number of epfd values associated to percentages of time, based on which the final mask – taking for instance the most restrictive value for every percentage of time - among the representative links can be established.

Annex 9

Study 9: Study of sharing between GSO and non-GSO FSS systems in the 50/40 GHz frequency bands

1 Introduction

WRC-19 agenda item 1.6 deals with the consideration of technical, operational and regulatory issues related to non-geostationary satellite systems in the 50/40 GHz frequency range, in accordance with **Resolution 159 (WRC-15)**: to consider the development of a regulatory framework for non-GSO FSS satellite systems that may operate in the frequency bands 37.5-39.5 GHz (space-to-Earth), 39.5-42.5 GHz (space-to-Earth), 47.2-50.2 GHz (Earth-to-space) and 50.4-51.4 GHz (Earth-to-space), in accordance with Resolution **159 (WRC-15)**.

Resolves 1 of Resolution **159 (WRC-15)** invites the ITU-R to conduct and complete in time for WRC-19 "studies of technical and operational issues and regulatory provisions for the operation of non-GSO FSS satellite systems in the frequency bands 37.5-42.5 GHz (space-to-Earth) and 47.2-48.9 GHz

(limited to feeder links only), 48.9-50.2 GHz and 50.4-51.4 GHz (all Earth-to-space), while ensuring protection of GSO satellite networks in the FSS, MSS and BSS, without limiting or unduly constraining the future development of GSO networks across those bands, and without modifying the provisions of Article **21**". *Resolves 2* specifies that "studies carried out under *resolves to invite ITU-R* 1 shall focus exclusively on the development of equivalent power flux-density limits produced at any point in the GSO by emissions from all the earth stations of a non-GSO system in the fixed-satellite service or into any geostationary FSS earth station, as appropriate".

2 Current approaches

The two main approaches to sharing between GSO and non-GSO FSS Systesms:

– Derive aggregate epfd curves and single-entry limits (approach used to derive single-entry limits found in RR Article **22**; Resolution **76 (Rev.WRC-15)** contains the aggregate values).

– Calculate the increase in unavailability to reference GSO links from the interference of non-GSO FSS systems. Recommendation ITU-R S.1323 allows for a 10% aggregate increase in the unavailability of GSO links.

See Annexes 1 to 3 for more detail on the pros and cons of each approach.

3 Study details and characteristics

A COTS software (Visualyse) was used to simulate the interference from a non-GSO system into the reference GSO links, using approach #2. The purpose of this study is to demonstrate the applicability of approach #2 in assessing the impact of interference from non-GSO systems into GSO systems.

Technical characteristics

Geostationary network				
Submission	**Luxembourg**	**Malaysia**	**Peru**	**Canada**
Link Direction	**GW to User**	**GW to User**	**GW to User**	**Exurbia FWD**
A) Performance objectives				
1.A.1 Threshold #1 (N/A for not applicable): $C/(N+I)$	12	12	12	N/A
(% of the year $C/(N+I)$ should be exceeded)	99.75	99.75	99.75	99.5
1.A.2 Threshold #2 (N/A for not applicable): $C/(N+I)$	20	20	20	-1.34
(% of the year $C/(N+I)$ should be exceeded)	99.6	99.6	99.6	99
1.A.3 Threshold #3 (N/A for not applicable): $C/(N+I)$	22	22	22	9.3

Geostationary network				
(% of the year $C/(N+I)$ should be exceeded)	99	99	99	(Clear Sky)
B) Waveform description				
1.B.1 Modulation type (e.g. FM, QPSK, BPSK)	32APSK	32APSK	32APSK	N/A
	128APSK	128APSK	128APSK	QPSK
	256APSK	256APSK	256APSK	8PSK
1.B.2 Noise bandwidth per carrier	500000	500000	500000	90000
C) Transmit earth station characteristics				
1.C.2 Latitude (+: North, –: South) from Equator	49.69	3.13	-12.1	52.1
1.C.3 Elevation angle	32	86	74	30.3
1.C.6 Rain model	ITU-R P.618	ITU-R P.618	ITU-R P.618	ITU-R P.618
1.C.9 On-axis Earth station transmit e.i.r.p.	80	80	80	72.3
1.C.12 Power control range (>0, 0 dB if none)	10	10	10	4.8
1.D.15 Antenna Diameter				9.0
1.D.16 On-Axis Antenna Gain				71.1
1.D.17 Uplink EIRP Density				-7.2
1.D.18 PSD at Antenna Flange				-78.3
D) Receive earth station characteristics				
1.D.2 Latitude (+: North, –: South) from Equator	-	-	-	48.4
1.D.5 Elevation angle	-	-	-	33.1
1.D.8 Earth station receive noise temperature (clear sky / faded link)	250/500	250/500	250/500	249.6
1.D.9 On-axis antenna gain	47.5	47.5	47.5	47.3

Geostationary network				
1.D.10 Antenna diameter	0.75	0.75	0.75	0.67
E) Space station receive characteristics				
1.E.1 Transponder bandwidth	500-600	500-600	500-600	800
1.E.2 Receive frequency	51	51	51	51
1.E.5 Peak receive antenna gain	51.8	51.8	51.8	54
1.E.6 Receive satellite antenna gain in the direction of transmit earth station	48.8	48.8	48.8	54
1.E.7 Satellite receive temperature	600	600	600	1000
1.E.11 Uplink *C/N*				24.8
F) Space station transmit characteristics				
1.F.1 Transmit frequency	38	38	38	38
1.F.4 Satellite e.i.r.p. in the direction of the receive earth station	71.5	71.5	71.5	69
1.F.9 Saturated Satellite e.i.r.p. density in direction of the receive earth station				-20.0
1.F.10 Satellite e.i.r.p. density in direction of the receive earth station (with OBO)				-24.5
1.F.11 Downlink *C/N*				10.9

The non-GSO characteristics:

FSS/BSS Downlink Parameters		
Frequency range (GHz)	38.2	38
CARRIER	Carrier #26	Carrier #19
Noise bandwidth (MHz)	50-500	62.5-1 000
EARTH STATION		
Other		
Additional Notes	Non-GSO system with a circular, orbit having an altitude of 1 400 km. *See discussion on protection criteria in covering liaison statement	Non-GSO system with a circular, orbit having an altitude of 1 200 km. *See discussion on protection criteria in covering liaison statement

FSS/BSS downlink parameters		
Frequency range (GHz)	38	38
SPACE STATION CARRIER	Carrier #26	Carrier #19
Peak transmit antenna gain (dBi)	45	34.5
Peak satellite e.i.r.p. spectral density **(**dBW/Hz)	-31.1	-29.2
Transmit antenna gain pattern and beamwidth	ITU-R Rec. S.1528 LS = −25 BW: 0.95	ITU-R Rec. S.1528 LS = −25 BW: 3.4
Other		
Additional Notes	Non-GSO system with an circular, orbit having an altitude of 1 400 km.	Non-GSO system with an circular, orbit having an altitude of 1 200 km.

FSS Uplink Parameters		
Frequency range (GHz)	51	51
CARRIER	Carrier #44	Carrier #33
Noise bandwidth (MHz)	50 - 500	62.5 - 500
Other		
Additional Notes	Non-GSO system with an circular, orbit having an altitude of 1 400 km. *See discussion on protection criteria in covering liaison statement	Non-GSO system with an circular, orbit having an altitude of 1 200 km. *See discussion on protection criteria in covering liaison statement

FSS Uplink Parameters		
Frequency range (GHz)	51	51
EARTH STATION CARRIER	Carrier #44	Carrier #33
Antenna diameter (m)	1	5.49
Peak transmit antenna gain (dBi)	53	63.3
Peak transmit power spectral density (clear sky) (dBW/Hz)	−85	−72.9
Antenna gain pattern (ITU Recommendation)	Rec. ITU-R 465-6	Rec. ITU-R 465-6
Minimum elevation angle of transmit earth station	25	40
Other		
Additional Notes	non-GSO system with an circular, orbit having an altitude of 1 400 km.	non-GSO system with an circular, orbit having an altitude of 1 200 km.

Methodology

Three identical GSO links were implemented in different locations. These forward links (gateway to user) were taken from input contributions to the ITU-R (Annex 13). The locations were selected to have different rain environment. Lima (Peru) has a typically dry climate, Betzdorf (Luxembourg) is considered to have a moderately humid climate while Kuala Lumpur (Malaysia) has a humid climate. For each link, rain fading was modelled using Recommendation ITU-R P.618, with the local rain rates provided by Recommendation ITU-R P.837. The fading noise temperature was calculated in accordance with rain characteristics. In accordance with the characteristics provided above, 10 dB of transmit power control was implemented on the gateway.

The impact of two different non-GSO systems, as well as the combined impact of these two systems, was simulated. These systems' characteristics are taken from ITU documentation. The gateways of the non-GSO systems were collocated with the GSO gateway. In order to avoid main-beam interference, GSO arc avoidance angles of 3º and 6º were implemented. No transmission occurred between an earth station and a satellite if the angle between the non-GSO satellite and the GSO arc was less than 3° or 6°, as measured at the earth station. Otherwise, the non-GSO gateway always communicates with the satellite with the highest elevation angle.

It was assumed that the rain fade of the wanted links and the interference links were 100% correlated in the space-to-Earth direction. Due to the limitation of the software, the correlation could only be set to either 0% or 100%. Considering that the fade of the wanted link and the interferer link both depend on the rain and atmospheric environment at the receiver's location, the correlation between their fading will be strong and it was determined that it is more realistic to assume 100% than 0%.

It was also assumed that the GSO user terminal was located 25 km from the non-GSO and GSO gateways. This distance is small enough that the user terminal receives the transmission from the main beam of one of the non-GSO satellite constellations.

The increase of the GSO unavailability due to the addition of interference from the non-GSO links was calculated as follows:

1 For each time step of the simulation, the C/N was determined in both the uplink and downlink direction.

2 The percentage of unavailability due to rain was determined for the overall uplink and downlink, using the respective *C*/*N* objective for each system.

The overall *C*/*N* is determined using the following formula:

$$\frac{C}{N} = \left(\left(\frac{C}{N} up \right)^{-1} + \left(\frac{C}{N} down \right)^{-1} \right)^{-1}$$

3 Then, for each time step of the simulation, the *C*/(*N*+*I*) was determined in both the uplink and downlink direction, including the combined impact of the rain and the non-GSO interference.

The overall *C*/(*N*+*I*) is determined using the following formula:

$$\frac{C}{N+I} = \left(\left(\frac{C}{N+I} up \right)^{-1} + \left(\frac{C}{N+I} down \right)^{-1} \right)^{-1}$$

The results are based on a simulated time of 30 days, using 1 second time steps. The increase in unavailability for the individual uplink and downlink direction has been included for reference.

Results

Percentage of increase in unavailability of the forward link for 0 degree GSO arc avoidance				
Location	**Direction**	**1 200 km**	**1 400 km**	**1 200 km+1 400 km**
Luxembourg (12 dB threshold)	Uplink	0%	0%	0%
	Downlink	0.12%	0.01%	0.12%
	Total	0.15%	0.01%	0.13%
Malaysia (12 dB threshold)	Uplink	0.13%	0.00%	0.10%
	Downlink	11.12%	0.20%	11.33%
	Total	9.24%	0.16%	9.35%
Peru (12 dB threshold)	Uplink	0.44%	0.00%	0.47%
	Downlink	72.06%	1.44%	73.50%
	Total	58.85%	1.15%	60.02%
Exurbia (9.3 dB threshold)	Uplink	0.00%	0.00%	0.00%
	Downlink	0.01%	0.00%	0.01%
	Total	0.01%	0.00%	0.00%

Percentage of increase in unavailability of the forward link for 3 degree GSO arc avoidance				
Location	**Direction**	**1 200 km**	**1 400 km**	**1 200 km+1 400 km**
Luxembourg (12 dB threshold)	Uplink	0%	0%	0%
	Downlink	0.12%	0.01%	0.12%
	Total	0.15%	0.01%	0.13%
Malaysia (12 dB threshold)	Uplink	0.00%	0.00%	0.01%
	Downlink	0.59%	0.00%	0.59%
	Total	0.69%	0.00%	0.70%
Peru (12 dB threshold)	Uplink	0.03%	0.00%	0.00%
	Downlink	0.44%	0.00%	0.44%
	Total	0.50%	0.00%	0.46%
Exurbia (9.3 dB threshold)	Uplink	0.00%	0.00%	0.00%
	Downlink	0.01%	0.00%	0.01%
	Total	0.01%	0.00%	0.00%

Percentage of increase in unavailability of the forward link for 6 degree GSO arc avoidance				
Location	**Direction**	**1 200 km**	**1 400 km**	**1200 km+1 400 km**
Luxembourg (12 dB threshold)	Uplink	0.00%	0.00%	0.00%
	Downlink	0.12%	0.01%	0.12%
	Total	0.15%	0.01%	0.15%
Malaysia (12 dB threshold)	Uplink	0.00%	0.00%	0.01%
	Downlink	0.29%	0.00%	0.30%
	Total	0.32%	0.00%	0.33%
Peru (12 dB threshold)	Uplink	0.03%	0.00%	0.00%
	Downlink	0.18%	0.00%	0.18%
	Total	0.23%	0.00%	0.23%
Exurbia (9.3 dB threshold)	Uplink	0.00%	0.00%	0.00%
	Downlink	0.01%	0.00%	0.01%
	Total	0.01%	0.00%	0.00%

Analysis

As shown above for forward links in all three locations, the highest increase in unavailability created by one non-GSO system using GSO arc avoidance is 0.7%. It can be noted that the increase in unavailability varies significantly between the two non-GSO systems used in the simulation. This result is due to the differences in system and orbital characteristics.

The impact of GSO arc avoidance is significant to the results. The larger the GSO arc avoidance angle, the smaller the increase in unavailability of the GSO link, and the absence of GSO arc avoidance leads to high increases in unavailability. These results suggest that GSO arc avoidance would be an effective mitigation technique to reduce the impact of interference from non-GSO systems.

However, it should be noted that the GSO arc avoidance has no impact on the GSO link situated in Luxembourg. This can be explained by the high latitude of the location. Since the GSO arc is located at a low elevation as seen from the non-GSO earth station, and that the earth station always communicates with the satellite with highest elevation angle, there is no event where the selected satellite crosses the GSO arc. Therefore, implementing GSO arc avoidance is not practical at this latitude. This finding suggests that GSO earth stations located at high latitudes would experience limited impact from non-GSO systems, since a natural geometrical separation will occur between the GSO and the non-GSO beams.

In addition, when comparing the increase in unavailability for between uplink and downlink segments, most of the increase in unavailability is caused by interference into the downlink segments of the GSO links. Consequently, mitigation measures or regulatory limits to protect GSO systems from interference from non-GSO systems would be more effective in the space-to-Earth direction.

Finally, we note that increase in unavailability due to the impact of two non-GSO FSS systems adds linearly. Further studies are needed to determine whether this addition holds for a more than two systems.

Conclusion

The above study shows how the calculation of the increase in unavailability can be used to evaluate the impact of the interference of one or two non-GSO systems on a GSO system. The results also reveal that factors such as the latitude of the GSO earth station, and mitigation techniques such as GSO arc avoidance, can facilitate sharing between GSO and non-GSO FSS systems. Finally, the results show the impact of interference from non-GSO systems is higher in the space-to-Earth direction.

In the future, a higher number of systems could be evaluated in order to determine the effect of multiple systems on the aggregate impact to the GSO links. Systems with different orbital characteristics, such as MEO and HEO could also be simulated.

The results of this study demonstrate the effectiveness of the methodology to determine the increase in unavailability to GSO reference links.

Attachment 1
to Annex 9

Analysis of interference into systems using transparent transponders: joint effects of uplink and downlink fading and interference

A.1 Technical Analysis

The uplink and the downlink clear-sky carrier-to-noise ratios are given by $\left(\frac{C_{cs}}{N\uparrow}\right)$ and $\left(\frac{C_{cs}}{N\downarrow}\right)$, respectively. If $I\uparrow$ and $I\downarrow$ denote the uplink and downlink time-varying interferences, the uplink and the downlink clear-sky carrier-to-noise ratios with time varying interference are given by are given by $\left(\frac{C_{cs}}{N\uparrow + I\uparrow}\right)$ and $\left(\frac{C_{cs}}{N\downarrow + I\downarrow}\right)$, respectively.

A.1.1 Uplink Analysis

The expression for the uplink carrier-to-noise ratio with interference and fading conditions can be written as:

$$\left(\frac{C}{N}\right)_{up} = \frac{C_{cs}}{F_u(Ac\uparrow)\left[G(Ac\uparrow)N\uparrow + \frac{I\uparrow}{F(Ai\uparrow)}\right]} = \left(\frac{C_{cs}}{N\uparrow}\right) \text{ x } \frac{1}{F_u(Ac\uparrow)\,G(Ac\uparrow)} \text{ x } \frac{1}{\left[1+\frac{1}{F(Ai\uparrow)G(Ac\uparrow)}\left(\frac{I\uparrow}{N\uparrow}\right)\right]} \quad \text{(A1)}$$

Note that the uplink interference is assumed to fade independently of the desired uplink carrier power.

Define the uplink degradation due fading of the desired carrier by X_{up} and the uplink degradation due to the interference by Y_{up} as follows:

$$X_{up} = F_u(Ac\uparrow)\,G(Ac\uparrow) \quad \text{(A2)}$$

and

$$Y_{up} = 1 + \frac{1}{F(Ai\uparrow)G(Ac\uparrow)}\left(\frac{I\uparrow}{N\uparrow}\right) \quad \text{(A3)}$$

Then the degradation in the uplink clear-sky carrier-to-noise ratio is given by:

$$\left(\frac{C_{cs}}{N\uparrow}\right)_{deg} = X_{up}Y_{up} \quad \text{(A4)}$$

where X_{up} and Y_{up} can be expressed as follows:

$$X_{up} = F_u(Ac\uparrow) \quad \text{(A5)}$$

and

$$Y_{up} = 1 + \frac{1}{F(Ai\uparrow)}\left(\frac{I\uparrow}{N\uparrow}\right) \quad \text{(A6)}$$

when we ignore the impact of noise enhancement on the uplink, as discussed in *Assumption 2*.

Note that:

X_{up} is a stochastic process which depends on the statistics of the uplink desired carrier fade $Ac\uparrow$.

Y_{up} is a stochastic process which depends on the statistics of the uplink desired carrier fade $Ac\uparrow$, the statistics of the uplink interference fade $Ai\uparrow$, and the statistics of the uplink interference $I\uparrow$.

The statistics of the uplink carrier-to-noise ratio can be obtained by determining the statistics of the degradation in the uplink clear-sky carrier-to-noise ratio, as it is assumed that the clear-sky carrier-to-noise ratio is set to a fixed value. Although generally speaking, X_{up} and Y_{up} are stochastic processes, at any instant in time, their values are random variables. The statistics of the degradation in the uplink clear-sky carrier-to-noise ratio is easy to obtain if we can assume that X_{up} and $Y_{up}$are independent. If we look at the expressions for X_{up} and Y_{up} given by equations (A2) and (A3), they are clearly not independent. However, if we consider the noise enhancement on the uplink, $G(Ac\uparrow)$ to be negligible, then for X_{up} and Y_{up} given by equations (A5) and (A6) could be considered essentially independent. To simplify the analysis, we express $\left(\frac{C_{cs}}{N\uparrow}\right)_{deg}$ in dB, as

$$\left(\frac{C_{cs}}{N\uparrow}\right)_{deg}(dB) = x + y \tag{A7}$$

where:

$$x = 10\ Log\{X_{up}\} \tag{A8}$$

$$y = 10\ Log\{Y_{up}\} \tag{A9}$$

Let

$$u = x + y \tag{A10}$$

On the basis that *x* and *y* are independent random variables, the probability distribution function $PDF_U(u)$ of the discrete random variable resulting from the addition of the discrete random variables *x* and *y* is obtained by taking the convolution of their respective probability distribution functions $PDF_X(x)$ and $PDF_Y(y)$, expressed as follows:

$$PDF_U(u) = PDF_X(u) * PDF_Y(u) \tag{A11}$$

Given $PDF_U(\zeta_i)$, the statistics of the degradation in the uplink clear-sky carrier-to-noise ratio are easily obtained.

A.1.2 Downlink Analysis with Transparent Transponder

Assuming a transparent transponder, the expression for the downlink carrier-to-noise ratio with interference and fading conditions can be written as:

$$\left(\frac{C}{N}\right)_{dn} = \frac{C_{cs}}{F_u(Ac\uparrow)\,F(Ac\downarrow)\left[G(Ac\downarrow)N\downarrow + \frac{I\downarrow}{F(Ac\downarrow)}\right]} = \left(\frac{C_{cs}}{N\downarrow}\right) \text{ x } \frac{1}{F_u(Ac\uparrow)\,\text{F(Ac}\downarrow)G(Ac\downarrow)} \text{ x } \frac{1}{\left[1+\frac{1}{F(Ac\downarrow)G(Ac\downarrow)}\left(\frac{I\downarrow}{N\downarrow}\right)\right]} \tag{A12}$$

Note that the downlink carrier (C/N) will be diminished due to rain attenuation under rain-faded conditions on the uplink.

Define the downlink degradation due fading of the desired carrier by X_{dn} and the downlink degradation due to the interference by Y_{dn} as follows:

$$X_{dn} = F_u(Ac\uparrow)\,F(Ac\downarrow)G(Ac\downarrow) \tag{A13}$$

and

$$Y_{dn} = 1 + \frac{1}{F(Ac\downarrow)G(Ac\downarrow)}\left(\frac{I\downarrow}{N\downarrow}\right) \tag{A14}$$

However, when uplink power control is implemented and possibly site diversity as well as automatic level control at the satellite, if the unavailability on the uplink due to uplink fading alone is much less than 1/10th than the unavailability on the downlink due to downlink fading alone one can assume that the clear-sky downlink carrier level will not be affected by the variations on the uplink. Then the degradation in the downlink clear-sky carrier-to-noise ratio is given by:

$$\left(\frac{C_{cs}}{N\downarrow}\right)_{deg} = X_{dn}Y_{dn} \tag{A15}$$

where X_{dn} and Y_{dn} become:

$$X_{dn} = F(Ac\downarrow)G(Ac\downarrow) \tag{A16}$$

and

$$Y_{dn} = 1 + \frac{1}{F(Ac\downarrow)G(Ac\downarrow)}\left(\frac{I\downarrow}{N\downarrow}\right) \tag{A17}$$

Note that:

X_{dn} is a stochastic process which depends only on the statistics of the downlink desired carrier fade $Ac\downarrow$ under the assumption just discussed above.

Y_{dn} is a stochastic process which depends on the statistics of the downlink desired carrier fade $Ac\downarrow$ and the statistics of the downlink interference $I\downarrow$.

Similarly, in the case of uplink, statistics of the downlink carrier-to-noise ratio can be obtained by determining the statistics of the degradation in the downlink clear-sky carrier-to-noise ratio, when it is assumed that the clear-sky carrier-to-noise ratio is set to a fixed value. Following a similar analysis to the previous section, we can express $\left(\frac{C_{cs}}{N\downarrow}\right)_{deg}$ in dB, as

$$\left(\frac{C_{cs}}{N\downarrow}\right)_{deg}(dB) = a + b \tag{A18}$$

where:

$$a = 10\,Log\{X_{dn}\} \tag{A19}$$

$$b = 10\,Log\{Y_{dn}\} \tag{A20}$$

However, in this case, it is clear that the random variables *a* and *b* are not independent, since Y_{dn} is a function of both the rain attenuation and the interference. Hence the classic approach of using the convolution is not appropriate in this case. An alternative approach is to keep the expression for $\left(\frac{C_{cs}}{N\downarrow}\right)_{deg}$ linear; in which case, it can be written simply as:

$$\left(\frac{C_{cs}}{N\downarrow}\right)_{deg} = S + T \quad \text{(linear)} \tag{A21}$$

where:

$$S = F(Ac\downarrow)G(Ac\downarrow) \tag{A22}$$

$$T = \left(\frac{I\downarrow}{N\downarrow}\right) \tag{A23}$$

Let

$$E = S + T \tag{A24}$$

Note that the random variable S and T separate the effects due to rain attenuation and due to interference, making these two random variables independent. On the basis that S and T are independent random variables, the probability distribution function $PDF_E(e)$ of the discrete random E resulting from the addition of the discrete random variables S and T is obtained by taking the convolution of their respective probability distribution functions $PDF_S(s)$ and $PDF_T(t)$, expressed as follows:

$$PDF_E(e) = PDF_S(e) * PDF_T(e) \tag{A25}$$

Given $PDF_E(e)$, the $PDF_D(d)$ of the degradation in the downlink clear-sky carrier-to-noise ratio expressed in dB can be obtained as follows:

$$PDF_D(d_i(dB)) = PDF_E(10Log(e_i(linear))) \tag{A26}$$

A.1.3 Combined Uplink/Downlink Analysis with Transparent Transponder

The overall carrier-to-noise ratio in the presence of uplink and downlink fading and interference can be written as:

$$\left(\frac{C}{N}\right) = \frac{\left(\frac{C}{N}\right)_{up}\left(\frac{C}{N}\right)_{dn}}{\left(\frac{C}{N}\right)_{up} + \left(\frac{C}{N}\right)_{dn}} \tag{A27}$$

After some simplification (see Attachment 2), the above expression can be written as

$$\left(\frac{C}{N}\right) = \frac{\left(\frac{C}{N}\right)_{cs}}{\left(aX_{up}Y_{up} + (1-a)X_{dn}Y_{dn}\right)} \tag{A28}$$

Where

$$\left(\frac{C}{N}\right)_{cs} = \frac{\left(\frac{C_{cs}}{N\uparrow}\right)\left(\frac{C_{cs}}{N\downarrow}\right)}{\left(\frac{C_{cs}}{N\uparrow}\right) + \left(\frac{C_{cs}}{N\downarrow}\right)} \tag{A29}$$

And

$$a = \frac{N\uparrow}{N\uparrow + N\downarrow} \tag{A30}$$

Then the degradation in the overall clear-sky carrier-to-noise ratio in the presence of uplink and downlink fading and interference can be written as:

$$\left(\frac{C}{N}\right)_{cs-deg} = \frac{N\uparrow}{N\uparrow + N\downarrow} X_{up}Y_{up} + \frac{N\downarrow}{N\uparrow + N\downarrow} X_{dn}Y_{dn} \tag{A31}$$

From the above equation, we note that the uplink degradations due to fading and interference increase the proportion of the uplink clear-sky noise contribution to the overall carrier-to-noise ratio, while the downlink degradations due to fading and interference similarly increase the proportion of the downlink clear-sky noise contribution to the overall carrier-to-noise ratio.

Equation (A31) could be written as:

$$\left(\frac{C}{N}\right)_{cs-deg} = P_1 + P_2 \tag{A32}$$

Where we have for P_1:

$$P_1 = X_1 X_{up} Y_{up} \tag{A33}$$

with

$$X_1 = \frac{N\uparrow}{N\uparrow + N\downarrow} \tag{A34}$$

$$X_{up} = F_u(Ac\uparrow) \tag{A35}$$

$$Y_{up} = 1 + \frac{1}{F(Ai\uparrow)}\left(\frac{I\uparrow}{N\uparrow}\right) \tag{A36}$$

Similarly, we have for P_2:

$$P_2 = X_2 X_{dn} Y_{dn} \tag{A37}$$

with

$$X_2 = \frac{N\downarrow}{N\uparrow + N\downarrow} \tag{A38}$$

$$X_{dn} = F(Ac\downarrow)G(Ac\downarrow) \tag{A39}$$

$$Y_{dn} = 1 + \frac{1}{F(Ac\downarrow)G(Ac\downarrow)}\left(\frac{I\downarrow}{N\downarrow}\right) \tag{A40}$$

By observation, we can see that the set of random variables which make up P_1 and the set of random variables which make up P_2 are independent of each other and hence the random variables $P_1$and P_2 are independent. The pdf of the degradation in the overall clear-sky carrier-to-noise ratio in the presence of uplink and downlink fading and interference $\left(\frac{C}{N}\right)_{cs-deg}$ can then be obtained by taking the convolution of the pdf of P_1 with the pdf of P_2.

To derive the pdf of P_1 it is convenient to work in dBs.

Let

$$p_1 = 10\ Log\{P_1\} \tag{A41}$$

$$x_1 = 10\ Log\{X_1\} \tag{A42}$$

$$x = 10\ Log\{X_{up}\} \tag{A43}$$

$$y = 10\ Log\{Y_{up}\} \tag{A44}$$

Let

$$u = x + y \tag{A45}$$

Then

$$p_1 = x_1 + u \tag{A46}$$

Note that x_1 is a constant and that the pdf of u was derived earlier and is given in equation (A11). It follows that the pdf of P_1 is given by:

$$PDF_{P_1}(p_1(dB)) = PDF_U(p_1(dB) - x_1(dB)) \tag{A47}$$

This represents the pdf of the values in dB of the uplink degradation due to the uplink effects on the wanted carrier and the uplink interference.

The next step is to derive the pdf of P_2. To derive the pdf of P_2 it is convenient to work with linear values. Let P_2 be expressed as:

$$P_2 = X_2\ (\mathrm{S} + \mathrm{T}) \tag{A48}$$

where:

$$X_2 = \frac{N\downarrow}{N\uparrow + N\downarrow} \tag{A49}$$

$$S = F(Ac\downarrow)G(Ac\downarrow) \tag{A50}$$

$$T = \left(\frac{I\downarrow}{N\downarrow}\right) \tag{A51}$$

Let

$$E = S + T \tag{A52}$$

Since *S* and *T* are independent random variables, the pdf of *E* is obtained by taking the convolution of the pdf of *S* and the pdf of *T*, as shown in § A.1.2. We have:

$$PDF_E(e) = PDF_S(e) * PDF_T(e) \tag{A53}$$

and

$$PDF_D(d_i(dB)) = PDF_E(10Log(e_i(linear))) \tag{A54}$$

The pdf of P_2 can be expresses as:

$$PDF_{P_2}(p_2) = PDF_E\left(\frac{p_2}{X_2}\right) \tag{A55}$$

The $PDF_{P_2}(p_2)$ can be expressed in dB as follows:

$$PDF_{P_2}(p_2\ (dB)) = PDF_E\left(10Log\left\{\left(\frac{p_2}{X_2}\right)(linear)\right\}\right) \tag{A56}$$

Let

$$x_2 = 10\ Log\{X_2\} \tag{A57}$$

The, we can write

$$PDF_{P_2}(p_2\ (dB)) = PDF_D(p_2\ (dB) - x_2\ (dB)) \tag{A58}$$

This represents the pdf of the values in dB of the downlink degradation due to the downlink effects on the wanted carrier and the downlink interference.

Let

$$P = P_1 + P_2 \tag{A59}$$

Then, the pdf of *P* will be the pdf of the degradation in the overall carrier-to-noise ratio in the uplink and downlink due to rain attenuation and interference. The pdf of *P* is obtained from the convolution of the pdf of P_1 with the pdf of P_2. The we have:

$$PDF_P(p(dB)) = PDF_{P_1} * PDF_{P_2}(p(dB)) \tag{A60}$$

$$= PDF_U\big(p(dB) - x_1(dB)\big) * PDF_D(p\ (dB) - x_2\ (dB)) \tag{A61}$$

$$= PDF_U * PDF_D(p\ (dB) - x_1(dB) - x_2\ (dB)) \tag{A62}$$

Equation (A60) gives us the pdf of the degradation in the overall carrier-to-noise ratio in the uplink and downlink due to rain attenuation and interference.

Attachment 2
to Annex 9

Derivation of overall uplink and downlink degradation in carrier-to-noise ratio

In this Attachment is derived a simple expression that defines the overall degradation in the carrier-to-noise ratio in terms of the uplink and downlink effects on the wanted signal and the interference terms for the uplink and the dowlink.

From equations (A1), (A2) and (A3), we express the uplink carrier-to-noise ratio as:

$$\left(\frac{C}{N}\right)_{up} = \left(\frac{C_{cs}}{N\uparrow}\right) \text{ x } \frac{1}{X_{up}} \text{ x } \frac{1}{Y_{up}} \tag{B1}$$

Let

$$x_1 = \left(\frac{C_{cs}}{N\uparrow}\right) \tag{B2}$$

$$\alpha = \frac{1}{X_{up}} \text{ x } \frac{1}{Y_{up}} \tag{B3}$$

Then

$$\left(\frac{C}{N}\right)_{up} = \alpha x_1 \tag{B4}$$

From equations (A12), (A16) and (A17), we can express the downlink carrier-to-noise ratio as:

$$\left(\frac{C}{N}\right)_{dn} = \left(\frac{C_{cs}}{N\downarrow}\right) \text{ x } \frac{1}{X_{dn}} \text{ x } \frac{1}{Y_{dn}} \tag{B5}$$

Let

$$x_2 = \left(\frac{C_{cs}}{N\downarrow}\right) \tag{B6}$$

$$\beta = \frac{1}{X_{dn}} \text{ x } \frac{1}{Y_{dn}} \tag{B7}$$

Then

$$\left(\frac{C}{N}\right)_{dn} = \beta x_2 \tag{B8}$$

Under clear-sky conditions, the overall carrier-to-noise ratio is given by:

$$\left(\frac{C}{N}\right)_{cs} = \frac{x_1 x_2}{x_1 + x_2} \tag{B9}$$

With rain attenuation and interference, the overall carrier-to-noise ratio is given by:

$$\left(\frac{C}{N}\right)_{att+int} = \frac{\alpha x_1 \ \beta x_2}{\alpha x_1 + \ \beta x_2} = \frac{\alpha x_1 \ \beta x_2}{\alpha x_1 + \ \beta x_2} \text{ x } \frac{x_1 + x_2}{x_1 + x_2} = \frac{x_1 x_2}{x_1 + x_2} \text{ x } \frac{\alpha\beta \ (x_1 + x_2)}{\alpha x_1 + \ \beta x_2} \tag{B10}$$

The degradation in the overall clear-sky carrier-to-noise ratio is given by the ratio:

$$\left(\frac{C}{N}\right)_{cs-deg} = \frac{\left(\frac{C}{N}\right)_{cs}}{\left(\frac{C}{N}\right)_{att+int}} = \frac{\frac{x_1 x_2}{x_1 + x_2}}{\frac{x_1 x_2}{x_1 + x_2} \text{ x } \frac{\alpha\beta \ (x_1 + x_2)}{\alpha x_1 + \ \beta x_2}} = \frac{\alpha x_1 + \ \beta x_2}{\alpha\beta \ (x_1 + x_2)} \tag{B11}$$

Equation (B11) can be written as:

$$\left(\frac{C}{N}\right)_{cs-deg} = \frac{1}{(x_1 + x_2)} \text{ x } \left(\frac{x_1}{\beta} + \frac{x_2}{\alpha}\right) \tag{B12}$$

Substituting back in for x_1 and x_2 , we get

$$\left(\frac{C}{N}\right)_{cs-deg} = \frac{1}{\left(\left(\frac{C_{CS}}{N\uparrow}\right)+\left(\frac{C_{CS}}{N\downarrow}\right)\right)} \text{ x } \left(\frac{\left(\frac{C_{CS}}{N\uparrow}\right)}{\beta} + \frac{\left(\frac{C_{CS}}{N\downarrow}\right)}{\alpha}\right) = \frac{1}{\left(\left(\frac{1}{N\uparrow}\right)+\left(\frac{1}{N\downarrow}\right)\right)} \text{ x } \left(\frac{\left(\frac{1}{N\uparrow}\right)}{\beta} + \frac{\left(\frac{1}{N\downarrow}\right)}{\alpha}\right) \quad \text{(B13)}$$

$$= \frac{N\uparrow N\downarrow}{N\downarrow + N\uparrow} \text{ x } \left(\frac{\left(\frac{1}{N\uparrow}\right)}{\beta} + \frac{\left(\frac{1}{N\downarrow}\right)}{\alpha}\right) \quad \text{(B14)}$$

$$= \frac{N\uparrow}{N\downarrow + N\uparrow} \text{ x } \frac{1}{\alpha} + \frac{N\downarrow}{N\downarrow + N\uparrow} \text{ x } \frac{1}{\beta} \quad \text{(B15)}$$

Substituting back in for α and β , we get:

$$\left(\frac{C}{N}\right)_{cs-deg} = \frac{N\uparrow}{N\downarrow + N\uparrow} X_{up}Y_{up} + \frac{N\downarrow}{N\downarrow + N\uparrow} X_{dn}Y_{dn} \quad \text{(B16)}$$

Which is the result shown in equation (A31).

Annex 10

Study 10: Sharing study relating (*I*/*N*) to spectral efficiency of satellite networks using ACM

Executive summary

This study was done in support of WRC-19 agenda item 1.6. The approach of studying systems using ACM was to address the impact of long-term decrease in spectral efficiency (measured as a decrease in throughput) of GSO FSS networks due to non-GSO interference. This approach is to be used in combination with approaches looking at increase in GSO FSS link unavailability.

This sharing study examines the long-term impact to throughput of a GSO system employing Adaptive Coding and Modulation (ACM) that is subjected to interference from a non-GSO system. Any reduction in throughput is ultimately reflected in a decrease in spectral efficiency.

The results show that during rain fading events, the reduction in throughput is mostly due to the degradation in the carrier-to-noise ratio, which results from rain and other types of atmospheric attenuation. A reduction in thoughput is a reduction in the long-term of the amount of data that can be transmitted and received.

Two interference scenarios from a non-GSO system into the downlink of a GSO network were considered. In the first case, the GSO earth station was at a higher lattitude (Saskatoon, Canada) and the interference had minimal impact on the spectral efficiency of a link employing ACM. In the second case, the GSO earth station was assumed to be at a lower lattitude (Lima, Peru). The analysis and calculations show that even with high peaks in *I*/*N* (up to 33 dB), the long-term spectral reduction in efficiency for the second case was about 2%.

In addition, an analysis relating the degradation in throughput (reduction in spectral efficiency) of a link employing ACM to the duration of *I*/*N* interference burst was performed. Taking into account the wide dynamic range of *C*/*N* over which ACM systems can operate, short bursts of interference with high *I*/*N* levels do not substantially degrade the performance of an ACM system.

Availability:

The study examined cases in which the rate of change in *I/N* exceeded 1dB/second and in which the *I*/*N* exceeds the dynamic range of the modem. In other words, when the excess path loss (e.g., loss in excess of that during clear-sky conditions) exceeds the dynamic range of the ACM system to compensate for such fades or when there are imperfections in the ACM system to mitigate the detected fade, there is an unavailability associated with those events. This additional unavailability is given in the paper.

Summary

This study clearly demonstrates that the additional loss of throughput as a result of interference is a small fraction of the loss in throughput due to propagation effects alone.

1 Introduction

In this study is investigated the impact on the spectral efficiency of a GSO network employing Adaptive Coding and Modulation (ACM) that is subjected to interference from a non-GSO network. The study considers the sensitivity of ACM systems to variations in the ratio of *I*/*N* rather than epfd.

Operation of V-Band non-GSO systems has the potential to cause interference to GSO networks operating in this band – downlinks in 37.5-42.5 GHz (space-to-Earth), and uplinks in 47.2-50.2 GHz (earth-to-space) and 50.4-51.4 GHz (Earth-to-space). The ITU has addressed similar concerns in FSS bands below 30 GHz by imposing epfd limits on non-GSO systems. In this study, we demonstrate that imposing fixed limits on epfd or *I*/*N* are not necessarily good protection measures considering the characteristics of the interference generated by non-GSO systems and the capabilities of satellite networks employing ACM; the spectral efficiency of an ACM system subject to interference is a better indicator.

This study uses as its basis methodologies being developed by the ITU-R.

This study looks at two cases studies; one where the northern latitude of the GSO earth station leads to minimal impact from the non-GSO system; and a second cases at lower latitude where the impact from the non-GSO system is more severe. The results, which address short term and long term impact demonstrate that systems employing ACM can cope with a very wide range of interference levels while maintaining a high spectral efficiency.

2 GSO Network Parameters

Annex 13 provides tables of FSS parameters for sharing studies. Although not specifically developed for these sharing studies, this Annex provides parameters of representative V-band FSS networks.

2.1 Earth Station Parameters

The key GSO network parameters for assessing the impact of interference are the Earth Station (ES) antenna diameter and noise temperature. ES antenna diameters range from 0.3 to 9 m and ES noise temperatures from 150 to 500 K based on “clear-sky” conditions using a value of sky noise that is not exceeded for more than 20% of the time. Removing outliers, the implied antenna efficiency ranges from 0.25 to 0.9. A representative value of ES noise temperature of 250 K, and an ES antenna efficiency of 0.7 are assumed for the analysis in this study.

2.2 Satellite Parameters

The key GSO network parameter for assessing the impact of aggregate interference in the (Earth-to-space) direction is the satellite receive beam G/T. The higher the G/T, the higher the sensitivity to

interference. ITU documentation provides parameters for 27 carriers in the 47.2-50.2 GHz and/or 50.4-51.4 GHz frequency bands. Satellite receive beam G/T ranges from 7.2 to 34.1 dB/K. Similar results are obtained from the ITU-R SNS database which contains 656 unique notices for GSO satellites operating uplinks in the 47.2-50.2 GHz and/or 50.4-51.4 GHz bands. The peak G/T values obtained from these notices range from 4.2 to 37.4 dB/K, with 439 notices having peaks between 21 and 22 dB/K and 114 having peaks between 34 and 35 dB/K.

3 Impact of degradation in (*C*/*N*) on spectral efficiency

Many of the current two-way satellite communications networks carry Internet traffic, where maintaining connections is more important than providing a constant bit rate. Modern GSO networks utilize adaptive coding and modulation (ACM), with power amplifier linearization techniques, to improve spectral efficiency and transmission performance. Linearization techniques allow the use of higher order, more spectrally efficient, modulations. ACM allows the maintenance of satellite connections in the face of degraded propagation, although, at the cost of a reduced throughput. ACM systems are sensitive and adapt rapidly to changes in the *C*/*N*. Thus, even small amounts of link degradation have significant impact on the network's performance.

ACM combats the link degradation resulting from fade impacts and interference by maintaining the connection, albeit with reduced throughput. This decrease in throughput results in decreased end-to-end capacity over the satellite link. The impact of degradation is related to decrease in satellite link capacity by the slope of the ACM modem operating curve. Modem performance has improved significantly over the last two decades and is expected to continue improving in the future, though such improvement will be more limited as the Shannon Limit is approached. Today's state-of-the-art modems provide DVB-S2X class performance.

Modem performance is bounded by the Shannon limit, which relates the maximum achievable spectral efficiency to the available C/N (in this context, N is the total noise in the link, including thermal and interference). The Shannon limit is:

$$\varepsilon(bps/Hz) = \log_2\left(1 + 10^{C/N\,(dB)/10}\right) \tag{39}$$

The sensitivity of spectral efficiency to *C*/*N* of an ideal (Shannon limit) modem is given by:

$$\dot{\varepsilon}\left(\frac{bps}{Hz}/dB\right) = \frac{d\varepsilon}{d(C/N)} = \frac{\ln(10)\times 10^{C/N\,(dB)/10-1}}{\ln(2)\times\left(1+10^{\,C/N(dB)/10}\right)} \tag{40}$$

And the relative sensitivity by:

$$S\left(\frac{1}{dB}\right) = \frac{\ln(10)\times 10^{C/N\,(dB)/10-1}}{\ln(2)\times\left(1+10^{C/N\,(dB)/10}\right)\times\log_2\left(1+10^{C/N\,(dB)/10}\right)} \tag{41}$$

Figure A10-1 shows the Shannon limit curve, the DVB-S2X modem MODCOD's, and the least squares 2nd degree polynomial fit to the MODCOD's.

FIGURE A10-1

Modem operating curve

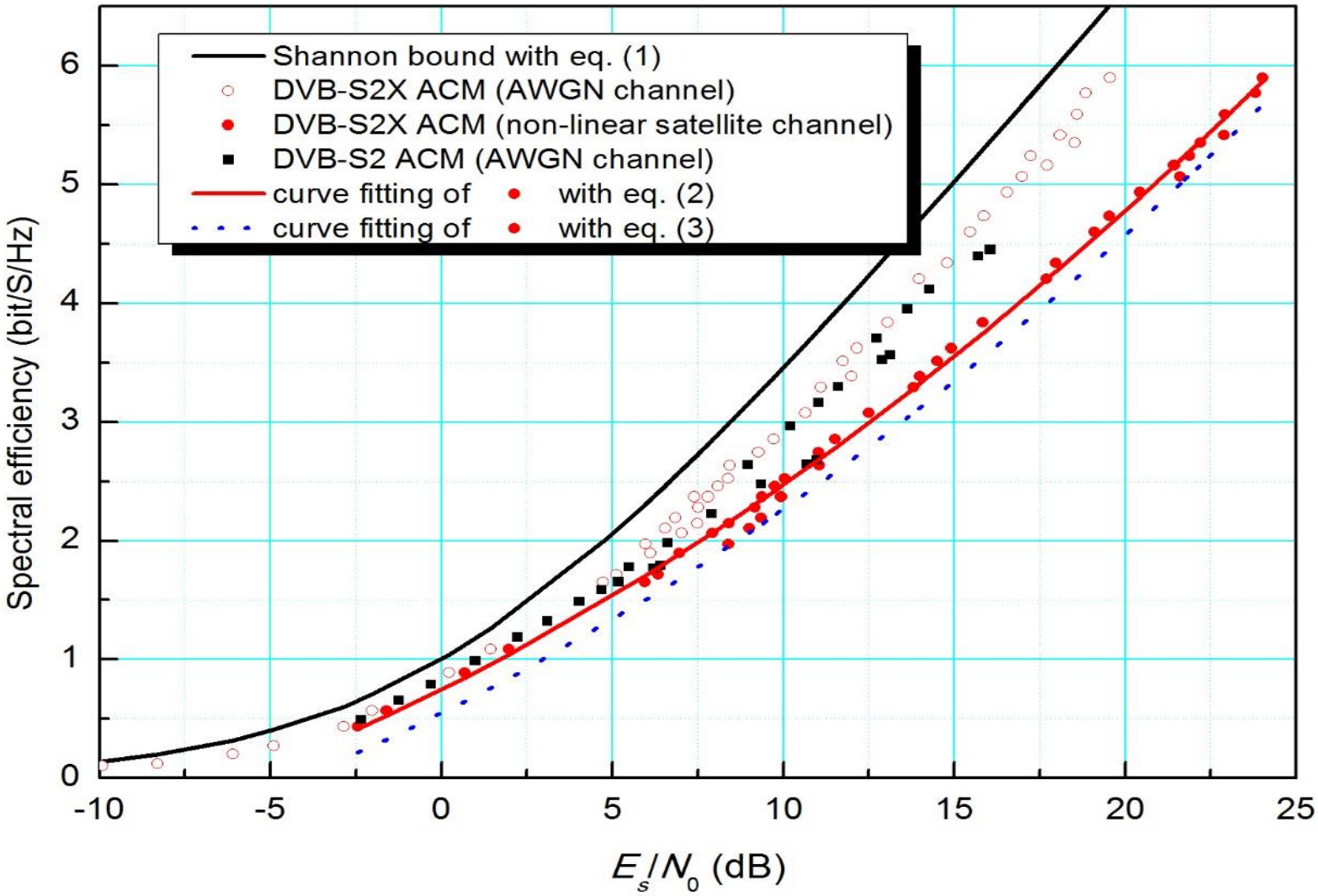

The fit equation,

$$\varepsilon\,(bps/Hz) = 0.00292 \times (C/N)^2 + 0.14337\ \times\ (C/N) + 0.74493 \tag{42}$$

facilitates calculation of the sensitivity of spectral efficiency of the DVB-S2X modem to *C*/*N*:

$$\dot{\varepsilon}\,(\frac{bps}{Hz}/dB) = 0.00584 \times (C/N) + 0.14337 \tag{43}$$

The relative sensitivity of the DVB-S2X modem is given by:

$$S\,\left(\frac{1}{dB}\right) = \frac{0.00584\times(C/N)+0.14337}{0.00292\times(C/N)^2+0.14337(C/N)+0.74493} \tag{44}$$

The DVB-S2X and Shannon relative sensitivities of spectral efficiency to changes in *C*/*N* are shown in Fig. A10-2. This Figure shows that the sensitivity is between 5% and 19% data rate reduction per dB for an ideal (Shannon limit) modem and between a 6% and 31% per dB for a DVB-S2X modem, depending on operating point. For example, a typical undegraded GSO operating point of 12.3 dB, the sensitivity is 8% per dB for today's state-of-the-art DVB-SX2 modems, and slightly less for an ideal (Shannon limit) modem.

FIGURE A10-2

Data rate sensitivity to changes in *C*/*N*

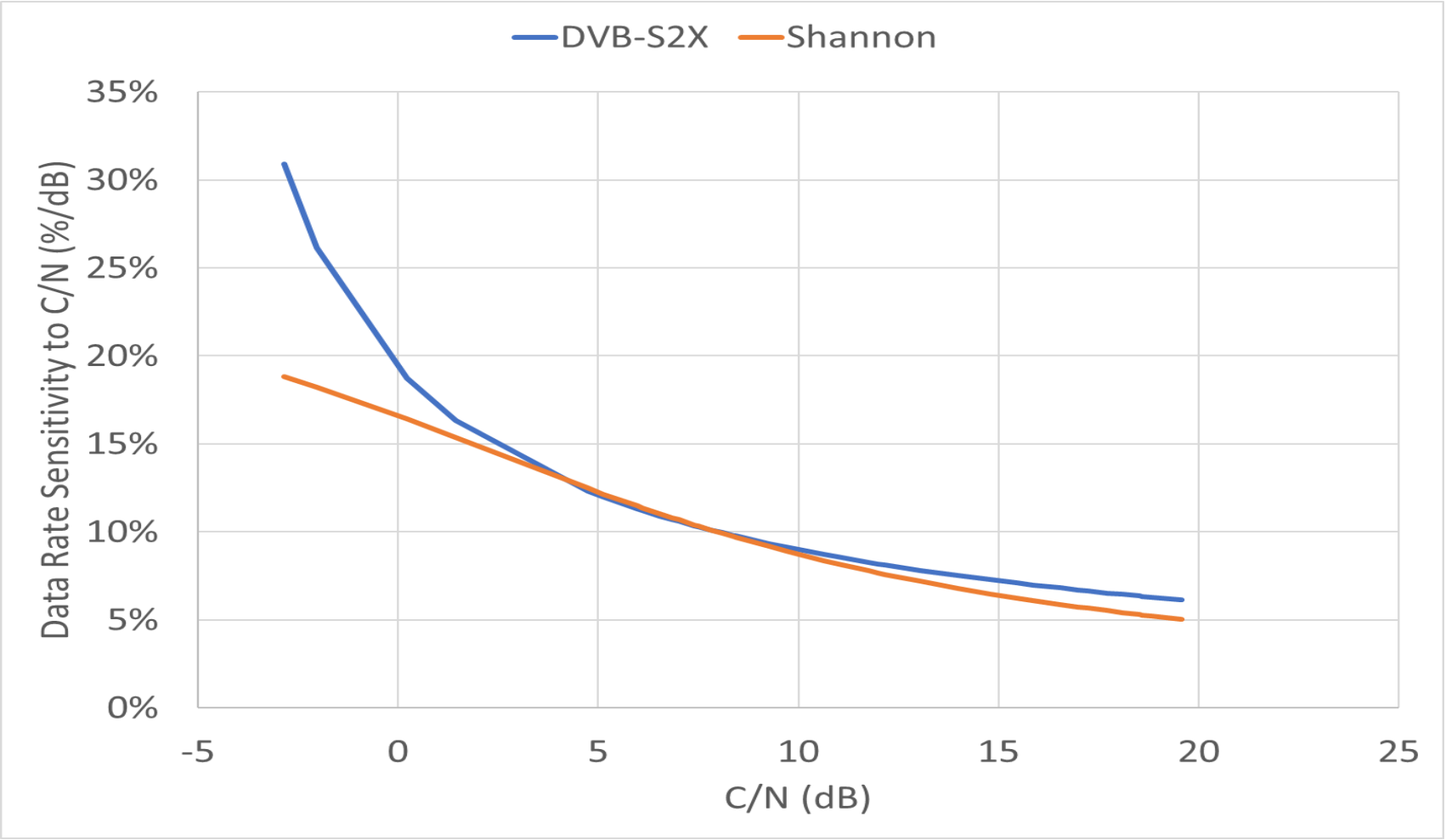

The percent degraded throughput, %DTp, is given by:

$$\%\mathrm{DTp}(\rho,\gamma) = 100\left[1 - \frac{\varepsilon(\rho-\gamma)}{\varepsilon(\rho)}\right] \quad (45)$$

where

ρ : undegraded C/N (dB)

γ: degradation (dB)

$\varepsilon(x)$: spectral efficiency function bits/s/Hz.

The average percent degraded throughput ($\overline{\%DTp}$) is given by:

$$\overline{\%DTp}(\rho) = 100\left[1 - \int_0^\infty p(\gamma)\frac{\varepsilon(\rho-\gamma)}{\varepsilon(\rho)}d\gamma\right] \quad (46)$$

where:

$p(\gamma)$ is the probability density function (pdf) of degradation γ resulting from interference specified as an, and is constrained by:

$$\int_0^\infty p(\gamma)\,d\gamma = 1 \quad (47)$$

The cumulative distribution function (cdf), the probability of degradation not exceeding γ, is given by:

$$cdf(\gamma) = \int_0^\gamma p(z)\,dz \quad (48)$$

4 Definitions and assumptions

In this section, the basis assumptions and definitions used throughout this study are provided.

4.1 Basic definitions

C : wanted power (W), which varies as a function of the uplink and downlink fades and also as a function of the transmission configuration (multiple access, use of uplink power control, etc.)

Ccs: wanted power (W), in clear-sky conditions (long-term condition)

N: total link (uplink or downlink) system noise (W) (i.e. the thermal power on uplink or downlink contributions at the demodulator input, the noise power resulting from the multi-carrier operation of the involved power amplifier –in the earth stations and in the space stations– , the cross polarization isolations of the different transmit and receive antennas, the thermal power increase due to increased path attenuation during rain events of which attenuation due to rain is the dominant factor, which also varies as a function of the transmission configuration and with the uplink and downlink fades. *N* also includes allocation for long-term (i.e. *not* time-varying) contributions from other GSO networks. The uplink and downlink system noise will be affected by fades

$N\uparrow$ and $N\downarrow$: uplink and downlink noise power in clear-sky conditions (long-term condition) (W)

$I\uparrow$ and $I\downarrow$: uplink and downlink time-varying interference power (W) generated by other networks.

4.2 Basic Assumptions

For the purpose of the technical analysis of the impact of co-frequency non-GSO FSS systems on GSO FSS links during fading events, the following assumptions are made:

Assumption 1: The two time-varying sources of degradation considered in the analysis are link fading plus any other time variations in the characteristics of the link and interference from other FSS networks.

Assumption 2: Let $F_u(Ac\uparrow)$ denote the degradation in the uplink clear-sky *C/N* due to fading of the carrier, F(Ai↑) be the fading of the uplink interference and F(Ac↓) denote the degradation in the downlink clear-sky carrier-to-noise ratio due to fading of the downlink carrier. It is assumed that for the uplink $F_u(Ac\uparrow)$ and F(Ai↑) are not correlated. Let G(Ac↑) and G(Ac↓) denote the increase in the uplink receiver noise temperature and the downlink receiver noise temperature, respectively. G(Ac↑) is included in the derivation of the equations for generality; however, typically the uplink increase in receiver noise temperature is ignored in the studies. Note that $F_u(Ac\uparrow)$ is generally not the simple attenuation of the uplink carrier due to rain and cloud fade and increases in fade due to increased gaseous attenuation during rain; it also represents the application of uplink power control, uplink site diversity and automatic level control in the satellite. The function F(A) and G(A) are defined in Recommendation ITU-R P.618.

Due to fading plus other time variations in the characteristics of the link, carrier and interference power reductions and noise enhancements due to fading can be accounted for by introducing the appropriate factor.

Assumption 3: This analysis assumes that, during a fading event in the downlink direction, the interfering carrier is attenuated by the same amount as the wanted carrier. This assumption results in some under-estimation of the total downlink degradation under circumstances where interference peaks and downlink fading occur simultaneously.

Assumption 4: The time allowances for each interference entry are obtained by dividing by *N* the time allowances associated with the total interference. This number *N* is related to the number of networks that can potentially cause time-varying interference and will be referred to as the equivalent number of networks. *N* may also vary with the time percentage considered.

5 Uplink considerations

5.1 Clear-sky conditions

This section derives the aggregate epfd↑ resulting from operation of co-frequency non-GSO FSS systems that would result in a specific percentage degradation of throughput on the uplink in clear-sky conditions.

For the case of clear sky conditions for both the uplink carrier and the interference, the equation for the uplink degradation due to interference reduces to (in terms of spectral densities):

$$Y_{up} = 1 + \left(\frac{I_0\uparrow}{N_0\uparrow}\right) \tag{49}$$

The clear-sky aggregate epfd↑ resulting from operation of co-frequency non-GSO FSS systems is potential interference into a GSO FSS uplink. The impact of this interference is characterized by the interference-spectral-density to thermal-noise-spectral-density ratio $\left(\frac{I_0\uparrow}{N_0\uparrow}\right)$, which can be calculated as:

$$\left(\frac{I_0\uparrow}{N_0\uparrow}\right) = epfd\uparrow(dBW/m^2) - 10\log_{10} B_R(Hz) + G/T(dB/K) - G_1(dB/m^2) - k(dBW/(K\cdot Hz)) \tag{50}$$

where:

epfd↑ is aggregate effective PFD in the uplink direction (dBW/m^2)

B_R is the reference bandwidth associated with the epfd↑ value (Hz)

G/T is the GSO satellite receive beam G/T (dB/K)

G_1 is the ideal gain of a 1-meter squared area at the uplink frequency (dB).

$$G_1(dB) = 10\log_{10}\left[\frac{4\pi\times F(Hz)^2}{c(m/s)^2}\right] \quad (51)$$

where:

F is the uplink frequency (Hz)

c is the speed of light, 299,792,458 m/s

k is Boltzmann's constant, −228.6 dBW/(K×Hz).

Plugging in the 40-kHz reference bandwidth and using 49.26 GHz as the uplink frequency (< 0.2 dB error across the two bands), gives

$$\left(\frac{I_0\uparrow}{N_0\uparrow}\right)(\text{dB}) = epfd_\uparrow\ (dBW/m^2) + G/T\ (dB/K) + 127.3\ dB \quad (52)$$

Alternatively, if the GSO satellite beam receive noise temperature, T (K), and effective antenna area are available, $\left(\frac{I_0\uparrow}{N_0\uparrow}\right)$, can calculated as

$$\left(\frac{I_0\uparrow}{N_0\uparrow}\right)(\text{dB}) = epfd_\uparrow(dBW/m^2) + A_{eff}(dBm^2) + 158.6\ dB \quad (53)$$

Where A_{eff} is the GSO satellite receive beam antenna effective area (dBm^2) and a 250 K noise temperature has been assumed. Although the earth station noise temperature will vary over propagation conditions varying from clear-sky to various levels of rain fade (corresponding to fades exceeded for small percentages of time, the relative change (in dB terms) will be comparatively small compared to the rain fade, thus the error of assuming a constant temperature is expected to be small. The degradation experienced by a GSO FSS uplink can be calculated as

$$L(dB) = 10\log_{10}\left[1 + \left(\frac{I_0\uparrow}{N_0\uparrow}\right)\right] \quad (54)$$

The relationship between aggregate $epfd_\uparrow$, satellite beam G/T, and uplink throughput reduction in terms of $\left(\frac{I_0\uparrow}{N_0\uparrow}\right)$ is shown in Table A10-1.

It is obvious from the results that for a given throughput reduction that the level of *I*/*N* required to produce it is independent of the G/T of the wanted satellite. This demonstrates an advantage of the *I*/*N* approach over that of the epfd approach as it does not depend on the specific system parameters of the interfered-with system.

TABLE A10-1

***I*/*N* (dB) that would result in indicated percentage throughput reduction (%DTp) for various satellite beam G/Ts (dB/K). These results assume a clear-sky *C*/*N* of 12.5 dB**

		I/N			
G/T (dB/K)	**Throughput reduction**				
	1%	**2%**	**3%**	**4%**	**5%**
33	-15.5	-12.3	-10.5	-9.1	-8.1
33.5	-15.5	-12.3	-10.5	-9.1	-8.1
34	-15.5	-12.3	-10.5	-9.1	-8.1
34.5	-15.5	-12.3	-10.5	-9.1	-8.1
35	-15.5	-12.3	-10.5	-9.1	-8.1
35.5	-15.5	-12.3	-10.5	-9.1	-8.1
36	-15.5	-12.3	-10.5	-9.1	-8.1

6 Downlink considerations

6.1 Clear-Sky conditions

This section derives the aggregate epfd↓ resulting from operation of co-frequency non-GSO FSS systems that would result in specific percent degraded throughput on the downlink in clear-sky conditions.

For the case of clear sky conditions for both the downlink carrier and the interference, the equation for the downlink degradation due to interference reduces to (in terms of spectral densities):

$$Y_{dn} = 1 + \left(\frac{I_0\downarrow}{N_0\downarrow}\right) \tag{55}$$

The clear-sky aggregate epfd↓ resulting from the operation of co-frequency non-GSO FSS systems is potential interference in addition to the fading of GSO FSS downlinks. The impact of this interference is characterized by the interference-spectral-density to thermal-noise-spectral-density ratio, $\left(\frac{I_0\downarrow}{N_0\downarrow}\right)$, which, under clear-sky conditions, can be calculated as:

$$\left(\frac{I_0\downarrow}{N_0\downarrow}\right)(\text{dB}) = epfd_{\downarrow}\,(dBW/m^2) - 10\log_{10} B_R\,(Hz) + A_{eff}\,(dBm^2) - T\,(dBK) - k\,(dBW/(K{\times}Hz)) \tag{56}$$

Where:

epfd↓ is aggregate effective pfd in the downlink direction (dBW/m^2)

B_R is the reference bandwidth associated with the epfd↓ value (Hz)

A_{eff} is the GSO satellite network ES antenna effective area (dBm^2)

$$A_{eff}(dBm^2) = 10\log_{10}\left[\frac{\pi{\times}D(m)^2{\times}\varepsilon}{4}\right] \tag{57}$$

where:

D is the antenna diameter (m)

ε is the antenna aperture efficiency

T is the ES noise temperature (K)

k is Boltzmann's constant, −228.6 dBW/(K × Hz)

Assuming a 40-kHz reference bandwidth, 0.7 ES antenna aperture efficiency, and 250 K ES noise temperature, reduces to:

$$\left(\frac{I_0\downarrow}{N_0\downarrow}\right)(dB) = epfd_{\downarrow}\,(dBW/m^2) + 20\log_{10}[D(m)] + 156\,dB \tag{58}$$

The degradation experienced by a GSO FSS downlink is a function of the $I_0\downarrow/N_0\downarrow$. It can be calculated as:

$$L(dB) = 10\log_{10}\left[1 + \left(\frac{I_0\downarrow}{N_0\downarrow}\right)\right] \tag{59}$$

The relationship between ES antenna diameter, and downlink data rate reduction is shown in Table A10-2 in terms of $\left(\frac{I_0\downarrow}{N_0\downarrow}\right)$.

Again, it is obvious from the results that for a given throughput reduction that the level of *I*/*N* required to produce it is independent of the G/T of the wanted satellite. This demonstrates an advantage of the *I*/*N* approach over that of the epfd approach as it does not depend on the specific system parameters of the interfered-with system.

TABLE A10-2

***I/N* (dB) that would result in indicated percentage throughput reduction (%DTp) for various ES antenna diameters (m). These results assume a clear-sky *C/N* of 12.5 dB**

I/N					
Antenna diameter (m)	**Throughput reduction**				
	1%	**2%**	**3%**	**4%**	**5%**
0.3	−15.6	−12.3	−10.6	−9.2	−8.1
0.45	−15.5	−12.2	−10.5	−9.1	−8.0
0.6	−15.5	−12.2	−10.5	−9.1	−8.0
1	−15.5	−12.3	−10.5	−9.1	−8.1
2	−15.5	−12.3	−10.5	−9.2	−8.1
5	−15.5	−12.3	−10.5	−9.1	−8.0

6.2 Rain faded conditions

6.2.1 Degradation in downlink carrier-to-noise ratio

In this section is considered the effect of rain fade on the spectral efficiency of a system employing ACM. The analysis provided here makes use of assumption 3, specifically, that during a fading event in the downlink direction, the interfering carrier is attenuated by the same amount as the wanted carrier.

From Attachment 1 to Annex 9, equations (A15), (A16) and (A17), the degradation in the downlink clear-sky carrier-to-noise ratio $\left(\frac{C_{cs}}{N\downarrow}\right)_{deg}$ is given by (in terms of spectral densities):

$$\left(\frac{C_{cs}}{N\downarrow}\right)_{deg} = X_{dn}Y_{dn} \tag{60}$$

where

$$X_{dn} = F(Ac\downarrow)G(Ac\downarrow) \tag{61}$$

$$Y_{dn} = 1 + \frac{1}{F(Ac\downarrow)G(Ac\downarrow)}\left(\frac{I_0\downarrow}{N_0\downarrow}\right) \tag{62}$$

The degradation in the downlink clear-sky carrier-to-noise ratio can be expressed in dB as:

$$\left(\frac{C_{cs}}{N\downarrow}\right)_{deg}(dB) = x + y \tag{63}$$

Where

$$x = 10\,Log\,\{X_{dn}\} = 10\,Log\,\{F(Ac\downarrow)G(Ac\downarrow)\} \tag{64}$$

$$y = 10\,Log\,\{Y_{dn}\} = 10\,Log\left\{1 + \frac{1}{F(Ac\downarrow)G(Ac\downarrow)}\left(\frac{I_0\downarrow}{N_0\downarrow}\right)\right\} \tag{65}$$

Then, the downlink carrier-to-noise ratio $\left(\frac{C}{N}\right)_{dn}$ becomes:

$$\left(\frac{C}{N}\right)_{dn}(dB) = \left(\frac{C_{cs}}{N\downarrow}\right)(dB) - x - y \tag{66}$$

In order to study specific cases, it is necessary to have the expressions for $F(Ac\downarrow)$ and $G(Ac\downarrow)$. The expressions are given by:

$$F(Ac\downarrow) = 10^{Ac\downarrow/10} \tag{67}$$

and

$$G(Ac\downarrow) = \frac{\Delta T_{sky} + T_{sys}}{T_{sys}} \quad (68)$$

where

$Ac\downarrow$: Total atmospheric attenuation excluding scintillation (for a given probability p as given by equation (60) in Rec. ITU-R P.618-13 during rainy conditions.

ΔT_{sky} : change in sky noise temperature (K) at the ground station antenna due to rain

attenuation

T_{sys} : ground station system noise temperature (K)

Note that since $F(Ac\downarrow) \geq 1$ and $G(Ac\downarrow) \geq 1$, then the greatest degradation in $\left(\frac{C}{N}\right)_{dn}$ due to interference occurs under clear sky conditions.

From Recommendation ITU-R P.618-13, T_{sky} is estimated as:

$$T_{sky} = T_{mr}\left(1 - 10^{-Ac\downarrow/10}\right) + 2.7 \text{ x } 10^{-Ac\downarrow/10} \quad (69)$$

where

T_{mr} : atmospheric mean radiating temperature (K)

From the above expression for T_{sky} and assuming the same medium radiating temperature for both clear-sky and rainy conditions, we have for ΔT_{sky} the following:

$$\Delta T_{sky} \approx T_{mr}\left(1 - 10^{-\Delta Ad\downarrow/10}\right) \quad (70)$$

Where

$$\Delta Ad\downarrow = A_T(p)\downarrow - Ac\downarrow \quad (71)$$

$A_T(p)$: Total atmospheric attenuation including scintillation (for a given probability p as given by equation (60) in Rec. ITU-R P.618-13 during rainy conditions.

In the absence of local data, an atmospheric mean temperature of 275 K may be used for clear and cloudy weather. Then, the expression for $G(Ac\downarrow)$ can be written as:

$$G(Ac\downarrow) = \frac{T_{mr}\left(1 - 10^{-Ac\downarrow/10}\right) + T_{sys}}{T_{sys}} \quad (72)$$

Substituting for $F(Ac\downarrow)$ and $G(Ac\downarrow)$ in the equation for $\left(\frac{C}{N}\right)_{dn}$, the degradation in $\left(\frac{C}{N}\right)_{dn}$ due to fading is given by:

$$x = 10\,Log\{\frac{10^{-Ac\downarrow/10}\left[\left(1 - 10^{-Ac\downarrow/10}\right) + T_{sys}\right]}{T_{sys}}\} \quad (73)$$

And the degradation in $\left(\frac{C}{N}\right)_{dn}$ due to the interference is given by:

$$y = 10\,Log\{1 + \frac{10^{-Ac\downarrow/10}\,T_{sys}}{T_{mr}\left(1 - 10^{-Ac\downarrow/10}\right) + T_{sys}}\left(\frac{I_0\downarrow}{N_0\downarrow}\right)\} \quad (74)$$

Figure A10-3 illustrates separately the degradation in downlink carrier-to-noise ratio $\left(\frac{C}{N}\right)_{dn}$ due to rain fade and due to interference for the case of a fixed level of interference set at $\left(\frac{I_0\downarrow}{N_0\downarrow}\right)$ = −12.2 dB, as a function of the fading on the downlink. The results shown in Fig. A10-3 clearly demonstrate that when the interference fades along with the desired signal, the impact on the downlink carrier-to-noise ratio is mostly due to the fading of the wanted carrier. The results show that with zero fading (clear-sky) condition, the degradation in $\left(\frac{C}{N}\right)_{dn}$ is about 0.25 dB as expected and the relative effect of the interference diminishes as the level of fading increases.

From the expression for *y*, see equation (51):

$$y = 10\,Log\left\{1 + \frac{1}{F(Ac\downarrow)G(Ac\downarrow)}\left(\frac{I_0\downarrow}{N_0\downarrow}\right)\right\} \tag{75}$$

It can be seen that the impact of clear-sky aggregate epfd$_\downarrow$ resulting from the operation of co-frequency non-GSO FSS systems is reduced under faded conditions, consequently, the clear-sky expression equation (56) for the interference-to-noise density under faded conditions becomes:

$$\left(\frac{I_0\downarrow}{N_0\downarrow}\right)_{Faded} = epfd_\downarrow - 10\text{Log}\{F(\,Ac\downarrow)G(\,Ac\downarrow)\} + 20\log_{10}[D(m)] + 156\,dB] \tag{76}$$

FIGURE A10-3

Comparison of degradation in $\left(\frac{C}{N}\right)_{dn}$ due to rain fade and interference from non-GSO system

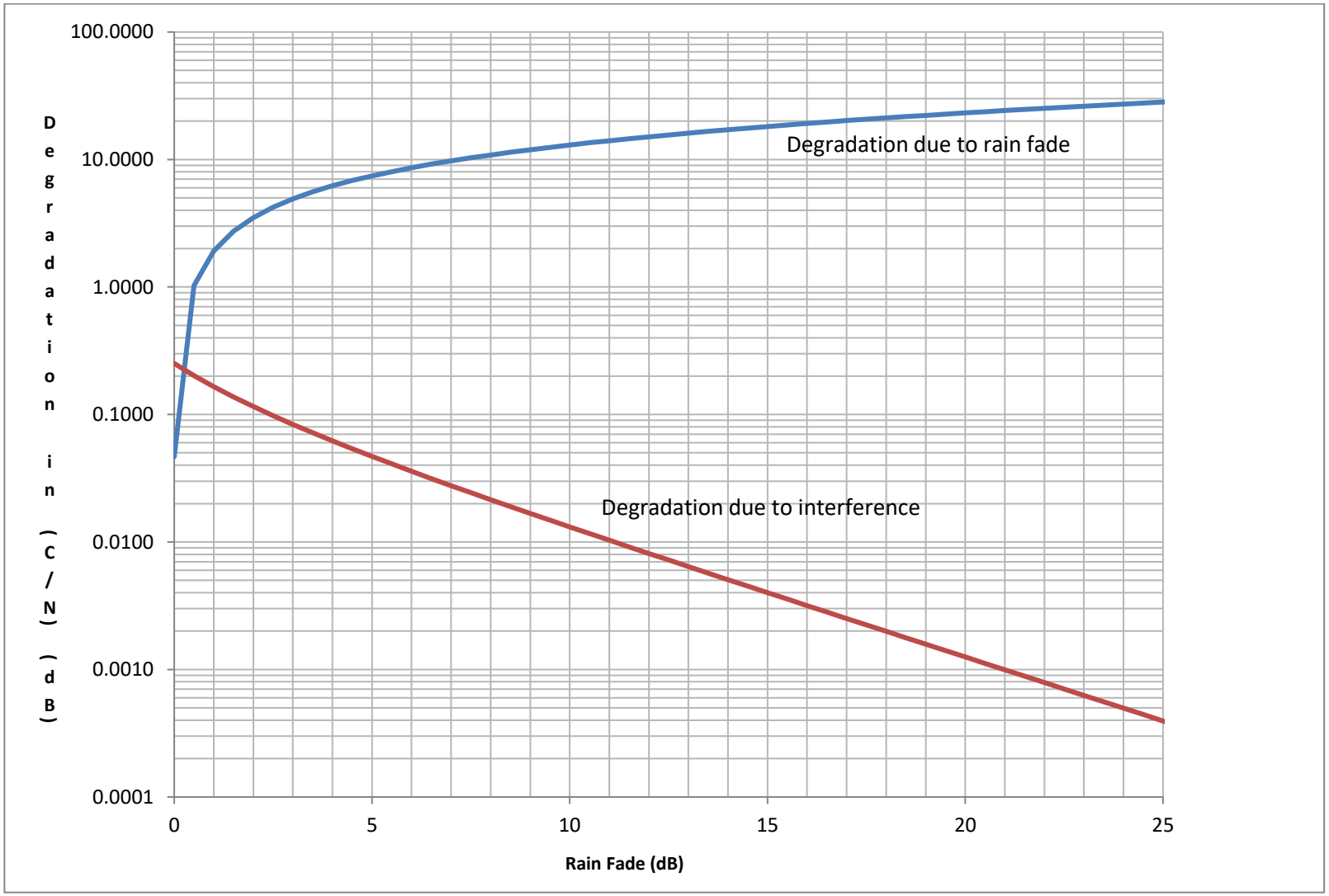

6.2.2 Effect of rain fade and interference on percent degraded throughput

In this section is considered the impact on the percent degraded throughput %DTp of a system employing DVB-S2X. For the purpose of the calculations, the polynomial fit equation from Recommendation ITU-R S.2131-0 was used. The fit equation, which was obtained by fitting the spectral efficiency of the DVB-S2X ACM operation over non-linear satellite channel with a least squared minimum error second order polynomial, is given by:

$$\eta(\gamma) = 0.74493 + 0.14337\,\gamma + 0.00292\,\gamma^2 \quad (77)$$

Figure A10-4 illustrates the sensitivity of the percent degraded throughput to the level of fading under assumption 3, (where the desired signal and interference in the downlink are subject to the same fading event). For the results show, the value of *I*o/*N*o is fixed at −12.2 dB.

From the results shown in Figs A10-3 and A10-4, it is clear that during downlink fade events, the degradation in $\left(\frac{C}{N}\right)_{dn}$ and %DTp resulting from interference subjected to the same fading as the wanted carrier will be minimal. Consequently, the majority of the %DTp caused by interference from a non-GSO system will occur during clear sky conditions. Table A10-3 illustrates the degradation in spectral efficiency due to the rain fade component and due to the interference component. The Table clearly indicates that during rain fades greater than a few dB, any reduction in the additional spectral efficiency caused by interference is minimal, given that when the interference is subject to the same fading as the desired signal. The data in Table A10-3 also assumes a clear sky fixed level of interference set at $\left(\frac{I_0\downarrow}{N_0\downarrow}\right)$ = −12.2 dB.

The results shown in Table A10-3 also clearly demonstrate that the interference will not have a quantitative effect on the availability of a system employing ACM, assuming the clear sky level of the interference was acceptable (say for instance $\left(\frac{I_0\downarrow}{N_0\downarrow}\right)$ = −12.2 dB or −6 dB). These results provide further support to the notion that the bandwidth efficiency of ACM systems is most sensitive to long-term interference. The results in Table A10-3 are for the two cases of $\left(\frac{I_0\downarrow}{N_0\downarrow}\right)$ = −12.2 dB and −6 dB.

FIGURE A10-4

Relative sensitivity of percent degraded throughput due to rain fade
This Figure assumes that the clear-sky *C*/*N* is 23.75 dB – the maximum level for which DVB-S2X has a defined spectral efficiency

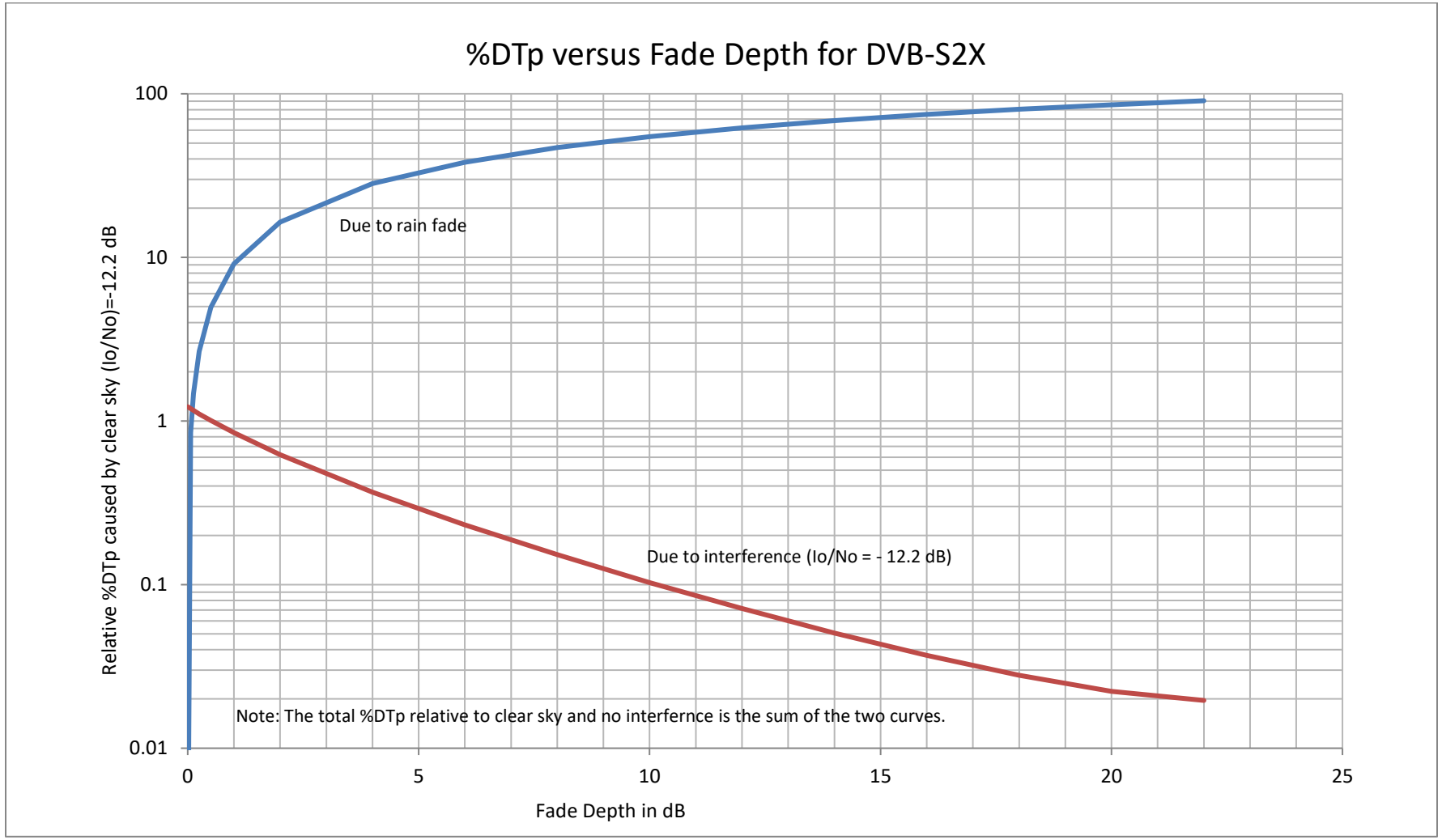

TABLE A10-3

Downlink rain fade and interference effect on spectral efficiency

Clear-sky C/N =	23.75	dB	Io/No = −12.2 dB	Io/No = −12.2 dB	Io/No = −12.2 dB	Io/No = −6 dB	Io/No = −6 dB	Io/No = −6 dB
	C/N degrad.	Spectral Eff.	C/N degrad.	Spectral Eff.	Decrease in	C/N degrad.	Spectral Eff.	Decrease in
Rain Fade	due to rain fade	(rain only deg.)	due to interf.	(rain + interf. deg.)	Spectral Eff.	due to interf.	(rain + interf. deg.)	Spectral Eff.
(dB)	(dB)	b/s/Hz	(dB)	b/s/Hz	(%)	(dB)	b/s/Hz	(%)
0	0.000	5.797	0.254	5.726	1.233	0.973	5.525	4.693
0.0625	0.130	5.760	0.247	5.691	1.198	0.947	5.496	4.583
0.125	0.258	5.724	0.240	5.657	1.171	0.927	5.468	4.472
0.25	0.509	5.654	0.227	5.591	1.114	0.876	5.412	4.280
0.5	0.991	5.520	0.204	5.464	1.014	0.792	5.304	3.913
1	1.886	5.275	0.166	5.231	0.834	0.655	5.099	3.336
2	3.480	4.851	0.116	4.821	0.618	0.464	4.730	2.494
4	6.207	4.159	0.062	4.144	0.361	0.254	4.097	1.491
6	8.610	3.585	0.036	3.577	0.223	0.148	3.551	0.948
8	10.846	3.081	0.022	3.077	0.130	0.089	3.062	0.617
10	12.989	2.626	0.013	2.623	0.114	0.055	2.615	0.419
12	15.076	2.208	0.008	2.207	0.045	0.034	2.202	0.272
14	17.131	1.822	0.005	1.821	0.055	0.021	1.818	0.220
16	19.165	1.464	0.003	1.463	0.068	0.013	1.461	0.205
18	21.186	1.132	0.002	1.131	0.088	0.008	1.130	0.177
20	23.199	0.8250	0.001	0.825	0.000	0.005	0.824	0.121
22	25.208	0.542	0.001	0.542	0.000	0.003	0.542	0.000
23.8	27.013	0.308	0.001	0.308	0.000	0.002	0.308	0.000

6.2.3 Case study of percent degraded throughput on downlink

6.2.3.1 pdf for degradation in carrier-to-noise ratio due to rain attenuation and interference from an non-GSO network

In this section is considered the impact on the percent degraded throughput, %DTp when the rain fading is characterized using the statistics developed from the application of Resolution ITU-R P.618-13 and the interference statistics are thise obtained using a Visualize simulation of a non-GSO satellite network consisting of 108 satellites in six planes, each with 18 satellites in polar orbits. The rain statistics are those representative of the Ottawa region in Canada.

From Attachment 1, the degradation in the clear-sky downlink carrier-to-noise ratio $\left(\frac{C_{cs}}{N\downarrow}\right)$, expressed in terms of spectral densities is given by:

$$\left(\frac{C_{cs}}{N\downarrow}\right)_{deg} = s + t \tag{78}$$

where

$$s = F(Ac\downarrow)G(Ac\downarrow) \tag{79}$$

$$t = \left(\frac{I_0\downarrow}{N_0\downarrow}\right)$$

Note that under clear-sky, *s = 1* and the equation for $\left(\frac{C_{cs}}{N\downarrow}\right)_{deg}$ becomes:

$$\left(\frac{C_{cs}}{N\downarrow}\right)_{deg} = 1 + \left(\frac{I_0\downarrow}{N_0\downarrow}\right) \tag{80}$$

In deep faded conditions, *s* becomes a large number relative to $\left(\frac{I_0\downarrow}{N_0\downarrow}\right)$; hence the equation for $\left(\frac{C_{cs}}{N\downarrow}\right)_{deg}$ tends to:

$$\left(\frac{C_{cs}}{N\downarrow}\right)_{deg} = F(Ac\downarrow)G(Ac\downarrow) \tag{81}$$

With *s* and *t* being independent random variables, the pdf of $e = s + t$ can be obtained through a convolution as discussed in Attachment 1 to Annex 9 and is given by:

$$PDF_E(e) = PDF_S(e) * PDF_T(e) \tag{82}$$

The next step in the process is to obtain $PDF_S(s)$ and $PDF_T(t)$. Using the definitions for $F(Ac\downarrow)$ and $G(Ac\downarrow)$ defined earlier in equations (67) and (72), respectively, we get:

$$s = \left\{\frac{10^{Ac\downarrow/10}\left(T_{mr}\left(1-10^{-Ac\downarrow/10}\right)+T_{sys}\right)}{T_{sys}}\right\} \tag{83}$$

The expression for *s* can be simplified if it is assumed that $T_{mr} \approx T_{sys}$. Then *s* simplifies to

$$s = 2 \text{ x } 10^{Ac\downarrow/10} - 1 \tag{84}$$

And expressing $Ac\downarrow$ linearly (not in dB), it is simply obtained:

$$s = 2Ac\downarrow - 1$$

Then the random variable e becomes:

$$e = 2Ac \downarrow -1 + \left(\frac{I_0 \downarrow}{N_0 \downarrow}\right) \quad (85)$$

Note that equation (85) consists of linear terms.

The application of Recommendation ITU-R P.618-13 gives us rain statistics for the Ottawa region in Canada; it is given below in Fig. A10-5. Note that Recommendation ITU-R P.618-13 applies for probabilities between .001% and 5%. For the purpose of our study, the results between 5% and 20% were extrapolated. This is in line with the accepted value of 80% of the time being clear-sky at lower frequency bands. From the results of Fig. A10-5, the pdf for the rain fade can be calculated, which is shown in Fig. A10-6 below. From the results of Fig. A10-6, the pdf of the degradation in the downlink carrier-to-noise ratio due rain fade can be calculated, which includes the noise enhancement. This pdf is shown in Fig. A10-7.

Note that the point at 20% in Fig. A10-5 is an added interpolation point based on the widely accepted treatment of clear-sky conditions for about 80% of the time. The balance of the analysis carries through with this interpolation.

FIGURE A10-5

Percentage of time the probability that rain fade exceeds a level

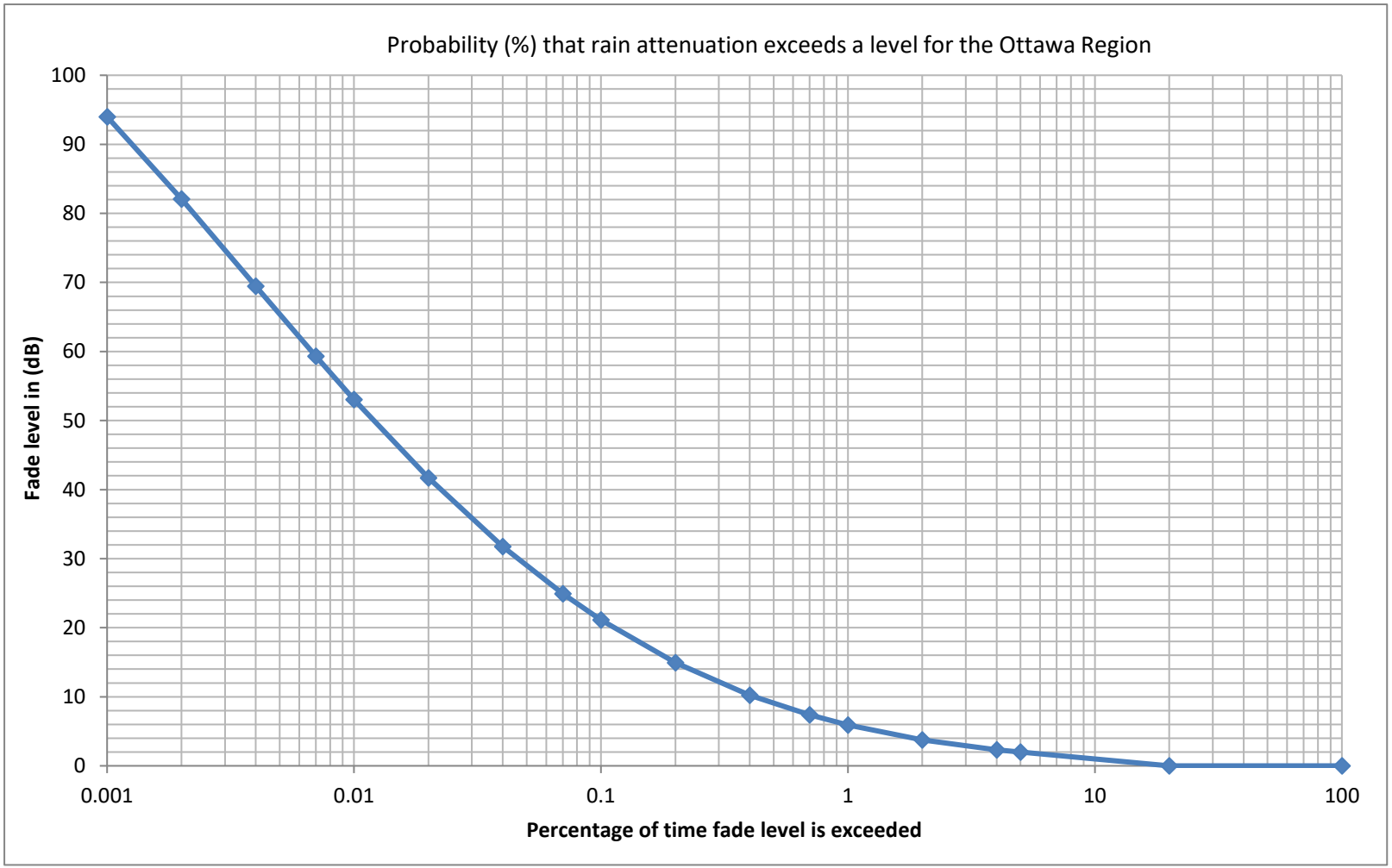

FIGURE A10-6

pdf of rain attenuation for the Ottawa region

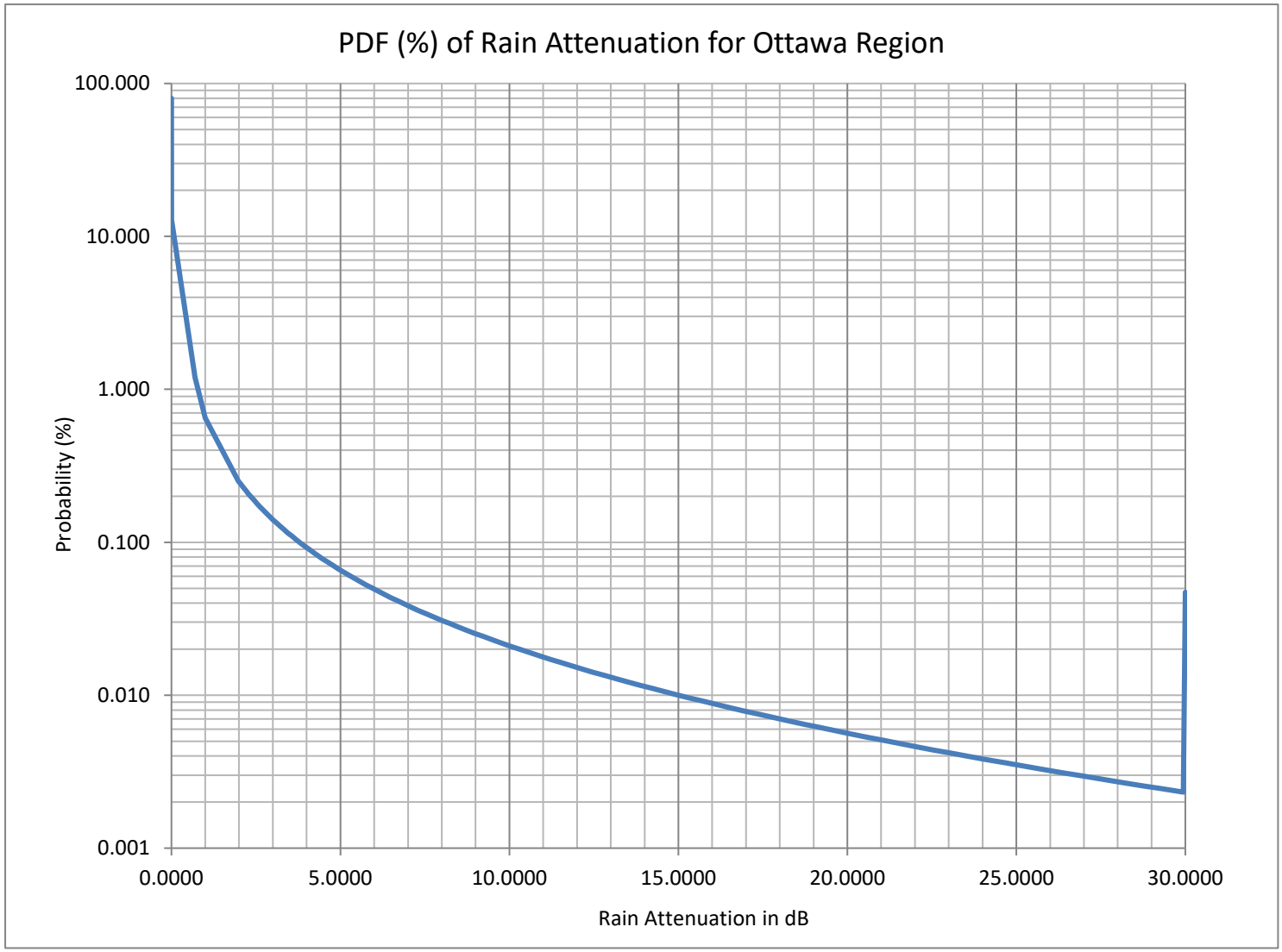

FIGURE A10-7

pdf of downlink degradation in carrier-to-noise ratio due to rain attenuation

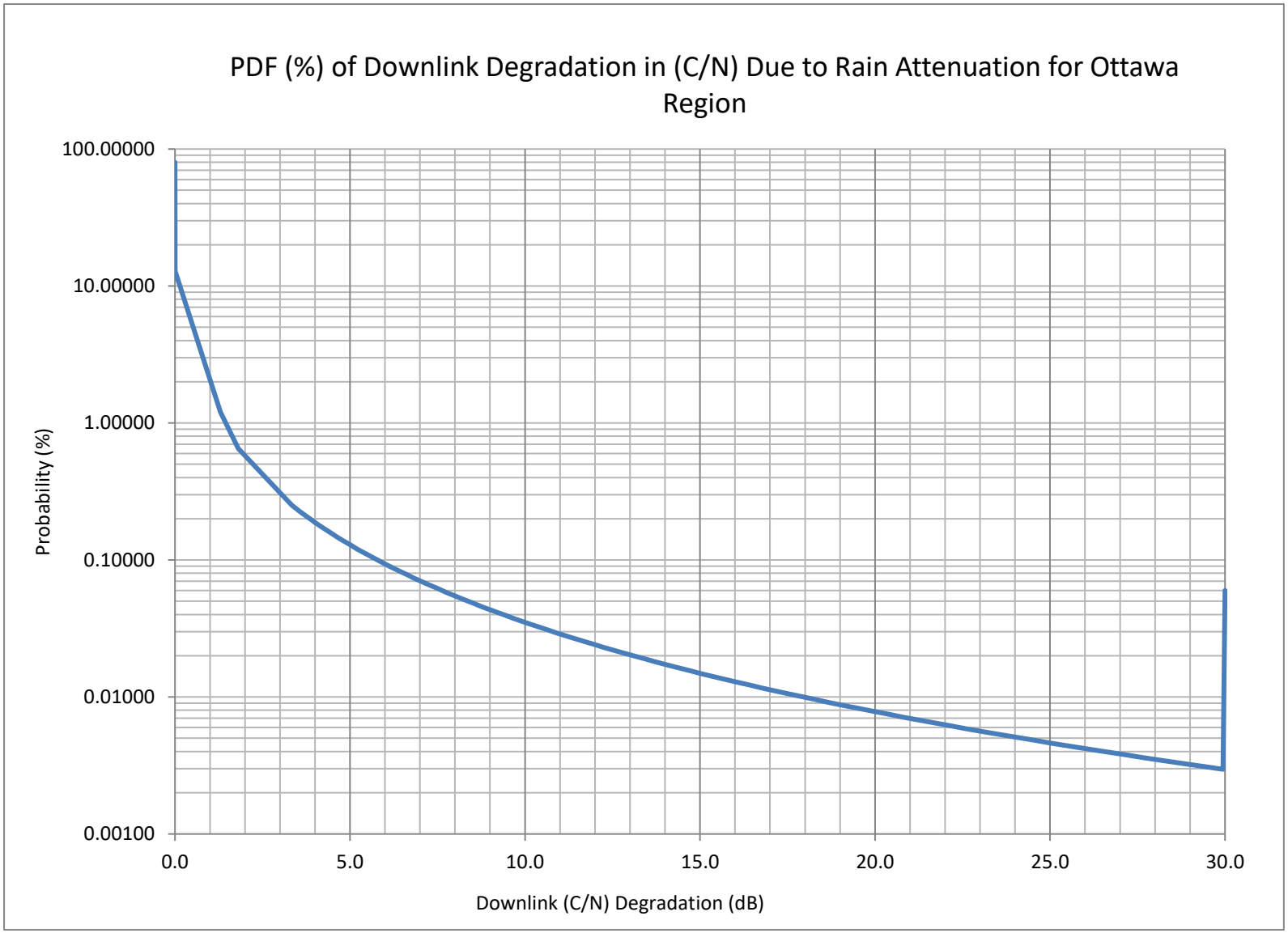

FIGURE A10-8

pdf of *I*/*N* from Non-GSO network (Saskatoon location)

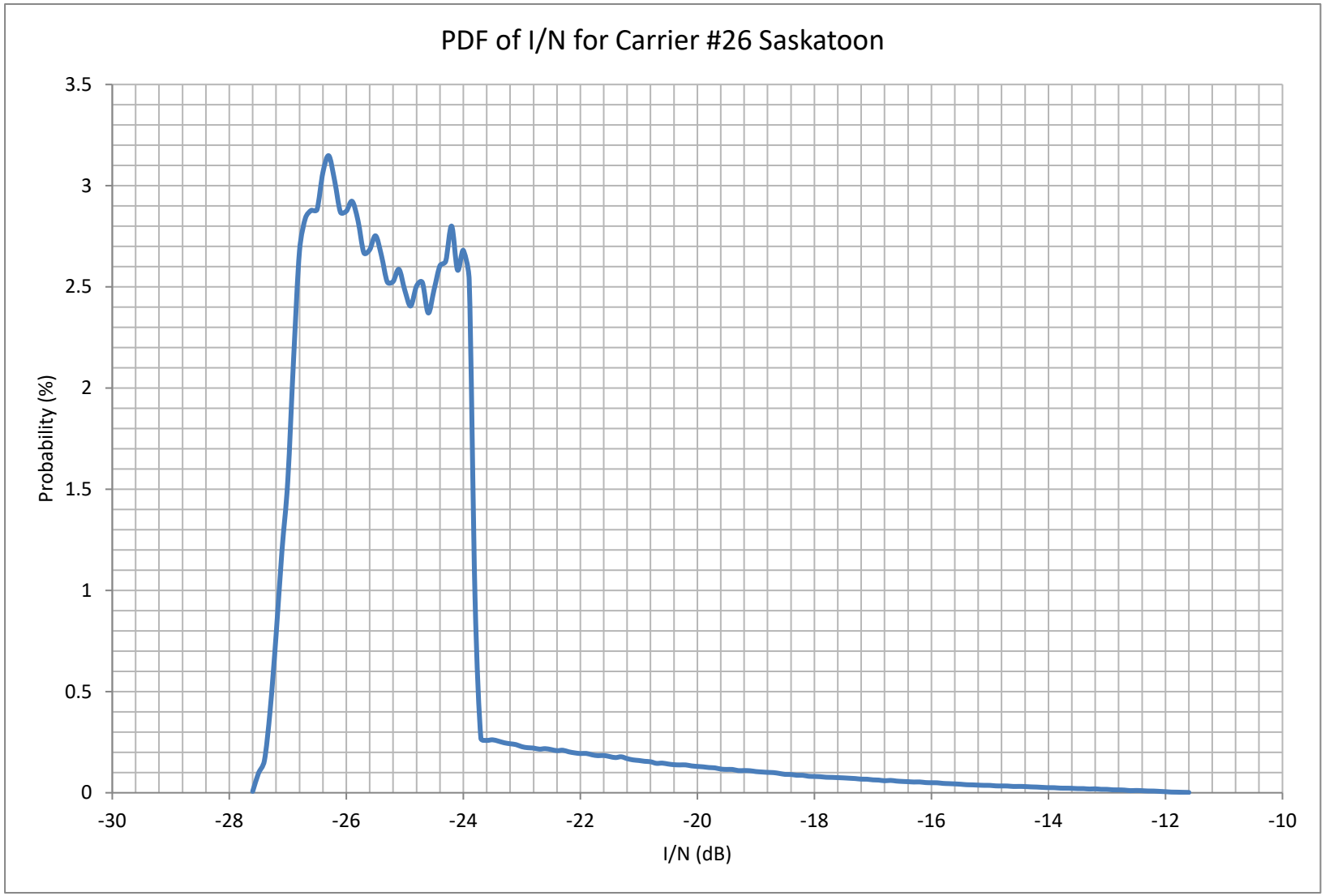

Case 1 (part 1): Earth station located in Saskatoon, Canada

For this case, the pdf of the dowlink I↓/N↓ is shown in Fig. A10-8. The convolution of the pdf of Fig. A10-6 and the pdf of Fig. A10-7 would give the pdf of the degradation in the downlink due to both the rain fade and the non-GSO interference. However, if the random variable e is taken from equation (85) and look at the range of its components, assuming rain attenuation in the range of 0 to 30 dB, then

$$1 \leq 2Ac\downarrow -1 \leq 1999 \tag{86}$$

And for $\left(\frac{I_0\downarrow}{N_0\downarrow}\right)$ less than -10 dB, then the linear value of $\left(\frac{I_0\downarrow}{N_0\downarrow}\right)$ is less than 0.1

Then for all intents

$$e = 2Ac\downarrow -1 \tag{87}$$

Hence, taking the convolution of the pdf of Fig. A10-7 and the pdf of Fig. A10-8 the results shown in Fig. A10-7 will not quantitaively change. This result is expected because it can be seen that most of the interference is a low levels, with a greater concentartion around −25 dB.

Case 2 (part 1): Eart station located in Lima, Peru

A second location for an earth station in Peru was selected because with the lower lattitude more intense interference events are expected. This is shown in Fig. A10-9, where the *I*/*N* peak with values greater than 30 dB is seen. For the purpose of the analysis in this study, have assumed the rain attenuation statistics of the Ottawa region for convenience in the calculations for this second case as well as the first case. The pdf of the degradation due to rain attenuation and interference was calculated by taking the convolution of the pdf shown in Fig. A10-7 with the pdf shown in Fig. A10-10.

With the results obtained for the pdf of the degradation in the downlink carrier-to-noise ratio for these two cases, we are now ready to lok at their impact on the spectram efficiency of satellite network using ACM on the downlink.

FIGURE A10-9

***I*/*N* as a function of time from non-GSO network (Peru location)**

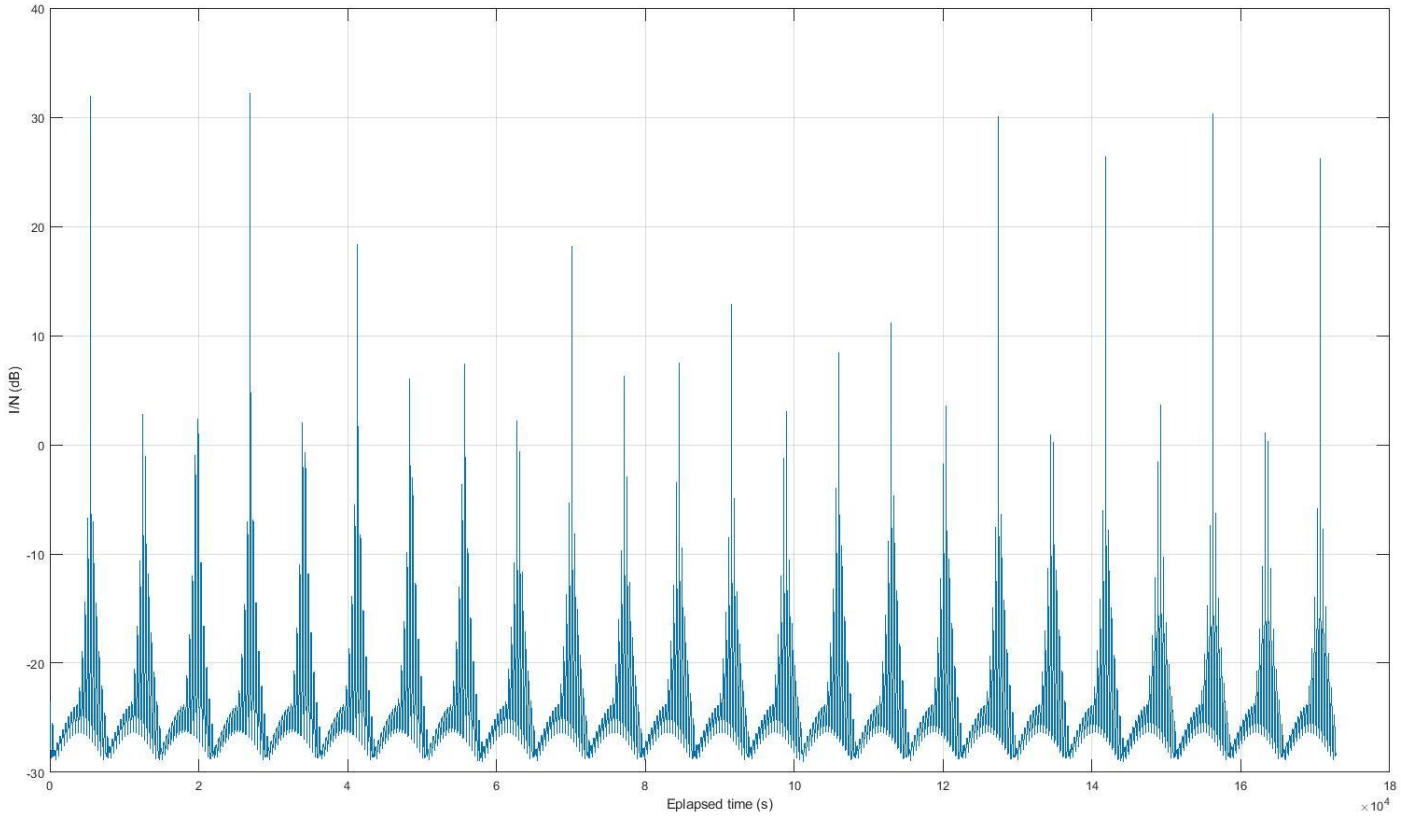

FIGURE A10-10

pdf of *I*/*N* from non-GSO network (Peru location)

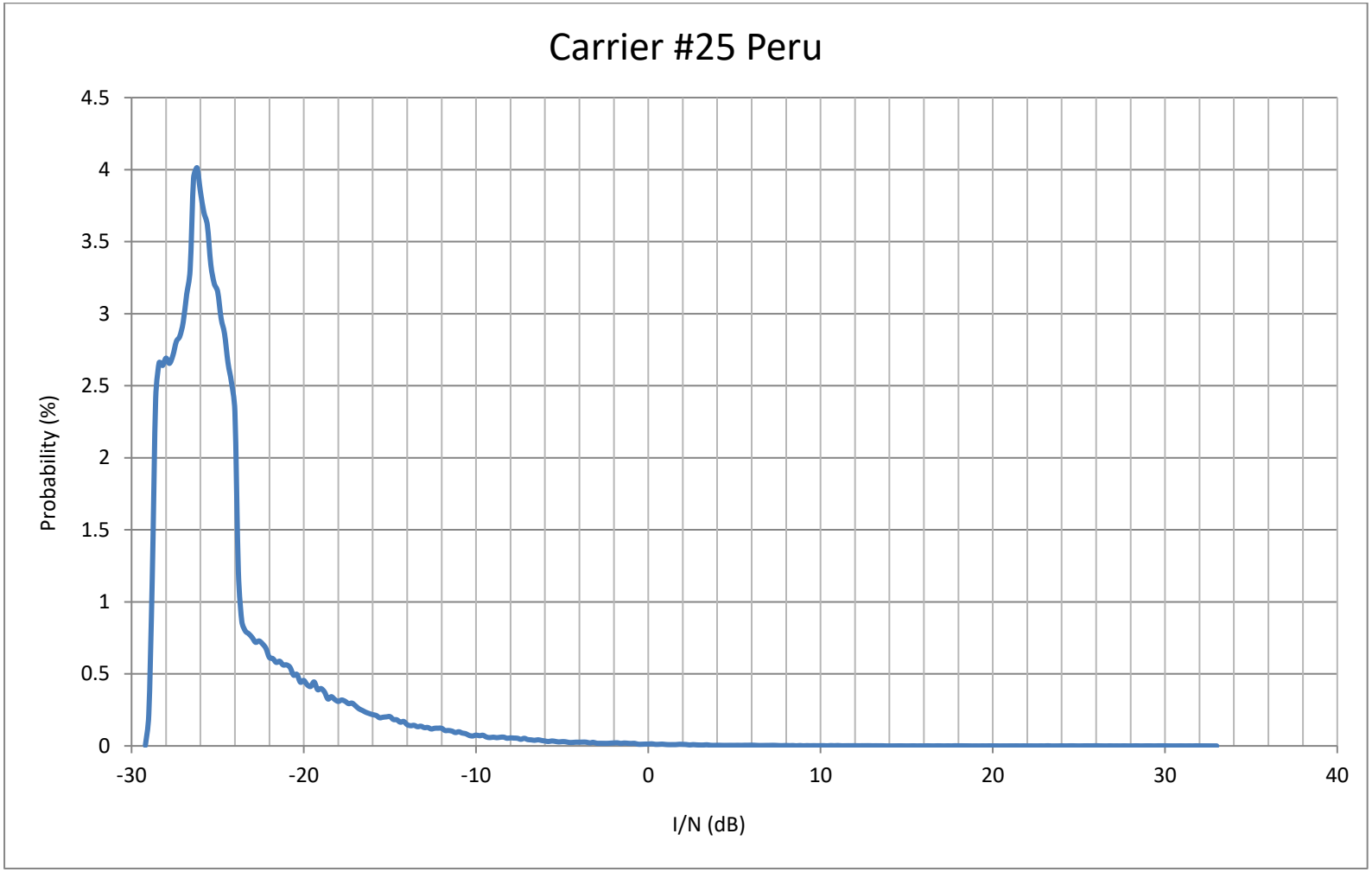

FIGURE A10-11

pdf of sum of degradation due to rain attenuation and interference obtained by convolution of the pdf shown in Fig. A10-7 with the pdf shown in Fig. A10-10

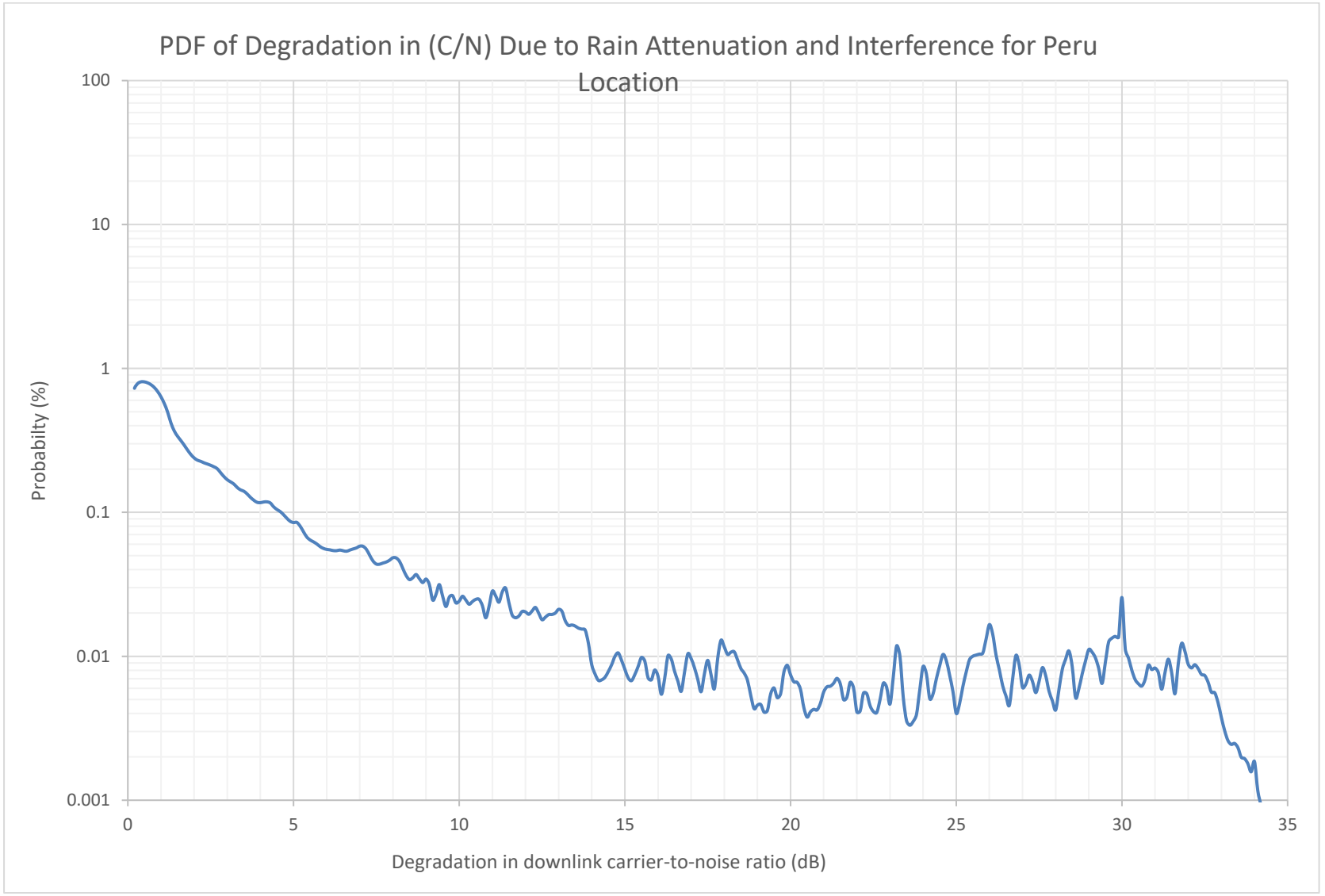

6.2.3.2 Long-term impact on Percent Degraded Throughput (%DTp) due to rain attenuation and interference from an non-GSO network

In this section, the effect on the spectral efficiency of a system using ACM caused by rain atttenuation and interference on the dowlink is investigated. The impact on spectral efficiency will be studied in two parts; the first when there in rain fade in the downlink – that is the impact on spectral efficiency will be solely due to the interference caused by the non-GSO network; and secondly when there is rain fade as well as interference from the non-GSO network.

It is noted from Fig. A10-5, that for about 80% of the time when we have clear-sky on the down link only the interference will be present and for the other 20% of the time we have both some rain attenuation and interference from the non-GSO network. There is an issue though with this 20% of the time because Recommendation ITU-R P.618 only applies for 5% of the time. This means that for the remaining 15% of the time, a suitable interpolation model is required for the "transition region" that bridges the clear-sky conditions (fades not exceeeded for 20% of the time) and where the rain model begins (fades exceeded for < 5% of the time) since we do not hve a model that has been validated by Study Group 3, the experts on propagation.

The expression for the impact on spectral efficiency is obtained by calculating the expected percent degraded throughput ($\overline{\%DTp}$) given by:

($\overline{\%DTp}$) = Expectation {%DTp | clear-sky and inteference} + Expectation { %DTp | rain attenuation and inteference} (88)

For our example, the expression for %DTp becomes

($\overline{\%DTp}$) = 0.80 x Expectation {%DTp | inteference} +
15 x Expectation { %DTp | rain(estimated) and interfence} +
.05 x Expectation { %DTp | rain(P.618) and interfence} (89)

Recall that it was showed earlier that during fading of both the interference and the wanted carrier on the downlink, the impact to %DTp caused by the interference is minimal compared to the impact caused by the rain attenuation. Hence the greatest impact on the average percent degraded throughput ($\overline{\%DTp}$) will occur during the 80% of the time when we have clear-sky, for this specific case; the long term situation.

Given the pdf of the interference and the pdf of the rain and attenuation it is simple to calculate the ($\overline{\%DTp}$) for this case using the general expression defined earlier

$$\overline{\%DTp}(\rho) = 100\left[1 - \int_0^\infty p(\gamma)\frac{\varepsilon(\rho-\gamma)}{\varepsilon(\rho)}d\gamma\right] \quad (90)$$

where

ρ : undegraded C/N (dB)

γ : degradation (dB)

$\varepsilon(x)$: spectral efficiency function (bits/s/Hz)

$p(\gamma)$: probability density function (pdf) of degradation γ, and is constrained by:

$$\int_0^\infty p(\gamma)\,d\gamma = 1 \quad (91)$$

For our situation, the expression for ($\overline{\%DTp}$) can be written as follows:

$$\overline{\%DTp}(\rho) = 80\% \text{ x } \left[1 - \int_0^\infty p(\gamma_1)\frac{\varepsilon(\rho-\gamma_1)}{\varepsilon(\rho)}d\gamma_1\right] + 15\% \text{ x } \left[1 - \int_0^\infty p(\gamma_2)\frac{\varepsilon(\rho-\gamma_2)}{\varepsilon(\rho)}d\gamma_2\right]$$
$$+5\% \text{ x } \left[1 - \int_0^\infty p(\gamma_3)\frac{\varepsilon(\rho-3)}{\varepsilon(\rho)}d\gamma_3\right] \quad (92)$$

where:

$p(\gamma_1)$: probability density function (pdf) of degradation due to interference only

$p(\gamma_2)$: probability density function (pdf) of degradation due to interference and rain attenuation (obtained by convolution). Rain attenuation was estimated by a simple linear interpolation (the rain attenuation is not expected to have an erratic behaviour); and

$p(\gamma_3)$: probability density function (pdf) of degradation due to interference and rain attenuation (obtained by convolution). Rain attenuation derived using P.618.

Case 1 (part 2): Saskatoon Location

Let us now apply equation (92) to calculate the %DTp for each of the three time-segments, assuming the *I*/*N* distribution as shown in Fig. A10-8.

1) Clear-Sky Situation (80% of the time)

   %DTp calculated for *I*/*N* pdf as described in Fig. A10-7 = 0.08254%

2) Rain (estimated) and Interference Situation (15% of the time)

   %DTp calculated for pdf as described in Fig. A10-6 (interpolated) = 1.3846%

3) Rain (P.618) and Interference Situation (5% of the time)

   %DTp calculated for pdf as described in Fig. A10-6 (P.618) = 30.8359%

Therefore, the expected percent degraded throughput ($\overline{\%DTp}$) is given by:

$$(\overline{\%DTp}) = .8 \text{ x } .08254 + .15 \text{ x } 1.3846 + .05 \text{ x } 30.8359$$
$$= 1.8155\ \% \quad (93)$$

In the absence of interference, the ($\overline{\%DTp}$) would be approximately the sum of the second and third term in the above equation. This gives:

$$(\overline{\%DTp}) = 1.7495\% \quad (94)$$

This tells us that an ACM system, which has the full dynamic range of DVB-S2X and a clear-sky *C*/*N* of 23.75 dB could expect a long-term average degradation in its %DTp of the order of 2% from rain attenuation alone. It should be noted that the dynamic range of the ACM system depends on the available clear-sky *C*/*N*.

Case 2 (part 2): Peru Location

Let us now apply equation (91) to calculate the % DTp for each of the three time-segments, assuming the *I*/*N* distribution as shown in Fig. A10-10.

1) Clear-Sky Situation (80% of the time)

   %DTp calculated for *I*/*N* pdf as described in Fig. A10-10 = 0.3055%

2) Rain (estimated) and interference situation (15% of the time)

%DTp calculated for pdf as described in Fig. A10-11 (interpolated) = 7.0089%

3) Rain (P.618) and interference situation (5% of the time)

%DTp calculated for pdf as described in Fig. A10-11 (P.618) = 50.2360%

Therefore, the expected percent degraded throughput ($\overline{\%DTp}$) is given by:

$$(\overline{\%DTp}) = .8 \text{ x } .3055 + .15 \text{ x } 7.0089 + .05 \text{ x } 50.2360$$

$$= 3.8075\ \% \quad (95)$$

In the absence of interference, the ($\overline{\%DTp}$) would be the same as derived for Case 1 (part 2) since the same rain statistics are assumed:

$$(\overline{\%DTp}) = 1.7495\% \quad (96)$$

From equations (95) and (96), it can be deducted that non-GSO interference as shown for the case of Peru would result in a reduction in overall spectral efficiency, including long-term, of about 2.1%. This is well within the 10% reduction in spectral efficiency stipulated in Recommendation ITU-R S.2131-0. The long-term reduction in spectral efficiency, given by the first term in equation (95), amounts to a reduction in spectral efficiency of about 0.24%. The spectral efficiency due to rain attenuation only would degrade from 98.25% without interference to 96.19% due to rain attenuation and non-GSO interference, i.e. for the long term, we have for the Peru example:

Spectral Efficiency (overall 100% of time): 98.25% → 96.19%

6.2.3.3 Impact GSO ACM system availability due to non-GSO *I*/*N*

In this section, we look at the impact on availability of a GSO FSS system using ACM due to the *I*/*N* from an non-GSO network. For the purpose of our study, it will be considered the specific case of an earth station located in Peru and subjected to interference from an non-GSO network characterized by the pdf shown in Fig. A10-10, which reflects the statistics of the *I*/*N* time function shown in Fig. A10-9.

In the analysis of availability considerations on a GSO system employing ACM, two characteristics of the interference need to be addressed. These are the rate of change of *I*/*N* and the levels reached by the *I*/*N*.

Regarding the rate of change of *I*/*N*, one of the assumptions in the development of Recommendation ITU-R S.2131-0 is that the ACM system can handle a 1 dB reduction in *C*/*N* during 1 second interval. This decrease may be due to any source of external interference and rain fading.

With regards to the levels reached by the *I*/*N*, it was mentioned in the previous section, that if the ACM system has a minimum clear-sky carrier-to-noise ratio of 23.75 dB, ignoring any imperfections on mitigating measures using feedback on detected fade to track and mitigate such fade,it will have a dynamic range of 27 dB. This means that under clear-sky conditions, the ACM system would be able to follow variations in *I*/*N* provided the rate of change of *I*/*N* does not exceed 1 dB in a 1 second interval, which can be expressed as:

$$10\ Log\ \left\{1 + \frac{I}{N}\right\} \leq 27\ dB \quad (97)$$

The two criteria that govern the capability of an ACM system operated with a clear-sky C/N of 23.75 dB, which allows the maximum dynamic range, are given. To be conservative, the dynamic range for variations was kept in *I*/*N* to be less than 24 dB. These criteria can be expressed as:

1) *I*/*N* rate of change criterion:

$$\frac{d\left(\frac{I}{N}\right)}{dt} \leq 1\ dB/s \tag{98}$$

2) *I/N* range constrained by:

$$10\ Log\ \left\{1 + \frac{I}{N}\right\} \leq 24\ dB \tag{99}$$

This means that if the time variations of the non-GSO interference is considered to be as shown in Fig. A10-9, then the ACM system will be able to cope with all the interference events except those where the *I*/*N* exceeds 24 dB and those where the rate of change of *I*/*N* exceeds 1dB/s. Figure A10-15 is a snap-shot of a short time period around the first interference peak shown in Fig. A10-9. This Figure clearly demonstrates that the variations in the interference levels are quite gradual and extend over many seconds, however, when the interference increases rapidly to reach the high peak values, its rate of change does in some cases exceed 1 dB per second. It was first considered the additional unavailability caused by the instances where the *I*/*N* exceeds 24 dB and then look at the instances where the rate of change of *I*/*N* exceeds 1 dB per second. For those events where the rate of change of the interference exceeds 1 dB/s or the level exceeds 24 dB, the interference would induce additional unavailability.

The amount of unavailable time due to high levels of interference during the clear-sky period is given by:

$$T_{.8\ unavail.high\ I/N} = 0.8 \text{ x } 8760 \text{ x } Prob\left(10\ Log\ \left\{1 + \frac{I}{N}\right\} > 24\ dB\right)\ hrs \tag{100}$$

Note the factor 0.8 as considering the 80% of the time which is clear-sky. For this specific case, $p_{.8}$ can be determined from the pdf of *I*/*N* shown in Fig. 10, or by taking the ratio of the simulation points in Fig. A10-9, where *I*/*N* is greater than 24 dB, to the total number of simulation points:

$$p_{.8\ high\ I/N} = Prob\left(10\ Log\ \left\{1 + \frac{I}{N}\right\} > 24\ dB\right) \tag{101}$$

$$\cong Prob\left(10\ Log\ \left\{\frac{I}{N}\right\} > 24\ dB\right) \tag{102}$$

The value of $p_{.8\ high\ I/N}$ was obtained by taking the ratio of simulation points, which satisfied the criterion of equation (101) to the total number of simulation points. Note that the simulation represented two days at ½ second intervals, i.e. 345,600 simulation points. This gave:

$$p_{.8\ high\ I/N} = 0.000153 \tag{103}$$

This results in an additional unavailable time due to high *I*/*N* of:

$$T_{.8\ unavail.high\ I/N} = 1.072\ hrs \tag{104}$$

It was then determined the probability that the rate of change of *I*/*N* would exceed 1 dB/s when the *I*/*N* was actually below 24 dBs. This probability can be expressed as:

$$p_{.8\ high\ rate\ I/N} = Prob\left(10\ Log\ \left\{1 + \frac{I}{N}\right\} < 24\ dB \quad \text{AND} \quad \frac{d\left(\frac{I}{N}\right)}{dt} > 1\ dB/s\right) \tag{105}$$

The value of $p_{.8\ high\ rate\ I/N}$ was obtained by taking the ratio of simulation points, which satisfied the criterion of equation (102) to the total number of simulation points. This gave:

$$p_{.8\ high\ rate\ I/N} = 0.0006091 \tag{106}$$

This results in an additional unavailable time due to high rate I/N of:

$$T_{.8\ unavail.high\ rate\ I/N} = 4.268\ hrs \quad (107)$$

It was then determined the additional unavailable time during the 15% time-period between the clear-sky time-period and the 5% time period where Recommendation ITU-R P.618-13 applies. During the 15% time-period the ACM system will not incur any unavailability due to rain attenuation, as the rain attenuation during this time-period is expected to be less than 2 dBs. It can be conservatively assumed a fixed value of 2 dB for the rain attenuation. Under this condition, the probability of unavailability due to high *I*/*N* given in equation (98) becomes:

$$p_{.15\ high\ I/N} = Prob\left(10\ Log\ \left\{1 + \frac{I}{N}\right\} > 22\ dB\right) \quad (108)$$

The probability of unavailability due to high rate I/N, given in equation (105) becomes:

$$p_{.15\ high\ rate\ I/N} = Prob\left(10\ Log\ \left\{1 + \frac{I}{N}\right\} < 22\ dB \quad \text{AND} \quad \frac{d\left(\frac{I}{N}\right)}{dt} > 1\ dB/s\right) \quad (109)$$

Note that the limit for *I*/*N* is reduced to 22 dB. The values $p_{.15\ high\ I/N}$ and $p_{.15\ high\ rate\ I/N}$ were obtained by taking the ratio of simulation points, which satisfied the criterion of equations (108) and (109) to the total number of simulation points. This gave:

$$p_{.15\ high\ I/N} = 0.0001765 \quad (110)$$

$$p_{.15\ high\ rate\ I/N} = 0.0005975 \quad (111)$$

From these:

$$T_{.15\ unavail.high\ I/N} = 0.2319\ hr \quad (112)$$

$$T_{.15\ unavail.high\ rate\ I/N} = 0.7851 hr \quad (113)$$

The next step is to calculate the additional unavailability introduced by the interference during the 5% time-period. The total unavailability during this time period is obtained from pdf shown in Fig. A10-11, by evaluating the probability that the *C*/*N* has degraded by more than 24 dB. The values were calculated to be:

$$p_{.05\ rain+int} = 0.007757 \quad (114)$$

For comparison, we can determine the unavailable time due to rain attenuation alone. This can be obtained from Fig. A10-7 by calculating the probability that the degradation in the clear-sky *C*/*N* exceeds 24 dB. Let $p_{.05}$ represent this probability. It was calculated to be:

$$p_{.05\ rain} = 0.0010706 \quad (115)$$

This corresponds to an unavailability of

$$T_{.05\ unavail.rain+int} = 0.007757 \text{ x } 8760 = 67.9513\ hrs \quad (116)$$

$$T_{.05\ unavail.rain} = 0.0010706 \text{ x } 8760 = 9.3784\ hrs \quad (117)$$

From the above results, the short-term availabilities can be calculated. The short-term availability due to rain attenuation is given by:

$$Avail_{rain}(short - term) = \left(\frac{8760 - 9.3784}{8760}\right) \text{ x } 100 = 99.89\% \quad (118)$$

The short-term (5% of the time) availability due to rain attenuation and interference is given by:

$$Avail_{rain+int}(short - term) = \left(\frac{8760 - 67.9513}{8760}\right) \text{ x } 100 = 99.22\% \quad (119)$$

Hence the short-term availability for the Peru example would be reduced from 99.89% to 99.22%.

Availability (Short-Term): 99.89% → 99.22%

The long-term availability due to interference is given by:

$$Avail_{rain+int} = \left(\frac{8760-1.072-4.268-.2319-.7851}{8760}\right) \text{ x } 100 = 99.93\% \qquad (120)$$

Hence during the long-term (95% of the time), the availability would be reduced from 100% to 99.93%.

Availability (Long-Term): 100.00% → 99.93%

Note that the spectral efficiencies derived in the previous section took accounted for the time when the system was not available.

7 Long-Term considerations on sensitivity of percent degraded throughput (%DTp) to *I*/*N* level in clear-sky

In this section, the sensitivity of the % DTP to various values of *I*/*N* in a clear-sky environment is studied.

Table A10-4 provides the %DTp degradations that would result assuming different clear-sky overall *C*/*N* values. In the first case (column 2), with a clear-sky *C*/*N* of 23.75 dB, the ACM system can take advantage of the full range of DVB-S2X MODCODs. The amount of degradation that satellite links will experience in the absence of interference will depend on the locations of the earth stations at either end of the link and the mitigation measures available to them (e.g., UPC and ACL). In the other two cases, with a clear-sky *C*/*N* of 15 dB or 10 dB, the ACM system cannot take advantage of the full dynamic range. The data from Table A10-4 is plotted in Fig. A10-12.

When looking at the pdf of interference shown in Fig. A10-7, it was noted that it tends to be concentrated around some levels with very low probability at other levels. The impact on the %DTp of the low probability of occurrence interference events will be minimal. Figure A10-13 illustrates the sensitivity of %DTp to various levels of *I*/*N* for different duty cycles. These results clearly illustrate that under clear-sky conditions (around 80% of the time in the Ottawa region), the %DTp is directly related to the duration of the interference events. Hence high levels of *I*/*N* with small duty cycle would have a relatively small impact on the overall spectral efficiency of a system employing ACM. Recall that a system employing the full capability of DVB-S2X (requires clear-sky *C*/*N* of approx. 24 dB) has a dynamic range of about 27 dB. This means that such a system could accommodate *I*/*N* variations up to about $I/N \approx 27$dB. Recall that we showed that a steady *I*/*N* of −12.2 dB, resulted in %DTp degradation of 1.2%. Hence an *I*/*N* of −12.2 dB for 10% of the time would result in a %DTp degradation of about 0.12% during the clear-sky period. The actual impact on the %DTp is defined by the durations of the high levels of interference.

Figure A10-13 clearly demonstrates the sensitivity of the spectral efficiency of an ACM system to the duration of high level interference events, i.e. their duty cycle. The practical implication of these results is that imposing a hard limit on the maximum allowable level of *I*/*N* is very conservative if the likelihood and duration of such levels is not considered.

TABLE A10-4

	Clear-sky conditions	**Clear-sky conditions**	**Clear-sky conditions**
	***C/N* = 23.75 dB**	***C/N* = 15 dB**	***C/N* = 10 dB**
I/N	**%DTp**	**%DTp**	**%DTp**
-20	0.2102	0.2808	0.3527
-19	0.2642	0.353	0.4434
-18	0.3321	0.4436	0.5572
-17	0.4171	0.5572	0.6998
-16	0.5237	0.6995	0.8785
-15	0.657	0.8776	1.1021
-14	0.8235	1.0999	1.3812
-13	1.0311	1.3771	1.7292
-12.2	1.2332	1.6468	2.0676
-12	1.2984	1.7218	2.1618
-11	1.6097	2.1492	2.698
-10	2.005	2.6771	3.3602
-9	2.4924	3.3264	4.1743
-8	3.0883	4.1205	5.1697
-7	3.813	5.0856	6.3787
-6	4.6878	6.2497	7.8362
-5	5.7346	7.6414	9.5772
-4	6.975	9.2884	11.6356
-3	8.4281	11.2153	14.041
-2	10.1096	13.4413	16.8162
-1	12.0296	15.9779	19.9376
0	14.191	18.8271	23.5133

FIGURE A10-12

Sensitivity of %DTP to *I*/*N* for clear-sky conditions and constant values of *I*/*N*

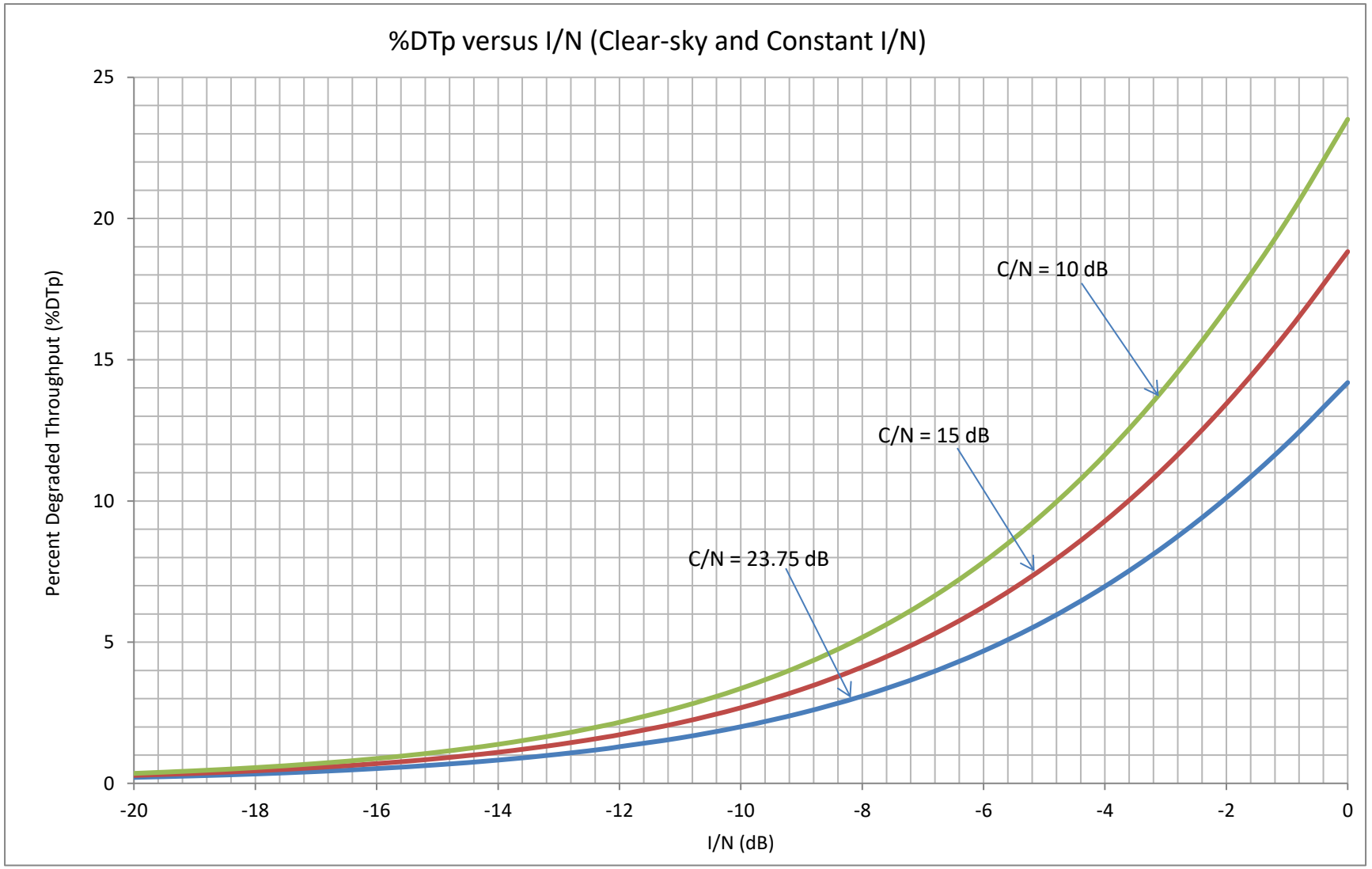

Figure A10-14 illustrates upper bounds on the duty cycle of various interference levels that would result in 1% and 3% degraded throughput. Two cases are illustrated, the first case assumes that the ACM system has access to the full dynamic range of DVB-S2X, about 27 dB for a clear-sky carrier-to-noise ratio of 23.75 dB, and the second case assumes that the ACM system starts with a clear-sky carrier-to-noise ratio of 15 dB, which would give it a dynamic range of about 18 dB. The results shown in Fig. A10-14 demonstrate that imposing the "classic" limit on I/N of −12.2 dB for sharing between non-GSO systems and GSO systems employing ACM is not a good measure to use to determine the feasibility of sharing between these systems.

A couple of points, $p1$ and $p2$, were indicated in Figs A10-13 and A10-14 to illustrate the link between the data in these two Figures.

FIGURE A10-13

Sensitivity of %DTp to the duty cycle of a given *I/N* ratio

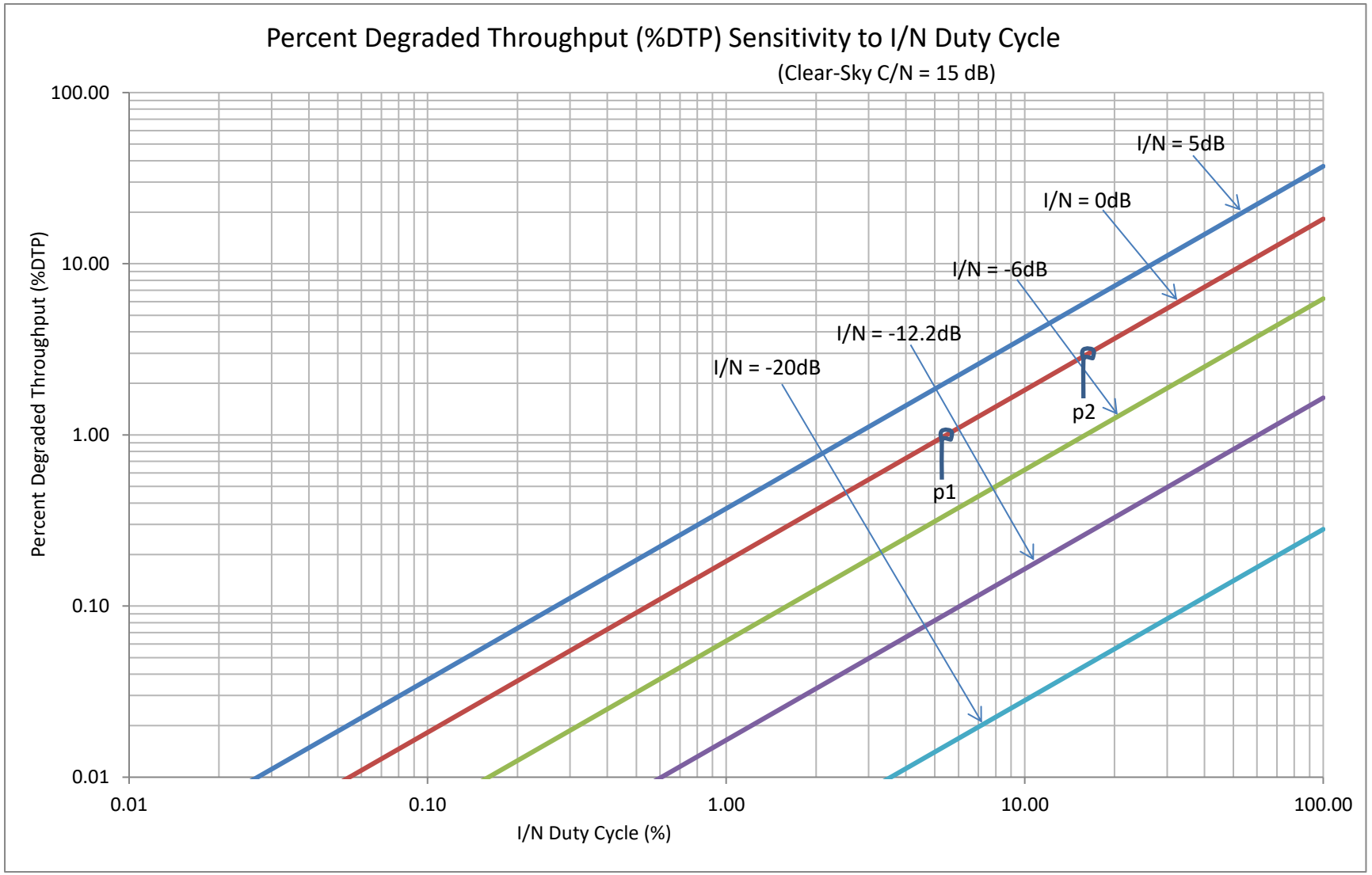

FIGURE A10-14

Allowable *I*/*N* interference level that would result in 1% degraded throughput

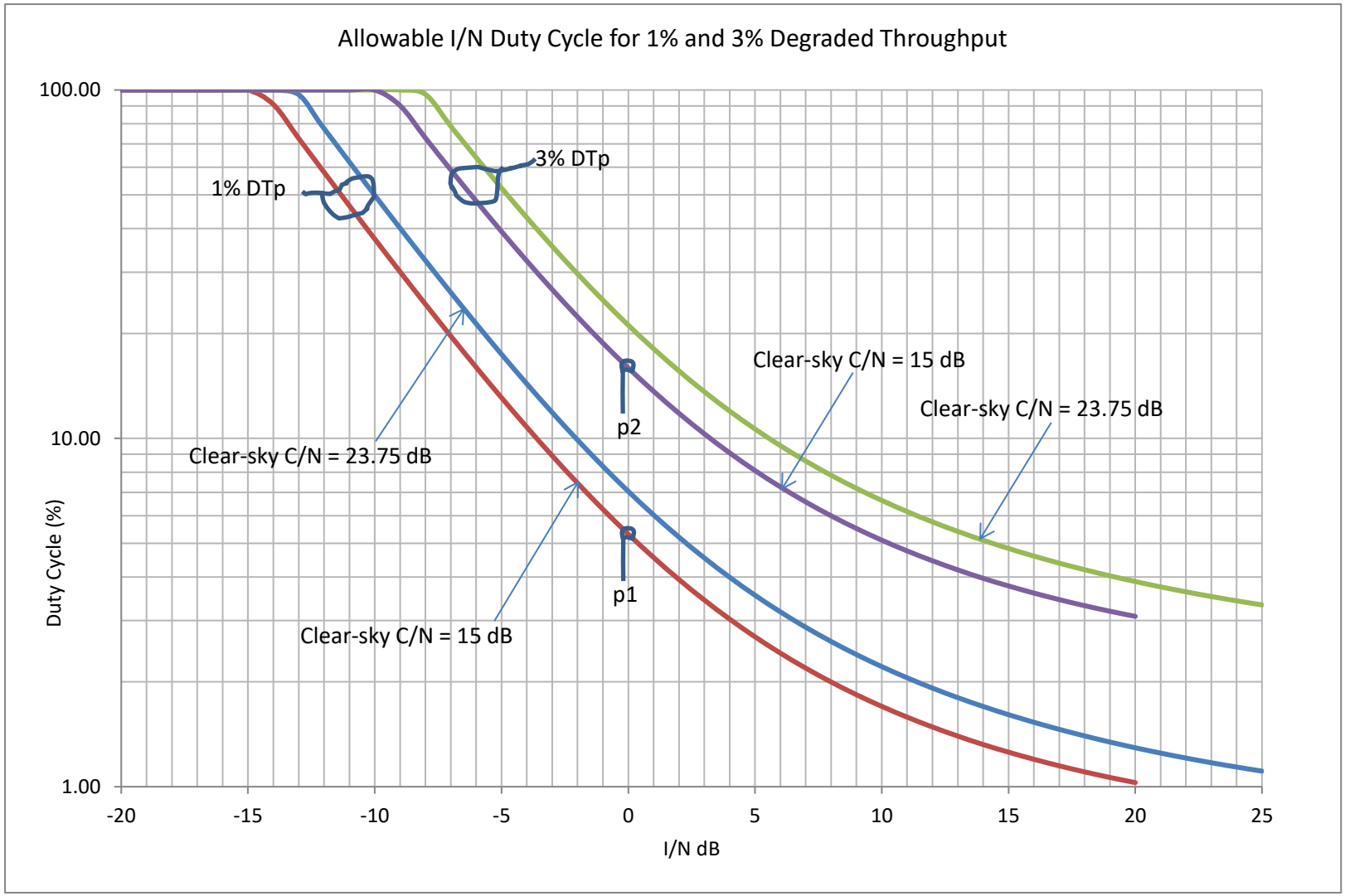

FIGURE A10-15

***I*/*N* as a function of time (short time window) from non-GSO network (Peru location)**

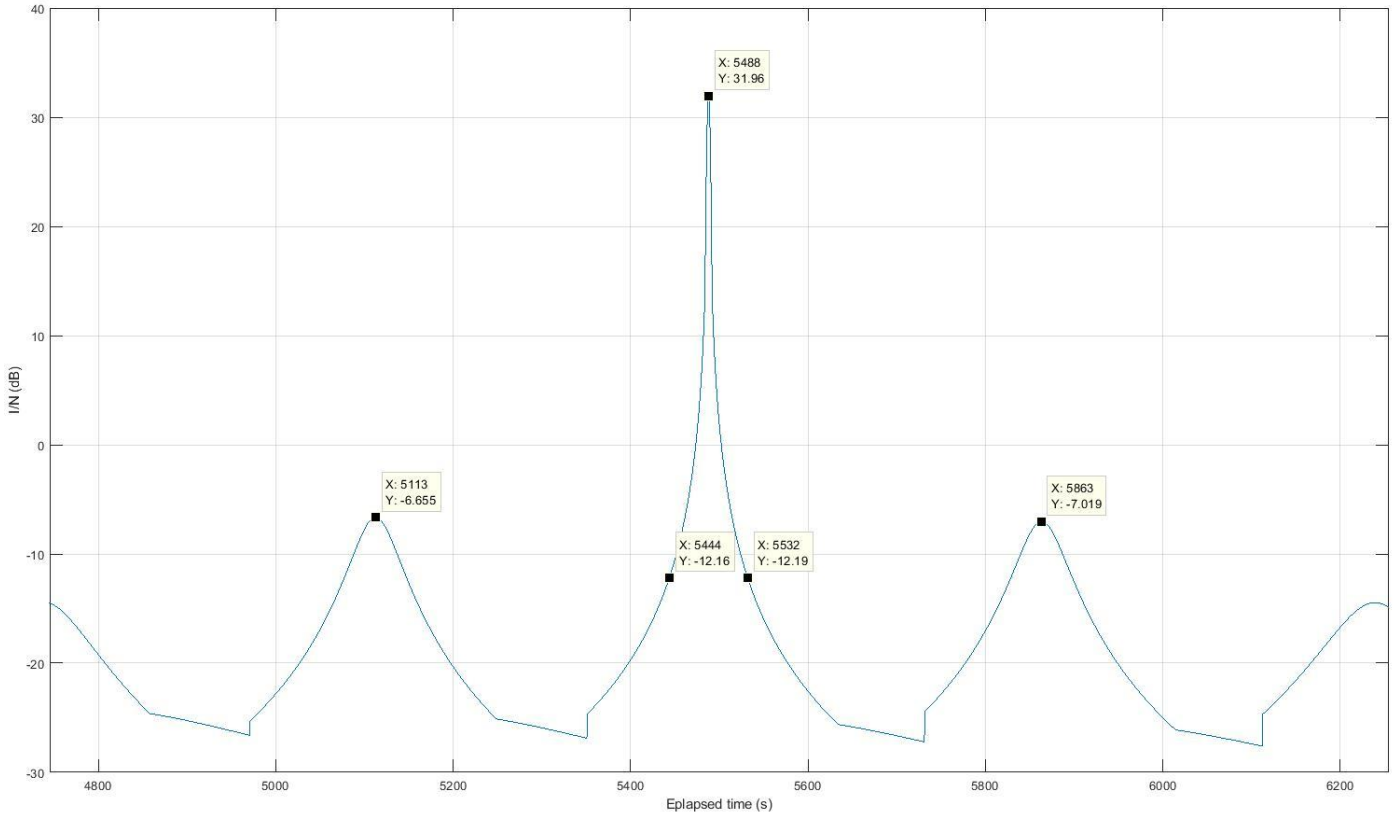

8 Conclusions

This study provides the basic equations that can be used to determine the degradation in *C*/*N* on the uplink, on the downlink, and the combined *C*/*N*. It was addressed in particular the case where the inteference and the wanted signal are correlated on the downlink. The analysis provides some simple equations and guidance when studying the performance of communications links subjected to interference and rain attenuation.

It was also considered various aspects of the sensitivity of the spectral efficiency of a satellite communication system employing ACM. The results show that during rain fading events, the reduction in spectral efficiency is mostly due to the degradation in the carrier-to-noise ratio due to rain attenuation.

Two scenarios of interference from a non-GSO system into the downlink of a GSO network were considered. In the first case, the GSO earth station was assumed to be at a higher lattitude (Saskatoon, Canada). In this case the interference had minimal impact on the spectral efficiency of a link employing ACM. In the second case, the GSO earth station was assumed to be at a lower lattitude (Peru). The time function of the interference for the second case, which had short duration *I*/*N* peaks at around 33 dB were provided. The analysis and calculations show that even with such high peaks in *I*/*N*, the long-term spectral reduction in efficiency for the second case was about 2%.

Finally, some analysis were done, which relates the degradation in spectral efficiency of a link employing ACM to the duration of *I*/*N* interference burst. The relationship between the duty cycle of the *I*/*N* bursts and the reduction in spectral efficiency is shown. It is demonstrated that taking into account the wide dynamic range of *C*/*N* over which ACM systems can operate, short bursts of interference with high *I*/*N* levels do not substantially degrade the performance of an ACM system.

These results demonstrate that imposing a constraint on epfd, which is equivalent to imposing a constraint on *I*/*N* is not an equitable sharing criteria. The results further support the concept of a criterion that limits the reduction in spectral efficiency for systems employing ACM.

Annex 11

Sharing studies relating to protection of GSO FSS networks using adaptive coding and modulation from the operation of non-GSO FSS systems

1 Introduction

Under WRC-19 agenda item 1.6, ITU-R studies concluded that the protection of GSO networks is possible based on protection criteria that considers both the short term performance objective and long term throughput performance of GSO links while enabling the use of these frequency bands by non-GSO FSS systems. These procedures allow for flexibility in the design and operation of non-GSO systems, while ensuring protection of GSO operations, therefore significantly enhancing spectrally efficient use of the 50/40 GHz bands. A draft Resolution has also been developed to ensure that the aggregate emissions from operating non-GSO FSS systems do not exceed aggregate protection requirements of GSO networks.

In studies that were carried out under this agenda item in ITU-R, the idea of the short term protection metric was for protection of traditional FSS systems from complete loss or unavailability and the idea of the long term protection metric was for protection of FSS systems utilizing adaptive coding and modulation (ACM) approaches. While the short-term criteria is focused on traditional satellite systems and the long term is focused on systems utilizing ACM, both the short-term criteria and long-term criteria apply equally to ACM systems to assure that the interference experienced by the satellite system does not translate to a unacceptable impact on system performance.

In the work that was carried out for protection of systems utilizing ACM, studies utilized the work being carried out by ITU-R on Recommendation ITU-R S.2131-0. This Recommendation presents a concept of percent degraded throughput as a means to calculate performance objectives for satellite systems utilizing adaptive coding and modulation. This annex provides an analysis of the concept of percent degraded throughput as developed for use in calculating sharing conditions between non-GSO and GSO satellite systems employing ACM.

2 Overview of percent degraded throughput concept

Next generation GSO and non-GSO FSS networks operating in the 50/40 GHz frequency bands will tend to carry Internet traffic, so maintaining connections is more important than providing a constant bit rate. Given the large propagation losses experienced in V-band, these systems may utilize mitigation techniques such as adaptive coding and modulation (ACM) and power control to overcome the effects of propagation losses and interference. ITU-R developed Recommendation ITU-R S.2131-0 to define performance objectives for satellite systems utilizing ACM.

Recommendation ITU-R S.2131-0 presents a concept of spectral efficiency as a function of *C*/*N*. In terms of satellite performance through fade, this concept is presented as the degradation of throughput or percent degraded throughput. The percent degraded throughput can be computed as a function of *C*/*N* which varies depending on the propagation and interference conditions of the satellite link. For changes of *C*/*N* due to propagation conditions, Recommendation ITU-R S.2131-0 refers to Recommendation ITU-R P.618, which computes the change in *C*/*N* due to propagation as a function of total time. It is important to note, that the concept of propagation conditions given in Recommendation ITU-R P.618 is a long term statistic, taken over an average year at a given location.

3 Overview of percent degraded throughput on sharing studies using time average approach

Studies conducted within the ITU-R applied the concept of percent degraded throughput using time average approach to develop sharing criteria for the operation of FSS systems in the 50/40 GHz frequency bands. These studies demonstrated that applying a long term protection criteria for protection of GSO FSS systems from non-GSO FSS networks of 3% for single-entry and 10% for aggregate allowances of percent degraded throughput would allow for sharing between non-GSO and GSO FSS systems in the 50/40 GHz frequency bands. The percent degraded throughput represents the achievable capacity of the FSS link due to propagation fading averaged over a year as compared to the achievable capacity of the FSS link due to the combined mechanism of propagation and interference over a year.

The concept of percent degraded throughput is evaluated based on the long term statistics of propagation fade based on Recommendation ITU-R P.618. In determining interference effects on a FSS link utilizing ACM, the calculation for percent degraded throughput can include both the long term statistics of propagation effects and effects due to interference. In terms of interference calculations, the long-term degradation of throughput over time based on the achievable capacity due to propagation fading is compared to the capacity in degraded throughput resulting from *C*/*N* degradations due to sources of interference and fading. The use of ACM to maintain the required

performance can then be computed as a function of *C*/*N* which varies in time depending on propagation, in relation to the *C*/*N* of the satellite link considering both fade and interference conditions on the satellite link.

In particular, the analyses conducted within ITU-R and reflected in the CPM Report on WRC-19 agenda item 1.6 utilizes the above described approach to compare the statistics of long-term *C*/*N* degraded throughput due to propagation fade with the long-term *C*/*N*+*I* degraded throughput due to propagation fade and interference effects. This approach follows the ITU guidance on the computation of percent degraded throughput on the basis of a long term operation of a FSS network. In applying this guidance on performance criteria to sharing considerations being considered by WRC-19 agenda item 1.6, the difference between percent degraded throughput computed over time due to propagation fading only and the percent degraded throughput due to the combined mechanism of propagation and interference cannot exceed 3% for single entry by any one non-GSO system and 10% for the aggregate for all operating non-GSO systems. Thus, the concept currently indicated in sharing studies and potential solutions under WRC-19 agenda item 1.6 can best be summarized by the below equations:

For victim systems employing ACM, the conditions to be verified for compliance with the single entry case is:

$$(SE_x - SE_z)/SE_x \leq 0.03 \quad (121)$$

For victim systems employing ACM, the conditions to be verified for compliance with the aggregate case is

$$(SE_x - SE_z)/SE_x \leq 0.1) \quad (122)$$

Where SE_x represents the achievable capacity of the FSS link due to propagation fading over a long term time period and SE_z represents the achievable capacity of the FSS link due to the combined mechanism of propagation and interference over the long term. These equations represent the conditions to be checked to ensure that the percent degraded throughput caused by interference fades does not exceed a certain threshold, when compared to fades caused by propagation conditions over a long term period of operation.

4 Percent degraded throughput as applied for non-GSO sharing computations

It should be noted that the recommendation that governs the calculation of epfd statistics within the ITU, Recommendation ITU-R S.1503, assumes maximum power operation for non-GSO systems in all aspects of their operation. This assumption is reasonable when looking to find the worst-case, short-term, epfd generated by a non-GSO system. However, because non-GSO systems will only utilize maximum power to overcome rain fade, which would in turn attenuate the epfd measured at the receiver, this assumption will significantly over-estimate the long term interference introduced by non-GSO systems.

As described above, the concept of percent degraded throughput for ACM systems is based on long-term statistics for rain fade. Therefore, the interference statistics should match the long term nature of ACM degradation due to rain fade conditions. Additionally, studies in have shown that propagation impairments in the 50/40 GHz frequency bands can be very high as compared to lower frequency bands. If ACM operations or mitigation of propagation impairments should be considered in the calculations of epfd statistics, the application of power control should similarly be applied to the calculation of interference statistics from non-GSO systems.

For example, if a GSO system employing ACM was to operate in clear sky conditions, an interfering non-GSO system would be operating in those same clear sky conditions. Therefore, the non-GSO system would typically be operating below maximum power, and the interference would be

significantly reduced. Within the current framework of using Recommendation ITU-R S.1503 to calculate epfd interference from non-GSO systems, the non-GSO system would always be assumed to operate at max power and at worst case geometries.

With this approach, where the GSO system is operating with no fade impacts and the interfering non-GSO system is computed as worst case, any consideration of impacts on ACM systems would grossly overestimate the interference levels and the impact of percent degraded throughput. For these reasons, among others, the ITU has adapted the approach of long term percent degraded throughput in the context of sharing between non-GSO systems in the 50/40 GHz frequency bands.

For an example of the use of percent degraded throughput, an analysis was conducted from a non-GSO system into a FSS GSO earth station located in New York operating at 40.0 GHz. Figure A11-1 presents the consideration of bandwidth efficiency for this analysis. In the Figure, the blue curve (BEx) represents the bandwidth efficiency CDF due to propagation fade, the green curve (BEy) represents the bandwidth efficiency CDF resulting from non-GSO interference into the GSO earth station, and the brown curve represents bandwidth efficiency CDF resulting from the convolution of the propagation fades and the interference fades. As can be clearly seen from this figure, in terms of long term ACM operations, the dominant factor in the consideration of bandwidth efficiency is propagation fades.

FIGURE A11-1

Analysis of non-GSO interference into GSO ES

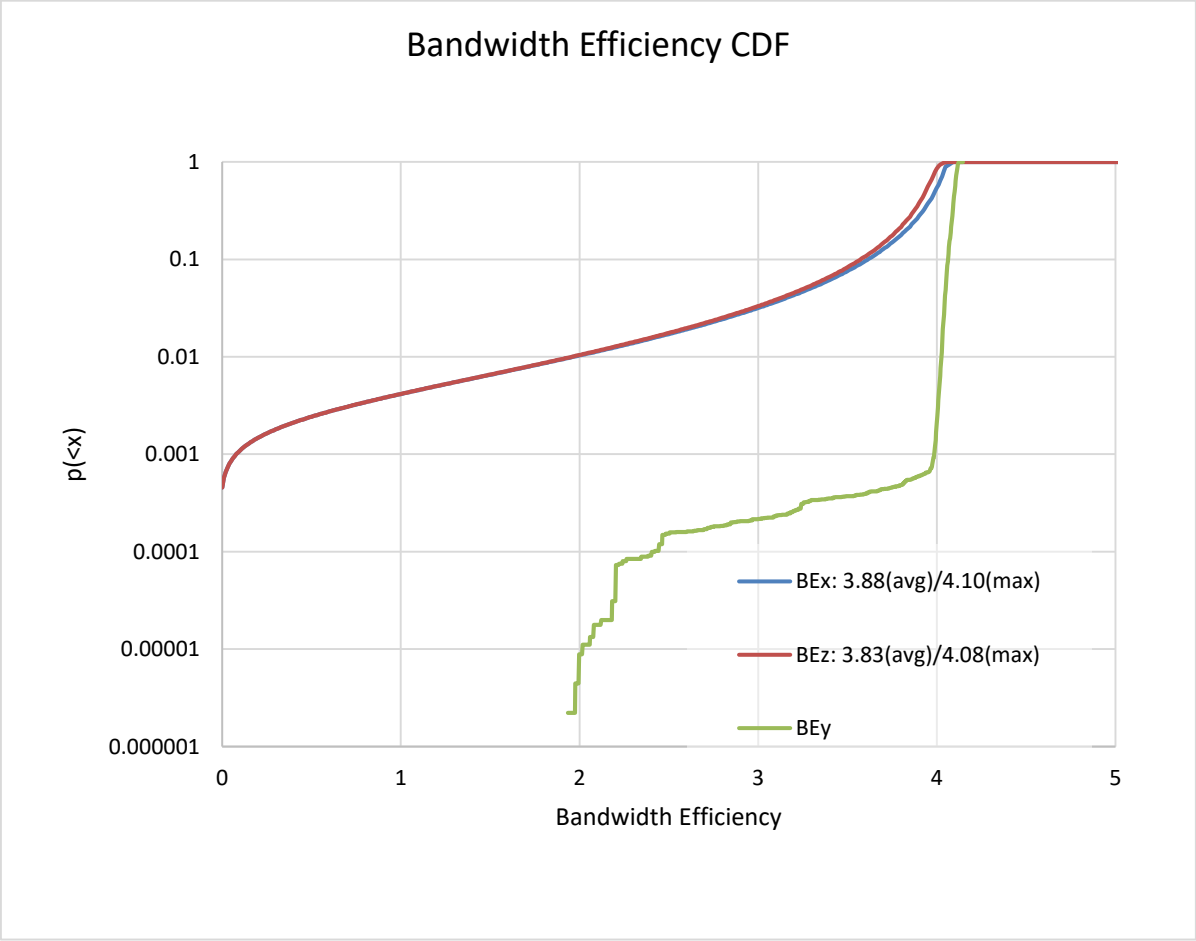

In terms of determining the percent degraded throughput, the difference between the bandwidth efficiency from the CDF curves of BEz and BEx should not exceed 3% for single entry and 10% for aggregate contributions. For this particular example, the bandwidth efficiency for the long term

operation of this system due to propagation alone is determined to be 3.88 bps and the bandwidth efficiency for the long term operation of this system due to propagation and interference is determined to be 3.83 bps. Thus, in applying the concept of percent degraded throughput, this analysis produces:

(3.88-3.83)/4.10 * 100% = 1.22% percent degraded throughput

As can be seen by the analysis presented above, the concept of percent degraded throughput as described by Recommendation ITU-R S.2131-0 can be used to ensure that the ACM performance by a satellite network meets the protection criterion given in Recommendation ITU-R S.1323 as compared to the capacity of percent degraded throughput for a system operating in rain fade conditions and a system operating in rain and interference conditions.

5 Overview of reserve capacity approach

During discussions regarding WRC-19 agenda item 1.6 at CPM19-2, the concept of reserve capacity was discussed as a potential alternate metric in the context of sharing between FSS systems in the 50/40 GHz frequency bands. It should be noted that the concept of reserve capacity has not been studied within ITU-R under WRC-19 agenda item 1.6.

The concept of reserve capacity was originally introduced in Recommendation ITU-R S.1323-2. This Recommendation discusses the maximum permissible levels of interference in a satellite network. It should be noted that Recommendation ITU-R S.1323-2 pertains to sharing between FSS networks below 30 GHz. Further, it is important to note that the concept of reserve capacity that is introduced in the Recommendation is noted as needing further studies and no specific example is provided in the application of the reserve capacity study.

One of the main limitations of Recommendation ITU-R S.1323-2 is that the sharing consideration does not account for propagation losses on the interfering path. As studied by ITU-R and confirmed by the relevant propagation experts within the ITU, propagation losses are significant for satellite operations in the 50/40 GHz and should be taken into account on both the wanted and interfering paths. For WRC-19 agenda item 1.6, the ITU-R has been developing a new Recommendation for sharing considerations of FSS systems above 30 GHz that takes into account propagation losses on both the wanted and interfering paths. In Recommendation ITU-R S.1323-2 the aggregate allowance of interference to systems employing ACM is 10%.

During the meeting of CPM19-2, some administrations inserted the concept of reserve capacity as an option in Method A of the draft CPM text for protection of FSS systems using ACM. Since the concept of reserve capacity in the 50/40 GHz frequency bands has not been studied within ITU-R, or clearly defined by the ITU-R, this concept is subject to interpretation on its meaning and application.

One possible interpretation of reserve capacity as defined in Recommendation ITU-R S.1323, is that the satellite network is able to maintain the same amount of throughput as it did without interference present. In other words, this refers to the ability of a satellite system to ensure that during the times when the ACM system is operating above the target throughput, the spectral efficiency is such that excess capacity can be stored in “reserve” to be used to ensure that during times of adverse propagation and increased interference, the operation of the satellite network does not drop below the target throughput. Thus, during times of fade, to ensure that the operational throughput required to account for external interference should not be reduced beyond a maximum of 10% of the capacity lost (“reserve capacity”) to account for rain fades.

As described above, the concept of reserve capacity has been proposed for frequency bands below 30 GHz. This concept is indicated in *resolves* 6.2 of Recommendation ITU-R S.1323:

> **6.2** in the case of networks using adaptive coding, provisionally be responsible for at most a 10% (until review by further studies) decrease in the amount of reserve capacity available to links that require heavier coding to compensate for rain fading, on the assumption that the

network maintains, with the use of this reserve capacity, the same level of performance as it did with no time-varying interference present. Further studies are needed to validate this approach;

As previously explained, while the use of the concept of reserve capacity is not supported by work on ACM systems by ITU-R, nevertheless, it can be shown that the use of the percent degraded throughput on a time averaged can meet the description as indicated in *resolves* 6.2. Referring again to Fig. A11-1 above, it can be seen that this particular link has a maximum bandwidth efficiency of 4.10 bps/Hz in the presence of propagation fades. The operational capacity for this system is 3.88 bps/Hz. Thus, according to *recommends* 6.2 of Recommendation ITU-R S.1323, the interfering system would need to provide at most a 10% aggregate decrease to maintain the same level of performance as it would without time-varying interference present. Based on this concept, the same logic as described above for percent degraded throughput applies, where the decreased ACM capacity available based on time-varying interference is 3.83 bps/Hz. Thus, the reserve capacity for time-varying interference would be the difference in service provided to compensate for rain fade, as compared to the ability of the ACM system to maintain the same level of performance with at most 10% decrease allowance, or:

$$(3.88\text{-}3.83)/3.88 * 100\% = 1.3\%$$

As shown above, this example of utilizing time averaged percent degraded throughput represents a 1.3% decrease caused by time-varying interference as compared to the performance of the link without time-varying interference present, which meets the criteria by a large margin.

6 Alternative reserve capacity approach

An alternate definition of reserve capacity was also presented. With this approach, the calculation of ACM degradation is not computed as a function of time associated with the rain and interference statics, but is computed based on an instantaneous impact on spectral efficiency. In contrast with the concept of degraded throughput, which strives to ensure that the ACM in the satellite system allows the maintaining of the required performance of the satellite system, this concept of "reserve capacity" strives to ensure that the operational throughput required to account for external interference should not be reduced beyond a maximum of 10% of the "reserve capacity" in excess of the operational capacity during operations of clear sky.

Based on this interpretation and referring back to Fig. A11-1, if the time averaged spectral efficiency for this system with no interference was set at 3.88 bps/Hz, the reserve capacity would be computed as the difference of the maximum capacity to the target capacity, or 4.10-3.88 bps/Hz = 0.22 bps/Hz. However, in this interpretation, we are comparing the maximum value (clear sky) achieved over a time period (a year) by a satellite system to a time average target capacity that can only be determined by applying long-term statistics of propagation fades. This particular interpretation of reserve capacity would then only allow 10% of 0.22 bps drop in spectral efficiency. This would essentially allow an interference allowance for all other satellite networks to impact only a 0.022 bps drop in spectral efficiency on an aggregate basis or 0.0067 bps drop in spectral efficiency for single entry on any one non-GSO system. As can be seen by the curve in Fig. A11-1, an allowance for such a small drop in spectral efficiency is not a realistic metric in the context of spectral efficiency losses accounted for by propagation fades.

Additionally, as explained previously the concept of operations of satellite systems employing ACM is to ensure that satellite connections are maintained during fade events. The fading events are computed as a long term statistic, respective to the calculation of rain fade. Figure A11-2 is taken from Recommendation ITU-R S.2131-0 and presents a curve for spectral efficiency and percent degraded throughput for a location in South Florida, USA. As can be seen from this curve, the

throughput of a system using ACM will change as a function of time. Additionally, in a practical analysis, the interference experienced by a certain link will also change as a function of time.

FIGURE A11-2

Attenuation due to propagation loss based on Recommendation ITU-R P.618 for a satellite connection utilizing ACM and operating in a climatological area similar to South Florida, USA

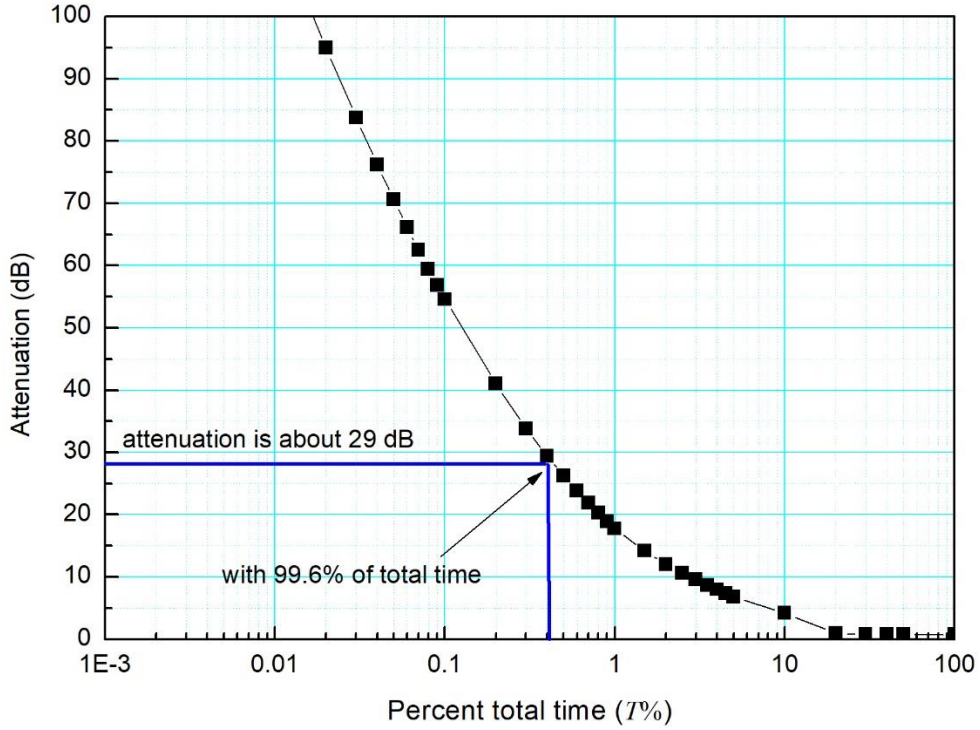

In the consideration of reserve capacity as described above, the periods for which the ACM systems will operate above the operational throughput will be in limited fading conditions (clear-sky and near clear-sky conditions). As shown by the Figure, the throughput of the victim satellite systems will change based on the long term considerations for which ACM systems are designed. Even in the consideration of reserve capacity given in Recommendation ITU-R S.1323, the assumption for time-varying fade statistics are implied. Thus, the concept of reserve capacity must be time dependent, as capacity, even in 'reserve', cannot be created nor used in any instant as capacity is a quantity which is consumed and measured over time. Consideration of interference allowance based on a short term, instantaneous metrics is not appropriate methodology for a long term operational approach such as discussed for ACM operations.

Furthermore, recall that for measurements of interference from non-GSO systems into GSO systems in ITU-R studies, Recommendation ITU-R S.1503 implies that the worst case epfd assumptions are always being computed. Consideration of a short term interference metric where the victim system is in best-case operating conditions and the interfering system is producing worst case interference is also not an appropriate metric for evaluating ACM operations.

Finally, in this interpretation, the concept of applying an interference criteria based on reserve capacity is not appropriate as the reserve capacity criteria represents capacity that is in excess. Consideration of reserve capacity in instantaneous, clear sky conditions would mean that there is no propagation fade and the interference allowance for other GSO and non-GSO satellite systems would be 0%. However, at the same time that the interference allowance is 0%, the reference GSO FSS satellite link is operating with reserve capacity, meaning that the wanted satellite operations are

generating capacity in excess of its designed operational throughput. The criteria for evaluating interference to an ACM system should be based on long term and predictable impacts on capacity such as with the percent degraded throughput concept.

7 Conclusion

This Annex considers concepts for the protection of FSS systems utilizing adaptive coding and modulation approached in the 50/40 GHz frequency bands. As described above and highlighted by the work carried out by ITU-R in developing Recommendation ITU-R S.2131-0, the use of adaptive coding and modulation allows a satellite to maintain a connection in spite of degraded conditions but at lower throughput data rates. To consider the impact to satellite systems using ACM, and to allow those systems to adjust to degraded link conditions, it is necessary to account for all foreseeable fade effects, such as time-varying propagation conditions and interference. As the analyses carried out within ITU and further presented in this document shows, the concept of percent degraded throughout as applied on a long-term basis presents a methodology that can provide a metric to protect the operations of satellite systems employing ACM.

Annex 12

Study #12 for the development for sharing between non-GSO and GSO in the 50/40 GHz frequency bands

In this study, the performance of the GSO link is evaluated through the following methodology:

Step 1: Set the parameters of the interfered-with GSO FSS link

As an example, the following subset of the parameters for a link was considered:

TABLE A12-1

Characteristics of the interfered-with GSO FSS link

Parameter	Value
Frequency (GHz)	40.0
Antenna diameter (m)	0.75
Max antenna gain (dBi)	48.0
Receiver Equivalent Noise Temperature (Clear-Sky) (K)	244.0
Satellite e.i.r.p. (dBW)	73.0
Carrier bandwidth (MHz)	600.0

Step 2: Set the parameters of the interfering non-GSO system

An example non-GSO system as characterized in Table A12-2 was used. It should be noted that this is just one possible example set of system parameters.

TABLE A12-2

Characteristics of the interfering non-GSO system

Parameter	Value
Frequency (GHz)	40.0
Number of orbits	18
Number of satellites per orbit	40
Total number of satellites	720
Separation angle between satellites in the same orbital plane (degree)	9.0
Separation angle between orbital planes (degree)	10.2
Altitude of the perigee and apogee for each orbit (km)	1200
Orbit inclination (degree)	87.9
GSO exclusion angle (aka "alpha angle") as per the relevant field in the non_geo table of the SRS database (degree)	6.0
Minimum elevation angle of the associated non-GSO e/s (degree)	5.0
Maximum number of satellites transmitting simultaneously	50.0
Power radiated by each of the satellites	See pfd mask4

Step 3: Set the location of the interfered-with GSO earth station

Recommendation ITU-R S.1503-3 was used to determine the location of the interfered-with GSO earth station and associated satellite. As it would not be feasible to analyse all possible geometries, Recommendation ITU-R S.1503-3 uses the Worst-Case Geometry Algorithm (WCGA) to determine the earth station and associated GSO satellite that would result in the highest single satellite epfd (or if there are multiple, the one with the lowest angular momentum / lowest elevation angle). Table A12-3 summarises the output of the WCGA for the non-GSO system whose characteristics are indicated in Table A12-2. A link budget for the computation of the clear-sky *C*/*N* at the WCG GSO earth station from the WCG GSO satellite is provided in Annex 1.

TABLE A12-3

Worst-Case GSO geometry studied

Parameter	Value
Longitude of the GSO satellite (degree)	−4.34
Latitude of the associated GSO e/s (degree)	67.83
Longitude of the associated GSO e/s (degree)	3.07
Elevation angle of the associated GSO e/s (degree)	13.50
Azimuth angle of the associated GSO e/s (degree)	−171.99
R001 rain rate at the associated GSO e/s (mm/hr)	20.838

Step 4: Compute the statistics of the Equivalent Power Flux Density (epfd) measured at the input of the receiver of the interfered-with GSO earth station

Following the methodology of Recommendation ITU-R S.1503-3, the Cumulative Density Function (CDF) of the epfd was computed. Figure A12-1 illustrates the results obtained.

[4] The PFD mask (in XML format) can be found in Attachment 1.

FIGURE A12-1

CDF of the epfd measured at the input of the GSO receiver

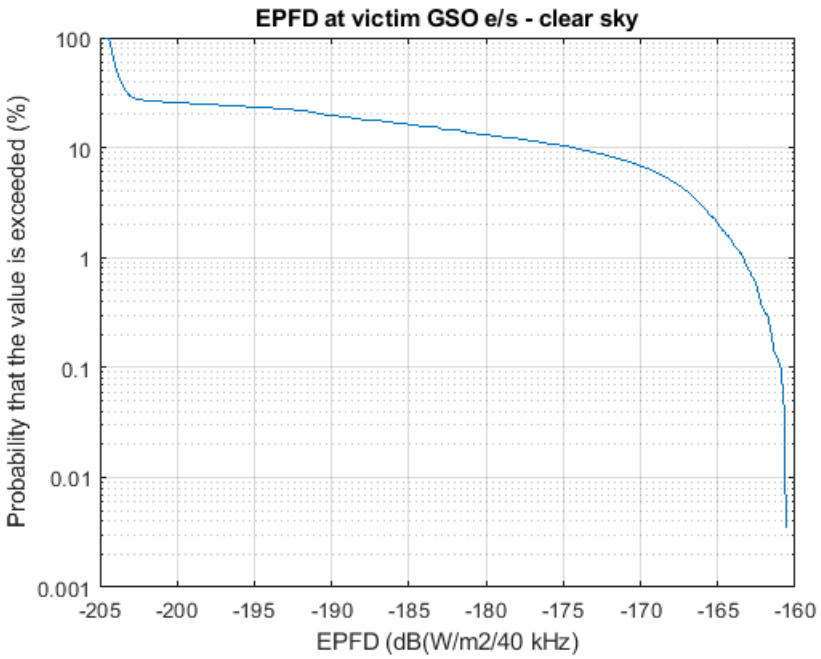

Step 5: Compute the rain statistics at the GSO earth station location

It is important take into account fading from rain when assessing the impact of interference caused by a non-GSO system into a GSO earth station. The methodology indicated by ITU-R was applied to calculate the rain statistics, in particular by setting the fading to 0 dB for percentages of unavailability larger than p_{max}. Where p_{max} is the minimum value of a) 10% and b) the probability of rain attenuation of a slant path calculated from § 2.2.1.2 of Recommendation ITU-R P.618-13.

FIGURE A12-2

CDF of the attenuation due to rain

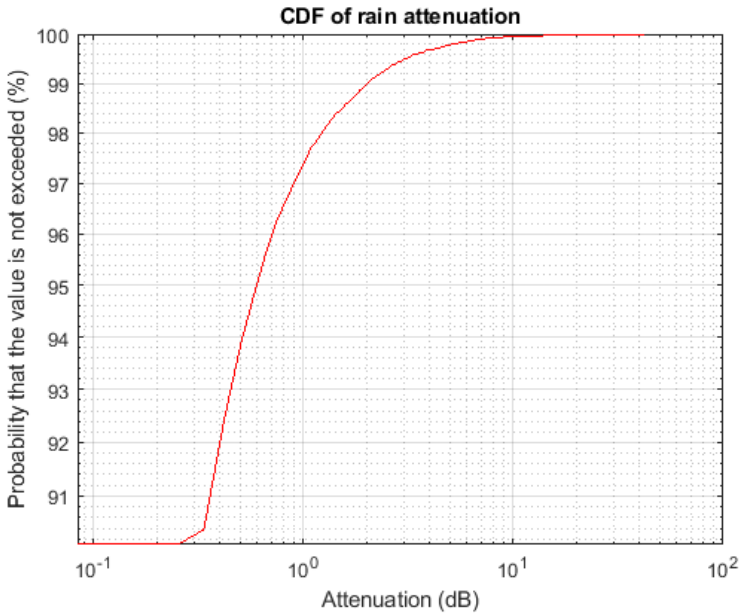

Step 6: Convolve the clear-sky *C*/*N* and epfd with the rain statistics

To assess the combined effects of interference and rain over the wanted GSO FSS link, the CDFs illustrated in Figs A12-1 and A12-2 were convolved. This convolution was achieved by combining the clear-sky wanted and interfering signal strength in the time domain from which the CDF in Fig. A12-1 was generated, with the rain attenuation in the time domain from which the CDF in Fig. A12-2 as generated. Additionally, the increase in the earth station receive thermal noise from rain fading was included. When performing the convolution, it was assumed that there was a full correlation between the fading of the wanted and interfering signal. Furthermore, the increase in equivalent noise power at the input of the GSO receiver was also computed by following the methodology illustrated in § 3 of Recommendation ITU-R P.618-13.

Step 7: Compute the CDF of the *C/N* and *C/(N+I)* ratios measured at the input of the receiver of the GSO earth station

Figure A12-3 compares the CDF of the *C/N* ratio measured at the input of the GSO receiver in presence of rain (blue line) and the CDF of the *C/(N+I)* ratio measured the input of the GSO receiver in presence of rain and interference (red curve).

FIGURE A12-3

CDF of the *C/N* and *C/(N+I)* ratios at the GSO receiver

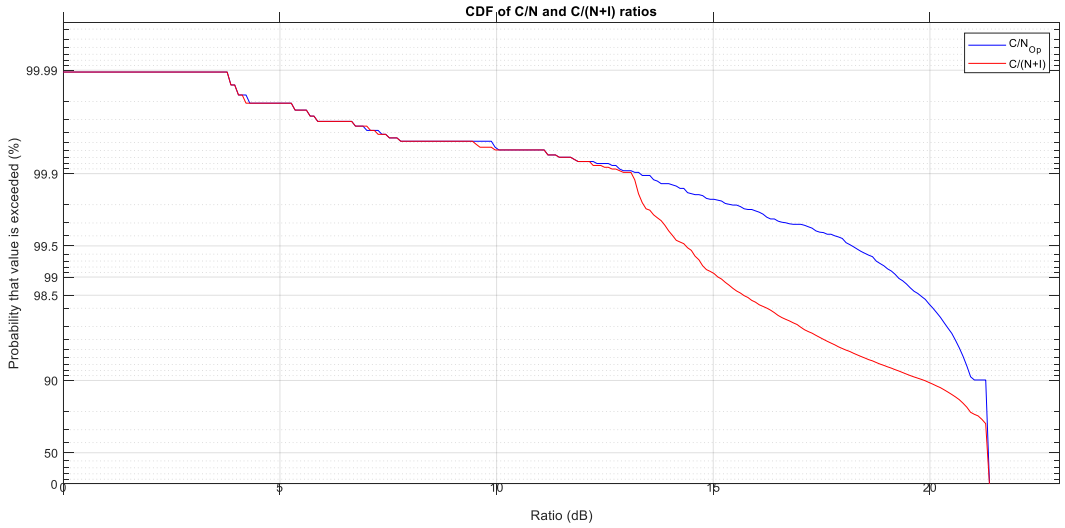

Assuming that the GSO link studied would become unavailable when the *C/N* or the *C/(N+I)* at the input of the receiver would fall below a $C/N_{thr} < 0$ dB, from the plots shown in Fig. A12-3 it can be seen that the interference caused by the non-GSO system would not increase the time allowance for degradation exceeding the minimum short-term performance objective of GSO FSS link studied. Therefore, the conditions of protection criteria being developed in the ITU-R would be met.

Step 8: Compute the CDF of the GSO spectral efficiency of the GSO link

Using equation (3) of the version of Recommendation ITU-R S.2131-0, the data generating the statistics illustrated in Fig. A12-3 were used to generate the CDF of the spectral efficiency of the GSO link in presence of rain only, and in presence of both rain and interference (blue and red curve, respectively, in Fig. A12-4).

From Fig. A12-4, the degradation in the SE exceeded for a certain % of time of an average year can be identified. In this example it can be seen that in presence of rain only, the or SE exceeded for 99% of an average year is equal to 4.39 bps/Hz in presence of rain only, while, with interference, the SE that is exceeded for 99% of an average year is equal to 3.38 bps/Hz (i.e. a degradation of 23.0%).

FIGURE A12-4

CDF of the spectral efficiency at the GSO receiver

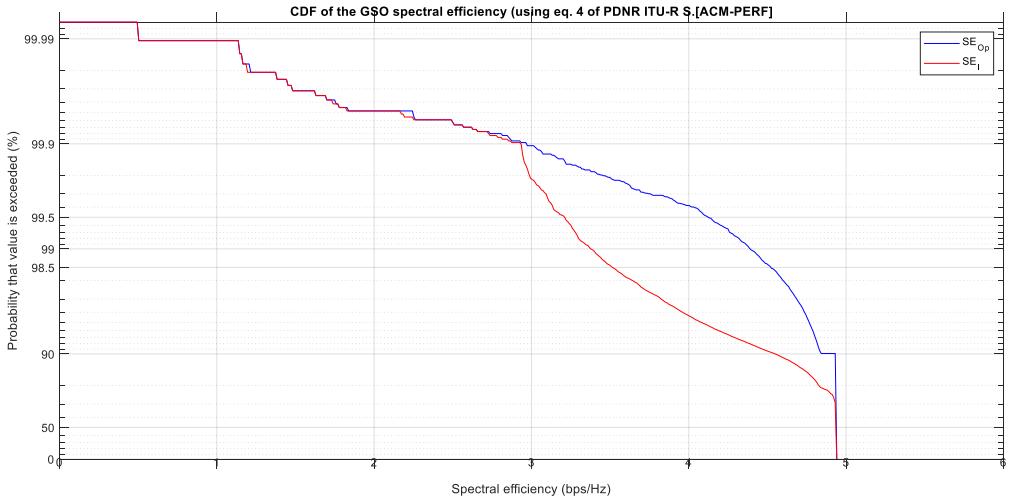

Step 9: Analyze the results

Table A12-4 summarises the results obtained.

TABLE A12-4

Analysis results

Parameter	Unit	Value
Average spectral efficiency in operational conditions (rain only)	bps/Hz	4.91
Average spectral efficiency in interfered conditions (rain + interference)	bps/Hz	4.82
Average degradation in spectral efficiency and annual throughput5	**%**	**1.83**
SE exceeded for 80% of an average year in operational conditions (rain only)	bps/Hz	4.84
SE exceeded for 80% of an average year in interfered conditions (rain + interference)	bps/Hz	4.83
Degradation in SE exceeded for 80% of an average year	**%**	**0.21**
SE exceeded for 95% of an average year in operational conditions (rain only)	bps/Hz	4.76
SE exceeded for 95% of an average year in interfered conditions (rain + interference)	bps/Hz	4.08
Degradation in SE exceeded for 95% of an average year	**%**	**14.32**
SE exceeded for 99% of an average year in operational conditions (rain only)	bps/Hz	4.39
SE exceeded for 99% of an average year in interfered conditions (rain + interference)	bps/Hz	3.38
Degradation in SE exceeded for 99% of an average year	**%**	**22.98**
SE exceeded for 99.5% of an average year in operational conditions (rain only)	bps/Hz	4.12
SE exceeded for 99.5% of an average year in interfered conditions (rain + interference)	bps/Hz	3.21
Degradation in SE exceeded for 99.5% of an average year	**%**	**22.07**
SE exceeded for 99.9% of an average year in operational conditions (rain only)	bps/Hz	2.93
SE exceeded for 99.9% of an average year in interfered conditions (rain + interference)	bps/Hz	2.93
Degradation in SE exceeded for 99.9% of an average year	**%**	**0.00**

5 Throughout this Annex, this metric is based on protection criteria being developed in the ITU-R.

The results above show that, in this example, assessing the degradation of the performance of an FSS link using ACM taking in to account the average degradation in spectral efficiency shows a degradation of 1.86% and therefore the single-entry 3% protection criterion being developed in the ITU-R would be met; however, the results also show that the interference would increase the degradation in SE exceeded for certain percentages of an average year by more than 3%. Therefore, in this example, the impact of the interference on a victim GSO FSS link benefits may not be deemed acceptable.

Attachment 1

to Annex 12

TABLE A12-15

GSO link budget (clear-sky)

Parameter	Unit	Value
Frequency	GHz	40.0
Longitude of the GSO satellite	deg	-4.34
Latitude of the associated GSO e/s	deg	67.83
Longitude of the associated GSO e/s	deg	3.079
Elevation angle of the associated GSO e/s	deg	13.50
Free space loss	dB	216.58
Satellite e.i.r.p. sd	dBW/Hz	-14.78
Bandwidth	kHz	40
Satellite e.i.r.p.	dBW	31.24
Max antenna gain	dBi	48.0
Receiver equivalent noise temperature (clear-sky)	K	244.0
C/*N* (clear-sky)	dB	21.37

Attachment 2

to Annex 12

PFD Mask.xml

Annex 13

GSO/FSS system parameters used in studies

Geostationary network	Units																
Link Direction		**Gateway to User**			**User to Gateway**			**Gateway to User**	**User to Gateway**	**Gateway to User**	**User to Gateway**	**GW to User**	**GW to User**	**GW to User**	**User to GW**	**User to GW**	**User to GW**
A) Performance objectives		Carrier#1	Carrier#2	Carrier#3	Carrier#4	Carrier#5	Carrier#6										
1.A.1 Threshold #1 (N/A for not applicable): $C/(N+I)$	(dB)	7.3	7.3	7.3	15.3	6	4.4	-2.7	1.4	-4.2	0.6	0	-3	5	0	-3	5
(% of the year $C/(N+I)$ should be exceeded)		99.59	99.58	99.56	99.88	99.96	99.91	99.60	99.60	99.60	99.60	99.9	99.8	99.9	99.9	99.8	99.9
1.A.2 Threshold #2 (N/A for not applicable): $C/(N+I)$	(dB)	N/A	N/A	N/A	N/A	N/A	N/A	14	12	13.3	11.8	9.7	6.8	8.6	7.2	4.7	7.5
(% of the year $C/(N+I)$ should be exceeded)								96	96	96	96	99.5	99.5	99.5	99.5	99.5	99.5
1.A.3 Threshold #3 (N/A for not applicable): $C/(N+I)$	(dB)	N/A	N/A	N/A	N/A	N/A	N/A	N/A	N/A	N/A	N/A	16	20.4	10.6	12	15	9
(% of the year $C/(N+I)$ should be exceeded)												90.0	90.0	90.0	90.0	90.0	90.0
B) Waveform description																	
1.B.1 Modulation type (e.g., FM, QPSK, BPSK)		QPSK, 8-PSK, 16-APSK	QPSK, 8-PSK, 16-APSK	QPSK, 8-PSK, 16-APSK	QPSK, 8-PSK, 16-APSK	QPSK, 8-PSK, 16-APSK	QPSK, 8-PSK, 16-APSK	BPSK 16APSK	QPSK 16APSK	BPSK 16APSK	QPSK 16APSK	QPSK 16APSK 64APSK	QPSK 16APSK 256APSK	8PSK 16APSK 16APSK	QPSK 16APSK 32APSK	QPSK 8APSK 64APSK	8PSK 16APSK 16APSK
1.B.2 Noise bandwidth per carrier	(kHz)	110,000	110,000	110,000	110,000	110,000	110,000	600,000	62,500	600,000	62,500	500,000	500,000	500,000	2,000	2,000	2,000
C) Transmit earth station characteristics																	
1.C.1 Altitude	(km)	0	0	0	0	0	0	0.01	0.01	0.01	0.01	0	0	0	0	0	0
1.C.2 Latitude (+: North, –: South) from Equator	(degree)	54.827031	54.827031	54.827031	54.827031	54.827031	54.827031	41.98	41.98	41.98	41.98	49.69	3.13	-12.1	-	-	-
1.C.3 Elevation angle	(degree)	25	25	25	25	25	25	40.1	40.1	40.1	40.1	32	86	74	-	-	-
1.C.4 Temperature at ground level	(°C)	25	25	25	25	25	25	10.5	10.5	10.5	10.5	25	25	25	25	25	25
1.C.5 Relative humidity	(%)	30	30	30	30	30	30	50	50	50	50	-	-	-	-	-	-

Geostationary network	**Units**															
Link Direction		**Gateway to User**			**User to Gateway**			**Gateway to User**	**User to Gateway**	**Gateway to User**	**User to Gateway**	**GW to User**	**GW to User**	**GW to User**	**User to GW**	**User to GW**	**User to GW**
1.C.6 Rain model	(ITU/ Crane)	ITU-R P.618	ITU-R P.618	ITU-R P.618	ITU-R P.618	ITU-R P.618	ITU-R P.618	ITU-R P.618	ITU-R P.618	ITU-R P.618	ITU-R P.618	ITU-R P.618	ITU-R P.618	ITU-R P.618	ITU-R P.618	ITU-R P.618	ITU-R P.618
1.C.7 Rain zone	(as per model)	C	C	C	C	C	C	-	-	–	–	-	-	-	-	-	-
1.C.8 Rain fall rate exceeded for 0.01% of an average year (mm/h) if available		15	15	15	15	15	15	50.1	50.1	50.1	50.1	28.23	99.13	6.01	-	-	-
1.C.9 On-axis Earth station transmit e.i.r.p.	(dBW)	86.2	83.5	81.7	83.5	56.9	51.9	87.6	58.9	88.0	60.2	80	80	80	59.1	59.1	59.1
1.C.10 Antenna pointing loss towards the geostationary satellite	(dB)	0.5	0.5	0.5	0.5	0.5	0.5	0	0.9	0	0.9	0.5	0.5	0.5	0.5	0.5	0.5
1.C.11 Inter modulation earth stations *C*/*I*	(dB)	20	20	20	20	20	20	40	100	40	100	35	35	35	35	35	35
1.C.12 Power control range (>0, 0 dB if none)	(dB)	0	0	0	0	0	0	7	0	7	0	10	10	10	0	0	0
1.C.13 Power control accuracy (applicable only if uplink power control used)	(dB)	-	-	-	-	-	-	0.5	NA	0.5	NA	0.25	0.25	0.25	0.25	0.25	0.25
1.C.14 Polarisation isolation (*C*/*I* of wanted to unwanted polarisation)	(dB)	28	28	28	28	28	28	27	100	27	100	30	30	30	25	25	25
D) Receive earth station characteristics																	
1.D.1 Altitude	(km)	0	0	0	0	0	0	0.01	0.01	0.01	0.01	-	-	-	0	0	0
1.D.2 Latitude (+: North, –: South) from Equator	(degree)	-47.2043	-47.2043	-47.2043	-47.2043	-47.2043	-47.2043	41.98	41.98	41.98	41.98	-	-	-	49.69	3.13	-12.1
1.D.3 Temperature at ground level	(°C)	25	25	25	25	25	25	10.5	10.5	10.5	10.5	25	25	25	25	25	25
1.D.4 Relative humidity	(%)	30	30	30	30	30	30	50	50	50	50	-	-	-	-	-	-
1.D.5 Elevation angle	(degree)	25	25	25	25	25	25	40.1	40.1	40.1	40.1	-	-	-	32	86	74
1.D.6 Rain zone	(as per model)	N	N	N	N	N	N	-	-	–	–	-	-	-	-	-	-
1.D.7 Rain fall rate exceeded for 0.01% of an average year (mm/h) if available		95	95	95	95	95	95	50.1	50.1	50.1	50.1	-	-	-	28.23	99.13	6.01

Geostationary network	Units																
Link Direction		**Gateway to User**			**User to Gateway**			**Gateway to User**	**User to Gateway**	**Gateway to User**	**User to Gateway**	**GW to User**	**GW to User**	**GW to User**	**User to GW**	**User to GW**	**User to GW**
1.D.8 Earth station receive noise temperature (clear sky / faded link)	(K)	250/500	250/500	250/500	250/500	250/500	250/500	250/500	200/450	250/500	200/450	250/500	250/500	250/500	250/500	250/500	250/500
1.D.9 On-axis antenna gain	(dBi)	42.8	42.8	42.8	56.6	56.6	56.6	43.4	67.0	43.4	67.0	47.5	47.5	47.5	57.6	57.6	57.6
1.D.10 Antenna diameter	(m)	0.45	0.45	0.45	2.2	2.2	2.2	0.45	6.8	0.45	6.8	0.75	0.75	0.75	2.4	2.4	2.4
1.D.11 Antenna pointing loss	(dB)	0.5	0.5	0.5	0.5	0.5	0.5	0.9	0	0.9	0	0.5	0.5	0.5	0.5	0.5	0.5
1.D.12 Polarisation isolation (*C*/*I* of wanted to unwanted polarisation)	(dB)	28	28	28	28	28	28	25	25	25	25	30	30	30	25	25	25
E) Space station receive characteristics																	
1.E.1 Transponder bandwidth	(MHz)	110	110	110	110	110	110	600	62.5	600	62.5	500-600	500-600	500-600	500-600	500-600	500-600
1.E.2 Receive frequency	(GHz)	42.5-51.4	42.5-51.4	42.5-51.4	42.5-51.4	42.5-51.4	42.5-51.4	48	48	50.5	50.5	42.5-51.4	42.5-51.4	42.5-51.4	42.5-51.4	42.5-51.4	42.5-51.4
1.E.3 Receive polarisation		C	C	C	C	C	C	C	C	C	C	C	C	C	C	C	C
(H: horizontal, V: Vertical, C: Circular)																	
1.E.4 Automatic level control range	(dB)	0	0	0	0	0	0	0	0	0	0	0	0	0	0	0	0
(0 if none)																	
1.E.5 Peak receive antenna gain	(dBi)	51.8	51.8	51.8	51.8	51.8	51.8	51.4	59.8	51.9	60.2	51.8	51.8	51.8	57.23	57.23	57.23
1.E.6 Receive satellite antenna gain in the direction of transmit earth station	(dBi)	48.8	48.8	48.8	48.8	48.8	48.8	51.4	56.8	51.9	57.2	48.8	48.8	48.8	52.2	52.2	52.2
1.E.7 Satellite receive temperature	(K)	700-1000	700-1000	700-1000	700-1000	700-1000	700-1000	600.0	600.0	600.0	600.0	600	600	600	600	600	600
1.E.8 Receive cross-polarisation isolation (*C*/*I*, 100 if not applicable)	(dB)	25	25	25	25	25	25	27	27	27	27	30	30	30	30	30	30
1.E.9 Receive frequency re-use isolation (*C*/*I*, 100 if not applicable)	(dB)	25	25	25	25	25	25	100	25	100	25	30	30	30	25	25	25
1.E.10 Transponder total input back-off	(dB)	2.5	2.5	2.5	2.5	2.5	2.5	0	0	0	0	2.5	2.5	2.5	2.5	2.5	2.5
F) Space station transmit characteristics																	

Geostationary network	Units																
Link Direction		**Gateway to User**			**User to Gateway**			**Gateway to User**	**User to Gateway**	**Gateway to User**	**User to Gateway**	**GW to User**	**GW to User**	**GW to User**	**User to GW**	**User to GW**	**User to GW**
1.F.1 Transmit frequency	(GHz)	37.5-50.2	37.5-50.2	37.5-50.2	37.5-50.2	37.5-50.2	37.5-50.2	40.5	40.5	40.5	40.5	37.5-50.2	37.5-50.2	37.5-50.2	37.5-50.2	37.5-50.2	37.5-50.2
1.F.2 Transmit polarisation (H: horizontal, V: Vertical, C: Circular)		C	C	C	C	C	C	C	C	C	C	C	C	C	C	C	C
1.F.3 Transponder total output back-off	(dB)	2.5	2.5	2.5	2.5	2.5	2.5	0.0	0.0	0.0	0.0	2.5	2.5	2.5	2.5	2.5	2.5
1.F.4 Satellite e.i.r.p. in the direction of the receive earth station	(dBW)	61.9	61.9	61.9	61.8	51.5	51.5	77.3	57.2	77.8	58.0	71.5	71.5	71.5	51.3	51.3	51.3
1.F.5 Transmit cross-polarisation isolation (*C*/*I*, 100 if not applicable)	(dB)	25	25	25	25	25	25	25	25	25	25	30	30	30	25	25	25
1.F.6 Transmit frequency re-use isolation (*C*/*I*, 100 if not applicable)	(dB)	25	25	25	25	25	25	23	100	23	100	35	35	35	35	35	35
1.F.7 Satellite adjacent transponder isolation	(dB)	25	25	25	25	25	25	100	100	100	100	30	30	30	30	30	30
1.F.8 Transponder inter modulation *C*/*I*	(dB)	20	20	20	20	20	20	100	18	100	18	25	25	25	25	25	25
G) Interference from other GSO networks and terrestrial services																	
1.G.1 Up link clear-sky *C*/*I* due to other geostationary networks	(dB)	24	24	24	24	24	24	42.6	27.9	37.2	23.3	30	30	30	23	23	23
1.G.2 Up link clear-sky *C*/*I* due to sharing with fixed service (100 dB if no sharing)	(dB)	100	100	100	100	100	100	48.8	34.1	43.4	29.5	33	33	33	33	33	33
1.G.3 Down link clear-sky *C*/*I* due to other geostationary networks	(dB)	23	23	23	23	23	23	27.5	44.5	27.8	45.3	23	23	23	30	30	30
1.G.4 Down link clear-sky *C*/*I* due to sharing with fixed services (100 dB if no sharing)	(dB)	100	100	100	100	100	100	33.7	50.7	34	51.5	33	33	33	33	33	33